Spatial mapping of air quality

for European scale assessment

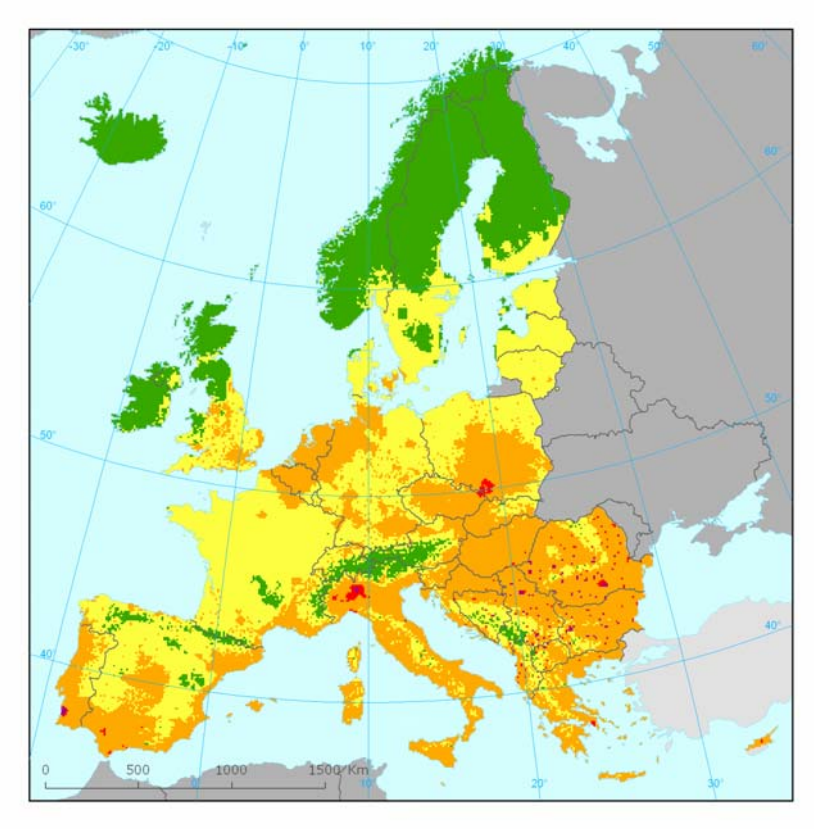

ETC/ACC Technical Paper 2006/6

March 2007

Jan Horálek, Bruce Denby, Peter de Smet, Frank de Leeuw,
Pavel Kurfürst, Rob Swart, Twan van Noije

European Topic Centre
on Air and Climate Change

The European Topic Centre on Air and Climate Change (ETC/ACC)

is a consortium of European institutes under contract of the European Environmental Agency

RIVM UBA-B UBA-V IIASA NILU AEAT AUTh CHMI DNMI NTUA ÖKO IEP TNO UEA

Front page picture: *Figure 8.1 Annual mean PM10 concentrations ($\mu g \cdot m^{-3}$), 2004.*

DISCLAIMER:

This ETC/ACC Technical Paper has not been subjected to European Environment Agency (EEA) member country review. It does not represent the formal views of the EEA.

Spatial mapping of air quality for European scale assessment

ETC/ACC Technical Paper 2006/6

March 2007

Final draft

Jan Horálek, Pavel Kurfürst, Czech Hydrometeorological Institute (CHMI), Praha

Peter de Smet, Frank de Leeuw, Rob Swart, Twan van Noije, Netherlands Environmental Assessment Agency (MNP), Bilthoven

Bruce Denby, Norwegian Institute of Air Research (NILU), Kjeller

EEA project manager: Jaroslav Fiala

Contents

Contents ... **5**

Abstract ... **9**

1 Introduction ... **11**

2 Interpolation methodologies and supplementary data selection ... **15**
2.1 Introduction ... *15*
2.2 Linear regression models without interpolation ... *17*
2.3 Interpolation methods using primarily measurements ... *17*
2.3.1 Inverse distance weighted interpolation (IDW) ... 17
2.3.2 Ordinary kriging (OK) ... 17
2.3.3 Ordinary cokriging (OC) ... 18
2.3.4 Lognormal kriging (LK) and lognormal cokriging (LC) ... 18
2.3.5 Variogram ... 18
2.4 Linear regression models plus interpolation of their residuals ... *20*
2.5 Use of various supplementary data sources ... *21*
2.6 Criteria for comparing spatial interpolations ... *22*
2.7 Criteria for the selection of an interpolation method ... *23*

3 Methods for the mapping of urban and rural areas ... **25**
3.1 Maps for rural areas ... *25*
3.2 Maps for urban areas ... *25*
3.3 Merging of rural and urban maps ... *25*

4 Input data ... **27**
4.1 Introduction ... *27*
4.2 Measured air quality data ... *27*
4.3 Altitude ... *28*
4.4 Output from the Unified EMEP model ... *28*
4.5 Meteorological parameters ... *29*
4.6 Climatological parameters ... *30*
4.7 Emissions ... *30*
4.8 Land cover ... *30*
4.9 Population density ... *31*

5 Analysis of mapping methodologies ... **33**
5.1 Rural mapping ... *33*
5.2 Rural areas – PM_{10} ... *33*
5.2.1 Comparison of linear regression models for rural PM_{10} indicators ... 33
5.2.2 Linear regression models after logarithmic transformation ... 35
5.2.3 Comparison of linear regression models using meteorological or climatological data ... 36
5.2.4 Comparison of linear regression models using altitude from AirBase or GTOPO30 ... 38
5.2.5 Conclusions on the linear regression models for rural PM_{10} ... 40
5.2.6 Comparison of spatial interpolation methods for rural PM_{10} ... 40
5.2.7 Conclusions on the spatial interpolation for PM_{10}, rural areas ... 48
5.3 Rural areas - Ozone ... *49*
5.3.1 Comparison of linear regression models for rural ozone indicators ... 49
5.3.2 Comparison of linear regression models using meteorological or climatological data ... 52
5.3.3 Conclusions on the linear regression models for rural ozone ... 53
5.3.4 Comparison of spatial interpolation methods for rural ozone ... 54
5.3.5 Conclusions on the spatial interpolation for ozone, rural areas ... 63
5.4 Rural areas - NO_x ... *63*
5.4.1 Relationships between NO_2 and NO_x data ... 63
5.4.2 Comparison of linear regression models for rural NO_x ... 65

5.4.3 Comparison of spatial interpolation methods for rural NO_x ... 66
5.4.4 Conclusions on the spatial interpolation for NO_x, rural areas ... 68
5.5 Rural areas - SO_2 ... *69*
5.5.1 Comparison of linear regression models for rural SO_2 ... 69
5.5.2 Comparison of spatial interpolation methods for rural SO_2 ... 69
5.6 Rural areas - $PM_{2.5}$ ... *72*
5.7 Urban mapping ... *73*
5.8 Urban areas - PM_{10} ... *74*
5.8.1 Comparison of linear regression models for urban PM_{10} ... 74
5.8.2 Conclusion of linear regression models for urban PM_{10} ... 76
5.8.3 Comparison of spatial interpolation methods for urban PM_{10} ... 77
5.8.4 Conclusions on the spatial interpolation for PM_{10}, urban areas ... 82
5.9 Urban areas - Ozone ... *82*
5.9.1 Comparison of linear regression models for urban ozone ... 82
5.9.2 Conclusion of linear regression models for urban ozone ... 83
5.9.3 Comparison of spatial interpolation methods for urban ozone ... 84
5.9.4 Conclusions on the spatial interpolation for ozone, urban areas ... 89

6 Comparison of exceedance mapping based on daily and annual statistics ... 91
6.1 Daily variation of interpolation parameters ... *92*
6.1.1 Station availability ... 92
6.1.2 Daily mean and standard deviation comparison ... 93
6.1.3 Regression parameters ... 93
6.1.4 Kriging parameters ... 94
6.1.5 Cross validation RMSE ... 95
6.2 Comparison of annual mean fields using daily and annual statistics ... *96*
6.3 Comparison of percentile fields using daily and annual statistics ... *98*
6.4 Comparison of number of exceedance days fields using daily and annual statistics ... *100*
6.5 Uncertainty analysis and mapping ... *102*
6.5.1 Uncertainty in the annual mean when using daily statistics ... 103
6.5.2 Uncertainty in the exceedance fields when using daily statistics ... 104
6.5.3 Comments on the kriging semivariogram ... 105
6.5.4 Conclusions on uncertainty mapping ... 106
6.6 Discussion and conclusions concerning the use of daily and annual statistics ... *106*

7 Uncertainty analyses on spatial interpolation ... 109
7.1 Introduction ... *109*
7.2 Comparison of measured and interpolated values ... *109*
7.3 Uncertainty maps ... *112*

8 Using the maps in impact assessments ... 117
8.1 Introduction ... *117*
8.2 Population exposure and health impacts ... *117*
8.2.1 Health impact of particulate matter ... 117
8.2.2 Health impact of ozone ... 121
8.2.3 Other pollutants ... 123
8.3 Exposure of vegetation ... *124*
8.3.2 Ozone ... 124
8.3.3. SO_2 and NO_x ... 129

9 Conclusions and recommendations ... 131
9.1 Summary of the interpolation methodologies and applications ... *131*
9.1.1 Methodologies assessed ... 131
9.1.2 Pollutants and indicators assessed ... 132
9.1.3 Monitoring and supplementary data used ... 132
9.1.4 Assessment and selection of the interpolation methodologies ... 132
9.2 Summary of the rural interpolation results ... *132*
9.2.1 PM_{10} ... 133
9.2.2 Ozone ... 133
9.2.3 NO_x ... 133

9.2.4 SO_2 ... 134
9.2.5 $PM_{2.5}$ ... 134
9.3 Summary of the urban interpolation results ... *134*
9.3.1 PM_{10} ... 134
9.3.2 Ozone ... 134
9.3.3 $PM_{2.5}$ ... 135
9.4 Summary of the use of daily or annual statistics ... *135*
9.5 Summary of the uncertainty analysis ... *136*
9.5.1 Spatial representativeness ... 136
9.5.2 Kriging variance ... 136
9.5.3 Uncertainty in the number of exceedances ... 137
9.6 Summary of the risk assessment ... *137*
9.6.1 Population exposure ... 137
9.6.2 Vegetation exposure ... 137
9.7 Considerations when recommending operational air quality mapping and risk assessment procedures ... *137*
9.8 Recommendations for further work ... *138*
9.8.1 Further discussions concerning methodologies, additional indicators, uncertainty and applications 138
9.8.2 Further analysis needs for the spatial assessment methodologies ... 139
9.8.3 Further pollutants and indicators ... 139
9.8.4 Uncertainty assessment and mapping ... 140
9.8.5 Further applications of the assessments ... 141

References ... 145

Annex. Final maps and summarizing tables for the year 2004 ... 149
Introduction ... *149*
Concentration maps ... 149
Exposure tables ... 150
Maps and Tables ... 151

Abstract

In this paper, interpolation techniques are applied for the construction of detailed air quality maps for Europe, based on a combination of primarily air quality monitoring data and secondarily, modelling and other supplementary data. We note that this approach is complementary to the analysis for the European Thematic Strategy that relies primarily on modelling results supporting air emission reduction strategy and feasibility assessments. Subsequently, these maps are used as the basis for an assessment of air pollution related risks for public health and ecosystems. The paper describes the improvement and application of various interpolation methods that were evaluated in a previous paper to develop high quality Europe-wide interpolated air quality maps for the European Environment Agency. The earlier work was expanded by including more recent data (2004) and more air quality indicators: PM_{10}, ozone, NO_x and SO_2 are now covered. Insufficient data were available to support the mapping of $PM_{2.5}$. Supplementary information used includes results from the Unified EMEP model calculations, altitude data, annual meteorological fields, and climatological fields. Separate urban and rural maps are merged using population density information. We conclude that kriging methods are generally to be preferred over inverse distance weighting, and in case of PM_{10} lognormal kriging over ordinary kriging. Methodologies based on linear regression using supplementary data are generally to be preferred over pure interpolation methods. The usage of concurrent meteorological data gives better results than climatological data. In the study, three types of uncertainty are addressed: spatial representativeness, kriging interpolation variance, and exceedance uncertainty.

The paper includes a preliminary combination of the interpolated air quality data with other data sets to analyse exposure and impacts of air pollution in terms of population and ecosystems at risk. We calculate the number of Europeans exposed to annual mean concentrations of PM_{10} above the European limit value of 40 $\mu g.m^{-3}$ at 6 % of the total population in 2004. The estimated number of premature deaths calculated using 2004 as the reference year is estimated between 246,000 and 327,000, depending on the choice of natural background concentration. The high end of this range is close to the estimates used in the CAFE strategy. For ecosystems, we find that more than 30 % of all agricultural land may be exposed to ozone exceeding the target value of 18 $mg.m^3.h$ and more than 80 % may be exposed to levels in excess of the long-term objective of 6 $mg.m^{-3}.h$. In southern countries more than 90 % is estimated to exceed the target values, while in northern Europe the estimated ozone levels are below the target value for nearly 70% of the agricultural area. For forests, in northern Europe the critical ozone reporting level of 20 $mg.m^{-3}.h$ is not exceeded in our calculations, but in southern Europe it is exceeded everywhere. The rural NO_x map shows a few regions where the NO_x limit value for the protection of vegetation is exceeded (the Benelux, the Rhone Valley and northern Italy). No significant exceedances for SO_2 were expected as the interpolated map of annual average SO_2 confirms.

In addition to the added value provided by visualization of air pollution indicators for public information purposes, the maps also improve the quality and relevance of the assessment of air pollution exposure and impacts in rural and urban areas across Europe. Potentially, it can be used for supporting the checking of compliance with air quality standards and for evaluation of national air quality reports. The current work focuses on longer-term indicators for European air quality. The application of the methods for near-real time reporting of air quality indicators might be a focus of future work. The paper provides suggestions for further work on methodologies (e.g., selection of the "best" methodology, alternative supplementary information), uncertainties (e.g., sub-grid variability, mapping of probabilities) and applications (e.g., combination with NATURA2000, near-real time mapping).

1 Introduction

Rationale and objectives

This project has been initiated with the objective of the European Environmental Agency of having interpolated maps primarily based on air quality measurements as reported by the countries through the Exchange of Information (EoI), next to the model-based European air quality maps (as applied e.g. in CAFÉ and City-Delta). The reported measurement data, including the stations meta-information is stored in the database AirBase (http://airbase.eionet.europa.eu), which is accessible through the internet. The maps of this project provide geospatially referenced information on air quality-related status and impact indicators that can be used in air pollution assessments. Typical status indicators are concentration levels, exceedances of thresholds and limit values as defined by the AQ-FWD and its Daughter Directives (DD) (EC, 1996, 1997, 1999, 2000, 2001, 2002, 2004). Examples of impact indicators are population at risk, potential number of deaths, and ecosystems, vegetation or crops at risk. In turn these impact indicators can provide input to indicators and assessments on potential yield reductions, economic and ecologic losses. However, these are beyond the scope of this paper.

For some air quality parameters, European-wide maps are missing and not provided by other projects and programmes. The maps produced in this project are primarily based on monitoring instead of modelling data and could lead to new insights and worthwhile conclusions related to European air pollution and its impacts. For example, these maps can serve as a '2nd opinion' in policy assessments of, e.g., limit value and target value exceedances and other indicators. They could provide support by comparing them with nationally reported air quality data and indicators, and in determining areas of compliance.

Earlier work

This is the final report of the task "Spatial air quality data" of the ETC/ACC Implementation Plan 2006, and represents a follow-up of the ETC/ACC Technical Papers 2005/7 (Denby et al., 2005) and 2005/8 (Horálek et al., 2005) on "Interpolation and assimilation methods for European scale air quality assessment and mapping".

In the ETC/ACC Technical Paper 2005/8 human health related indicator maps were created for the annual average and 36th maximum daily average value for PM_{10} and for the ozone indicators SOMO35. As vegetation related indicator AOT40-maps have been prepared for crops (accumulated over 3 months), the methods used for the creation of these maps for the years 2000–2003 were produced in three steps:

1. for the rural areas: linear regression of the measured and supplementary data followed by interpolation of the residuals;
2. for the urban areas: interpolation of the differences between the measurements and the rural background interpolated concentration field followed by the addition of the interpolated difference field to the rural background field;
3. merging of the interpolated maps for the rural and urban areas on the basis of the population density map.

In all cases the supplementary data used in the linear regression included output from the Unified EMEP model as well as altitude and sunshine duration. In the case of AOT40, relative humidity was also used. Both sunshine duration and relative humidity were extracted from climatological fields (averaged over the period 1961–1990). The analysis was performed on the basis of the annual statistics.

For all pollutants the maps for rural and urban areas were created separately and consequently merged on the basis of the population density. This approach tries to provide an objective method for dealing with the differences found between the rural and urban interpolated concentration fields in some areas in Europe.

Extension and improvements in this paper

This report deals with the improvement of methods and data input sources for producing air quality maps for Europe, with the extension of the set of pollutants for which these maps are created, and with the detailed analysis of uncertainties of the individual maps and the use of interpolation methods based on daily averages versus annual averages from measurements. Specifically, the examined methods are applied for creating maps for the year 2004, which are used in EEA's air quality related Core Set Indicators (CSI004 and CSI005) and in EEA Air Pollution reports.

In this report the mapping methods are further developed in two directions:

- improvement of the methods for those pollutants and indicators mapped previously (related to PM_{10} and ozone);
- development and application of methods for other pollutants and their indicators (SO_2, NO_x, $PM_{2.5}$, AOT40 for forests and the 26th highest maximum 8-hour daily average concentration for ozone).

Usage of additional data sources

In relation to the improvements on methodological aspects, we focused on the use of actual meteorological data for the same year as the monitoring data, as well as on selecting those meteorological parameters which show a better correlation with the air quality data. For example, now we take the 6-hourly values for 2004 for solar surface radiation of the ECMWF MARS database (www.ecmwf.int/services/archive), instead of the 30-year annual averaged sunshine duration of the CRU climatological database (New et al., 2002). The actual data is expected to improve the interpolation results due to its better temporal correlation and resolution, despite its somewhat lower spatial resolution. For PM_{10} and ozone this paper discusses these expected improvements for the year 2004.

The use of the altitude parameters from the European-wide high resolution dataset GTOPO30 (30 seconds grid cells) instead of the altitudes reported with the AirBase monitoring data, is compared for the rural background stations in the production of the maps of PM_{10} annual averages and the 36th maximum daily averages.

It is expected that auxiliary data with a high spatial resolution such as traffic density maps or emission inventories, will further improve the interpolation. However, no suitable high resolution traffic density database with European wide coverage appears to be available for this purpose. Spatial emission data for NO_x from the APMoSPHERE project (Briggs et al., 2005) is used in Section 5.8 only, as one of the supplementary parameters for estimation of urban PM_{10} pollution. One could think of including environmental satellite imagery data. However, such data is not considered. The conversion of the aerosol layer characteristics measured by satellites into ground level pollutant concentrations is not well established yet. An illustrative example of such a study is Koelemeijer et. al. (2006a) on $PM_{2.5}$. Another reason for not using satellite data is the voluminous data processing related to it and the limitations on project resources.

Exploration of improved methods, their applicability and associated uncertainties

Another improvement focuses on the analysis of the effects of using different temporal resolutions of observational data in particular using daily instead of annual statistics. The outcomes could contribute to the refinement of the calculation methods of exceedances proposed for legislations. Case studies use the annual mean, the 36th highest daily mean and the number of exceedance days derived from the PM_{10} monitoring data for the year 2003. Chapter 6 discusses the results, including its uncertainties.

Kalman Filter techniques were considered for explorative use in the data assimilations, but due to their complexity and capacity demands we decided not to include them in this project. It is however advised to follow their developments in the application in the field of air pollution and consider their usage at some time in the coming years.

Finally, we report on the quantification of uncertainties and errors in more detail. For this reason we focus additionally on the three following items:

1. Cross-validation of errors between parameters by using the root-mean square error (RMSE) and several other statistical indicators, which is discussed throughout the paper in the sections on the spatial interpolations;
2. Actual measurements compared to the interpolated and/or modelled values based on cross-validation, also to be found throughout the paper;
3. Spatial maps of the errors in the interpolation maps: maps with prediction standard error or standard deviations (SD). In Chapter 6 and 7 a first attempt is presented of producing such maps.

The current work focuses on the mapping of annual related limit or threshold values. The applicability of the methods for near-real time or even forecast reports of air quality is not the primary scope of this project, but might be a focus of future work. Nevertheless, we emphasise that there is a need to stay alert and to recognise synergies across the diversity of thee project types. We can image that at some point in the future interpolation techniques and methodologies of this project could become applicable in a way for EEA's near-real time projects. For example, applying methods from this project for spatial interpolation using meteorological forecasts and other supplementary data, for which in the future a correlation with air quality concentrations might be established, to derive spatially interpolated air quality indicator prediction maps for Europe. Therefore, we should try to build bridges across projects and aim for shared and robust methods.

Extensions for analysis of exposure and impacts

In relation to the extension to the other pollutants and their indicators, we updated the indicator maps for the year 2004. This concerns the human health status indicators annual average and 36th maximum daily averages for PM10, and for ozone the indicator SOMO35, and the vegetation related indicator AOT40 for vegetation/crops, with addition of the AOT40 or forests.

Additional to these updates, a preliminary human health impact assessment was performed. The approach follows as much as possible the algorithms of the relative risk functions on health impact due to air pollution as used in other (model based) assessment programmes and projects (CAFÉ). The assessment provides tables with the estimated population at risk per country and for Europe as a whole. Next to tables, the spatial distribution over Europe is presented in maps. Both tables and maps are intended to be included in future updates of the EEA Core Indicator on urban air quality (CSI004). For the vegetation-related indicators similar impact maps and tables were prepared expressing the areas of each land-cover type at risk, i.e. subject to damage, change or yield reduction.

With respect to reaching current and future health-related limit or target values, the paper presents indicator maps based on 2004 data for PM_{10} with the number of exceedance days, for ozone with the 26th highest 8-hour daily means. Vegetation-related indicator maps have been prepared for the SO_2 and NO_x limit values set for the protection of ecosystems and vegetation. They are both relevant within the context of CSI005 of EEA, which includes impact estimates and maps. The paper includes preliminary Europe-wide maps of ecosystems and agricultural land at risk.

Finally, options for interpolation and mapping of $PM_{2.5}$ are explored on special request of EEA. Both EEA and DG-ENV are highly interested in such information based on monitoring data next to results coming from model-based projects. However, in many countries the implementation of a $PM_{2.5}$ monitoring network is currently in progress: in 2004 only a limited number of $PM_{2.5}$ monitoring stations are reported to AirBase. In the course of time this problem is expected to be solved by itself, when the networks and country reporting come into full operation according to the intentions of the directives. Until then, interpolated maps produced on the basis of $PM_{2.5}$ measurements contain large uncertainties.

Road map to the report

The setup of this report is as follows:

- **Chapter 2** presents the basic mapping methods, which are used in this report.
- **Chapter 3** gives in introduction on the separate rural and urban mapping including the method applied for their merger.
- **Chapter 4** documents all input data as well as the process of their preparation for the use in the analysis and mapping.
- **Chapter 5** addresses the further development of the mapping methods, detailed uncertainty analysis of these methods based on cross-validation and the extension of the number of mapped pollutants. Rural mapping is dealt with in Sections 5.1 - 5.6, urban mapping is covered in Section 5.7 - 5.9. Both in the case of rural and urban maps, individual pollutants are dealt with in separate sections of Chapter 5. In the case of rural maps this is applied for all examined pollutants, in the case of urban maps only pollutants PM and ozone affecting human health is covered.
- **Chapter 6** presents the detailed analysis of the comparison of exceedances mapping based on daily and annual statistics, including a discussion on uncertainty.
- **Chapter 7** presents the detailed analysis of uncertainties on the indicators dealt with in Chapter 5 including uncertainty mapping.
- **Chapter 8** describes the resulting combined rural and urban European maps for the relevant air pollution indicators and also some human health and ecosystem based risk maps with their related tables with areas and population numbers at risk.
- **Chapter 9** concludes and recommends on follow-up to this study.
- **The Annex** presents the final set of maps and tables for the year 2004 that are described in the Chapter 8.

2 Interpolation methodologies and supplementary data selection

2.1 Introduction

Air pollution measurements from ground stations are the most accurate source of air quality information. As the number of measuring sites is limited, the information obtained from these measurements has to be generalized to improve the spatial coverage. There are various ways to arrive at spatial maps on the basis of the data from the monitoring stations. One of the simplest is the use of *linear regression models*, where the regression is made with relevant supplementary data from other sources. A second approach is through *spatial interpolation*. If spatial interpolation does not use any further information (except altitude in some cases) in addition to the measurements (so called primary data), we speak about *interpolation using primarily monitoring data only*. If we include more supplementary information in the interpolation, one would expect that the results would become more accurate. The linear regression approach is primarily interesting to identify the most promising supplementary data sources that can be used in a third approach, that being *linear regression models plus interpolation of their residuals* and which generally provides better results. In some cases however, the additional benefit of this approach may only be marginal as compared to linear regression without interpolation.

In summary, the types of methods are as follows:

1. Linear regression models without interpolation (Section 2.2)
2. Interpolation methods using primarily monitoring data (Section 2.3)
3. Linear regression models plus interpolation of their residuals (Section 2.4)

Different interpolation methods are applied only in the case of interpolation using primarily monitoring data only. These are Inverse Distance Weighting (IDW), ordinary kriging, ordinary cokriging, and lognormal cokriging.

In urban areas one additional spatial interpolation type is examined: the interpolation using the urban increments, the Delta, added to the interpolated rural background concentration field, as explained in Section 3.2. This approach can be considered as a fourth type of spatial interpolation.

One important source of supplementary (or secondary) data is formed by the results of chemistry transport and dispersion models. These have the advantage of full coverage of the whole territory, but are generally less reliable than the measured data. Secondary data also include other supplementary parameters which show statistical correlation with air pollution data and give spatially more resolved information on the whole territory than the pure air quality measurements, such as meteorological or topographical data, population density, or emissions.

The basic mapping methods used in this report are the methods presented in Denby et al. (2005), especially the methods developed and presented in Horálek et al. (2005). The detailed description of these methods is presented in the respective reports; a brief description is given in the following sections.

Linear regression models (type 1) can be used for combining the information from measurements with supplementary data. These are presented in Section 2.2. The methods of interpolation, using primarily the measurements only (type 2), are described in Section 2.3. The residuals resulting from the linear regression models can be further interpolated – the methods using the interpolation of residuals (type 3) are described in Section 2.4. The method for the selection of preferred parameters for several linear regression models is described in Section 2.5, as well as the way of comparing these models. The methodology for comparing different mapping methods and different parameters used in these methods is described in Section 2.6.

Figure 2.1 presents a flow chart with a schematic impression on how air quality indicator concentration and exceedance maps and their exposure estimates are derived, using monitoring data, supplementary data, linear regressions and /or interpolation techniques.

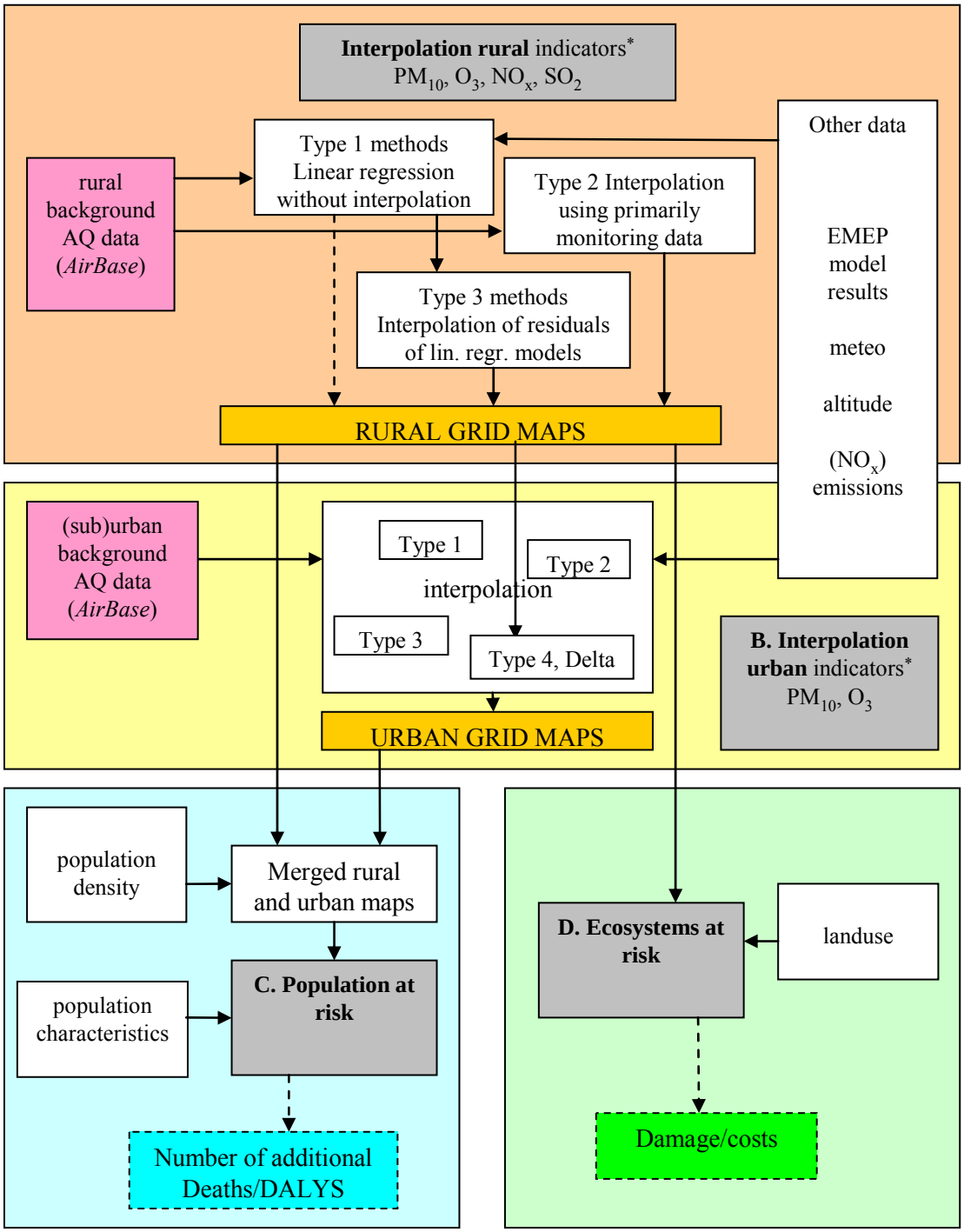

* indicators: concentrations, but also derived statistics such as exposure indicators SOMO35, AOT40 and Number Of Exceedances.

Figure 2.1 Flow chart providing a schematic impression on how air quality indicator concentration and exceedance maps and their exposure estimates are derived, using monitoring data, supplementary data, linear regressions and /or interpolation techniques.

2.2 Linear regression models without interpolation

In these methods, apart from the monitoring data, different secondary data sources that cover the mapping area are used. As in Horálek et al. (2005), the basic linear regression model equation considered is:

$$Z(s) = c + a_1*X_1(s) + a_2*X_2(s) + \ldots + \varepsilon(s) \quad (2.1)$$

where $Z(s)$ are (measured) air quality concentrations at the point s

$X_i(s)$ are different supplementary parameters at the point s, for i = 1, 2, …

$c, a_1, a_2, \ldots$ are the parameters of the linear regression model

$\varepsilon(s)$ is the residual of the linear regression model at the point s.

For details, see Horálek et al. (2005), Section 4.1.

Alternatively, linear regression models can be defined after the logarithmic transformation of the observed variables, according the equation:

$$\ln(Z(s)) = c + a_1*X_1(s) + a_2*Y_2(s) + \ldots + \varepsilon(s) \quad (2.2)$$

2.3 Interpolation methods using primarily measurements

Interpolation methods can be divided into deterministic methods and geostatistical methods. Deterministic methods include e.g. IDW methods or radial basis functions (RBF); Geostatistical methods utilize knowledge of the spatial structure of air quality field (variogram) and include various types of kriging. All these methods use the information at the points of the measuring stations only.

In the formulas presented in the following sections the following notation is applied:

$\hat{Z}(s_0)$ is the interpolated value of the air pollutant concentration at the point s_0,

$Z(s_i)$ is the measured value of the concentration at the i-th point, with $i=1,\ldots, n$.

n is the number of surrounding stations from which the interpolation is computed.

2.3.1 Inverse distance weighted interpolation (IDW)

Interpolation is carried out according to the relation

$$\hat{Z}(s_0) = \frac{\sum_{i=1}^{n} \frac{Z(s_i)}{d_{0i}^{\beta}}}{\sum_{i=1}^{n} \frac{1}{d_{0i}^{\beta}}} \quad (2.3)$$

where d_{0i} is the distance between the interpolated point and the i-th station,

β is the weighting power.

2.3.2 Ordinary kriging (OK)

A detailed description of geostatistical methods is given in Cressie (1993). Variograms are used to describe and quantify geostatistical structures. Section 2.3.5 briefly explains the principle and provides definitions of the variogram and its parameters, including the parameter settings used in this project.

Ordinary kriging is the most often used geostatistical method. It considers the basic statistical model

$$Z(s) = \mu + \eta(s) + \varepsilon(s) \quad (2.4)$$

where μ represents the constant mean structure of the air quality field,

$\eta(s)$ is the (zero-mean) (*) stochastic part; its statistical structure is described by a variogram,

$\varepsilon(s)$ is the measurement error or noise (zero-mean).

(*) zero-mean is sliding all data in a profile such that their average is zero.

Interpolation is carried out according to the relation

$$\hat{Z}(s_0) = \sum_{i=1}^{n} \lambda_i Z(s_i), \quad \sum_{i=1}^{n} \lambda_i = 1 \tag{2.5}$$

where $\lambda_1, \ldots, \lambda_n$ are the weights assumed on the basis of a variogram (Section 2.3.5) in order to minimize the mean-square-error.

2.3.3 Ordinary cokriging (OC)

Ordinary cokriging uses, in addition to primary measured data, also supplementary quantities, for example altitude and temperature. The values of these quantities are considered only at the measuring sites (contrary to the methods presented in Section 2.2 where the complete parameter field is considered).

Interpolation is carried out according to the relation

$$\hat{Z}(s_0) = \sum_{i=1}^{n} \lambda_i Z(s_i) + \sum_{j=1}^{m} \sum_{i=1}^{n} \eta_{ij} Y_j(s_i) \tag{2.6}$$

where λ_i and η_{ij} are the weights assumed on the basis of a variogram and crossvariograms,

$Y_j(s_i)$ are the values of supplementary quantities ($j=1, \ldots, m$) in the i-th point, with $i=1, \ldots, n$.

2.3.4 Lognormal kriging (LK) and lognormal cokriging (LC)

Lognormal kriging and cokriging can be used in case the considered quantity (e.g. measured concentrations) has a lognormal distribution (i.e. if the values gained by logarithmic transformations show a Gauss normal distribution).

This is similar to ordinary kriging and cokriging performed after logarithmic transformation. The interpolated field is back-transformed by exponentiation $exp(Z+\sigma^2/2)$, where Z is the interpolated field and σ^2 is the kriging error (Cressie, 1993).

2.3.5 Variogram

The variogram $2\gamma(h)$, or semivariogram $\gamma(h)$, is a measure of spatial correlation, i.e. of the relation between pairs of measuring stations s_1 and s_2, under the condition

$$2\gamma(h) = 2\gamma(s_1 - s_2) = \mathrm{var}((Z(s_1) - Z(s_2)), \quad \text{for all } s_1, s_2, \tag{2.7}$$

where *var* is the variance and h is two-dimensional distance (which can be expressed by distance and direction). If the variogram is the same for all directions, i.e. $2\gamma(h) = 2\gamma(|h|)$, then it is called *isotropic*.

The empirical variogram $2\gamma_e$ is calculated by the equation:

$$2\gamma_e(\mathrm{h}) = \frac{1}{n} \sum_{i=1}^{n} \{Z(\mathrm{s}_i) - Z(\mathrm{s}_i + \mathrm{h})\}^2, \tag{2.8}$$

where $Z(s_i)$ and $Z(s_i + h)$ are the measurements in the points $\mathbf{s}_i$ and $s_i + h$,

n is the number of distinct pairs of points, the distance h of which is in interval

$(h_{i-1}-\delta, h_i+\delta)$, so-called *lag size*, where (h_{i-1}, h_i) is the distance of i-th lag and δ is the lag tolerance.

In empirical variogram calculation, several classes of (two-dimensional) distances are considered, so-called *lags*, see Figure 2.2. The number of lags is one of the parameters of empirical variogram.

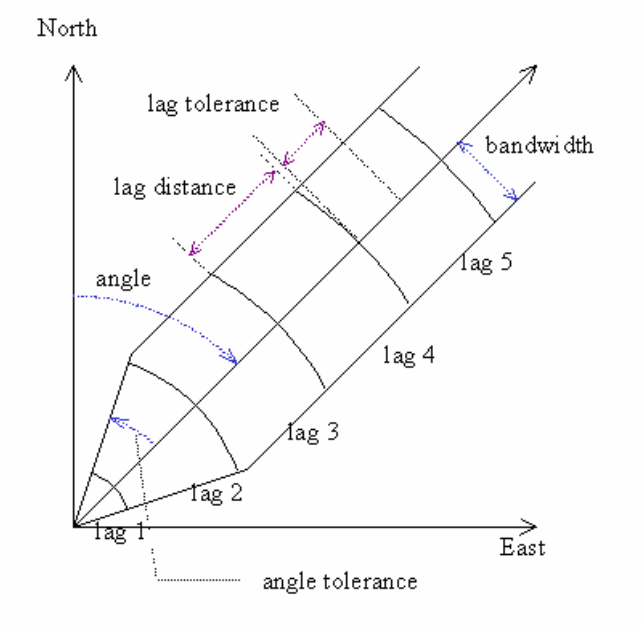

Figure 2.2 Graph showing the separation of distances between the pairs of stations into lags.

For use in kriging, the empirical variogram needs to be fitted (or estimated) by an analytical function - e.g. *spherical*, *exponential*, *Gaussian*. In Figure 2.3 an example of a spherical function can is presented.

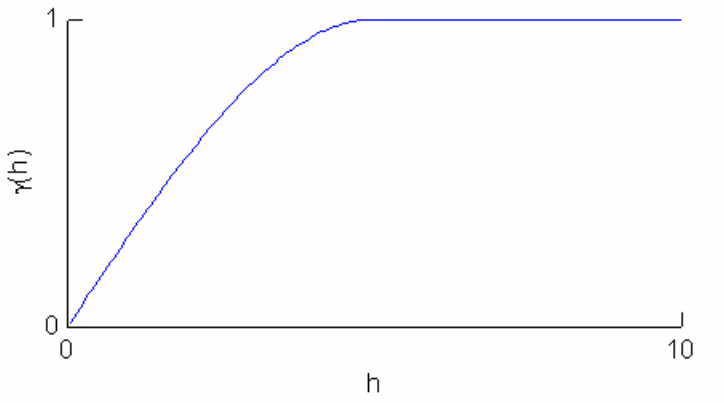

Figure 2.3 Graph showing the spherical curve.

The basic parameters of the variogram are called nugget, sill and range, see Figure 2.4.

Sill is the value at which the spatial variability doesn't change with distance (plateau); *range* is the distance at which the spatial variability doesn't change. The range gives information about the size of the search window as it is not interesting to account for those points where spatial variance is not related to distance. If the range is large, the long-range variation dominates; if small then the short distances dominate the variation. *Nugget* is the y-intercept, which represents the spatial uncorrelated noise and errors, since at zero distance we would expect no variability. The difference *sill-nugget* is sometimes called *partial sill*.

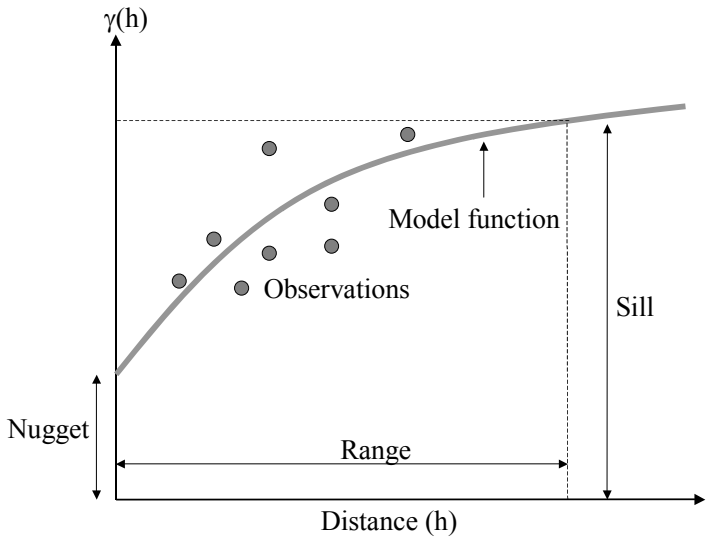

Figure 2.4 Diagram showing the important parameters that describe the variogram, 2γ(h), used in kriging

In this report, only isotropic variograms are used. Empirical variograms are fitted by the spherical function (being generally the most commonly used).

Two methods for estimating the variogram parameters of range, nugget and sill are used throughout the study: These are

1. Automatic fitting of the variogram function by GIS software, with the chosen parameters: number of lags = 12 and the lag size = 50 km
2. Manual minimization of the RMSE in the cross-validation.

2.4 Linear regression models plus interpolation of their residuals

This method combines the linear regression models of Section 2.2 and the interpolation methods of Section 2.3. The following statistical model is considered:

$$Z(s) = \mu(s) + \eta(s) + \varepsilon(s) \qquad (2.9)$$

where $\mu(s)$ represents the fixed part (which models mean concentration using regression models),

$\eta(s)$ is the (zero-mean) stochastic part; its statistical structure is described by a variogram,

$\varepsilon(s)$ is the measurement error or noise (zero-mean).

The method used is the spatial interpolation of the residuals of a linear regression model. Here interpolation is carried out according to the relation:

$$\hat{Z}(s_0) = c + a_1.X_1(s_0) + a_2.X_2(s_0) + ... + \eta(s_0) \qquad (2.10)$$

where $\hat{Z}(s_0)$ is the estimated value of the air pollution parameter at the point s_o

$X_1(s_0)$, $X_2(s_0)$, … are the individual supplementary quantities at the point s_o

c, a_1, a_2, are the parameters of the linear regression model calculated at the points of measurement,

$\eta(s)$ is the spatial interpolation of the residuals of the linear regression model at the points of measurement.

Different linear regression models use different supplementary data, for example, besides output from a dispersion model they can include altitude or various meteorological parameters. The dispersion model can be used alone or in combination with other parameters.

The spatial interpolation of residuals is carried out using interpolation methods, described in Section 2.3, with the exception of lognormal kriging and lognormal cokriging because residuals have no lognormal distribution.

2.5 Use of various supplementary data sources

Different sources of supplementary data in linear regression models (as described in Section 2.2 and 2.5) are used and their usage is mutually compared. Three basic varieties of the linear regression model equation 2.1 are used:

1. Regression models using the Unified EMEP model
2. Regression models using the Unified EMEP model + supplementary sources (e.g. altitude, meteorological parameters)
3. Regression models using supplementary sources only (e.g. altitude, meteorological parameters)

The basic reason for examining these three varieties is to verify the assumption that by using output from a chemistry transport model together with other supplementary data more accurate estimates can be obtained than by the use of output from a chemistry transport model alone or by the use of other supplementary data only.

Within the varieties 1 and 3 several submodels can be constructed and examined. For preferred submodel selection, different approaches can be used. Firstly, it is necessary to choose supplementary data that really brings some additional information. Submodel selection is also a compromise between bias and variance: by decreasing the number of parameters, the predictive capability can improve (i.e. the variance decreases), while the bias increases. So we need to arrive at an optimal selection of parameters meeting sufficient accuracy of interpolation results as well as sufficient suppression of uncertainties.

The most often used approaches for submodel selection are forward selection, backward elimination, stepwise regression (forward or backward type) and all subsets. Forward selection begins with the "best" predictor and adds the next "best" to improve the fit. Backward selection begins with all variables and removes the least useful as long as the fit is not substantially "worsened". Stepwise regression allows "good" predictors to re-enter at any step into the model. All improvements should lie within defined statistical criteria.

In the APMoSPHERE project, for example, the so-called approach of "supervised forward stepwise procedure" is used to construct regression models. Only variables that (i) increased the adjusted R^2 by more than 1%, and (ii) had coefficients that conformed to the pre-specified directions (Briggs et al., 2005) were included.

In this study backward elimination is used and confirmed by automatic stepwise regression. For possible further elimination and for comparison purposes, several other submodels are also analysed. The list of examined submodels is stated separately for each component. Individual submodels are mutually compared by evaluating the coefficient of determination R^2, adjusted R^2 and the root-mean square error RMSE:

$$R^2 = \frac{\left(\sum_{i=1}^{n}\left(Z(s_i)-\overline{Z}\right)\left(\hat{Z}(s_i)-\overline{\hat{Z}}\right)\right)^2}{\sum_{i=1}^{n}\left(Z(s_i)-\overline{Z}\right)^2 . \sum_{i=1}^{n}\left(\hat{Z}(s_i)-\overline{\hat{Z}}\right)^2} = 1 - \frac{\sum_{i=1}^{n}\left(Z(s_i)-\hat{Z}(s_i)\right)^2}{\sum_{i=1}^{n}\left(Z(s_i)-\overline{Z}\right)^2} \quad , \tag{2.11}$$

where $Z(s_i)$ is the measured concentration at the i-th point, $i = 1, ..., N$,

$\hat{Z}(s_i)$ is the estimated concentration at the *i*-th point using other points,

$\overline{Z}$ is the arithmetic average of $Z(s_1), \ldots, Z(s_N)$,

$\overline{\hat{Z}}$ is the arithmetic average of $\hat{Z}(s_1),\ldots,\hat{Z}(s_N)$.

$$adjusted\_R^2 = R^2 - \frac{p-1}{(N-p)}.(1-R^2) \tag{2.12}$$

where N is the number of the measuring points,

p is the number of parameters (i.e. $c, a_1, a_2, \ldots$) of the lin. regr. model (2.1),

$$RMSE = \sqrt{\frac{1}{N}\sum_{i=1}^{N}(Z(s_i)-\hat{Z}(s_i))^2} \tag{2.13}$$

Coefficients R^2 and adjusted R^2 are reported together in the whole report (where R^2 is mentioned in the text, both coefficient R^2 and adjusted R^2 are implied). However, for supplementary data selection adjusted R^2 is preferred.

As was concluded and recommended in Horálek et al. (2005) it is further investigated as to what extent an improvement can be obtained when using logarithmically transformed air quality parameter values in the linear regression models.

2.6 Criteria for comparing spatial interpolations

Several interpolation methods are applied and mutually compared. The main criterion for comparison analysed in this paper is RMSE from cross-validation, followed by other statistical indicators from cross-validation. The cross-validation method computes the spatial interpolation for each measurement point using all the available information except from that one point (i.e. it withholds one data point and then makes a prediction at the spatial location of that point). The predicted and measured values are then compared and the procedure is repeated for all points. This way the performance of the various interpolation methods at areas without measurements can be evaluated. (Cross-validation simulates and examines the behaviour of the interpolation in the places with no measurement.)

For each examined method several statistical indicators are presented. The particular indicators used in cross-validation are the following:

root mean squared error (RMSE), according to the equation (2.13)

mean prediction error (MPE), $$MPE = \frac{1}{N}\sum_{i=1}^{N}(Z(s_i)-\hat{Z}(s_i)) \tag{2.14}$$

which is the same as the average bias.

mean absolute error (MAE) $$MAE = \frac{1}{N}\sum_{i=1}^{N}\left|Z(s_i)-\hat{Z}(s_i)\right| \tag{2.15}$$

standard deviation of error $$sd = \sqrt{\frac{1}{N}\sum_{i=1}^{N}\left(\left(Z(s_i)-\hat{Z}(s_i)\right)-\frac{1}{N}\sum_{i=1}^{N}\left(Z(s_i)-\hat{Z}(s_i)\right)\right)^2} \tag{2.16}$$

minimum error, i.e. $\min\left\{Z(s_i)-\hat{Z}(s_i); i=1\ldots N\right\}$

maximum error, i.e. $\max\left\{Z(s_i)-\hat{Z}(s_i); i=1\ldots N\right\}$

median of absolute error (MedAE), i.e. $median\left\{\left|Z(s_i)-\hat{Z}(s_i)\right|; i=1\ldots N\right\}$

coefficient of determination R^2 of cross-validation scatterplot, according to the equation (2.11)

mean prediction standard error (MPSE) which is the arithmetic average of the kriging standard errors.

In the case of the methods described in Section 2.4 the cross-validation analysis is carried out only for residuals (not for the whole approach), because of calculation reasons. We suppose the difference would not be large (as the number of stations is large). For these methods R^2 is not computed, because the results would not be comparable with other methods. (Another possibility would be to calculate R^2 after adding the residuals to the linear regression results. This is a potential issue for the future.)

For interpolation methods using primarily monitoring data, the scatter plots are presented in Chapter 5 showing the interpolation estimates on the basis of cross-validation versus the measured values. In the case of an ideal linear correlation between the interpolation estimates and the measurements, the regression line fitted by the values of the scatter plot would be $y = a \cdot x$ with $a=1$, and with a *coefficient of determination* $R^2=1$. *RMSE* and *MAE* should be as small as possible, and *MPE* as close to zero as possible. The *standard deviation of error* and the *median of absolute error* should be as small as possible. Both *minimum error* and *maximum error* values should be as close to zero as possible.

The results of the cross-validation analysis are presented in Chapter 5 for each pollutant indicator, separately for the rural and urban areas. For the pollutant indicator the interpolation methods using primarily measurements are presented first, followed by the methods on interpolation of the residuals of the different linear regression models. For the geostatistical methods the two methods for variogram fitting, Section 2.3.5, are applied.

2.7 Criteria for the selection of an interpolation method

While for this report we have selected the RMSE as the main criterion for comparing interpolation results, it is important to note that the final selection of the best interpolation method depends also on application requirements of the assessment (e.g. EEA assessments and fact sheets) and therefore may relate to other (pragmatic) criteria as well. Such criteria include:

a. *Spatial coverage quality and extend*. Some data sources may lead to better results of RMSE, but may have poorer spatial coverage. Some data sources may provide larger European coverage.

b. *Observations versus model results*. It may be attractive to base the maps exclusively on observations, even if this may lead to lower spatial coverage.

c. *Continuity and robustness from year to year*. The eventual availability of time series is interesting for assessments. Even if for a more recent year the optimal method, in terms of RMSE, is a method different from previous the same method as in previous years may be preferred. This is especially true for those cases in which the differences are relatively small. In case the differences are large, it may be considered to recalculate previous years with the new method.

d. *Resource intensity, physical basis for the supplementary data inclusion and the technical platform*. The more (complex) supplementary data used, the more time, resources and sometimes more advanced computer facilities and capacity are needed. Choosing a second best option in terms of RMSE may therefore be sometimes preferred to keep demands within limits.

e. *Availability and reliability of the data*. The analysis becomes dependent on the date and resolution that these data become available and will be updated or refreshed. Choosing a second best option, for example in terms of timeliness or reliable cyclic updating, therefore be sometimes preferred.

f. *Methodologically consistency to meet homogeneity between pollutants and indicators*. This criterion is especially of interest in the case of different indicators of one pollutant type, such as AOT40 for crops and AOT40 for forests where it useful to select the same method for consistency and compatibility between the two AOT40 indicators. This is especially relevant when the different methods show small differences in terms of RMSE, since the interpolation result will likely differ little using one or the other method.

g. *Agreement of the quality of the interpolated values versus the measured values at monitoring sites.* Many interpolation methods do not preserve the measured value when the interpolation is made at, or very close to, the measurement point. Such methods are generally better in terms of RMSE from cross-validation. However, for some purposes it may be desirable to produce maps where the interpolation has an exact correspondence at the measurement sites.

Because different people will weigh these criteria differently, this paper does not make definite recommendations for the selection of best methods. Rather, the results are meant to provide input into a broader discussion on mapping of air quality.

In this context it is also important to put the results in perspective. The uncertainties addressed in this paper are limited to the uncertainties caused by the process of interpolation between data from monitoring stations. Uncertainties in the supplementary data sources are not specifically addressed, nor are uncertainties related to the measurements instruments and procedures. These uncertainties may be larger than the uncertainties addressed in this paper.

3 Methods for the mapping of urban and rural areas

One of the conclusions presented in Horálek et al. (2005) is that it is better to create air pollution maps separately for rural and urban areas. The reason lies in the different character of urban and rural air pollution. The final maps are constructed by merging the rural and urban maps together.

3.1 Maps for rural areas

For the creation of maps for rural areas the basic methods described in Chapter 2 are used and mutually compared. The methods are applied on rural background stations only (according to the AirBase classification).

3.2 Maps for urban areas

Two different approaches are considered in the creation of interpolated maps of urban areas:

i) The first is the interpolation of the values measured at the urban and suburban background stations with the use of methods described in Chapter 2.

ii) The second approach is the interpolation of the urban increment. This urban incremental concentration, the so called *Delta,* is the difference between the urban background station measurement and the interpolated rural background concentration field at the station coordinate. The Deltas are interpolated by ordinary kriging or IDW and the interpolated Delta concentration field is subsequently added to the interpolated rural background concentration field. The resulting European wide concentrations are now supposed to represent the urban backgound concentration field. This approach was explored earlier in Horálek et al. (2005). The advantage of this approach is its simplicity: the already interpolated result of the rural background concentration field is used again for the urban spatial interpolation. It is assumed that the interpolation improvements reached by using the supplementary parameters at the rural concentration fields propagate into the (sub)urban area interpolation results to a similar extend. The urban increment is calculated according to:

$$\Delta(s_i) = Z_{urb}(s_i) - \hat{Z}_{rur}(s_i) \tag{3.1}$$

where $Z_{urb}(s_i)$ is the measured value at the point s_i, being an (sub)urban background station,

$\hat{Z}_{rur}(s_i)$ is the estimated value of the rural background field at the point s_i,

$\Delta(s_i)$ is urban increment Delta at the point s_i.

The final urban map is given by

$$\hat{Z}_{urb}(s_i) = \hat{Z}_{rur}(s_i) + \hat{\Delta}(s_i) \tag{3.2}$$

Interpolation of $\Delta(s_i)$ is carried out using the methods described in Chapter 2. The methods are applied on urban and suburban background stations only.

3.3 Merging of rural and urban maps

The European-wide population density grid is used for merging the rural and urban maps into one combined air quality indicator map. Both the rural map and the urban map are created for the whole of Europe. The population density grid helps to determine for which part of the area the respective map is used.

For areas with population density less than the defined value of α_1, the rural map is applied, and for areas with population density grids greater than the defined value α_2, the urban map is applied. For areas with population density within the interval (α_1, α_2) the following relation is applied

$$\hat{Z}(s) = \frac{\alpha_2 - \alpha(s)}{\alpha_2 - \alpha_1}.R(s) + \frac{\alpha(s) - \alpha_1}{\alpha_2 - \alpha_1}.U(s) \qquad (3.3)$$

where $\hat{Z}(s)$ is the resulting value of concentration at the point *s*,

R(s) is the concentration at the point *s* for the rural map,

U(s) is the concentration at the point *s* for the urban map,

α(s) is the density of population at the point *s*.

4 Input data

4.1 Introduction

The input data used depends on the mapping methodology applied. The minimum input data necessary for interpolation are the measured air pollution concentrations with the respective geographical coordinates of the stations at which they were measured. The station altitude is also considered in this study. The advanced mapping methods use supplementary parameters, such as output from the Unified EMEP model, altitude data covering the whole study area, meteorological parameters, climatological parameters, emissions, land cover and population density. The resolution of such input data should be better than or comparable to the resolution of the maps constructed, which is 10 x 10 km.

In most cases the input data were supplied as raw data – in various formats and time intervals. It was necessary to modify them before further processing.

4.2 Measured air quality data

The air quality data were extracted from the European monitoring database *AirBase*, supplemented by several rural EMEP stations which are not reported to AirBase. Only data for *rural*, *suburban* and *urban* stations, classified in by AirBase and EMEP as the type *background* were used. *Industrial* and *traffic* station types are not considered, since they represent local scale concentration levels that not applicable at the mapping resolution employed. The following components were considered:

PM_{10} – daily average values [$\mu g.m^{-3}$], year 2003
– annual average [$\mu g.m^{-3}$], years 2003 and 2004
– 36th maximum daily average value [$\mu g.m^{-3}$], years 2003 and 2004

$PM_{2.5}$ – annual average [$\mu g.m^{-3}$], years 2003 and 2004

Ozone – SOMO35 [$\mu g.m^{-3}$.day], years 2003 and 2004
– 26th highest daily maximum 8-hour average value [$\mu g.m^{-3}$], year 2004
– AOT40 for crops [$\mu g.m^{-3}$.hour], year 2004
– AOT40 for forests [$\mu g.m^{-3}$.hour], year 2004

SO_2 – annual average [$\mu g.m^{-3}$], year 2004

NO_x – annual average [$\mu g.m^{-3}$], year 2004

NO_2 – annual average [$\mu g.m^{-3}$], year 2004 (NO_x mapping only)

NO – annual average [$\mu g.m^{-3}$], year 2004 (NO_x mapping only)

SOMO35 is the annual sum of maximum daily 8-hour concentrations above 35 ppb (i.e. 70 $\mu g.m^{-3}$). AOT40 is the sum of the differences between hourly concentrations greater than 40 ppb (i.e. 80 $\mu g.m^{-3}$) and 40 ppb, using only values measured between 7:00 and 19:00 UTC, calculated over the three months from May to July (AOT40 for crops), respectively over the six months from April to September (AOT40 for forests).

In case of components affecting human health data from *rural*, *urban* and *suburban* background stations were considered. This applies to the components PM_{10}, $PM_{2.5}$ and to the ozone parameters SOMO35 and 26th highest daily maximum 8-hour average value. In case of components affecting vegetation (SO_2, NO_x and both AOT40 parameters for ozone) only *rural* background stations were considered.

In the case of annual indicators only the stations that have temporal data coverage of at least 75 percent are used. For PM_{10} 176 rural background stations and 656 urban/suburban background stations are used. For $PM_{2.5}$ 14 rural background stations and 68 urban/suburban background stations are used. For ozone 418 rural background stations and 731 urban/suburban background stations are used. For NO_x 82 rural background stations with reported NO_X data are used, supplemented by other 189 rural

background stations with reported both NO_2 and NO data and also with other 23 rural background stations with reported NO_2 data only (from which NO_x is calculated and estimated, see Section 5.4). For SO_2 253 rural background stations are used. The air quality data have been extracted from AirBase, with addition of a few rural EMEP stations (these are 4 PM_{10} stations, helpful for spatial coverage).

The measured air pollution concentration data were obtained from the AirBase database as Excel tables. Since most geostatistical calculations are done in ArcGIS they were converted to ArcGIS format. Data from the stations that measured less than 75 % of the year were deleted. Furthermore, coordinates were checked. At 7 stations incorrect coordinates were detected; 3 stations were deleted from further processing and the coordinates of 4 stations were corrected (latitude and longitude were mutually exchanged). Additionally, two ozone stations (GR0110R, MK0042A) with highly questionable data were excluded from the analysis. The purified files were converted into *dbf* format and imported into ArcGIS on the basis of their geographic coordinates at the sites of the measuring stations. Finally, ArcGIS shape files were created and were consequently transformed from the geographical system WGS1984 (corresponding to geographic coordinates) into geographic projection system ETRS89-LAEA5210, which is the most commonly used EEA standard map projection. All maps presented in this paper comply with this projection with the map EEA predefined extent 1c (www.eionet.europa.eu/gis).

4.3 Altitude

In addition to the altitude presented with the measurement data in the AirBase (or EMEP) database a European covering gridded altitude dataset is used, namely GTOPO30 (Global Digital Elevation Model) at a resolution of 30 x 30 arcsec. (source: ESRI, Redlands, California, USA, 2005). The original format was the ArcGIS shapefile in the WGS1984 coordinate system. It was necessary to convert this grid to the geographic projection system ETRS89-LAEA5210 to enable further processing. This conversion was carried out with the use of ArcGIS to the resulting grid of 200x200 meters. The altitude is always given in meters.

4.4 Output from the Unified EMEP model

The chemistry transport model used is the photochemical version of the Unified EMEP model (revision rv2_5_beta2), which is a Eulerian model with a resolution of 50 x 50 km. Output from this model is used for a subset of the measured parameters listed in Section 4.2:

PM_{10} – daily average values [$\mu g.m^{-3}$], year 2003,
– annual average [$\mu g.m^{-3}$], years 2003 and 2004,
– 36^{th} maximum daily average value [$\mu g.m^{-3}$], years 2003 and 2004,

$PM_{2.5}$ – annual average [$\mu g.m^{-3}$], year 2004,

Ozone – SOMO35 [$\mu g.m^{-3}$.day], year 2004,
– AOT40 for crops [$\mu g.m^{-3}$.hour], year 2004,
– AOT40 for forests [$\mu g.m^{-3}$.hour], year 2004,

SO_2 – annual average [$\mu g.m^{-3}$], year 2004,

NO_x – annual average [$\mu g.m^{-3}$], year 2004.

The model is described by Simpson et al. (2003) and Fagerli et al. (2004). The model results are based on different emissions for each year (i.e. 2006-Trend2003-V7 and 2006-Trend2004-V7, as documented in Appendices A of EMEP Status Reports 1/2006 and 4/2006, see Tarassón et al., 2006 and Yttri et al., 2006) and actual meteorological data (from PARLAM-PS, i.e. special dedicated 2000 version of HIRLAM numerical weather prediction model, with parallel architecture, see Sandnes Lenschow and Tsyro, 2000).

In the original *netCDF* format each grid cell was represented by a point at its centre. Each such netCDF file was converted into *dbf* format and imported into *ArcGIS* as the point shapefile by its geographic coordinates of the centre of the grid cells. The ultimate grid (at resolution 10 x 10 km) was

created from this layer using IDW interpolation with the number of neighbouring points *n=4* and the weight $\beta=10$, see Section 2.3.1. This setting of parameters ensures that the created interpolation is almost identical to the original EMEP grid.

4.5 Meteorological parameters

Actual meteorological surface layer parameter data for the years 2003 and 2004 are extracted from the Meteorological Archival and Retrieval System (MARS) of the ECMWF (European Centre for Medium-range Weather Forecasts; http://www.ecmwf.int). MARS is the main repository of meteorological data at ECMWF from which registered users can freely extract archived data. It contains terabytes of a wide diversity of operational and research meteorological data as well as data from special projects. The datasets from which we extracted parameter data needed to provide a complete data coverage for the continuous period of at least 2000-2004 but preferably 1990-to date and for the complete area of study. At a later stage it allows for carrying out trend analyses on European-wide air quality indicators using any data of AirBase combined with a consistent set of concurrent meteorological parameter data with a comparable temporal resolution.

Specifications of the data, including its exact MARS parameter code references, ultimately extracted are:

Spatial grid resolution: 0.25 x 0.25 degrees latitude/longitude, i.e. 15 x 15 minutes.
Geographic window: Lower left corner 34 x -42 dgrs lat/long, Upper right corner 72 x 59.5 dgrs lat/long, i.e. covering the European-wide study area.
Years: 2003 - 2004

Data format: GRIB

From dataset: Operational Surface Analysis Data Sets ('oper')
Time resolution: Daily 6-hour averages (00:00, 06:00, 12:00, 18:00)

Parameters: Name	Remark	Abbrev.	Units	Code (Table 128)
10 meter wind U	(W→ E)	10U	$m.s^{-1}$	165
10m wind V	(N → S)	10V	$m.s^{-1}$	166
2 meter temperature		2T	K	167
2m dew point temperature		2D	K	168

From dataset: Tropical Ocean and Global Atmosphere ('toga')
Time resolution: Daily 12:00 average, derived from 24-hour forecast values, with values accumulated between time step 12 and time step 36 of the forecast

Parameters: Name	Abbrev.	Units	Code (Table 128)
Total precipitation	TS	$m.day^{-1}$	228
Surface solar radiation	SSR	$Ws.m^{-2}$	176

Wind speed as used in the calculations, is derived from the 10 meter height wind speed in U (*10U*) and V (*10V*) direction with magnitude $\sqrt{(10U)^2 + (10V)^2}$.

Temperature units were converted to [°C] using the relation T [°C] = T [K] + 273.15

Surface solar radiation units were converted from [$W.s.m^{-2}$] to [$MW.s.m^{-2}$], by dividing by 10^6.

Relative humidity (%) is derived by means of the saturated water vapour pressure (e_t) as a function of the temperature and of the dew point temperature at 2 meter height, according

$RH = \frac{e_{2D}}{e_{2T}} \cdot 100$, with $e_t = 6.1365^{(17.502 \cdot t/(240.97+t))}$ where t is 2T and 2D respectively [°C].

It should be noted that the 0.25 degrees spatial grid resolution is just above the current highest possible MARS grid resolution of 0.225 degrees (13.5 minutes) for extracting data through interpolation. Its cause lies in a typographic error in the extraction script discovered after finalisation of the extractions. It was decided not to repeat the extractions, since the resolution loss is acceptably small and the extraction is quite time and resource consuming.

The meteorological gridded data for the years 2003 and 2004 was transformed into ESRI GRID format. The averaging of both the original 6-hour and the daily meteorological parameter values into annual averages on the given grid resolution needed to be executed in two steps as a way to cope with the limited calculation capacity of the relevant ArcGIS procedure. As a first step the 6-hour values were averaged into half-month values and the daily values into two-month averages. As second step the annual averages were derived from these intermediate average values.

4.6 Climatological parameters

The input data also includes the 10 x 10 minute grid of climatological averages for the 30-years period 1961–1990 (source: CRU CL 2.0, www.cru.uea.ac.uk/cru/data/; New et al., 2002). The individual parameters are as follows:

- Temperature [K] – units subsequently converted to [°C]
- Precipitation [mm.year-1]
- Sunshine duration [%]
- Wind speed [m.s-1]
- Relative humidity [%]

In the original format the data are given in *txt* files where each grid cell is represented by the point at its left bottom corner. Each such *txt* file was transformed into *dbf* format and imported into *ArcGIS* as the point shapefile by its geographic coordinates recalculated into the centre of the grid cell. The ultimate grid (in resolution 2 x 2 km) corresponding to the original grid was created from this layer using IDW interpolation with a number of neighbouring points $n=4$ and a weight $\beta=10$.

4.7 Emissions

Emissions are used for NO_x only. Here the input data are given as NO_x emissions [$\mu g.m^{-2}.day^{-1}$] on a grid of 1 x 1 km in ArcGIS raster format, covering the western part of Europe (EU-15, Switzerland and Norway). These data are the output of the APMoSHERE project (Briggs et al., 2005) and the project concluded that NO_x emissions validated well against the AirBase data. No other emission data are used due to the incomplete reporting by some countries. The intention behind the use of the emission data is to include emission information at a higher resolution than the EMEP model can currently provide.

4.8 Land cover

The input data from CORINE Land Cover 2000 (CLC2000) – grid 250 x 250 m, version 8/2005 version 2, (Source and owner: EEA, lceugr250_00) is used. The countries missing in this database are Island, Norway, Switzerland, Serbia, Montenegro and Turkey.

In an effort to reduce the time demanding calculations on large data quantity involved with the 250 x 250 m grid resolution an aggregation to a 500 x 500 m grid resolution is performed first, before the exceedance mapping and table extraction takes place. The ultimate map and table results are not influenced by this resolution aggregation.

4.9 Population density

Population density [inhbs.km^{-2}] is given at a resolution of 100 x 100 m (Source EEA, pop01c00v3int, official version Aug. 2006; Owner: JRC). These data are based on the degree of urbanisation from Eurostat and the population census of the European communes 2001, mapped on the basis of CLC2000 land cover.

The current version of the population density database does not include the European countries Andorra, Albania, Bosnia-Herzegovina, Cyprus, Island, Lichtenstein, FYR of Macedonia, Norway, Serbia and Montenegro, Switzerland, and Turkey. An important objective of this project is to deliver European wide interpolated maps covering at least all EEA member and collaborating countries. Furthermore, spatial interpolations will perform better when gaps in the mapping area are avoided. To overcome the gaps the missing countries in the JRC population density database are filled with population density data from an alternative source, the ORNL LandScan (2002) Global Population Dataset. Its original resolution of 30 arc seconds was resampled to a 100 m grid resolution before merging it with the JRC database. To avoid possible non-continuous coverage at the borders between the JRC and ORNL databases the area of countries using the ORNL database in was enlarged with a 5 km buffer at the borders.

To enable further processing a two-step spatial data aggregation was carried out in ArcGIS. The first step resulted in the creation of a 1 x 1 km grid by coarse graining of the original 100 x 100 m grid. This aggregation is done to stay below the critical hardware limitations on the calculations capacity of current computer technology. In the second step each cell of the 1 x 1 km grid is given the average value of the surrounding 10 x 10 km square. This results in a grid at 1 x 1 km where each grid cell represents the average population density of the surrounding 10 x 10 km. This is done in order to be consistent with the grid resolution 10 x 10 in the final mapping.

5 Analysis of mapping methodologies

5.1 Rural mapping

The development of methods for mapping air quality in rural areas concerns mainly those using both the primary data (measured air pollution concentrations, or their parameters) and the secondary (supplementary) data, i.e. the methods described in Section 2.4. As compared with the approach used in Horálek et al. (2005), meteorological parameters (characteristic for the year 2004) are used as secondary data, instead of climatological parameters (averaged over the years 1961–1990). The presumption, that the concurrent meteorological data is better correlated with the air quality of the same year than the climatological data, is tested.

The examined pollutants are PM_{10}, ozone, NO_x, SO_2 and $PM_{2.5}$. For each pollutant its relevant ecosystem, vegetation and human health indicators in the context of protocols and directives are subject of investigation, for example, for PM_{10} different interpolation methods are examined for the 36th maximum daily average value and for the number of exceedance days. For the rural areas each pollutant is dealt with in a separate section.

For each pollutant various linear regression models (as described in Section 2.2) are examined and mutually compared according to the procedure described in Section 2.5, followed by various methods of spatial interpolation as described in Section 2.3 and 2.4. Both pure interpolation methods as well as interpolation methods based on the residuals of those linear regression models are considered. All the interpolation methods are compared using cross-validation scatter plots and statistical parameters, as described in Section 2.6. Apart from its use for comparison purposes, cross-validation analysis enables the interpolation uncertainty to be estimated.

For PM_{10} a comparison is made of the interpolation results for the 36th maximum daily average and the number of exceedance days. This is intended to distinguish any differences that may occur as a result of the interpolation of two fields that should show the same exceedence contours.

5.2 Rural areas – PM_{10}

5.2.1 Comparison of linear regression models for rural PM_{10} indicators

Several linear regression models or submodels (Section 2.5) of model equation 2.1 are examined:

Submodel	Input parameters
P.1	EMEP model output
P.2a	EMEP model output, altitude, wind speed, surface solar radiation, temperature
P.2b	EMEP model output, altitude, wind speed, surface solar radiation
P.2c	EMEP model output, altitude, wind speed, temperature
P.2d	EMEP model output, altitude, wind speed, relative humidity
P.3a	altitude, wind speed, temperature
P.3b	altitude, wind speed, surface solar radiation

The input parameters for the stepwise selection are altitude, meteorological parameters (i.e. wind speed, surface solar radiation, temperature, relative humidity, total precipitation) and EMEP model output (only for submodel type 2 selection). The basic submodel of type 2 arrived at after a stepwise regression with a backward elimination of parameters (Section 2.5) is P.2a for the annual average and P.2b for the 36th maximum daily average value. Because of colinearity of temperature and solar radiation (see below), the submodels P.2b and P.2c are examined as well, each excluding one of the two parameters. Additionally, one other submodel, P.2d, is considered, with both temperature and solar radiation replaced by relative humidity, in order to illustrate the "best" submodel with use of relative humidity.

The basic submodel of type 3 (i.e. without output from the EMEP model) selected by stepwise selection of backward type is model P.3a. Again for colinearity of temperature and solar radiation submodel P.3b is examined as well.

Altitude from GTOPO30 (see Section 4.3) is used, after having tested its correlation with the AirBase altitude values at measurement stations, see the Section 5.2.3.

The performance of the different linear regression models is compared in Tables 5.1 and 5.2, which give the parameters *c, a1, ..., a6* for the different submodels.

In the forthcoming tables the characteristics of the correlation coefficient R^2 and the RMSE are presented for each submodel showing the closeness of the linear relation with the measured air pollution values. R^2 should be as close as possible to 1 and RMSE as low as possible. If a parameter is not statistically significant, this is indicated by "n. sign.".

Table 5.1 shows the results for the PM_{10} annual average concentration. The values of R^2 and RMSE for the submodels of the type 1 and 2 show quite clearly that the addition of supplementary parameters substantially improves the closeness of the regression relation by an increased R^2 of about 0.35 and a decreased RMSE by approximately 1.35, i.e. one fifth. Similarly, the R^2 and RMSE for the submodels of types 2 and 3 indicate that the closeness of regression is higher when the EMEP modelled concentration field is used in addition, than when only supplementary parameters are used.

The best results (with regard to R^2 and RMSE) are obtained with model P.2a. However, there is a rather large correlation between temperature and solar radiation. This means it is possible that only one of the parameters, temperature or solar radiation, could be used; as model P.2d shows, the majority of the information that contributes to the accuracy improvement of the linear regression model is included in the other parameters. The comparison between models P.2b and P.2c shows that a better correlation is obtained by the model P.2b, because its R^2 is 0.05 higher and its RMSE is 0.22 $\mu g.m^{-3}$ lower, meaning that solar radiation improves the accuracy more than temperature as a supplementary parameter.

The above mentioned findings lead to the preferred selection of the regression model P.2b, in which the EMEP model output and supplementary parameters altitude, wind speed, and solar radiation are used.

Table 5.1 Comparison of different submodels of the linear regression model equation 2.1 describing the relation between the measured annual average PM_{10} concentration for 2004 and various supplementary parameters in the rural areas.

lin.regr.model (2.1)	P.1	P.2a	P.2b	P.2c	P.2d	P.3a	P.3b
c (constant)	12.0	n.sign.	n.sign.	16.9	209.1	25.0	21.4
a1 (altitude GTOPO)	not used	-0.0122	-0.0100	-0.0089	-0.0098	-0.0114	-0.0134
a2 (temperature 2004)	not used	-0.716	not used	0.852	not used	0.728	not used
a3 (wind speed 2004)	not used	-2.43	-2.32	-2.95	-1.64	-2.45	-2.18
a4 (relative humidity 2004)	not used	not used	not used	not used	-2.02	not used	not used
a5 (s. solar radiation 2004)	not used	2.71	1.94	not used	not used	not used	1.0436
a6 (EMEP model 2004)	0.83	1.28	1.24	0.82	1.06	not used	not used
R^2	**0.109**	**0.456**	**0.446**	**0.395**	**0.411**	**0.314**	**0.313**
adjusted R^2	**0.104**	**0.440**	**0.433**	**0.380**	**0.397**	**0.302**	**0.301**
RMSE [$\mu g.m^{-3}$]	**6.83**	**5.34**	**5.41**	**5.63**	**5.56**	**6.00**	**6.00**

Table 5.2 shows the results for the 36th maximum daily average PM_{10} value. By comparing the submodels of types 1, 2 and 3 (using R^2 and RMSE) similar results are obtained as for the annual average: The addition of supplementary parameters substantially improves the closeness of the regression relation (by an increased R^2 of 0.33 and a decreased RMSE of about one fifth); the closeness of the regression improves when output from the EMEP model is used in combination with supplementary parameters. The best results are provided by model P.2b.

Table 5.2 Comparison of different submodels of linear regression model equation 2.1 describing the relation between the measured 36th maximum daily mean PM_{10} concentration for 2004 and various supplementary parameters in the rural areas.

lin. regr. model (2.1)	P.1	P.2a	P.2b	P.2c	P.2d	P.3a	P.3b
c (constant)	23.7	n. sign.	n. sign.	30.2	375.2	44.1	39.2
a1 (altitude GTOPO30)	not used	-0.0151	-0.0151	-0.0135	-0.0149	-0.0179	-0.0212
a2 (temperature 2004)	not used	n. sign.	not used	1.511	not used	1.2041	not used
a3 (wind speed 2004)	not used	-4.74	-4.74	-5.63	-3.37	-4.63	-4.23
a4 (relative humidity 2004)	not used	not used	not used	not used	-3.63	not used	not used
a5 (s. solar radiation 2004)	not used	3.44	3.44	not used	not used	not used	1.6410
a6 (EMEP model 2004)	0.50	1.02	1.02	0.63	0.84	not used	not used
R^2	**0.062**	**0.390**	**0.390**	**0.348**	**0.364**	**0.281**	**0.275**
adjusted R^2	**0.056**	**0.376**	**0.376**	**0.332**	**0.349**	**0.269**	**0.262**
RMSE [µg.m^{-3}]	**12.04**	**9.74**	**9.74**	**10.04**	**9.92**	**10.54**	**10.59**

The results are similar to the findings in Section 4.3.5 of Horálek et al. (2005) on the selection of the most suitable supplementary data, but with the difference that we now use actual solar radiation instead of the 30-year averaged sunshine duration. A special remark should be made for the use of wind speed as a parameter. Whereas the 30-year average wind speed was not found to be significant in the findings of Section 4.3.4 of Horálek et al. (2005), the concurrent meteorological wind speed appears to significantly improve the linear regression results. See Section 5.2.3 for further discussion.

5.2.2 Linear regression models after logarithmic transformation

Following the recommendation made in Horálek et al. (2005) we further investigated the extent to which the linear regression results can be improved by logarithmic transformation of the measured air quality parameters, according to model equation 2.6. The results for the annual average concentration of PM_{10} for the different submodels are listed in Table 5.3.

Table 5.3 Comparison of different submodels of linear regression model equation 2.2 describing the relation between the logarithm of the measured annual average PM_{10} concentration for 2004 and various supplementary parameters in the rural areas.

lin. regr. model (2.2)	P.1	P.2a	P.2b	P.2c	P.2d	P.3a	P.3b
c (constant)	2.48	1.85	2.08	2.70	12.94	3.15	2.98
a1 (altitude GTOPO)	not used	-0.0006	-0.0005	-0.0004	-0.0005	-0.0006	-0.0007
a2 (temperature 2004)	not used	-0.037	not used	0.043	not used	0.0360	not used
a3 (wind speed 2004)	not used	-0.112	-0.120	-0.137	-0.067	-0.110	-0.097
a4 (relative humidity 2004)	not used	not used	not used	not used	-0.108	not used	not used
a5 (s. solar radiation 2004)	not used	0.137	0.086	not used	not used	not used	0.0505
a6 (EMEP model 2004)	0.047	0.068	0.061	0.045	0.059	not used	not used
R^2	**0.147**	**0.506**	**0.494**	**0.438**	**0.468**	**0.335**	**0.331**
adjusted R^2	**0.142**	**0.491**	**0.482**	**0.425**	**0.456**	**0.323**	**0.319**
RMSE, using backtransf. [µg.m^{-3}]	**6.86**	**5.33**	**5.37**	**5.59**	**5.56**	**5.99**	**6.02**

In addition, the same linear regression model equation 2.2 was examined for the 36th maximum daily mean value of PM_{10} (see Table 5.4).

Table 5.4 Comparison of different submodels of linear regression model equation 2.2 describing the relation between logarithm of PM_{10} measurement parameter 36th maximum daily mean value for 2004 and different supplementary parameters in the rural areas.

lin. regr. model (2.2)	P.1	P.2a	P.2b	P.2c	P.2d	P.3a	P.3b
c (constant)	3.11	2.56	2.56	3.22	14.18	3.70	3.57
a1 (altitude GTOPO)	not used	-0.0004	-0.0004	-0.0004	-0.0004	-0.0005	-0.0006
a2 (temperature 2004)	not used	n. sign.	not used	0.046	not used	0.0352	not used
a3 (wind speed 2004)	not used	-0.138	-0.138	-0.152	-0.080	-0.118	-0.107
a4 (relative humidity 2004)	not used	not used	not used	not used	-0.116	not used	not used
a5 (s. solar radiation 2004)	not used	0.091	0.091	not used	not used	not used	0.0465
a6 (EMEP model 2004)	0.017	0.030	0.030	0.021	0.028	not used	not used
R^2	**0.098**	**0.443**	**0.443**	**0.390**	**0.422**	**0.289**	**0.279**
adjusted R^2	**0.093**	**0.430**	**0.430**	**0.376**	**0.408**	**0.277**	**0.266**
RMSE, using backtransf. [µg.m^{-3}]	**12.13**	**9.69**	**9.69**	**10.00**	**9.96**	**10.56**	**10.63**

In comparison with the Tables 5.1 and 5.2 it can be seen that the measured values after logarithmic transformation show a closer regression relation with supplementary data than the data without this transformation. In all cases R^2 is higher by about 0.05–0.06 when using the logarithmic transformation of the measured air quality parameter values in the linear regression.

Thus it seems that the logarithmic transformation leads to a significant improvement of the linear regression models. This improvement can be utilized in two different ways: The simplest is the back transposing of the regression results. It can be seen that for the "best" methods the results are improved by this approach, back-transformed RMSE can be compared with RMSE from Tables 5.1 and 5.2. The second approach is direct spatial interpolation of the residuals of the linear regression model (2.2) and subsequent back transposition. Such back transposition, however, is rather complicated, as the bias must be corrected (for details, see Cressie, 1993).

The eventual improvement of the estimation with the use of logarithmic transformation should also be verified in the analysis of interpolation methods. Another question is whether there are differences in regression relations in different parts of Europe, as in Section 5.4.1, Figure 5.19. These points can be the subject of further study.

5.2.3 Comparison of linear regression models using meteorological or climatological data

Unlike in Horálek et al. (2005), now the annual averaged meteorological parameters from the specific year of interest are available. Comparison of the individual submodels of linear regression model equation 2.1 for PM_{10} indicators was carried out with the use of both actual meteorological data (year 2004, ECMWF) and climatological data (averages for 1961–1990, CRU), using similar or comparable parameters. Most parameters in the two datasets are the same with the exception of the meteorological data representing global radiation, surface solar radiation, and the climatological data, sunshine duration. The comparison was carried out on the basis of the coefficient of determination R^2.

The results are presented in Tables 5.5 and 5.6, for both the annual average and 36th maximum daily average value. It can be seen that inclusion of the actual annual averaged meteorological parameters (ECMWF) brings model improvement in comparison with using similar or comparable parameters based on 30-year averaged climatological data sources (CRU). It means that the use of meteorological parameters in both the linear regression model equations 2.1 and 2.2 leads to a better estimation of PM_{10} concentrations. This holds in general for all the examined regression models (R^2 is by 0.03-0.09 higher in case of using actual meteorological data).

Table 5.5 Comparison of submodels of linear regression model equation 2.1 using R^2 using the meteorological parameters for the specific year of interest (ECMWF) resp. 30-year averaged climatological data (CRU), for the rural areas.

type of regression model (2.1)	R^2 - annual average		R^2 - max. 36th d. v.	
	meteo_04	clim_61-90	meteo_04	clim_61-90
P.2a (altit., w.sp., sol.rad/sunsh.dur., temp., EMEP)	0.46	0.43	0.39	0.36
P.2b (altit., w.speed, sol.rad/sunsh.dur., EMEP)	0.45	0.42	0.39	0.35
P.2c (altit., w.speed, temp., EMEP)	0.39	0.32	0.35	0.26
P.2d (altit., w.speed, rel.humidity, EMEP)	0.41	0.37	0.36	0.31
P.3a (altit., w.speed, temp.)	0.31	0.26	0.28	0.21
P.3b (altit., w.speed, sol.rad/sunsh.dur.)	0.31	0.27	0.27	0.23
average	**0.39**	**0.35**	**0.34**	**0.29**

Table 5.6 Comparison of submodels of linear regression model equation 2.2 (i.e. using logarithm of PM_{10} parameters) using R^2 using the meteorological parameters for the specific year of interest (ECMWF) resp. 30-year averaged climatological data (CRU), for the rural areas.

type of regression model equation 2.2	R^2 - annual average		R^2 - max. 36th d. v.	
	meteo_04	clim_61-90	meteo_04	clim_61-90
P.2a (altit., w.sp., sol.rad/sunsh.dur., temp., EMEP)	0.51	0.50	0.44	0.44
P.2b (altit., w.speed, sol.rad/sunsh.dur., EMEP)	0.49	0.48	0.44	0.43
P.2c (altit., w.speed, temp., EMEP)	0.44	0.39	0.39	0.32
P.2d (altit., w.speed, rel.humidity, EMEP)	0.47	0.44	0.42	0.39
P.3a (altit., w.speed, temp.)	0.33	0.31	0.29	0.25
P.3b (altit., w.speed, sol.rad/sunsh.dur.)	0.33	0.30	0.28	0.24
average	**0.43**	**0.40**	**0.38**	**0.35**

Additionally, the correlation between the investigated parameters from the two different data sources, being the actual 2004 annual averaged ECMWF meteorological parameters versus the 30-year (1961–1990) averaged climatological parameters, was examined. The degrees of this correlation are demonstrated in Figures 5.1 and 5.2 below.

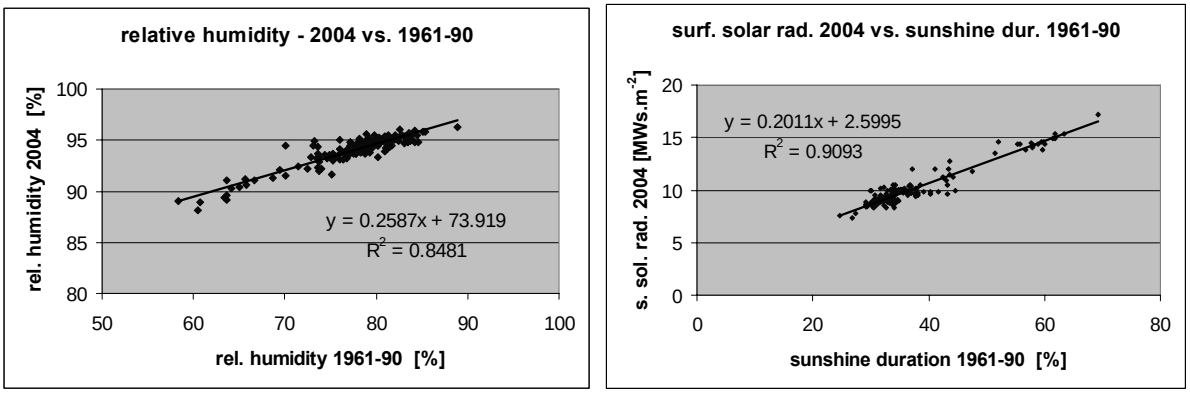

Figure 5.1 Correlations between actual meteorological 2004 (ECMWF, y-axis) and climatological 1961–1990 data (CRU, x-axis) for relative humidity (left) and surface solar radiation, resp. sunshine duration (right) at the locations of rural background stations with PM_{10} data.

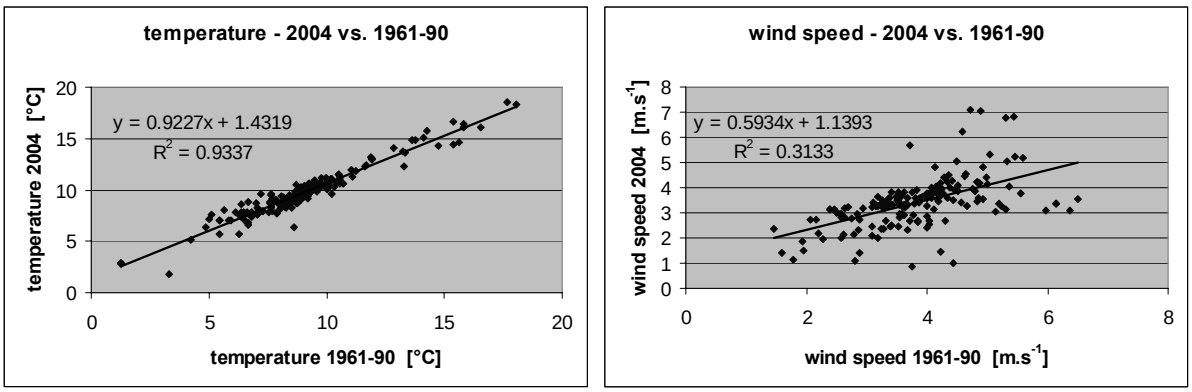

Figure 5.2 Correlation between actual meteorological 2004 (ECMWF, y-axis) and climatological 1961–1990 data (CRU, x-axis) for temperature (left) and wind speed (right) at the locations of rural background stations with PM_{10} data.

Figures 5.1 and 5.2 show the largest and significant difference (smallest R^2) between actual ECMWF and CRU climatological data is observed for wind speed. This is probably the reason why the 2004 annual averaged wind speed of ECMWF shows substantial better correlation coefficients (R^2) for PM_{10} in Tables 5.1 and 5.2, contrary to the poor correlation results with the 30-year averaged wind speed of CRU obtained in Horálek et al. (2005) for PM_{10}. It is concluded that the use of actual meteorological data instead of climatological data improves the closeness of the regression relation (with regard to R^2). The ECMWF yearly data will be further used in this study.

5.2.4 Comparison of linear regression models using altitude from AirBase or GTOPO30

As the basis of the linear regression relations, the supplementary parameters utilized should be representative for the whole of Europe for the purposes of AQ mapping. We have the altitude as raster of GTOPO30 (Section 4.3) covering the whole of Europe next to the AirBase altitude data only representative for the station (point) locations. Due to its character of complete European coverage it would be most appropriate to use GTOPO30 in the regression analyses. On the other hand, this project is primarily aimed to investigate the suitability of AirBase for European-wide spatial interpolations for AQ mapping. Therefore, we consider the altitude point data stored in AirBase as an important data source and we compare it with a European covering altitude data source GTOPO which is widely used and known for its reliability.

At first, AirBase altitude is compared with altitude from GTOPO30. Further, the comparison of individual submodels of linear regression model equations 2.1 and 2.2 is carried out with the use of AirBase altitude and altitude of GTOPO30. The comparison gives us an estimate of the degree of correlation between GTOPO30 and the altitudes reported by countries in AirBase GTOPO30 altitude. Moreover, it provides insight into which data source we should use for reaching the best results in the interpolation calculations

Figure 5.3 shows the close linear relation between the two altitudes. The coefficient of determination R^2 is 0.97, i.e. 97 % of the variability is explained by linear regression. It means that both altitudes are quite similar. The remaining differences are related to the fact that AirBase gives altitude information for a specific location, whereas GTOPO30 gives average values for about 600 x 600 m grid (after transposing from 30 x 30 arcsec grid). Especially in complex terrains differences are to be expected.

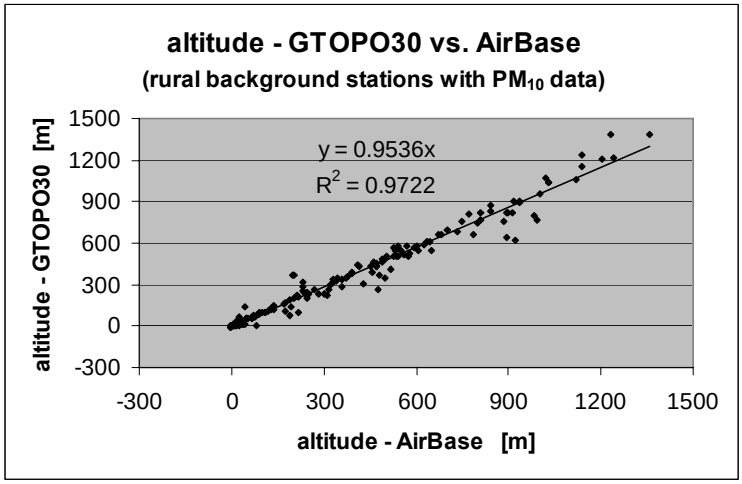

Figure 5.3 Correlation between the altitude from AirBase and GTOPO30 at the locations of rural background stations with PM_{10} data.

Tables 5.6 and 5.7 give an overview of the different submodels of linear regression model equations 2.1 and 2.2, respectively, (i.e. the models with and without logarithmic transformation) using altitude from AirBase and GTOPO30. The comparison is carried out on the basis of the coefficient of determination R^2.

Table 5.6 Comparison of submodels of linear regression model equation 2.1 with the use of altitude from AirBase (at rural background stations with PM_{10} data, for the year 2004) and GTOPO30, respectively.

type of regression model (2.1)	R^2 - annual average		R^2 - max36d	
	AirBase	GTOPO30	AirBase	GTOPO30
P.2a (altitude, w.speed, s.solar rad., temp., EMEP)	0.49	0.46	0.41	0.39
P.2b (altitude, w.speed, s.solar rad., EMEP)	0.47	0.45	0.40	0.39
P.2c (altitude, w.speed, temp., EMEP)	0.41	0.39	0.35	0.35
P.2d (altitude, w.speed, rel.humidity, EMEP)	0.43	0.41	0.37	0.36
P.3a (altitude, w.speed, temp.)	0.33	0.31	0.29	0.27
P.3b (altitude, w.speed, s.solar rad.)	0.33	0.31	0.29	0.28
average	**0.41**	**0.39**	**0.35**	**0.34**

Table 5.7 Comparison of submodels of linear regression model equation 2.2 (i.e. with logarithmic transformation of the measured concentrations, for the year 2004) with the use of altitude from AirBase (at rural background stations with PM_{10} data) and GTOPO3, respectively.

type of regression model (2.2)	R^2 - annual average		R^2 - max36d	
	AirBase	GTOPO30	AirBase	GTOPO30
P.2a (altitude, w.speed, s.solar rad., temp., EMEP)	0.54	0.51	0.47	0.44
P.2b (altitude, w.speed, s.solar rad., EMEP)	0.52	0.49	0.46	0.44
P.2c (altitude, w.speed, temp., EMEP)	0.46	0.44	0.40	0.39
P.2d (altitude, w.speed, rel.humidity, EMEP)	0.49	0.47	0.43	0.42
P.3a (altitude, w.speed, temp.)	0.36	0.33	0.30	0.28
P.3b (altitude, w.speed, s.solar rad.)	0.36	0.33	0.30	0.29
average	**0.45**	**0.43**	**0.39**	**0.38**

It can be seen that rather similar results are obtained in the regression models for the two different altitude sources. The use of GTOPO30 generally gives slightly smaller R^2 in all models, meaning that the AirBase altitudes perform best in the linear regressions. However, given that the correlation is only 1 – 2 % lower, we think it is justified to give preference to the GTOPO30 data, which has the advantage that they cover the whole

of Europe. These findings enable the usage of GTOPO30 data in mapping through linear regression and interpolation of residuals (type 3).

5.2.5 Conclusions on the linear regression models for rural PM_{10}

Different submodels of linear regression model equation 2.1 were examined for the two PM_{10} indicators, being the annual average and the 36th maximum daily average value for rural areas, using different supplementary data.

- It is concluded that the use of supplementary data together with output from the Unified EMEP model substantially improves the closeness of the regression relation (both with regard to R^2 and RMSE).
- It is concluded that the use of actual meteorological data instead of climatological data improves the closeness of the regression relation (with regard to R^2).
- It is concluded that GTOPO30 as source for altitude (which is available throughout the whole European area) can be used instead of AirBase altitude.
- The comparison of submodels with and without output from the Unified EMEP model shows that the closeness of regression is higher in case the EMEP model is used (P.2) as compared to a situation in which models with supplementary parameters only are used.
- Different types of linear regression models with logarithmic transformation were examined. The observed correlation coefficient values (R^2) after logarithmic transformation indicate that the logarithmic transformation leads to a significant improvement of the linear regression models. However, this transformation is not further examined in the next spatial interpolation section, due to the theoretical problems in back-transformation of spatial interpolation (see Cressie, 1993). This can be issue of further examination.
- The preferred submodel for both the annual average and 36th maximum daily average value is P.2b (EMEP model, altitude, wind speed and surf. solar radiation). This submodel will be further examined in the spatial interpolation comparisons of the next section. The other submodels (P.1, P.2a, P.2c, P.2d and P.3a) are included for comparison.

5.2.6 Comparison of spatial interpolation methods for rural PM_{10}

Various methods were used for spatial interpolation and were compared with each other using RMSE and other statistical indicators from cross-validation. The results are also compared with various types of the linear regression model without interpolation (equation 2.1) of Section 5.2.1. The various submodels for the PM_{10} indicators are coded the same as in Section 5.2.1. The compared methods are as follows:

1.Linear regression models without interpolation

P.1	EMEP
P.2a	EMEP, altitude, wind speed, surface solar radiation, temperature
P.2b	EMEP, altitude, wind speed, surface solar radiation
P.2d	EMEP, altitude, relative humidity, wind speed
P.3a	altitude, wind speed, temperature
P.clim	EMEP, altitude, climatological sunshine duration (i.e. method used in TP 8/2005)

2. Interpolation methods using primarily monitoring data

a. IDW
b. Ordinary kriging (OK) – parameters of variogram selected automatically (b1) and manually fitted (b2)
c. Ordinary cokriging (OC) – parameters of variogram selected automatically (c1) and manually fitted (c2)
d. Lognormal cokriging (LC) – parameters of variogram selected automatically (d1) and manually fitted (d2)

3. Interpolation of the residuals of linear regression models, using the interpolation methods

a. IDW
b. Ordinary kriging (OK) – parameters of variogram selected automatically (b1) and manually fitted (b2)

For all geostatistical methods (i.e. OK, OC, LC) variogram parameters (Section 2.3.2) are estimated in two ways: Automatically (optimisation/fitting of the variogram function) and manually (minimization of the cross-validation RMSE), see Section 2.3.5. The comparison of the results obtained by these two methods of parameter setting enables the influence of an eventual automatic routine, as is used in the ArcGIS software, to be evaluated. Note that the minimisation procedure will always provide an equivalent or reduced cross validation RMSE, in comparison to the automatic fit.

For the methods of linear regression, followed by interpolation of residuals (type 3), only IDW and ordinary kriging were performed. No ordinary cokriging or lognormal kriging is performed for the reasons explained in Section 2.4. Linear regression models with logarithmic transformation are not performed for the reasons explained in Section 5.2.5.

The comparison of individual interpolation methods was carried out with the use of the root-mean square error (RMSE) and the other statistical uncertainty and error indicators from cross-validation (Section 2.6, Equations 2.14 to 2.16). Moreover, cross-validation scatter plots are presented for interpolation methods using primarily monitoring data.

Apart from their use for comparison purposes, the results of the cross-validation analysis are useful for expressing of the maps uncertainties. Scatter plots show the correlation between measured and cross-validation estimates. Indicators such as RMSE express the total uncertainty of the whole map (in $\mu g.m^{-3}$). The nature of cross-validation (concentration measured in the estimated point is not used for estimation) enables the quality of the interpolation in the places with no measurement to be evaluated. (The quality of the interpolation at the position of the measurements is also examined in Section 7.2.)

Figure 5.4 shows the cross-validation scatter plots for the annual average PM_{10} concentrations for several interpolation methods using primarily monitoring data (i.e. only for interpolation methods of type 2), namely ordinary kriging, ordinary cokriging and lognormal cokriging, all with two setting of variogram parameters. The plots show that the best results among these methods, i.e. the highest R^2, are obtained by lognormal cokriging with the manual optimization of variogram parameters using RMSE minimization (2-d2).

The plots show that for all three methods the concentrations are smoothed. This is visible on the one hand from the linear regression equation ($y = a \cdot x + c$ when $a < 1$ and $c > 0$), and on the other hand directly from the graphs (comparing the values in the x and y axes).

The smoothing is smaller in case of the manually fitted parameters (for all methods) and also for both ordinary and lognormal cokriging in comparison with ordinary kriging. This is visible e.g. from the parameters of linear regression: Smaller smoothing means higher slope a and lower intercept c. (High intercept means overestimation of low values, low slope means underestimation of high values.)

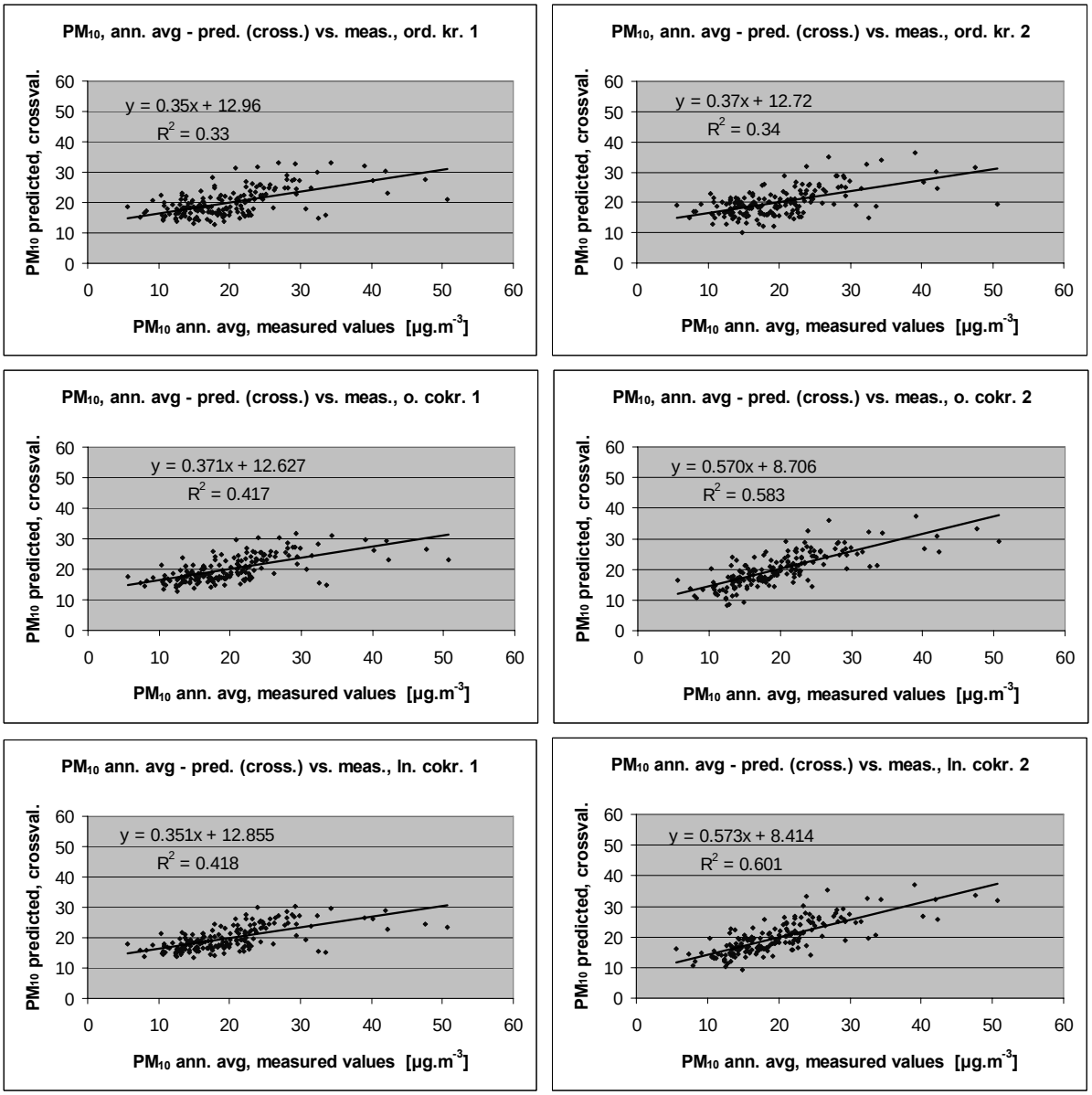

Figure 5.4 Correlation between cross-validation predicted values (y-axis) and measurements (x-axis) for the PM_{10} annual average for rural areas in 2004, for ordinary kriging (top), ordinary cokriging using altitude (centre) and lognormal cokriging (bottom), with parameters of variogram estimated automatically (left) and manually (right).

Figure 5.5 shows the cross-validation scatter plot for the 36th maximum daily average value for various interpolation methods using primarily monitoring data. Again: the best results are obtained by lognormal cokriging with the manual optimisation of the variogram parameters using RMSE minimization (2-d2). Manual optimisation of the variogram parameters gives better results for all examined methods. (R^2 is higher and underestimation of high values is smaller.)

The plots show that the high concentrations are underestimated and small concentrations are overestimated outside the measuring sites using all examined methods; the underestimation is smaller in the case of the manually fitted parameters of the variogram.

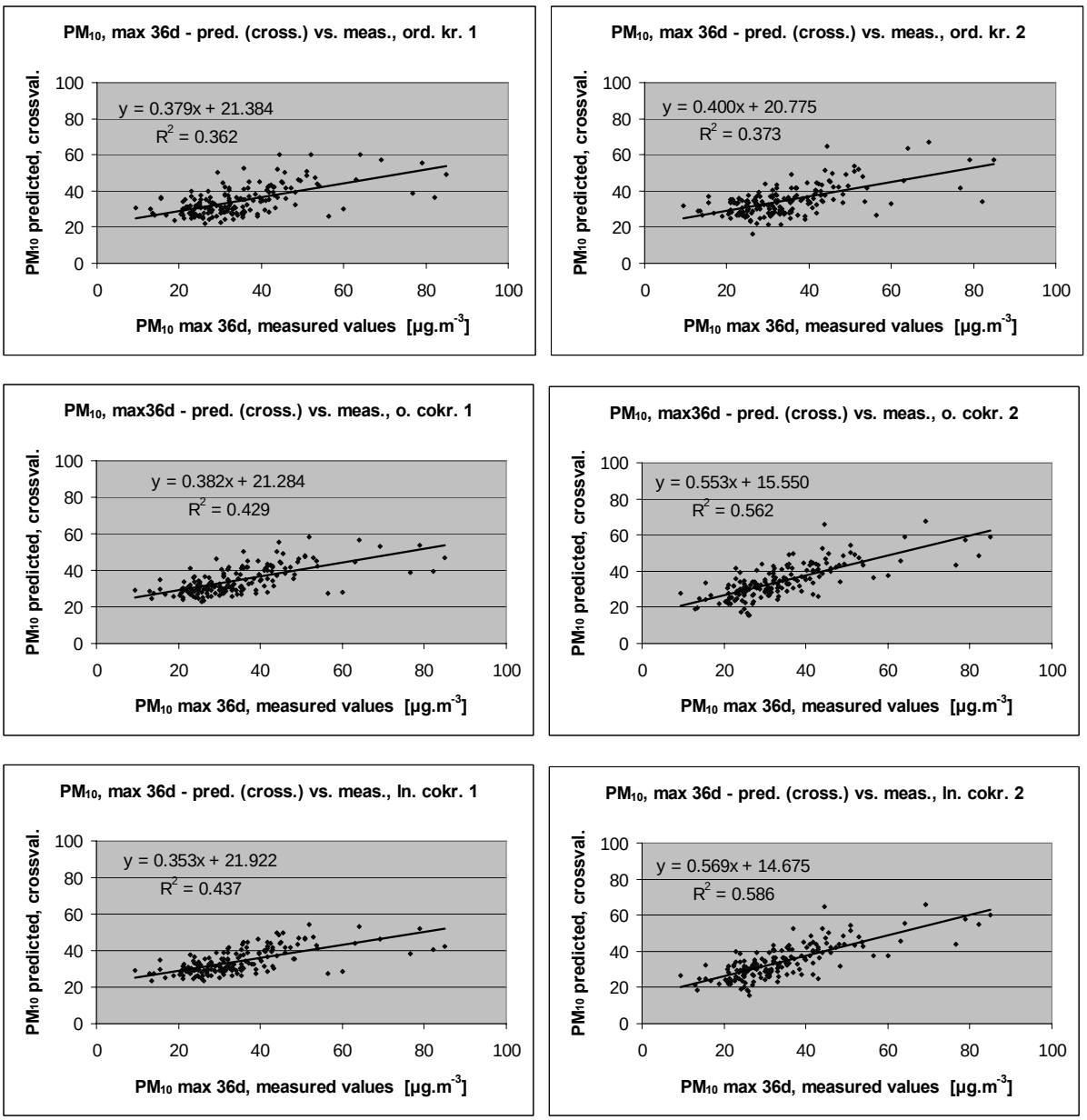

Figure 5.5 Correlation between cross-validation predicted values (y-axis) and measurements (x-axis) for, the 36th maximum daily average PM_{10} values for rural areas in 2004, for ordinary kriging (top), ordinary cokriging using altitude (centre) and lognormal cokriging (bottom) with parameters of variogram estimated automatically (left) and manually (right).

The comparison of the different methods of all types against the other statistical indicators of the cross-validation is presented in Table 5.8 for both the annual averages and the 36th maximum daily averages. The main criterion is RMSE, followed by MAE, MPE, MedAE and other indicators. Mean prediction standard error (MPSE) in principle can be computed for geostatistical methods only, thus its application is limited only to these methods. Similarly, also R^2 is not computed for all methods (see Section 2.6). SD gives, in general, very similar results as RMSE.

RMSE, SD, MAE, median of absolute error and MPSE should be as small as possible. MPE, minimum error and maximum error should be as near to zero as possible; R^2 should be as close to 1 as possible. All the indicators, with exception of R^2, are expressed in $\mu g.m^{-3}$.

Table 5.8 Comparison of different interpolation methods showing RMSE and the other statistics for the PM_{10} indicators annual averages and the 36th maximum daily averages for 2004 in rural areas. The smaller RMSE means the more accurate the estimation by the mapping method. Similarly, SD, MAE, median of absolute error and MPSE should be as small as possible; MPE, minimum error and maximum error should be as near to zero as possible; R^2 should be as close to 1 as possible. Apart of R^2, all other statistical indicators are in $\mu g.m^{-3}$.

mapping method		annual average PM_{10} [$\mu g.m^{-3}$]									36th maximum daily average [$\mu g.m^{-3}$]								
		RMSE	MPE	SD (error)	min (error)	max (error)	MAE	MedAE	R^2	MPSE	RMSE	MPE	SD (error)	min (error)	max (error)	MAE	MedAE	R^2	MPSE
1-P.1	lin. regr. P.1	6.83	0.00	6.83	-12.49	34.38	4.92	3.90	0.109		12.04	0.00	12.04	-21.32	53.54	8.65	6.71	0.062	
1-P.2a	lin. regr. P.2a	5.34	0.00	5.34	-12.14	22.45	3.86	2.89	0.456		9.74	0.07	9.74	-22.59	45.74	7.04	5.31	0.390	
1-P.2b	lin. regr. P.2b	5.41	0.04	5.41	-11.62	23.21	3.93	2.97	0.446		9.74	0.07	9.74	-22.59	45.74	7.04	5.31	0.390	
1-P.2d	lin. regr. P.2d	5.56	0.00	5.56	-12.44	24.01	3.99	2.81	0.411		9.92	0.00	9.92	-21.99	44.00	7.09	5.42	0.364	
1-P.3a	lin. regr. P.3a	6.00	0.00	6.00	-14.40	27.04	4.38	3.15	0.314		10.54	0.00	10.54	-24.21	49.89	7.85	6.09	0.281	
1-P.clim.	lin. regr. "clim."	5.63	-0.09	5.63	-10.31	24.31	4.08	3.35	0.398		10.29	-0.14	10.29	-20.37	47.64	7.34	5.43	0.319	
2-a	interp. IDW	5.84	0.30	5.83	-30.23	14.30	4.27	3.33	0.357		9.89	0.67	9.87	-46.67	27.89	7.19	5.46	0.378	
2-b1	interp. OKrig-aut	5.95	0.17	5.94	-29.68	13.18	4.27	3.09	0.328	4.97	9.95	0.36	9.94	-45.96	21.38	7.06	5.42	0.362	8.29
2-b2	interp. OKrig-fit	5.91	0.21	5.90	-31.11	13.66	4.32	3.17	0.338	5.15	9.88	0.45	9.87	-48.24	22.38	7.25	5.34	0.373	8.45
2-c1	interp. OCokr-aut (altit.)	5.55	0.18	5.55	-27.57	12.15	3.91	2.77	0.417	5.04	9.44	0.36	9.43	-42.47	19.68	6.65	5.13	0.429	8.42
2-c2	interp. OCokr-fit (altit.)	4.68	0.19	4.68	-21.37	10.96	3.29	2.33	0.583	3.89	8.24	0.42	8.23	-33.44	21.19	5.94	4.18	0.562	6.47
2-d1	interp. LnCokr-aut (altit.)	5.57	0.02	5.57	-27.05	12.29	3.88	2.87	0.418	5.31	9.46	0.00	9.46	-42.40	19.85	6.52	5.07	0.439	8.57
2-d2	interp. LnCokr-fit (altit.)	4.58	-0.04	4.58	-18.76	10.51	3.27	2.31	0.601	3.33	8.01	0.07	8.01	-33.00	20.30	5.88	4.22	0.586	5.57
3-P.1-a	lin. regr. 1 + IDW	5.51	0.06	5.50	-29.78	11.76	4.02	3.29			9.47	0.37	9.46	-46.20	27.12	6.94	5.33		
3-P.1-b1	lin. regr. 1 + OKrig-aut	5.60	-0.02	5.60	-29.84	10.97	4.01	3.01		4.77	9.53	0.11	9.53	-46.30	19.61	6.81	5.55		8.03
3-P.1-b2	lin. regr. 1 + OKrig-fit	5.54	-0.03	5.54	-31.07	10.38	4.02	3.21		4.87	9.41	0.14	9.41	-48.42	20.09	6.94	5.15		7.67
3-P.2a-a	lin. regr. 2a + IDW	4.75	0.09	4.75	-22.71	12.90	3.46	2.45			8.34	0.28	8.34	-34.85	28.28	6.09	4.63		
3-P.2a-b1	lin. regr. 2a + OKrig-aut	4.64	0.03	4.64	-22.30	9.20	3.33	2.43		4.04	8.09	0.10	8.09	-33.64	18.67	5.85	4.65		6.93
3-P.2a-b2	lin. regr. 2a + OKrig-fit	4.61	0.06	4.61	-22.07	9.98	3.34	2.32		3.76	8.07	0.13	8.07	-33.33	21.68	5.83	4.54		6.47
3-P.2b-a	lin. regr. 2b + IDW	4.77	0.09	4.77	-22.56	12.71	3.49	2.50			8.34	0.28	8.34	-34.85	28.28	6.09	4.63		
3-P.2b-b1	lin. regr. 2b + OKrig-aut	4.65	0.03	4.65	-21.98	9.37	3.34	2.33		4.07	8.09	0.10	8.09	-33.64	18.67	5.85	4.65		6.93
3-P.2b-b2	lin. regr. 2b + OKrig-fit	4.61	0.06	4.61	-21.72	10.12	3.33	2.30		3.73	8.07	0.13	8.07	-33.33	21.68	5.83	4.54		6.47
3-P.2d-a	lin. regr. 2d + IDW	4.86	0.10	4.86	-25.27	12.85	3.46	2.39			8.45	0.33	8.44	-39.63	25.79	5.92	4.27		
3-P.2d-b1	lin. regr. 2d + OKrig-aut	4.67	0.06	4.67	-23.96	10.69	3.30	2.40		4.16	8.09	0.17	8.09	-37.31	19.40	5.67	4.32		7.02
3-P.2d-b2	lin. regr. 2d + OKrig-fit	4.65	0.09	4.65	-23.92	11.14	3.29	2.25		3.95	8.07	0.19	8.07	-37.18	20.31	5.68	4.22		6.69
3-P.3b-a	lin. regr. 3b + IDW	5.05	0.37	5.04	-21.99	15.10	3.64	2.42			8.83	0.77	8.79	-34.07	29.62	6.34	4.55		
3-P.3b-b1	lin. regr. 3b + OKrig-aut	4.85	0.23	4.85	-21.02	13.51	3.43	2.25		4.17	8.43	0.45	8.42	-35.27	22.52	6.01	4.53		7.05
3-P.3b-b2	lin. regr. 3b + OKrig-fit	4.83	0.25	4.82	-20.74	13.45	3.44	2.26		3.98	8.42	0.48	8.40	-34.75	22.48	6.04	4.45		6.68
3-P.clim-a	lin. regr. 'clim' + IDW	4.82	0.23	4.82	-24.33	13.23	3.49	2.55			8.48	0.58	8.46	-38.23	29.19	6.15	4.67		
3-P.clim-b1	lin. regr. "clim" + OKrig-aut	4.68	0.09	4.68	-23.59	8.77	3.35	2.63		4.04	8.17	0.24	8.17	-36.83	17.44	5.82	4.63		7.00
3-P.clim-b2	lin. regr. "clim" + OKrig-fit	4.64	0.12	4.64	-23.32	10.18	3.35	2.55		3.74	8.12	0.29	8.12	-36.58	21.92	5.85	4.37		6.48

A number of points can be concluded from the results provided in Table 5.8.

- It can be seen that individual interpolation methods give similar results for both the annual average and the 36th maximum daily average value of PM_{10}.
- The use of interpolation methods, both interpolation using primarily monitoring data (type 2) and interpolation of the residuals of linear regression (type 3), give better results with regard to RMSE (and also MAE, SD, MedAE) than the methods using linear regression models without interpolation (type 1).
- In the case of methods of interpolation with monitoring data only (type 2) the best results (with regard to RMSE and all other indicators) are obtained by lognormal cokriging using altitude, method 2-d. This confirms the results presented in the Horálek et al. (2005).
- In the case of linear regression with interpolation of its residuals the best results (with regard to RMSE, MAE, MedAE, SD, MPSE) are obtained by (ordinary) kriging of the residuals of the linear regression model P.2b (method 3-P.2b-b), which uses EMEP model output, altitude, solar radiation and wind speed. In comparison with the results presented in the Horálek et al. (2005) meteorological data instead of climatological data were used, and wind speed was also considered.
- An intercomparison of the best methods of the types 1, 2 and 3 shows slightly better results for lognormal cokriging (in spite of the fact that it is no more than an interpolation method using primarily monitoring data), based on RMSE (and also SD, MAE and MPSE; MedAE is better for the 3-P.2b-b method). The reason is that this method uses logarithmic transformation which corresponds to a logarithmic-normal distribution of PM_{10}. For future applications we therefore recommend the examination of methods that enable logarithmic transformation of PM_{10} values and the use of supplementary parameters.
- If comparing the setting of variogram's parameters, the manual optimization using RMSE is the best (naturally) based on RMSE, but also based on MAE, MedAE, SD and MPSE (for almost all methods). This leads to selection of this setting of parameters. However, MPE is slightly better for automatic optization of variogram function for all methods. This is an issue for further examination.

The resulting rural maps for the annual mean PM_{10} concentrations and 36th maximum daily average PM_{10} using the two best methods, interpolation methods 2-d2 and 3-P.2b-b2, are shown in Figure 5.6 and 5.7 below. The main difference directly visible in the maps is the effect of the inclusion of altitude and solar radiation (seen in the latitudinal variation) as regression parameters.

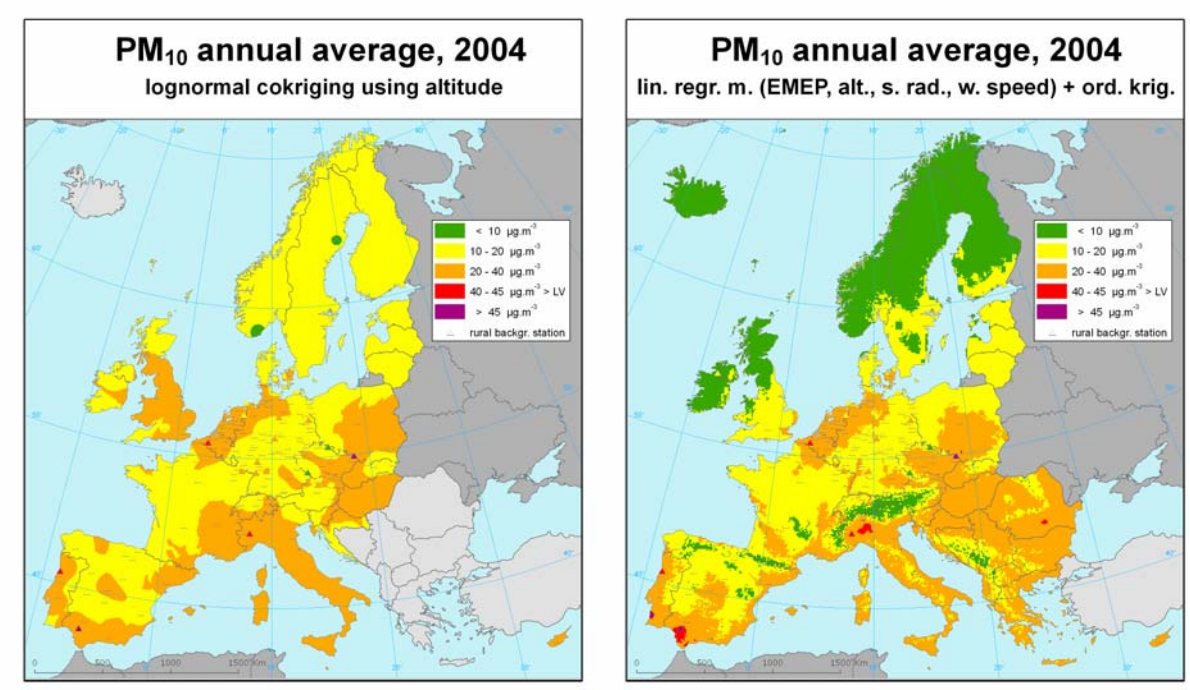

Figure 5.6 Maps showing the annual average PM_{10} concentration (in $\mu g.m^{-3}$) on the European scale for rural areas in 2004, 10 x 10 km grid resolution, as a result of the interpolation methods 2-d2 (left) and 3-P.2b-b2 (right). Uncertainty of both these maps expressed by RMSE is 4.6 $\mu g.m^{-3}$.

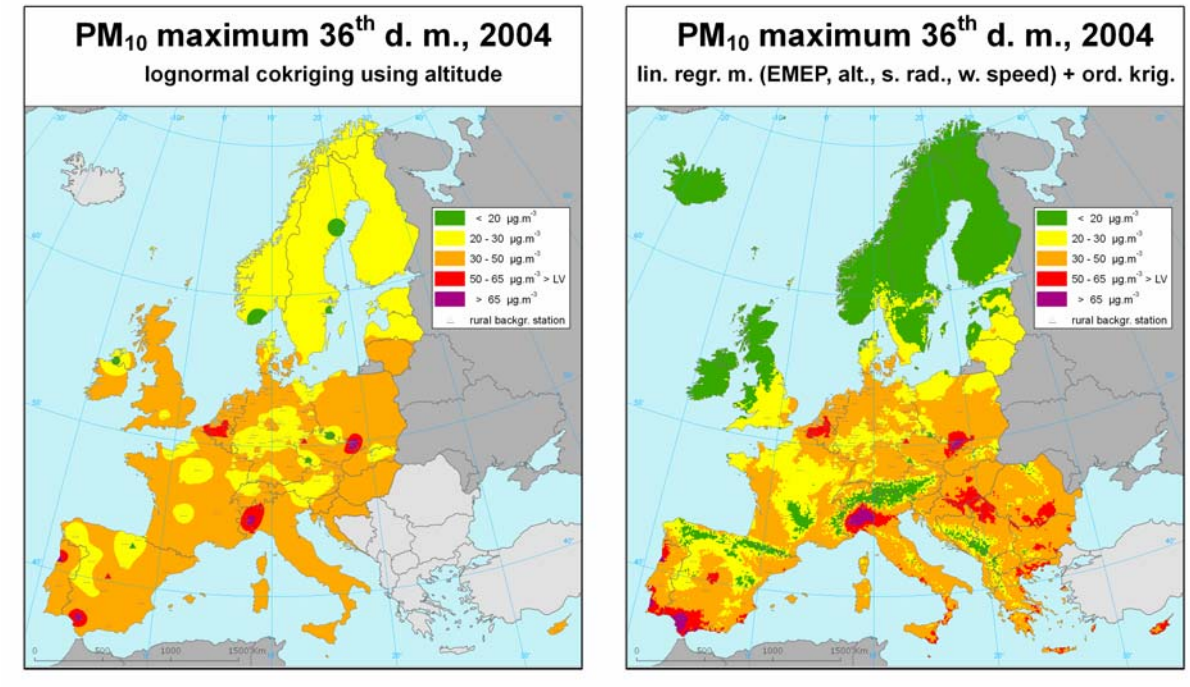

Figure 5.7 Maps showing the 36th maximum daily average PM_{10} values (in $\mu g.m^{-3}$) on the European scale for rural areas in 2004, 10 x 10 km grid resolution, as a result of interpolation method 2-d2 (left) and 3-P.2b-b2 (right). Uncertainty of these maps expressed by RMSE is 8.0 $\mu g.m^{-3}$.(left) and 8.1 $\mu g.m^{-3}$ (right).

Using RMSE (i.e. the most common indicator) the uncertainty of the maps can be expressed, in $\mu g.m^{-3}$. Alternatively, this uncertainty can be also expressed as a percentage of the mean of the values of relevant indicators across all stations. The relative uncertainty of the rural PM_{10} annual average map is

23.1% for the method 2-d2 and 23.3% for the method 3-P.2b-b2. The relative uncertainty of the rural map of 36th maximum daily average PM_{10} values is 23.6% for the method 2-d2 and 23.8% for the method 3-P.2b-b2.

We now turn to the other PM_{10} indicators of direct relevance to the current legislation. The daily PM_{10} concentration limit value is expressed as the tolerated exceedance, i.e. it is allowed to exceed the limit value of 50 $\mu g.m^{-3}$ on 35 days in one year (see Directive 1999/30/EC). Thus the critical exceedance contour can be derived on the basis of two approaches, either from the map of the 36th maximum daily average concentration or from the map of the number of exceedance (NOE) days of the limit 50 $\mu g.m^{-3}$. The aim of the comparison presented here is to find out whether the results of both procedures correspond, as should in principal be the case.

The comparison must use a comparable methodology. However, for the number of exceedance days the EMEP model cannot be used in the linear regression model. Although the model produces output for this parameter, the model strongly underestimates the concentrations and, consequently, the vast majority of the territory shows no exceedance. Unlike the other PM_{10} indicators such as the annual average concentration or the 36th maximum daily average value, a linear regression between the EMEP model output and the measured values would not be useful for this indicator. (The use of linear regression model using only variables other than EMEP model would be in principle possible, but it was not tested.)

The comparison was carried out only for the interpolation methods using primarily monitoring data, i.e. for IDW, ordinary kriging, and ordinary cokriging. Neither lognormal kriging nor lognormal cokriging can be used in case of the number of exceedance days because the value of the number of exceedance days may be zero, which does not enable logarithmic transformation. The possibility of using geostatistical methods (i.e. various types of kriging) for the mapping of the number of exceedances – although it is a discrete quantity – is demonstrated by Van de Kassteele (2006).

Furthermore the comparison was carried out only for rural areas. Only those AirBase stations with valid values for both parameters (i.e. the 36th maximum daily average value and the number of exceedance days) were taken into account.

Table 5.9 presents, for each of the three examined interpolation methods of type 2, their mapping results concerning the two exceedance indicators, including the share of the study area with values above the limit value and below the limit values. The examined interpolation methods are:

- IDW (method 2-a)
- Ordinary kriging (method 2-b2)
- Ordinary cokriging (method 2-c2)

Table 5.9 Comparison of the area (as percentage of the total mapped area) above or below the limit value (LV) for the interpolation of 36th maximum daily average value and for the interpolation of the number of exceedances (NOE) days, using different interpolation methods (rural areas, 2004).

Area with indicator values	IDW	ord. kriging	ord. cokriging
below LV, according to both maps	97.73%	99.36%	99.19%
below LV acc. to max36d, above LV acc. to NOE	1.30%	0.08%	0.12%
above LV acc. to max36d, below LV acc. to NOE	0.02%	0.14%	0.11%
above LV, according to both maps	0.95%	0.42%	0.58%

The ideal results would show zero at the 2nd and 3rd row of Table 5.9, i.e. whole area should be either below or above the limit value, according to both approaches. The table shows that the correspondence of both maps with regard to the above-the-limit territory is bigger in the case of more precise geostatistical methods (ordinary kriging and cokriging) than with the simpler IDW method. Furthermore, it can be stated that the difference in the definition of the territory based on the 36th

maximum daily average value and the number of exceedances is comparable with the difference in the definition of the territory based on various interpolation methods.

Figure 5.8 shows the maps of air pollution limit exceedances, constructed with the use of ordinary cokriging using altitude, based on the 36th maximum daily average value and the number of exceedance days. It can be seen that the differences are relatively small.

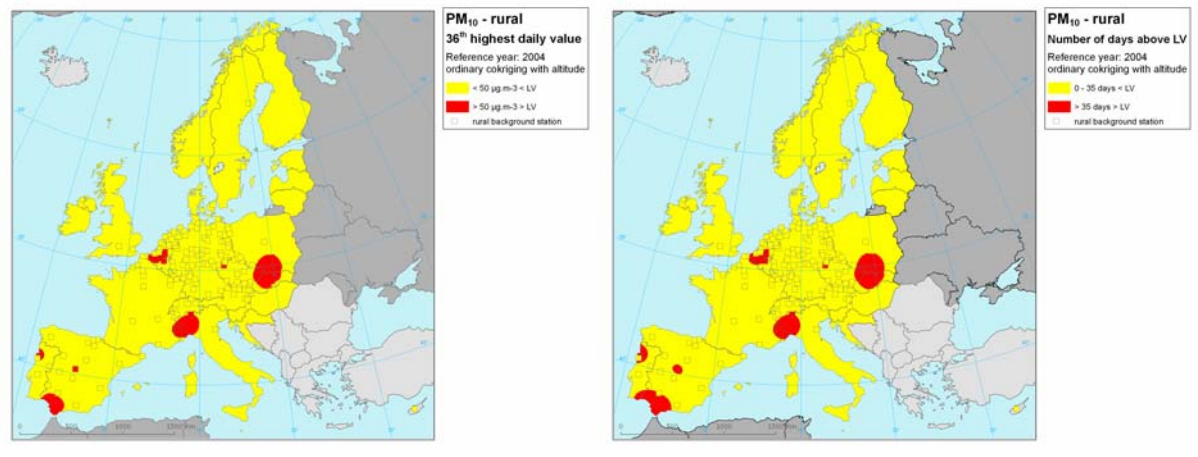

Figure 5.8 Rural areas above the limit value (LV) according to the interpolation of the 36th highest daily average value (left) and the number of exceedance days (right) for 2004, using ordinary cokriging with altitude.

It can be concluded that when geostatistical methods are used the size of the above-the-limit territory defined by the 36th maximum daily average value and by the number of exceedance days is comparable for the year tested, but not equivalent. In Chapter 6 a similar test is applied for 2003 data, a year with a larger spatial exceedance territory, as part of the study on the use of daily mean interpolations. In that case, regression with the EMEP model was used and the differences between the two methods become visible more significant. This indicates that the residual kriging methods may not lead to coincident above-the-limit territories. This aspect of the interpolations should be clearly determined in future studies.

5.2.7 Conclusions on the spatial interpolation for PM_{10}, rural areas

Various methods were used for spatial interpolation and were mutually compared using RMSE and other statistical indicators from cross-validation.

- The best results, with regard to RMSE, were obtained by the interpolation method using lognormal cokriging of monitoring data with altitude, method 2-d.
- The second best results were obtained by ordinary kriging of the residuals of the linear regression model, which uses EMEP model output, altitude, solar radiation and wind speed (method 3-P.2b-b). This method is similar to the method preferred in Horálek et al. (2005), with two small differences: the use of meteorological data instead of climatological data, and the additional inclusion of wind speed.
- For the final mapping of both PM_{10} indicators, the 36th maximum daily average value and the number of exceedance days, method 3-P.2b-b were selected for several reasons. Firstly, method 3-P.2b-b shows performances approaching the results of method 2-d. Secondly, only with the help of supplementary data is it possible to map the areas without measurement (e.g. rural map of Balkan). The third reason is better comparability with previous years results. In addition to this, the tests in Horálek et al. (2005) were executed for four years, i.e. the comparison of different methods is more robust.

- On the basis of cross-validation analysis the uncertainty of the constructed maps was estimated.
- Additionally, the two indicators for delimiting the area above the "daily" limit value, i.e. the 36th maximum daily average value and the number of exceedance days, were compared by using three different spatial interpolation methods. The conclusion is that the two indicators show similar results when only spatial interpolation is used. Type 3 methods using regression and residual interpolation were not tested. The differences are smaller than the differences in the interpolation methods used within each indicator type.

5.3 Rural areas - Ozone

A similar comparison as for PM_{10} was also carried out for ozone. Parameters relevant for human health (SOMO35 and the 26th highest daily maximum 8-hour average concentration) and for vegetation (AOT40 for crops and AOT40 for forests) were examined. First the relations between the measured values and various supplementary parameters were examined and individual linear regression models were compared. Furthermore individual interpolation methods were compared.

5.3.1 Comparison of linear regression models for rural ozone indicators

Several linear regression models (equation 2.1) are examined, for the different ozone indicators:

Submodel	Input parameters
O.1	EMEP dispersion model
O.2a	EMEP dispersion model, altitude, surface solar radiation, relative humidity
O.2b	EMEP dispersion model, altitude, relative humidity, wind speed
O.2c	EMEP dispersion model, altitude, surface solar radiation
O.2d	EMEP dispersion model, altitude, relative humidity
O.2e	EMEP dispersion model, wind speed
O.3a	altitude, relative humidity, surface solar radiation, wind speed
O.3b	altitude, relative humidity, surface solar radiation
O.3c	altitude, relative humidity, temperature
O.3d	altitude, surface solar radiation
O.3e	altitude, relative humidity

The input parameters into the stepwise selection are altitude, meteorological parameters (i.e. wind speed, surface solar radiation, temperature, relative humidity, total precipitation) and EMEP model output (only for submodel type 2 selection). The basic submodel of type 2 selected by stepwise selection of backward type is O.2b for SOMO35 and O.2a for both AOT40 parameters. To examine whether inclusion of several meteorological parameters results in substantial improvement of the models, also submodels of the type O.2c, O.2d and O.2e, each with only one meteorological parameter type, is included in the comparison.

The basic submodel of type 3 selected by stepwise selection of backward type is O.3b for SOMO35, submodel O.3a for AOT40 for crops, and submodel O.3c for AOT40 for forests. Supplementary comparison is carried out with the submodels O.3d and O.3e, where O.3d was best scoring on R^2 and RMSE. To limit the size of Table 5.10, only the better results for O.3d are included.

As for the 26th highest daily maximum 8-hour average value no EMEP model concentration field was available, the types 1 and 2 of the linear regression model could not be included in the comparison. The basic submodels of type 3 selected by stepwise selection of backward type is O.3f, supplemented by O.3g, are:

O.3f	altitude, temperature, relative humidity, wind speed
O.3g	altitude, relative humidity, wind speed

The performance of the different linear regression models is compared in Table 5.10 which gives the parameters *c, a1, ..., a6* for the different submodels on SOMO35. Furthermore, characteristics of R^2

and RMSE are presented for each submodel showing the closeness of the linear relation of the respective submodel with the measured air pollution values. The R^2 should be as close as possible to 1 and RMSE as low as possible. If a parameter is not statistically significant, this is indicated by "n. sign.".

Table 5.10 Comparison of different submodels of linear regression model equation 2.1 describing the relation between ozone measurement parameter SOMO35 for 2004 and different supplementary parameters in the rural areas.

lin. regr. model (2.1)	O.1	O.2a	O.2b	O.2c	O.2d	O.2e	O.3a=O3b	O.3c	O.3d
c (constant)	1214.6	22662	46866	-1450	41593	1039	31458	48800	-2171
a1 (altitude GTOPO30)	n. used	3.48	3.78	3.47	3.42	3.32	3.84	4.51	3.88
a2 (temperature 2004)	n. used	n. used	n. used	n. used	n. used	n. used	n. used	199	n. used
a3 (wind speed 2004)	n. used	n. used	348.0	n. used	n. used	n. used	n. sign.	n. used	n. used
a4 (rel. hum. 2004)	n. used	-241.0	-493.6	n. used	-420.6	n. used	-335.4	-498.2	n. used
a5 (s. solar rad. 2004)	n. used	238.3	n. used	366.5	n. used	n. used	415.7	n. used	620.1
a6 (EMEP model 2004)	0.95	0.40	0.54	0.43	0.48	1.40	n. used	n. used	n. used
R^2	**0.329**	**0.580**	**0.581**	**0.575**	**0.573**	**0.544**	**0.552**	**0.545**	**0.541**
adjusted R^2	**0.327**	**0.576**	**0.577**	**0.572**	**0.569**	**0.542**	**0.549**	**0.542**	**0.539**
RMSE [µg.m^{-3}.days]	**2410**	**1904**	**1902**	**1917**	**1921**	**1911**	**1966**	**1982**	**1991**

For SOMO35 (Table 5.10) the comparison of R^2 and RMSE for the submodels of types 1 and 2 shows quite clearly that the addition of supplementary parameters substantially improves the closeness of the regression relation with an increase of R^2 by 0.25 and a decreased RMSE by approximately one fifth. The comparison of submodels of type 2 and 3 shows the closeness of the linear relation, expressed by R^2 and RMSE, being naturally better in the case of submodels of type 2 using the EMEP model data. However, the difference is much smaller than in the case of PM_{10}, which indicates that the EMEP dispersion model output could be substituted by supplementary parameters for the major part, in case of necessity, using preferably submodel O.3b.

The submodels O.2a, O.2b, O.2c and O.2d give rather similar results with differences of R^2 less then 0.01. In the case of similar results the use of fewer parameters is preferred (see Section 2.5), resulting in the selection of submodels O.2c and O.2d, with preference for O.2c with its slightly better (higher) R^2 and the best (lowest) RSME for all types of submodels.

Table 5.11 presents the comparison of the individual types of the linear regression model equation 2.1 for the 26th highest daily maximum 8-hour average value of type 3 only. The types 1 and 2 could not be tested due to lacking EMEP model data. The best R^2 and RMSE values are achieved by submodel O.3f (altitude, temperature, wind speed, relative humidity), however, submodel O.3g (altitude, relative humidity, wind speed) has almost a similar R^2 (0.01 lower) against the advantage of using less parameters and is hence preferred.

Table 5.11 Comparison of different submodels of linear regression model equation 2.1 describing the relation between ozone measurement parameter 26th highest daily maximum 8-hour average values for 2004 and different supplementary parameters in the rural areas. Types 1 and 2 are not in due to lack of EMEP model data.

lin. regr. model (2.1)	O.3a	O.3b=O.3c=O.3e	O.3d	O.3f	O.3g
c (constant)	353.0	552.9	79.7	366.5	486.3
a1 (altitude GTOPO30)	0.0097	0.0133	0.0137	0.0121	0.0104
a2 (temperature 2004)	not used	n. sign.	not used	0.8	not used
a3 (wind speed 2004)	-2.90	not used	not used	-3.06	-2.45
a4 (rel. hum. 2004)	-2.58	-4.7	not used	-2.7	-3.9
a5 (s. solar radiation 2004)	1.17	n.sign.	3.1	not used	not used
R^2	**0.408**	**0.383**	**0.326**	**0.411**	**0.400**
adjusted R^2	**0.402**	**0.380**	**0.323**	**0.405**	**0.396**
RMSE [µg.m^{-3}]	**11.94**	**12.19**	**12.74**	**11.91**	**12.02**

The comparison of the R^2 in Table 5.10 with Table 5.11 shows that the closeness of the linear relation of the measured values with the linear regression model is remarkably worse in the case of the 26th highest daily maximum 8-hour average concentration. This may be caused by the lower spatial variability of this parameter.

Tables 5.12 and 5.13 present the comparison of individual types of linear regression model (equation 2.1) for AOT40 for crops and AOT40 for forests respectively. The comparison of results of the individual submodels for types 1, 2 and 3 for both AOT40 indicators lead to a conclusion similar to the one for SOMO35: the addition of supplementary parameters substantially improves the closeness of the regression relations with increases of R^2 by more than 0.2 and decreases RMSE by approximately one quarter. Output from the EMEP model can be replaced by other supplementary parameters with only minor loss of performance, using preferably submodel O.3b (which has a smaller number of parameters and only slightly worse R^2 in comparing with O.3a).

In case of AOT40 for crops the submodels of type 2 present overall the best R^2 and RMSE with best performing submodel O.2a, which is therefore the submodel of first preference. Submodel O.2d scores best for those with a lower number of supplementary parameters and could be used as second best alternative, since its R^2 is only 0.02 lower and it RSME is second lowest.

Table 5.12 Comparison of different submodels of linear regression model equation 2.1 describing the relation between ozone measurement parameter AOT40 for crops for 2004 and different supplementary parameters (in the rural areas).

lin. regr. model (2.1)	O.1	O.2a	O.2b=O.2c	O.2d	O.2e	O.3a	O.3b	O.3c	O.3e
c (constant)	n. sign.	186456	-16875	284234	5223	178894	225688	288571	388370
a1 (altitude GTOPO30)	n. used	7.38	7.41	7.21	5.65	7.28	8.65	11.19	8.77
a2 (temperature 2004)	n. used	n. used	n. used	n. used	n. used	n. used	n. used	792	n. used
a3 (wind speed 2004)	n. used	n. used	n. sign.	n. used	-1034	-1049	n. used	n. used	n. used
a4 (rel. hum. 2004)	n. used	-2032	n. used	-2962	n. used	-1931	-2451	-3041	-4011
a5 (s. solar rad. 2004)	n. used	1113	2209	n. used	n. used	1781	1579	n. used	n. used
a6 (EMEP model 2004)	1.32	0.47	0.57	0.56	1.94	n. used	n. used	n. used	n. used
R^2	**0.444**	**0.692**	**0.654**	**0.674**	**0.537**	**0.661**	**0.654**	**0.647**	**0.616**
adjusted R^2	**0.443**	**0.689**	**0.652**	**0.672**	**0.533**	**0.658**	**0.651**	**0.644**	**0.614**
RMSE [µg.m^{-3}.hours]	**7117**	**5283**	**5597**	**5431**	**6477**	**5538**	**5598**	**5659**	**5900**

As in the crops indicator, the AOT40 for forests shows the best results for both R^2 and RMSE at submodel O.2a. However, in this case the submodel O.2d scores best of those with a lower number of supplementary parameters, with a R^2 of only 0.007 lower and a RSME just above 1% higher, concluding that its use is preferred over O.2a, leading to similar rural mapping results.

Table 5.13 Comparison of different submodels of linear regression model equation 2.1 describing the relation between ozone measurement parameter AOT40 for forests for 2004 and different supplementary parameters (in the rural areas).

lin. regr. model (2.1)	O.1	O.2a	O.2b	O.2c	O.2d	O.2e	O.3a=O.3b	O.3c	O.3e
c (constant)	5259	292686	419567	-18799	397687	3406	362104	418045	559928
a1 (altitude GTOPO30)	n. used	14.01	15.39	14.22	13.87	13.92	16.23	19.79	16.33
a2 (temperature 2004)	n. used	n. used	n. used	n. used	n. used	n. used	n. used	1121	n. used
a3 (wind speed 2004)	n. used	n. used	1290	n. used	n. used	n. sign.	n. sign.	n. used	n. used
a4 (rel. hum. 2004)	n. used	-3111	-4408	n. used	-4115	n. used	-3832.5	-4351	-5732
a5 (s. solar rad. 2004)	n. used	1135	n. used	2843	n. used	n. used	1903.3	n. used	n. used
a6 (EMEP model 2004)	0.99	0.46	0.53	0.52	0.50	1.63	n. used	n. used	n. used
R^2	**0.402**	**0.654**	**0.652**	**0.621**	**0.647**	**0.533**	**0.598**	**0.601**	**0.577**
adjusted R^2	**0.400**	**0.651**	**0.648**	**0.618**	**0.644**	**0.531**	**0.595**	**0.598**	**0.575**
RMSE [µg.m^{-3}.hours]	**11968**	**9073**	**9110**	**9502**	**9167**	**10541**	**9782**	**9753**	**10039**

The results for SOMO35 and AOT40 for crops are similar to the findings in Section 4.2.5 of Horálek et al. (2005) on the selection of the most suitable supplementary data, but with the difference that we use now concurrent surface solar radiation instead of the 30-year averaged sunshine duration.

5.3.2 Comparison of linear regression models using meteorological or climatological data

Similar to PM_{10}, a comparison of individual submodels for ozone parameters was carried out with the use of both actual meteorological data ECMWF (year 2004) and climatic data (averages 1961–1990). All parameters are the same; however, the meteorological data for surface solar radiation are compared with climatological sunshine duration. The comparison, based on the coefficient of determination R^2, is presented in Tables 5.14 and 5.15. Unlike the case for PM_{10} the use of actual meteorological instead of climatological data yields only a small improvement. (One of the reasons can be that the lifetime of ozone is about 25 days; thus on the annual basis the spatial pattern can be reasonably well described with climatological data.) In addition Table 5.14 shows a poorer relation at the 26th highest daily maximum 8-hour average concentration than at all other ozone indicators.

Table 5.14 The comparison of submodels of linear regression model equation 2.1 for ozone parameters SOMO35 and 26th highest daily maximum 8-hour average concentration (both for 2004) with the use of meteo-parameters for the actual year 2004 (ECMWF), resp. 30-year averaged climatic data (CRU), using R2, for the rural areas. (No EMEP model data are available at the 26th highest daily max 8-hour average values and is greyed out).

type of regression model (2.1)	R^2 - SOMO35		R^2 - max. 26th highest 8h	
	clim_61-90	meteo_04	clim_61-90	meteo_04
O.2a (altit., rel. hum., sol.rad./sunsh.dur., EMEP)	0.57	0.58		
O.2b (altit., w.speed, rel. hum., EMEP)	0.56	0.58		
O.2c (altit., sol.rad./sunsh.dur., EMEP)	0.57	0.57		
O.2d (altit., rel. humidity, EMEP)	0.56	0.57		
O.2e (altit., wind speed, EMEP)	0.54	0.54		
O.3a (altit., rel. hum., sol.rad./sunsh.dur., w.sp.)	0.56	0.55	0.42	0.41
O.3b (altit., rel. hum., sol.rad./sunsh.dur.)	0.55	0.55	0.36	0.38
O.3c (altit., temperature, rel. hum.)	0.53	0.55	0.36	0.38
O.3d (altit., sol.rad./sunsh.dur.)	0.55	0.54	0.33	0.33
O.3e (altit., rel. hum.)	0.51	0.52	0.35	0.38
average	**0.55**	**0.56**	**0.36**	**0.38**

Table 5.15 The comparison of submodels of linear regression model equation 2.1 for the ozone parameters AOT40 for crops and for forests (both for 2004) with the use of meteo-parameters for the actual year 2004 (ECMWF), resp. 30-year averaged climatic data (CRU), using R2, for the rural areas.

type of regression model (2.1)	R^2 - AOT40 for crops		R^2 - AOT40 for forests	
	clim_61-90	meteo_04	clim_61-90	meteo_04
O.2a (altit., rel. hum., sol.rad./sunsh.dur., EMEP)	0.67	0.69	0.62	0.65
O.2b (altit., w.speed, rel. hum., EMEP)	0.63	0.65	0.60	0.65
O.2c (altit., sol.rad./sunsh.dur., EMEP)	0.67	0.65	0.62	0.62
O.2d (altit., rel. humidity, EMEP)	0.62	0.67	0.60	0.65
O.2e (altit., wind speed, EMEP)	0.53	0.54	0.53	0.54
O.3a (altit., rel. hum., sol.rad./sunsh.dur., w.sp.)	0.64	0.66	0.57	0.60
O.3b (altit., rel. hum., sol.rad./sunsh.dur.)	0.63	0.65	0.56	0.60
O.3c (altit., temperature, rel. hum.)	0.62	0.65	0.56	0.60
O.3d (altit., sol.rad./sunsh.dur.)	0.62	0.60	0.55	0.55
O.3e (altit., rel. hum.)	0.56	0.62	0.52	0.58
average	**0.62**	**0.64**	**0.58**	**0.60**

5.3.3 Conclusions on the linear regression models for rural ozone

Different submodels of linear regression model (equation 2.1) were examined for four ozone indicators; these being SOMO35, 26th highest daily maximum 8-hour average concentration, AOT40 for crops and AOT40 for forests for rural areas, using the output of the EMEP dispersion model and/or supplementary data. A number of conclusions are drawn.

- The use of supplementary data together with the EMEP dispersion model concentration field substantially improves the closeness of the regression relation with regard to both R^2 and RMSE.
- The use of actual meteorological instead of climatic data improves the closeness of the regression relation with regard to R^2. However, this improvement is only small compared to the results at PM_{10}.
- For indicators for which output from the EMEP model were available, the best regression results were obtained with the submodels:
  - O.2c (EMEP model output, altitude and surface solar radiation) for SOMO35
  - O.2a (EMEP model output, altitude, surf. solar radiation and relative humidity) for AOT40 for crops
  - O.2d (EMEP model output, altitude and relative humidity) for AOT40 for forests.

  However, the results of these three submodels are quite similar for all three indicators, thus all three will be subsequently examined when comparing different spatial interpolation methods in Section 5.3.4.
- The comparison of submodels with and without output from the Unified EMEP model shows that the EMEP model output can to a large extent be replaced by other supplementary parameters if required.
- The preferred submodel for the 26th highest daily maximum 8-hour average concentration (for which output from the EMEP model was not available) was found to be:
  - O.3g (altitude, relative humidity and wind speed).

  This submodel is thus further examined in the next section on the spatial interpolation comparisons for this indicator. In addition, this comparison also includes submodel O.3b (altitude, surface solar radiation and relative humidity), which would be preferred for SOMO35 and AOT40 for crops if model output was not available for these parameters.

5.3.4 Comparison of spatial interpolation methods for rural ozone

Several methods were used in spatial interpolation. These methods were subsequently compared on the basis of the RMSE and other cross-validation parameters. For comparison, various types of linear regression model without interpolation (according to Section 5.3.1) are also presented. The compared methods are as follows:

1. Linear regression model, without interpolation

   O.1 EMEP model output
   O.2a EMEP model output, altitude, surface solar radiation, relative humidity
   O.2c EMEP model output, altitude, surface solar radiation
   O.2d EMEP model output, altitude, relative humidity
   O.3b altitude, relative humidity, surface solar radiation
   O.3g altitude, relative humidity, wind speed

2. Interpolation methods using primarily monitoring data

   a. IDW
   b. Ordinary kriging (OK) – parameters of variogram selected automatically (b1) and manually fitted (b2)
   c. Ordinary cokriging (OC) – parameters of variogram selected automatically (c1) and manually fitted (c2)

3. Interpolation of the residuals of linear regression, using the interpolation methods

   a. IDW
   b. Ordinary kriging (OK) – parameters of variogram selected automatically (b1) and manually fitted (b2)

Neither lognormal kriging nor lognormal cokriging is used for the following reasons: The three ozone indicators (namely SOMO35, AOT40 for crops and AOT40 for forests) can give zero values, which makes the logarithmic transformation impossible. The fourth parameter, i.e. 26^{th} highest daily maximum 8-hour value does not have a spatial lognormal distribution.

For the human health indicator SOMO35, Figure 5.9 shows the cross-validation scatter plot for several interpolation methods using primarily monitoring data (i.e. only for interpolation methods of type 2). The best results of examined methods (using R^2) are obtained by ordinary cokriging with the optimisation of variogram parameters using RMSE minimization. The plots show, similarly to the PM_{10} indicators, that the high concentrations are underestimated by the interpolation. This underestimation of high values is the smallest in case of ordinary cokriging, for manually fitted parameters.

The other human health ozone indicator examined is the 26^{th} highest daily maximum 8-hour value. Figure 5.10 shows the cross-validation scatter plots for this indicator for different interpolation methods using primarily monitoring data. In comparing SOMO35 to the other ozone health-related indicators, the 26^{th} highest daily maximum 8-hour value gives the lower R^2 in the cross-validation scatter plots, see Figures 5.9 and 5.10.

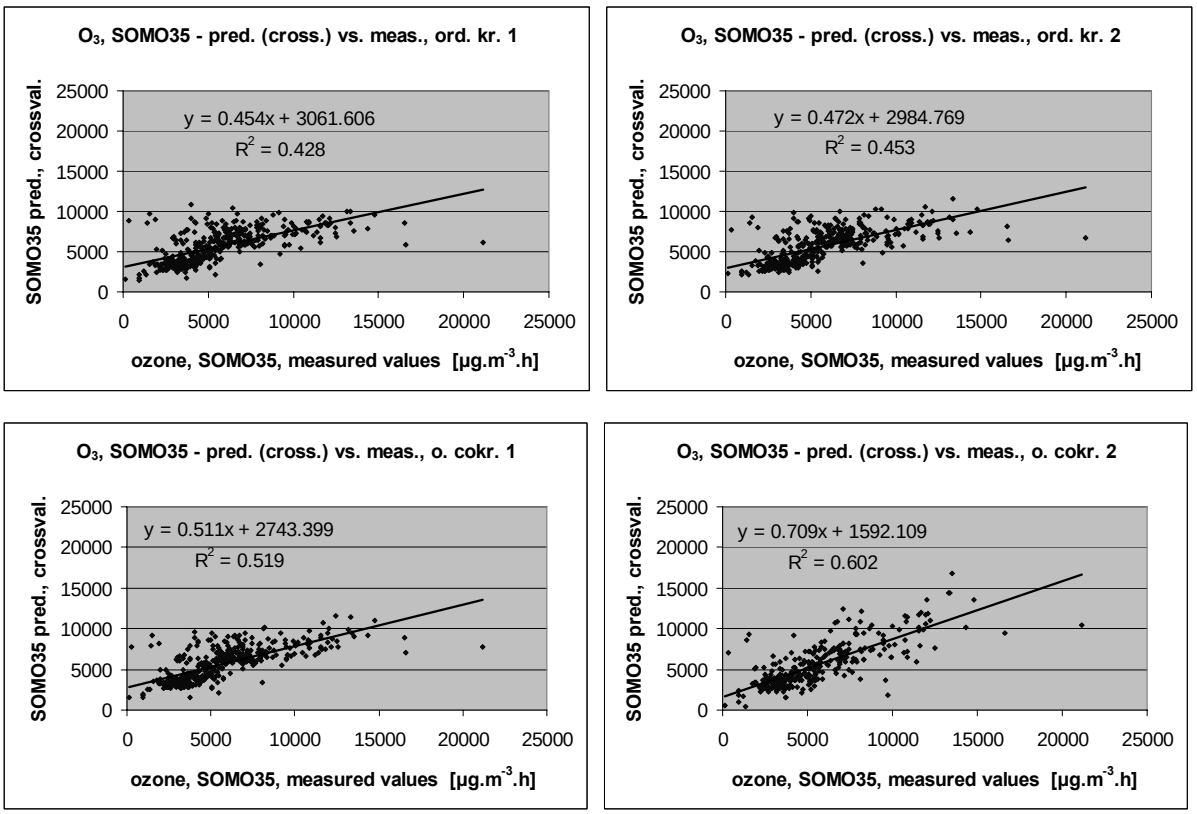

Figure 5.9 Correlation between cross-validation predicted values (y-axis) and measurements (x-axis) for the ozone indicator SOMO35 for 2004 in rural areas, for ordinary kriging (top) and ordinary cokriging using altitude (bottom), with parameters of variogram estimated automatically (left) and manually (right).

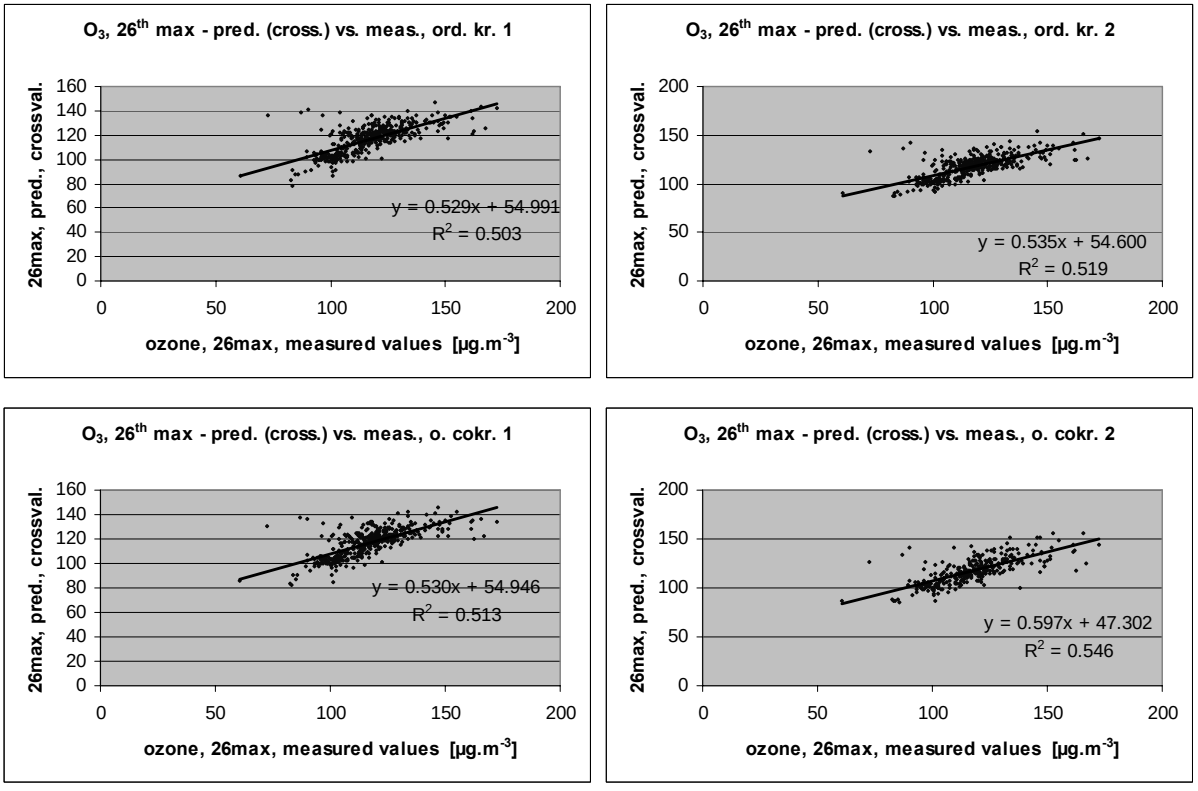

Figure 5.10 Correlation between cross-validation predicted values (y-axis) and measurements (x-axis) for the 26th highest max. 8-hr daily ozone for rural areas in 2004, for ordinary kriging (top) and ordinary cokriging using altitude (bottom), with parameters of variogram estimated automatically (left) and manually (right).

The cross-validation scatter plots for AOT40 for crops for different interpolation methods using primarily monitoring data are presented in Figure 5.11.

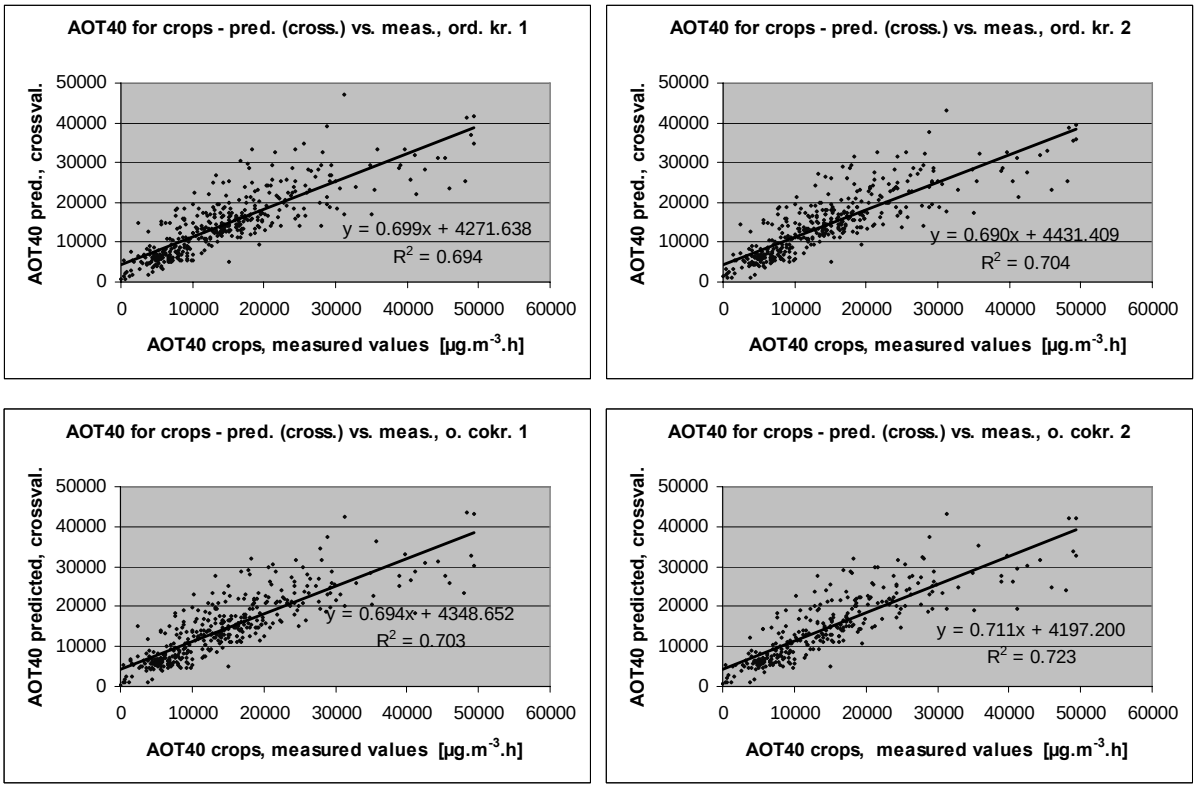

Figure 5.11 Correlation between cross-validation predicted values (y-axis) and measurements (x-axis) for ozone accumulation indicator AOT40 for crops for 2004 in rural areas, for ordinary kriging (top) and ordinary cokriging using altitude (bottom), with parameters of variogram estimated automatically (left) and manually (right).

In Figure 5.12 the cross-validation scatter plots for AOT40 for forests are presented for different interpolation methods using primarily monitoring data.

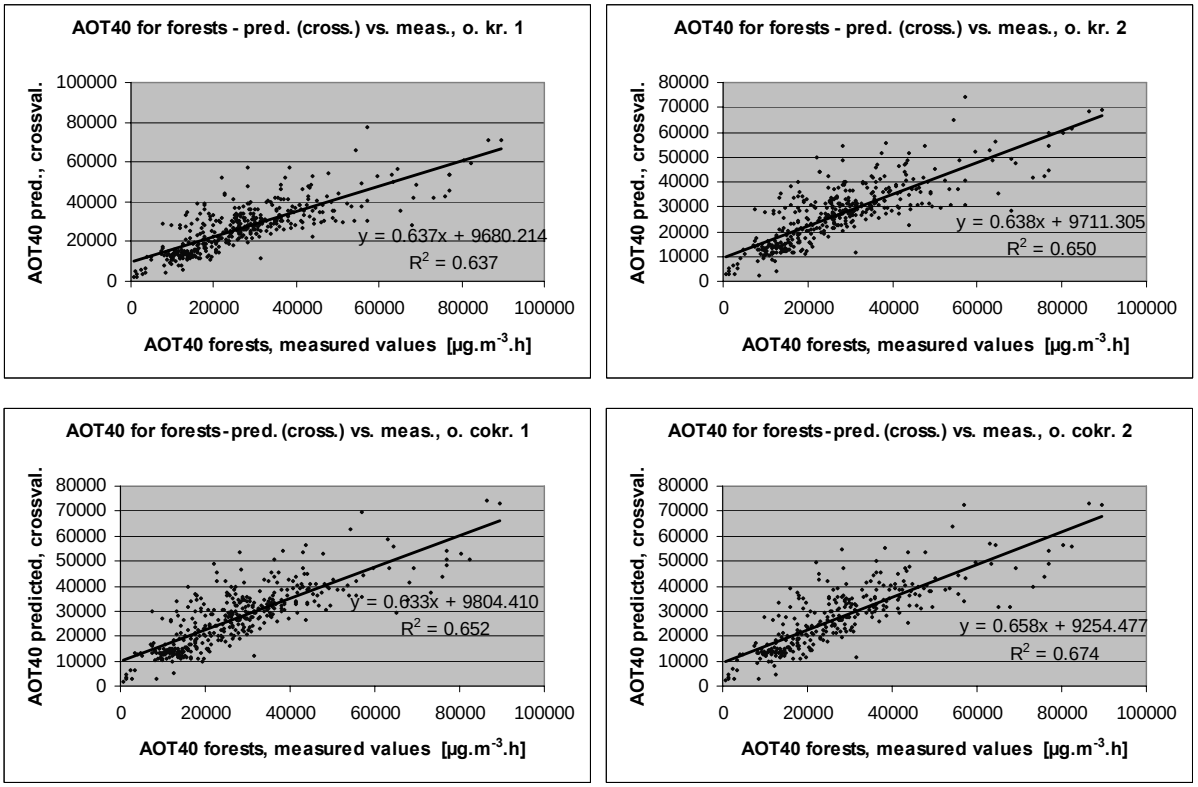

Figure 5.12 Correlation between cross-validation predicted values (y-axis) and measurements (x-axis) for the AOT40 for forests for 2004 in rural areas, for ordinary kriging (top) and ordinary cokriging using altitude (bottom), with parameters of variogram estimated automatically (left) and manually (right).

The comparison of all methods was carried out using the RMSE and other cross-validation parameters and is presented in Table 5.16.

Table 5.16 Comparison of different interpolation methods showing RMSE and the other statistical indicators for ozone indicators SOMO35, 26th highest daily maximum 8-hour average value, AOT40 for crops and AOT40 for forests (for the year 2004, rural areas). The smaller RMSE means the more accurate estimation by the mapping method. Similarly, SD, MAE, MedAE and MPSE should be as small as possible; MPE, minimum error and maximum error should be as near to zero as possible; R^2 should be as close to 1 as possible. Apart of R^2, all other statistical indicators are in the units of relevant ozone parameters.

mapping method		SOMO35 [µg.m^{-3}.d]									26th maximum daily 8-hour mean [µg.m^{-3}]								
		RMSE	MPE	SD (error)	min (error)	max (error)	MAE	MedAE	R^2	MPSE	RMSE	MPE	SD (error)	min (error)	max (error)	MAE	MedAE	R^2	MPSE
1-O.1	lin. regr. O.1	2410	2	2410	-9930	10275	1709	1300	0.329										
1-O.2a	lin. regr. O.2a	1904	0	1904	-6999	7487	1304	857	0.580										
1-O.2c	lin. regr. O.2c	1917	0	1917	-6879	7170	1337	925	0.575										
1-O.2d	lin. regr. O.2d	1921	0	1921	-7254	8180	1300	862	0.573										
1-O.3b	lin. regr. O.3b	1966	0	1966	-6010	6858	1350	901	0.552		12.19	0.00	12.19	-44.50	23.24	8.90	7.02	0.383	
1-O.3g	lin. regr. O.3g										12.02	0.00	12.02	-43.31	24.08	8.80	6.81	0.400	
2-a	interp. IDW	2247	-24	2247	-14982	8273	5688	5130	0.416		11.23	0.27	11.23	-42.65	63.65	116.79	116.63	0.478	
2-b1	interp. OK-aut	2225	-47	2225	-15064	8577	1447	884	0.428	1943	10.96	-0.07	10.96	-41.90	63.12	7.39	4.92	0.503	10.44
2-b2	interp. OK-fit	2175	-20	2175	-14398	7786	1446	945	0.453	2112	10.78	0.27	10.78	-40.94	60.16	7.43	5.24	0.519	10.50
2-c1	interp. OC-aut (altit.)	2038	-36	2038	-13357	7711	1374	868	0.519	1824	10.84	0.02	10.84	-45.11	57.97	7.42	4.80	0.513	10.13
2-c2	interp. OC-fit (altit.)	1872	-70	1871	-10689	7844	1265	901	0.602	473	10.51	0.01	10.51	-44.79	54.70	7.29	5.11	0.548	7.91
3-O.1-a	lin. regr. O.1 + IDW	2330	-59	2329	-15874	9414	1709	1300											
3-O.1-b1	lin. regr. O.1 + OK-aut	2321	-50	2321	-15182	9729	1534	981		2046									
3-O.1-b2	lin. regr. O.1 + OK-fit	2261	-46	2261	-14969	9201	1505	951		2027									
3-O.2a-a	lin. regr. O.2a + IDW	1955	-78	1954	-12818	8426	1304	857											
3-O.2a-b1	lin. regr. O.2a + OK-aut	1915	-39	1914	-12565	8025	1258	854		1639									
3-O.2a-b2	lin. regr. O.2a + OK-fit	1880	-41	1880	-12526	7836	1245	800		1659									
3-O.2c-a	lin. regr. O.2c + IDW	1943	-69	1942	-12704	8441	1337	925											
3-O.2c-b1	lin. regr. O.2c + OK-aut	1908	-37	1908	-12477	8045	1253	838		1663									
3-O.2c-b2	lin. regr. O.2c + OK-fit	1865	-38	1865	-12373	7793	1237	805		1667									
3-O.2d-a	lin. regr. O.2d + IDW	1993	-92	1990	-13034	8432	1300	862											
3-O.2d-b1	lin. regr. O.2d + OK-aut	1948	-44	1947	-12721	8086	1280	878		1635									
3-O.2d-b2	lin. regr. O.2d + OK-fit	1919	-51	1919	-12746	7872	1269	842		1724									
3-O.3b-a	lin. regr. O.3b + IDW	1931	-66	1930	-12251	8316	1350	901			11.03	-0.01	11.03	-43.39	55.71	8.90	7.02		
3-O.3b-b1	lin. regr. O.3b + OK-aut	1896	-31	1896	-12218	7806	1253	865		1636	10.84	0.03	10.84	-43.74	54.81	7.36	5.10		10.16
3-O.3b-b2	lin. regr. O.3b + OK-fit	1855	-29	1855	-12059	7574	1242	831		1650	10.68	0.20	10.67	-42.22	53.49	7.43	5.14		10.17
3-O.3g-a	lin. regr. O.3g + IDW										11.22	-0.04	11.22	-41.72	56.73	8.80	6.81		
3-O.3g-b1	lin. regr. O.3g + OK-aut										11.04	0.04	11.04	-41.99	56.10	7.56	5.16		10.19
3-O.3g-b2	lin. regr. O.3g + OK-fit										10.85	0.18	10.85	-40.74	54.38	7.63	5.26		10.23

(Table 5.16 continued at next page)

(Table 5.16 continued)

mapping method		AOT40 for crops [µg.m^{-3}.hours]									AOT40 for forests [µg.m^{-3}.hours]								
		RMSE	MPE	SD (error)	min (error)	max (error)	MAE	MedAE	R^2	MPSE	RMSE	MPE	SD (error)	min (error)	max (error)	MAE	MedAE	R^2	MPSE (st. err.)
1-O.1	lin. regr. O.1	7117	-245	7112	-28032	16859	5277	3994	0.444		11968	-6	11968	-50025	28194	8763	6697	0.402	
1-O.2a	lin. regr. O.2a	5283	0	5283	-25534	15795	3576	2516	0.692		9073	0	9073	-39322	25935	6439	4749	0.654	
1-O.2c	lin. regr. O.2c	5597	0	5597	-25797	15367	3943	2755	0.654		9502	0	9502	-37864	26572	6970	5210	0.621	
1-O.2d	lin. regr. O.2d	5431	0	5431	-26047	16848	3708	2573	0.573		9167	0	9167	-45295	26901	6458	4809	0.647	
1-O.3b	lin. regr. O.3b	5598	0	5598	-29890	17142	3769	2545	0.552		9782	0	9782	-48749	33006	6838	4733	0.598	
1-O.3g	lin. regr. O.3g																		
2-a	interp. IDW	5395	3	5395	-23268	12636	14420	13151	0.680		9546	40	9546	-34769	27532	27077	25743	0.619	
2-b1	interp. OK-aut	5274	-67	5273	-22802	15677	3624	2179	0.694	4955	9313	-156	9311	-40014	30100	6512	4491	0.637	8849
2-b2	interp. OK-fit	5187	-37	5187	-22814	13935	3551	2120	0.704	5349	9146	-90	9146	-39667	27825	6405	4331	0.650	9053
2-c1	interp. OC-aut (altit.)	5195	-70	5194	-24815	14351	3598	2212	0.703	4786	9126	-132	9125	-35565	26941	6440	4260	0.652	8536
2-c2	interp. OC-fit (altit.)	5158	-79	5158	-24056	14298	3566	2166	0.723	5195	9062	-178	9060	-36568	27575	6389	4232	0.674	8765
3-O.1-a	lin. regr. O.1 + IDW	6014	251	6009	-18112	24109	5277	3994			10930	404	10925	-38528	40325	9130	7011		
3-O.1-b1	lin. regr. O.1 + OK-aut	5991	121	5990	-18632	24023	4189	2600		5498	11000	323	10998	-39573	42795	7737	5236		10545
3-O.1-b2	lin. regr. O.1 + OK-fit	5923	53	5923	-19542	23935	4140	2539		4698	10900	447	10896	-39928	45227	7706	5289		10395
3-O.2a-a	lin. regr. O.2a + IDW	4944	207	4940	-15097	23449	3576	2516			9486	409	9478	-41816	31957	6874	4868		
3-O.2a-b1	lin. regr. O.2a + OK-aut	4854	60	4854	-16240	23567	3378	2221		4372	9409	226	9406	-43458	32801	6550	4509		8942
3-O.2a-b2	lin. regr. O.2a + OK-fit	4854	61	4854	-16274	23519	3379	2222		4426	9367	225	9364	-43288	32649	6568	4687		8910
3-O.2c-a	lin. regr. O.2c + IDW	5042	156	5039	-15658	23878	3943	2755			9397	328	9391	-34883	32783	7383	5309		
3-O.2c-b1	lin. regr. O.2c + OK-aut	4931	48	4930	-16998	23348	3426	2370		4502	9321	192	9319	-37023	32943	6567	4649		9121
3-O.2c-b2	lin. regr. O.2c + OK-fit	4930	46	4930	-17128	23303	3427	2389		4411	9285	308	9280	-36146	35019	6612	4802		9285
3-O.2d-a	lin. regr. O.2d + IDW	5082	267	5075	-15115	23385	3708	2573			9687	469	9676	-44223	34280	6901	4912		
3-O.2d-b1	lin. regr. O.2d + OK-aut	4994	81	4993	-15943	23117	3501	2346		4437	9616	260	9612	-46061	35565	6687	4706		8978
3-O.2d-b2	lin. regr. O.2d + OK-fit	4994	74	4994	-16072	23033	3502	2400		4332	9576	266	9572	-45841	34089	6694	4842		8957
3-O.3b-a	lin. regr. O.3b + IDW	4953	138	4951	-15678	25447	3769	2545			9430	273	9426	-42068	35909	7255	4869		
3-O.3b-b1	lin. regr. O.3b + OK-aut	4866	27	4866	-16949	25882	3388	2408		4357	9349	111	9348	-43524	36890	6484	4471		8928
3-O.3b-b2	lin. regr. O.3b + OK-fit	4863	26	4863	-17001	25816	3387	2415		4356	9295	92	9295	-43933	36195	6472	4618		9003
3-O.3g-a	lin. regr. O.3g + IDW																		
3-O.3g-b1	lin. regr. O.3g + OK-aut																		
3-O.3g-b2	lin. regr. O.3g + OK-fit																		

In Figures 5.13 to 5.16 the resulting European maps are shown for SOMO35, 26th highest daily maximum 8-hour average and the two AOT40 indicators based on the two best methods of interpolation of the particular indicators. Visually the maps are very similar with extra detail visible in the residual maps chiefly due to the inclusion of altitude in the regression model.

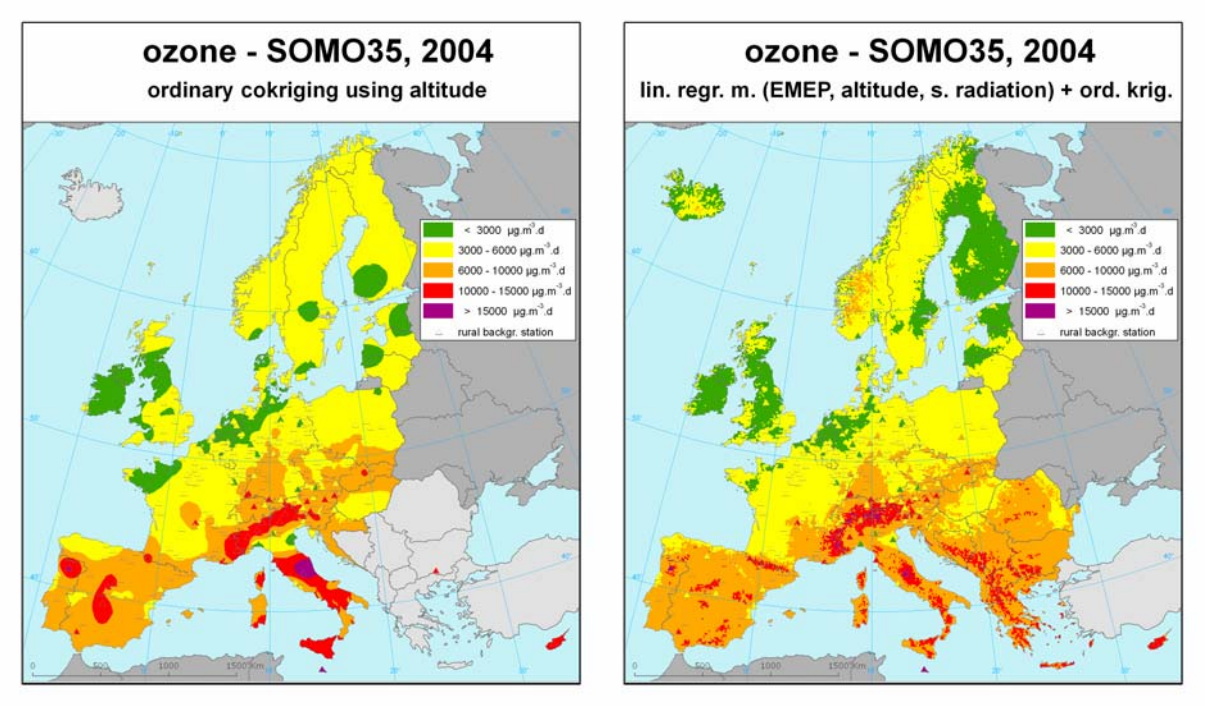

Figure 5.13 Maps showing values of ozone parameter SOMO35 (in µg.m^{-3}.days) on European scale for rural areas in 2004, 10 x 10 km grid resolution, as a result of interpolation method 2-c2 (left) and 3-O.2c-b2 (right). The uncertainty of these maps expressed by RMSE is 1872 µg.m^{-3}.days (left) and 1865 µg.m^{-3}.days (right).

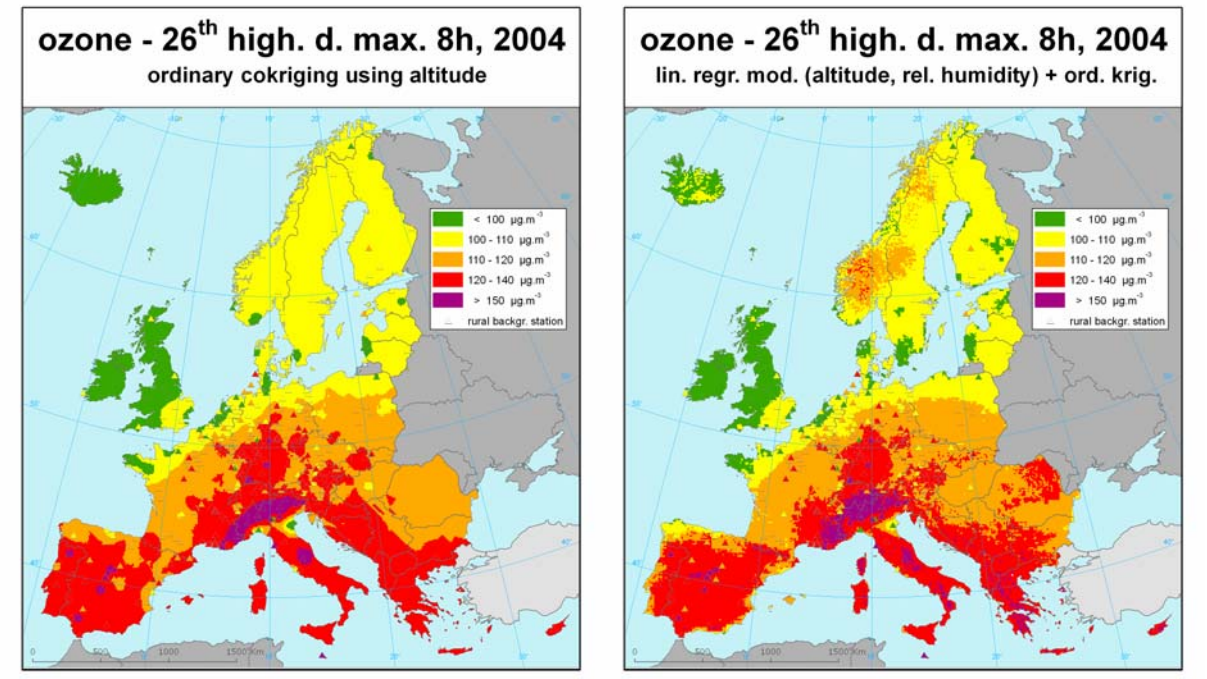

Figure 5.14 Maps showing values of ozone parameter 26th highest daily maximum 8-hour average values (in µg.m^{-3}) on European scale for rural areas in 2004, 10 x 10 km grid resolution, as a result of

interpolation method 2-c2 (left) and 3-O.3b-b2 (right). Uncertainty of these maps expressed by RMSE is 10.5 µg.m^{-3} (left) and 10.7 µg.m^{-3} (right).

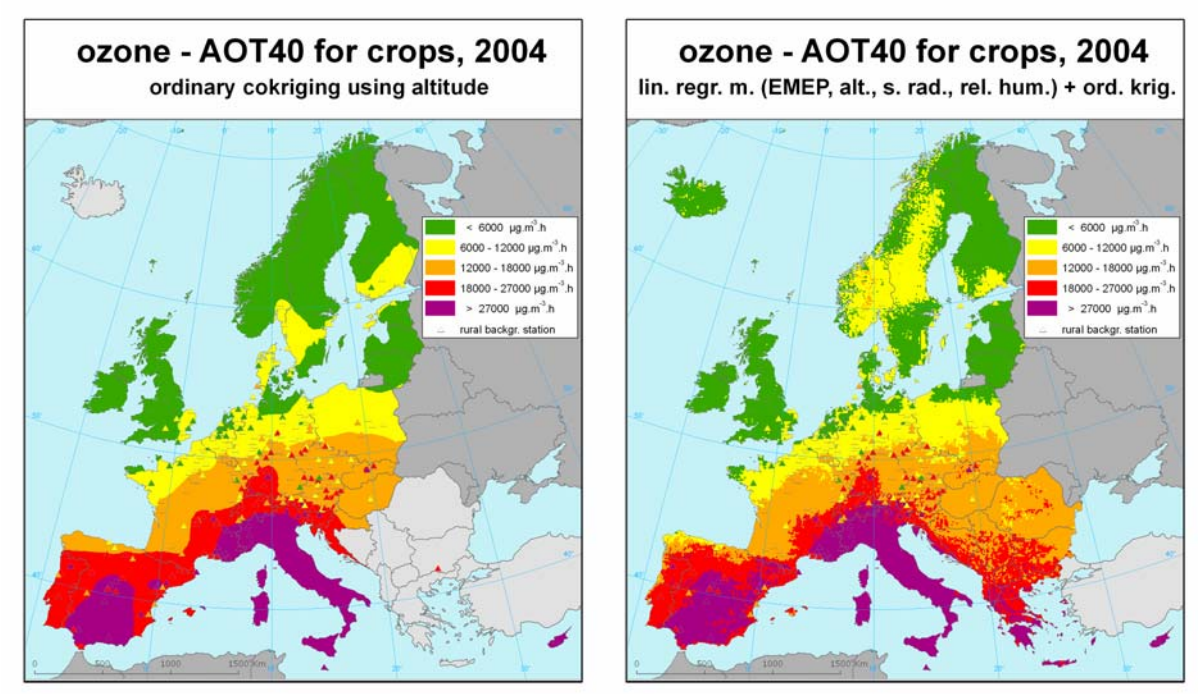

Figure 5.15 Maps showing values of ozone parameter AOT40 for crops (in µg.m^{-3}.h) on European scale for rural areas in 2004 in 10 x 10 km grid resolution as a result of interpolation method 2-c2 (left) and 3-O.2a-b2 (right). Uncertainty of these maps expressed by RMSE is 5158 µg.m^{-3}.hour (left) and 4854 µg.m^{-3} .hour (right).

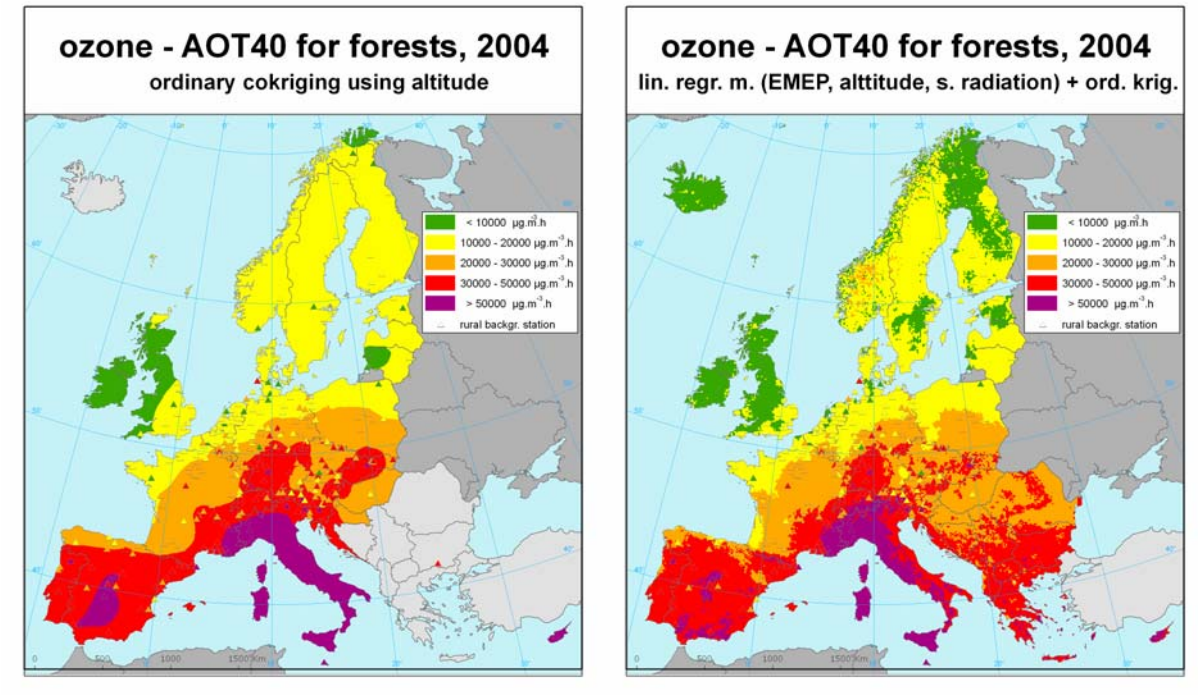

Figure 5.16 Maps showing values of ozone parameter AOT40 for crops (in µg.m^{-3}.h) on European scale for rural areas in 2004 in 10 x 10 km grid resolution as a result of interpolation method 2-c2 (left) and 3-O.2c-b2 (right). Uncertainty of these maps expressed by RMSE is 9062 µg.m^{-3}.hour (left) and 9285 µg.m^{-3}.hour (right).

The following specific conclusions are drawn:

- The use of interpolation methods, both interpolation using primarily monitoring data (type 2) and interpolation of the residuals of linear regression models (type 3), give better results with regard to RMSE (and all other statistical indicators with exception of MPE) than the methods using linear regression models without interpolation (type 1).
- In the case of interpolation methods of type 2, the best results based on RMSE (and also SD, MAE, R^2, MPSE) for both health-related indicators are obtained with ordinary cokriging with the use of altitude, method 2-c. The same method is the best also for the both AOT40 indicators, based on RMSE and also SD, MAE, MedAE and R^2. This confirms the results presented in Horálek et al. (2005) where SOMO35 and AOT40 for crops were examined.
- In the case of interpolation of residuals of the linear regression, type 3, the best results for AOT40 for forests are achieved by method 3-O.2c-b (based on RMSE and SD; based on MAE and MPSE it would be 3-O.2a-b) and for AOT40 for crops by the method 3-O.2a-b (based on RMSE, SD, MAE, MedAE). In case of the 26th highest daily maximum 8-hour average value (for which output from the EMEP model was not available) the best method is 3-O.3b-b (based on RMSE and almost all other statistical indicators). For SOMO35 the results of the method 3-O.3b-b (better by RMSE, SD, MPSE) and the method 3-O.2c-b (better by MAE, MedAE) are almost the same. In comparison with the results presented in the Horálek et al. (2005) the main difference is that meteorological data were used instead of climatological fields.
- In case of SOMO35 and AOT40 for crops the results are in agreement with the submodel selection of Section 5.3.1, whereas for the 26th highest daily maximum 8-hour average value and AOT40 for forests interpolation methods were selected based on different regression submodels compared to the submodels selected in Section 5.3.1.
- When comparing the setting of variogram parameters, the manual optimization using RMSE is the best (naturally) based on RMSE, but also based ona majority other indicators. This leads to selection of this methodology for setting these parameters.
- Mutual comparison of the best methods of the respective types shows that for SOMO35 (based on RMSE and almost all other indicators) and AOT40 for crops (based on RMSE, MAE, MPSE) better results are obtained with methods based on interpolation of residuals of linear regression models (type 3). However, in case of SOMO35 the difference between using type 2 or type 3 is only small with regard to the RMSE. In case of the 26th highest daily maximum 8-hour average value and AOT40 for forests interpolation methods of type 2 give in general somewhat better results (in both cases based on RMSE and almost all other indicators).
- The maps created by the best (or almost best) methods of types 2 (i.e 2-c2) and 3 (i.e. 3-O.2c-b2 in the case of SOMO35 and AOT40 for forests, 3-O.3b-b2 in the case of 26th highest maximum 8-hour daily value and 3-O.2a-b2 in the case of AOT40 for crops) are presented in Figures 5.13-5.16.

The uncertainty of the ozone maps can be expressed by RMSE (i.e. the most common indicator, see Table 5.16), in units relevant to the given indicator. Alternatively, this uncertainty can also be expressed as percentage of the mean of the values of relevant indicator across all stations. The relative uncertainty of the rural SOMO35 map is 32.8% for the method 2-c2 and 32.9% for the method 3-O.2c-b2. The relative uncertainty of the rural map of 26th highest maximum 8-hour daily value is 9% for the method 2-d2 and 9.1% for the method 3-O.3b-b2. The relative uncertainty of the map of AOT40 for crops is 33.7% for the method 2-c2 and 35.8% for the method 3-O.2a-b2. The relative uncertainty of the map of AOT40 for forests is 33.5% for the method 2-c2 and 34.3% for the method 3-O.2c-b2.

5.3.5 Conclusions on the spatial interpolation for ozone, rural areas

Various methods were used for the spatial interpolation and were mutually compared using RMSE and other statistical indicators from cross-validation, for all four examined ozone indicators. General conclusions to be drawn are:

- It is verified that the use of interpolation methods, both interpolation using primarily monitoring data (type 2) and interpolation of the residuals of linear regression models (type 3), give better results with regard to RMSE than the methods using linear regression models without interpolation
- The best results for SOMO35 were obtained with method 3-O.3b-b and almost the same results are given by method 3-O.2c-b2. Due to this non significant difference in RMSE (< 1%) for the final mapping method 3-O.2c-b was selected to allow for comparison with last year's results, since the same method as was selected in Horálek et al. (2005).
- The best results for 26th highest daily maximum 8-hour average value were obtained by interpolation method 2-c, i.e. ordinary cokriging using altitude. This method was selected for the final mapping.
- The best results for AOT40 for crops are given by 3-O.2a-b, whereas the best results for AOT40 for forests are given by ordinary cokriging with the use of altitude, method 2-c. However, for methodologically consistency and compatibility between the two AOT40 indicators it is preferred to select only one common method for the mapping. The selected method is 2-c, despite its reduced performance (6% higher RMSE than best performer) in the interpolation for AOT40 for crops. The main reasons to choose this method is to assure the continuity in indicator assessments made in previous years on past years (1996-2003) and it is the best performing method for AOT40 for forest.

5.4 Rural areas - NO_x

NO_x is a pollutant monitored with regard to its negative impact on vegetation. In the first Daughter Directive a limit value of 30 µg.m^{-3} as annual mean has been set for the protection of vegetation.

However, a preliminary analysis showed that for a large number of stations NO_x is measured but not reported as such, but separately as NO and NO_2. If this is the case (e.g. Spain, France and Germany) we have calculated the NO_x concentrations. In this way the 82 rural background stations reporting NO_x are extended with 189 stations with NO_x data calculated from the reported NO and NO_2 concentrations, according to the equation:

$$NO_x = NO_2 + 46/30.NO \qquad (5.1)$$

where all components are expressed in µg.m^{-3}, with a molecular mass for NO of 30 and for NO_2 of 46 g.mol^{-1}.

However, even after the addition of this set of stations there are still a number of countries without reported NO_x measurements for 2004 at the rural background stations in AirBase: Norway, Finland, Sweden, United Kingdom, Estonia, Lithuania, Latvia and Poland. For several of these countries there are NO_2 stations, but no NO stations (in total 23 stations). Since these countries together show quite large spatial gaps in Europe, it led to the idea try to translate NO_2 into NO_x to fill in some of these gaps. The next section explains how the conversion is calculated. One can examine for the station set that does measure NO_2, but no NO, the mutual regression relation between NO_x and NO_2 and learn whether NO_2 concentrations can be used for the construction of the NO_x field.

5.4.1 Relationships between NO_2 and NO_x data

Primarily, the mutual regression relation between NO_2 and NO_x was examined independent of the geographical distribution over Europe. Figure 5.17 shows the strong regression relation with a coefficient of determination $R^2 = 0.95$, meaning 95 % of variability is explained by linear regression.

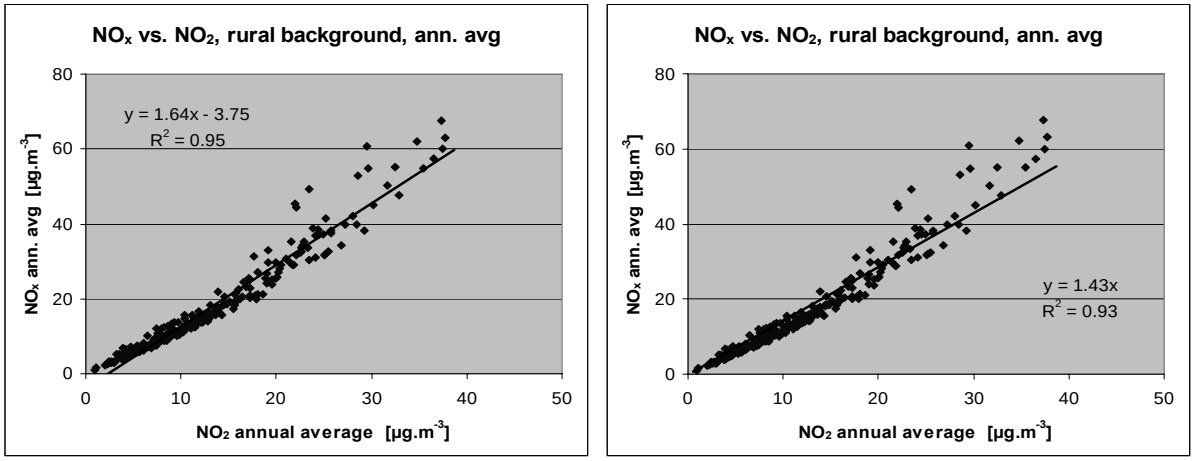

Figure 5.17 The graphs represent the results of the linear regression with (left) and without (right) intercept indicating the level of correlation between the annual averages of NO_x (y-axis) versus NO_2 (x-axis) in 2004 for rural background stations.

However it also becomes clear from the left-hand graph of Figure 5.17 that the linear correlation becomes weaker at higher concentrations. Therefore the dependence of the NO_x/NO_2 ratio on the NO_x concentration was examined. The left-hand graph of Figure 5.18 shows that at increasing NO_x concentrations the ratio increases (i.e. the share of NO, which contributes to the NO_x concentrations value, is increasing). This is likely the effect of photo-stationary equilibrium with ozone that directly affects this ratio. It is therefore not possible to apply the same ratio, and consequently the same regression coefficient, to random concentrations. It seems more appropriate to use, instead of the regression type $y = ax + b$, the quadratic regression $y = ax^2 + bx + c$. The right-hand graph of Figure 5.18 shows that this quadratic fit indeed corresponds better to the measurements of NO_x and NO_2.

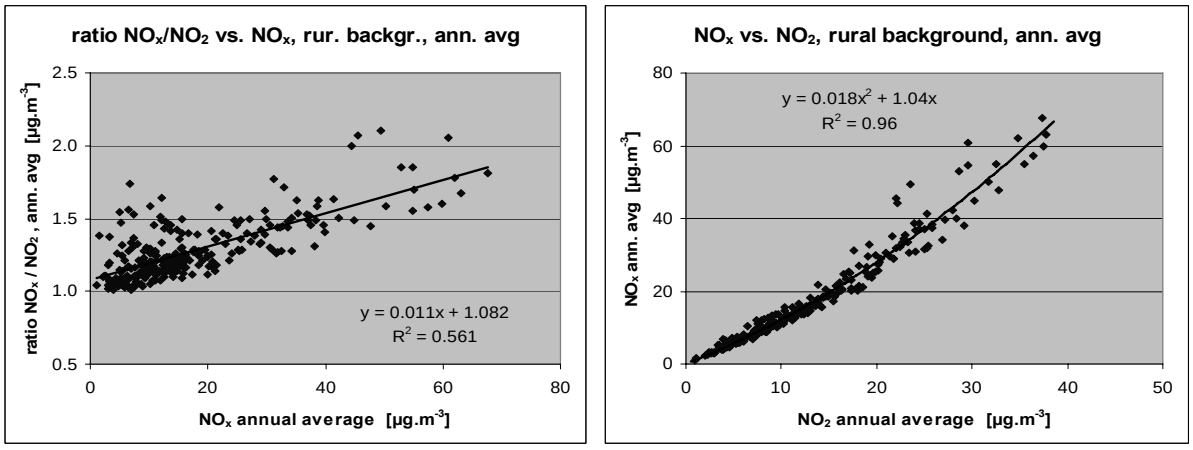

Figure 5.18 The graphs represent the results of the linear regression of the type $y = ax + b$ (left) and $y = ax^2 + bx + c$ (right) indicating the level of correlation between the ratio NO_x/NO_2 (y-axis) and NO_x (x-axis) (left) and between of NO_x (y-axis) versus NO_2 (x-axis) (right) for the 2004 annual averages of the rural background stations.

Before applying this result, the dependence between NO_2 and NO_x was examined for the individual European regions as used in EEA ozone reports (e.g. EEA, 2006). Figure 5.19 shows that although the regression relation in the individual European regions is slightly different, the closeness of this relation is high in all four regions investigated.

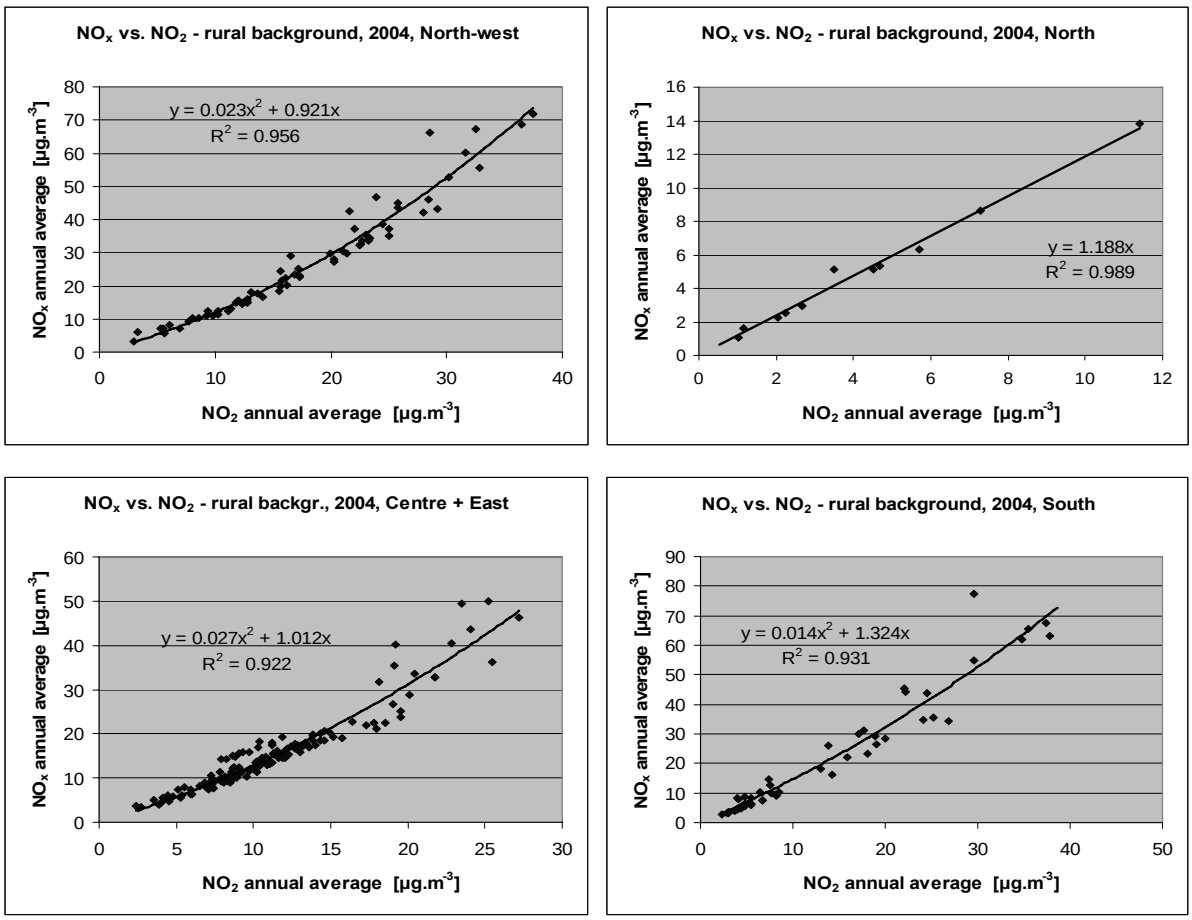

Figure 5.19 The graphs represent the results of the regression of the type $y = ax^2 + bx + c$ indicating the level of correlation between the annual averages of NO_x (y-axis) versus NO_2 (x-axis), for the year 2004, for rural background stations in the North-west (top-left), North (top-right), Centre + East (bottom-left) and South (bottom-right) regions of Europe.

It can be concluded that NO_2 and NO_x concentrations show sufficiently close regression relation. At the stations that do not measure NO_x (in total 23 stations), NO_2 concentrations were therefore used to estimate the corresponding NO_x levels. The recalculation was carried out separately for the four regions with the use of the regression relations found.

5.4.2 Comparison of linear regression models for rural NO_x

Two different submodels of linear regression model (equation 2.1) are examined:

Submodel	Input parameters
N.1	EMEP dispersion model
N.2	EMEP model output, altitude

The correlation between NO_x and meteorological parameters was not examined further, since the priority in this project was focussed on such examinations for PM_{10} and ozone indicators. The examination of correlation with meteorological parameters including pressure is possibly a task for future activities.

The relationship between measurements and output from the Unified EMEP model was examined, separately for the set of 271 stations (NO_x measurement only) and for the set of 294 stations (both NO_x measurements and recalculated NO_2). Table 5.17 shows that both cases give quite poor correlation.

Table 5.17 Comparison of different submodels of linear regression model equation 2.1 describing the relation between NO_x annual average for 2004 and different supplementary parameters.

linear regression model 2.1	NO_x only		NO_x and NO_2 recalc.	
	N.1	N.2	N.1	N.2
c (constant)	9.7	15.8	8.7	13.3
a1 (altitude)	not used	-0.0097	not used	-0.0079
a2 (EMEP model 2004)	3.21	2.36	3.50	2.90
R^2	**0.149**	**0.204**	**0.171**	**0.206**
adjusted R^2	**0.146**	**0.198**	**0.168**	**0.200**
RMSE [$\mu g.m^{-3}$]	**13.64**	**13.23**	**13.79**	**13.50**

Submodel N.2, which uses both EMEP model output and altitude, gives slightly better results than submodel N.1, which uses EMEP model output only. However, the level of correlation is low for all cases. The usefulness of the regression relations for spatial interpolation is further examined in the next section.

5.4.3 Comparison of spatial interpolation methods for rural NO_x

Spatial interpolation for the annual average NO_x was carried out using various interpolation methods, which were then compared. Interpolation was performed on the basis of data from 271 stations measuring NO_x supplemented by data from 23 stations measuring NO_2. The latter are translated into NO_x levels using the relations derived in Section 5.4.1.

The examined interpolation methods are:

1. Linear regression model without interpolation

   N.1 EMEP model output
   N.2 EMEP model output, altitude

2. Interpolation methods using primarily monitoring data

   a. IDW
   b. Ordinary kriging (OK) – parameters of variogram selected automatically (b1) and manually fitted (b2)
   c. Ordinary cokriging (OC) with altitude – parameters of variogram selected automatically (b1) and manually fitted (b2)
   d. Lognormal cokriging (LC) with altitude – parameters of variogram selected automatically (d1) and manually fitted (d2)

3. Interpolation of the residuals of linear regression models, with supplementary data

   N.1 EMEP model output
   N.2 EMEP model output, altitude

   using the interpolation methods

   a. IDW
   b. Ordinary kriging (OK) – parameters of variogram selected automatically (b1) and manually fitted (b2)

Figure 5.20 shows the cross-validation scatter plots for the annual average NO_x concentrations for several interpolation methods using primarily monitoring data (i.e. only for interpolation methods of type 2), namely ordinary cokriging and lognormal cokriging, all with the two different methods for setting variogram parameters. The plots show that the best results among these methods, i.e. the highest R^2, are obtained by lognormal cokriging with the manual optimisation of variogram parameters using RMSE minimization (2-d2).

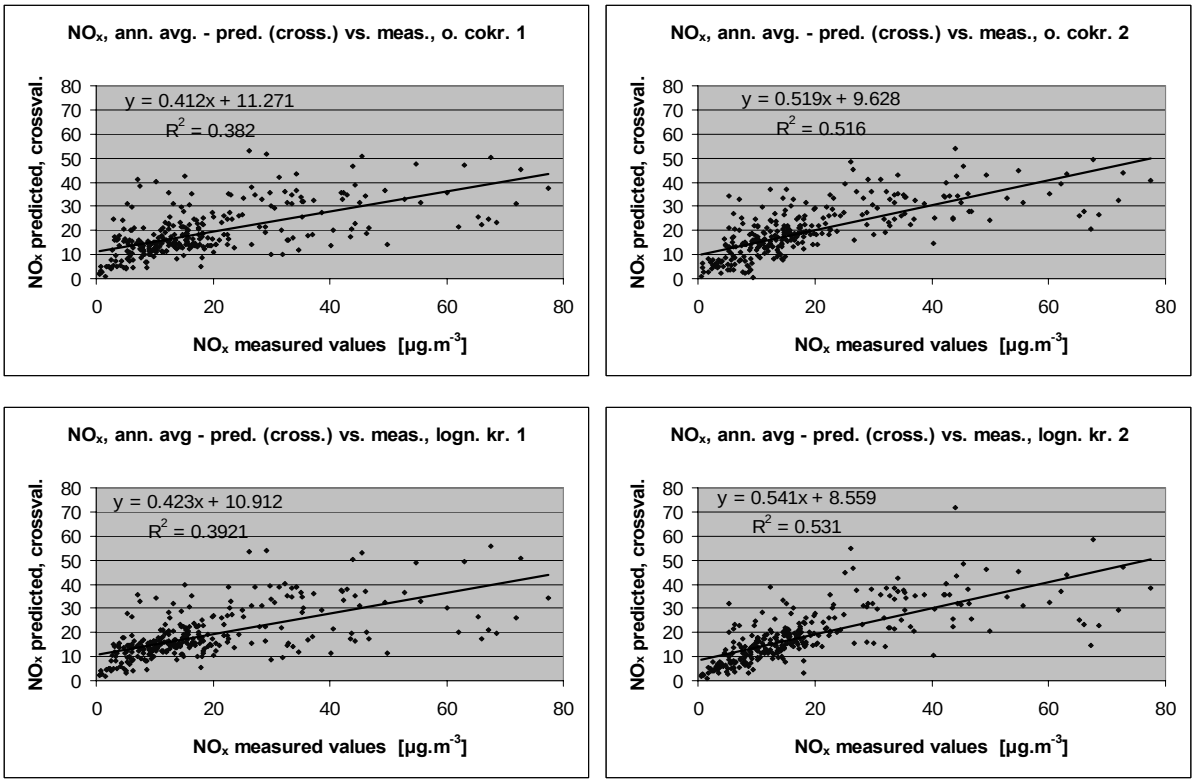

Figure 5.20 Correlation between cross-validation predicted values (y-axis) and measurements (x-axis) for the NO_x annual average for rural areas in 2004, for ordinary cokriging using altitude (top) and lognormal kriging (bottom), with parameters of variogram estimated automatically (left) and manually (right).

The interpolation results for all the different methods are presented in Table 5.18. The table shows that, as in the earlier discussed indicators, the geostatistical methods perform better (lower RMSE and other relevant statistical indicators) than IDW at the annual average NO_x. With regard to the relation of the NO_x measurements with altitude, more accurate interpolation is achieved by the applying cokriging. A further improvement is achieved by applying logarithmic transformation.

Overall, the best results with regard to RMSE and almost all other statistical indicators are obtained with pure interpolation through logarithmic cokriging, i.e. method 2-d2.

The best method using supplementary data and covering the complete study area is method 3-N.2-b2, i.e. linear regression model using EMEP dispersion model and altitude, and interpolation of its residuals by ordinary kriging. The maps created by the best methods of types 2 and 3 (i.e. 2-d2 and 3-N.2-b2) are presented in Figure 5.6.

The uncertainty of these maps expressed by RMSE in $\mu g.m^{-3}$ can be seen in Table 5.18. The relative uncertainty of the rural NO_x annual average map is 55.7% for the method 2-d2 and 57.6% for the method 3-P.2b-b2.

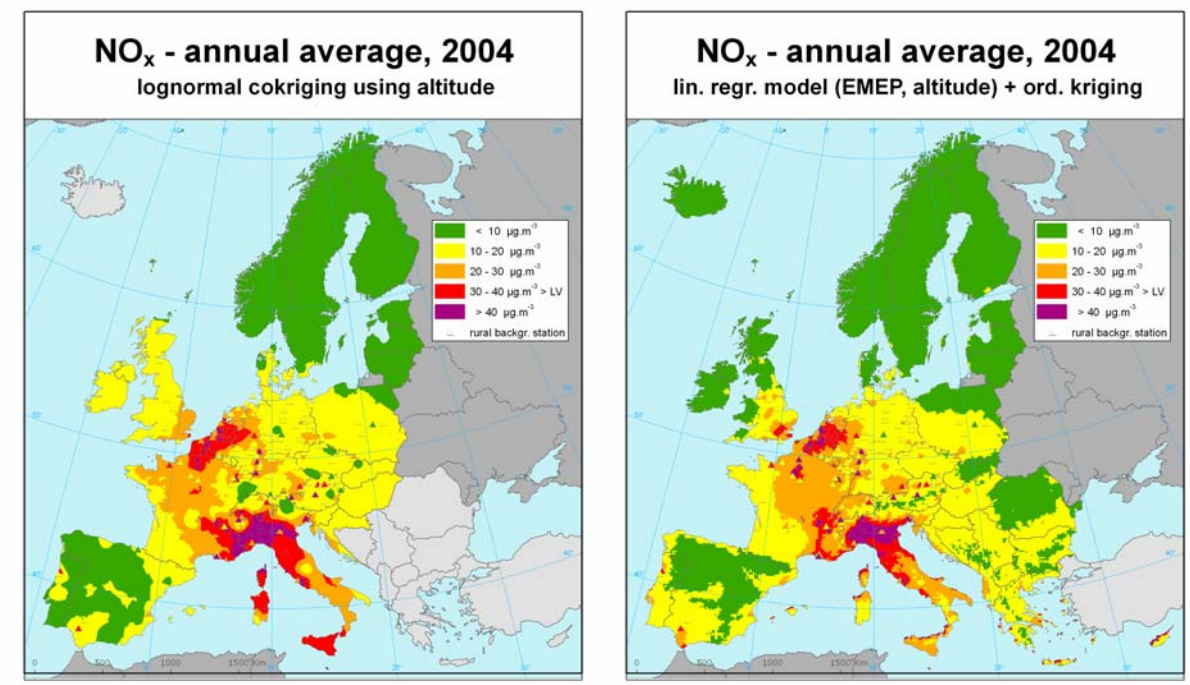

Figure 5.21 Maps showing the annual average NO_x concentration (in $\mu g.m^{-3}$) on European scale for rural areas in 2004, 10 x 10 km grid resolution, as a result of interpolation method 2-d2 (left) and 3-N.2-b2 (right). Uncertainty of these maps expressed by RMSE is 10.4 $\mu g.m^{-3}$ (left) and 10.7 $\mu g.m^{-3}$ (right).

Table 5.18 Comparison of different interpolation methods showing RMSE and the other statistical indicators for NO_x annual average in 2004 for rural areas.

mapping method		NO_x [$\mu.m^{-3}$]								
		RMSE	MPE	SD (error)	min (error)	max (error)	MAE	MedAE	R^2	MPSE
1-N.1	lin. regr. N.1	13.79	0.00	13.79	-19.24	59.89	9.60	7.10	0.171	
1-N.2	lin. regr. N.2	13.50	0.00	13.50	-19.61	58.92	9.34	6.71	0.206	
2 -a	interp. IDW	12.42	1.07	12.38	-49.52	37.19	18.61	14.44	0.344	
2-b1	interp. OK-aut	12.20	0.24	12.20	-46.34	33.05	8.27	5.23	0.355	11.73
2-b2	interp. OK-fit	12.09	0.12	12.09	-47.04	31.00	8.25	5.12	0.363	12.24
2-c1	interp. OC-aut (alt.)	11.93	0.33	11.93	-45.15	34.16	8.06	5.16	0.382	11.65
2-c2	interp. OC-fit (alt.)	10.56	0.68	10.54	-46.70	29.08	7.26	4.91	0.516	11.52
2-d1	interp. LC-aut (alt.)	11.83	0.17	11.83	-48.82	28.74	7.86	5.14	0.392	11.85
2-d2	interp. LC-fit (alt.)	10.37	0.01	10.37	-52.59	28.40	6.44	3.53	0.531	9.23
3-N.1-a	lin. regr. N.1 + IDW	11.98	0.55	11.97	-48.72	35.83	9.60	7.10		
3-N.1-b1	lin. regr. N.1 + OK-aut	11.70	0.12	11.70	-46.49	31.68	7.74	4.63		11.14
3-N.1-b2	lin. regr. N.1 + OK-fit	11.53	0.08	11.53	-48.32	26.85	7.70	4.54		12.29
3-N.2-a	lin. regr. N.2 + IDW	11.25	0.67	11.23	-47.29	35.60	9.34	6.71		
3-N.2-b1	lin. regr. N.2 + OK-aut	10.94	0.12	10.94	-44.39	31.67	7.11	3.97		10.27
3-N.2-b2	lin. regr. N.2 + OK-fit	10.73	0.09	10.73	-46.03	26.39	7.07	4.22		11.88

5.4.4 Conclusions on the spatial interpolation for NO_x, rural areas

Various methods were used for spatial interpolation and were mutually compared using RMSE and other statistical indicators from cross-validation.

- The best results (with regard to indicators like RMSE) were obtained by interpolation method 2-d, i.e. lognormal cokriging using altitude.
- The second best results were obtained by ordinary kriging of the residuals of the linear regression model 3-N.2-b, which uses EMEP model output and altitude.

- For the final mapping method 3-N.2-b was selected, because only with the help of European wide covering supplementary data it is possible to map also the areas without measurements (e.g. rural map of Balkan).
- On the basis of cross-validation analysis the uncertainty of the constructed maps was estimated.

5.5 Rural areas - SO_2

5.5.1 Comparison of linear regression models for rural SO_2

Sulphur dioxide emitted from anthropogenic sources originates especially from burning of fossil fuels and from smelting ores which contain sulphur. Directive 1999/30/EC establishes two types of limit values for SO_2, one for impacts on human health and one on ecosystems. In this study only the mapping of ecosystem impacts is executed. Two limit values for ecosystem acidification are defined by the Directive: annual average and winter season average, both with a limit value set to 20 $\mu g.m^{-3}$. In this study only annual average is examined.

For SO_2, the only submodel of linear regression model (equation 2.1) examined is:

Submodel	Input parameters
S.1	EMEP model output

The relation with meteorological parameters or altitude was not examined in the case of SO_2 for the same reasons as given in Section 5.4.2 on NO_x.

The resulting parameters of this submodel are shown in Table 5.19. R^2 is the level of correlation showing that about 29% of the variability is explained by the regression model. ¨

Table 5.19 Examination of linear regression model equation 2.1 describing the relation between SO_2 annual average for 2004 and EMEP model output.

linear regression model 2.1	**S.1**
c (constant)	1.43
a1 (EMEP model 2004)	1.54
R^2	**0.292**
adjusted R^2	**0.289**
RMSE [$\mu g.m^{-3}$]	**2.33**

The examined regression relation is further utilized in spatial interpolation. The level of correlation is rather low. The usefulness of the regression relation for spatial interpolation is further examined in the next section.

5.5.2 Comparison of spatial interpolation methods for rural SO_2

Spatial interpolation was carried out with the use of various interpolation methods that were then compared

The examined interpolation methods are as follows:

1. Linear regression model without interpolation
   S.1 EMEP model output
2. Pure interpolation methods using monitoring data only
   a. IDW
   b. Ordinary kriging (OK) – parameters of variogram selected automatically (b1) and manually fitted (b2)

e. Lognormal kriging (LK) – parameters of variogram selected automatically (e1) and manually (e2)

3. Interpolation of the residuals of linear regression models, with supplementary data

   S.1 EMEP model output

   using the interpolation methods

   a. IDW
   b. Ord. kriging (OK) – parameters of variogram selected automatically (b1) and manually fitted (b2)

Figure 5.22 shows the cross-validation scatter plots for the annual average SO_2 concentrations for several interpolation methods using primarily monitoring data (i.e. only for interpolation methods of type 2), namely ordinary kriging and lognormal kriging, all with two settings of the variogram parameters. The plots show that the best results among these methods, i.e. the highest R^2, are obtained by lognormal kriging with the manual optimisation of the variogram parameters using RMSE minimization (2-e2).

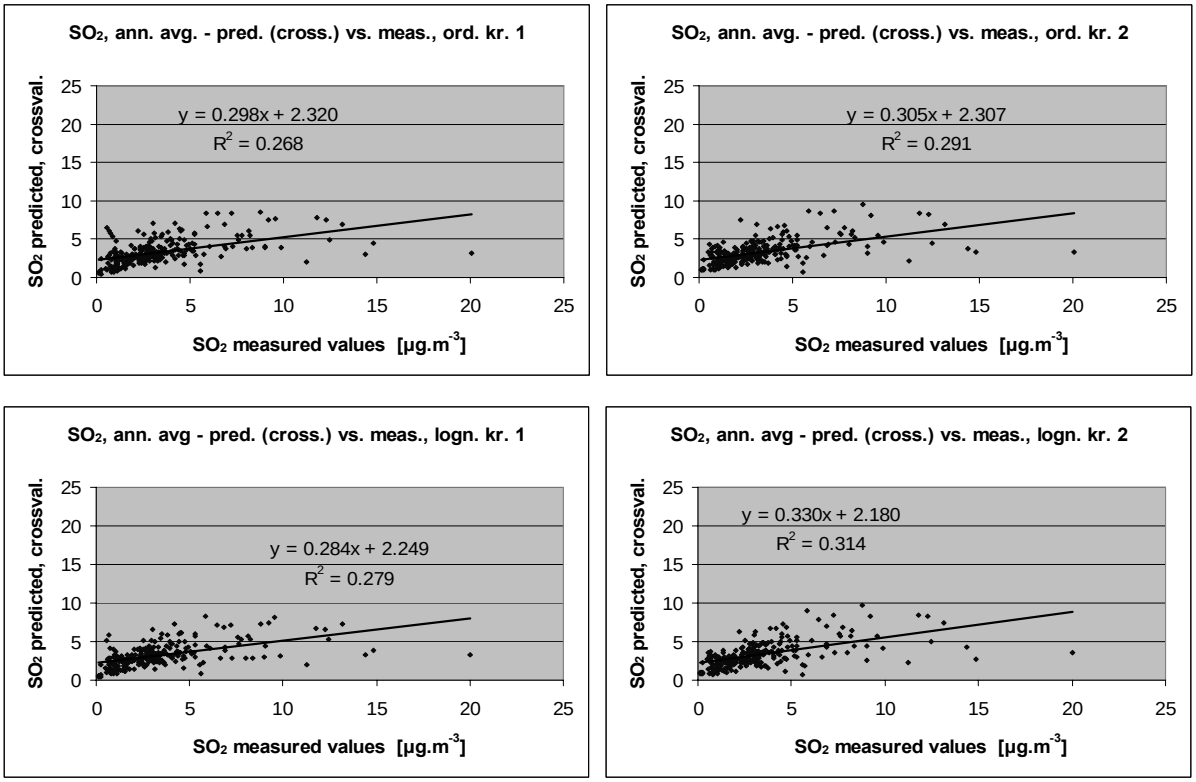

Figure 5.22 Correlation between cross-validation predicted values (y-axis) and measurements (x-axis) for the SO_2 annual average for rural areas in 2004, for ordinary kriging (top) and lognormal cokriging (bottom), with parameters of variogram estimated automatically (left) and manually (right).

The results of cross-validation analysis are shown in Table 5.20, for the different interpolation methods. All examined methods are compared with regard to cross-validation RMSE and the other statistical parameters.

Table 5.20 Comparison of different interpolation methods showing RMSE and the other statistical indicators for SO_2 annual average in 2004 for rural areas.

mapping method		SO_2 [µ.m^{-3}]								
		RMSE	MPE	SD (error)	min (error)	max (error)	MAE	MedAE	R^2	MPSE
1-S.1	lin. regr. S.1 (EMEP)	2.33	0.00	2.33	-5.07	15.03	1.55	1.16	0.292	
2-a	interp. IDW	2.39	0.08	2.39	-17.00	6.03	3.36	2.79	0.260	
2-b1	interp. OK-aut	2.37	-0.04	2.37	-16.80	6.02	1.44	0.84	0.268	1.70
2-b2	interp. OK-fit	2.33	-0.03	2.33	-16.66	5.28	1.43	0.97	0.291	1.73
2-e1	interp. LK-aut	2.36	-0.16	2.35	-16.80	5.24	1.41	0.83	0.279	1.94
2-e2	interp. LK-fit	2.29	-0.07	2.29	-16.51	4.03	1.39	0.93	0.314	1.87
3-S.1-a	lin. regr. S.1 + IDW	2.05	0.03	2.05	-14.85	4.81	1.55	1.16		
3-S.1-b1	lin. regr. S.1 + OKrig-aut	2.06	-0.06	2.06	-15.17	4.84	1.26	0.80		1.51
3-S.1-b2	lin. regr. S.1 + OKrig-fit	2.01	-0.07	2.01	-14.97	5.04	1.22	0.82		1.70

Of the methods not using supplementary data the best method is 2-e, i.e. lognormal kriging (according the comparison based on RMSE and almost all other indicators).

The best results with regard to RMSE (and also SD, MAE, MedAE, and MPSE) are obtained with method 3-S.1-b2, i.e. linear regression using EMEP model output followed by interpolation of the residuals by ordinary kriging on the basis of a variogram with manually selected parameters. This method is used in Chapter 8 for the final mapping of the interpolated SO_2 annual average concentrations.

The maps created by the best methods of types 2 and 3 (i.e. 2-e2 and 3-S.1-b2) are presented in Figure 5.23.

The uncertainty of these maps expressed by RMSE in µg.m^{-3} can be seen in Table 5.20. The relative uncertainty of the rural SO_2 annual average map is 68.1% for the method 2-e2 and 59.8% for the method 3-P.2b-b2.

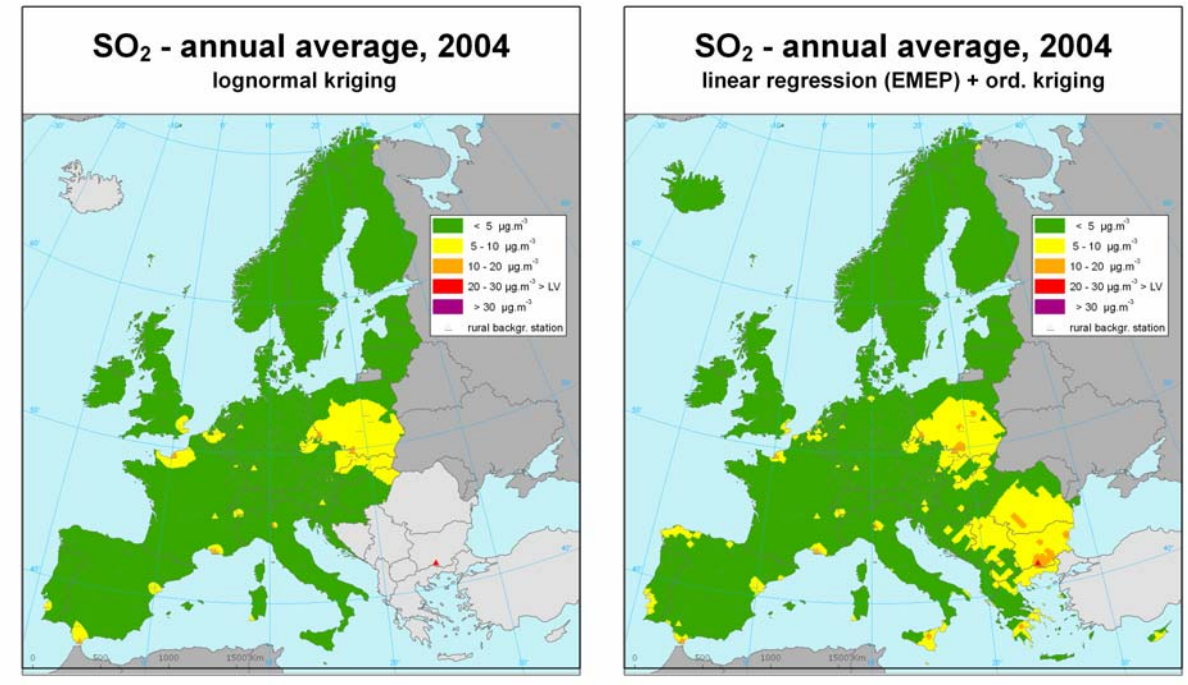

Figure 5.23 Maps showing the annual average SO_x concentration (in µg.m^{-3}) on European scale for rural areas in 2004, 10 x 10 km grid resolution, as a result of interpolation method 2-e2 (left) and 3-S.1-b2 (right). Uncertainty of these maps expressed by RMSE is 2.3 µg.m^{-3}.(left) and 2.0 µg.m^{-3} (right).

5.6 Rural areas - $PM_{2.5}$

On special request from EEA, options were explored to somehow use the PM_{10} data for producing an interpolated $PM_{2.5}$ map for Europe. Both EEA and DG-ENV are highly interested in such $PM_{2.5}$ maps based on monitoring data next to results currently provided by model-based projects only. However, in many countries the implementation of stations measuring $PM_{2.5}$ is still in the phase of being established, resulting so far in few $PM_{2.5}$ monitoring data reported in AirBase. In the course of time this lack of reported data is expected to be resolved when the $PM_{2.5}$ measurements and their national reporting go into full operation according to the intentions of the 1st daughter directive, but until then interpolated maps produced on the basis of $PM_{2.5}$ measurements have large uncertainties. This section explores the feasibility of preparing an interpolated $PM_{2.5}$ map, based on the few $PM_{2.5}$ measurements and supported by the correlation between PM_{10} and $PM_{2.5}$ measurements that should 'overcome' the current lack of $PM_{2.5}$ measurements. Furthermore, the correlation between the EMEP model output on $PM_{2.5}$ and the few $PM_{2.5}$ measurements is examined to determine if EMEP model output could help improving the interpolation.

First the relation between the valid annual averages of $PM_{2.5}$ and PM_{10} is examined at those rural background stations measuring both pollutants. Their correlation could be used to reduce the uncertainties in the $PM_{2.5}$ interpolations in areas where only PM_{10} measurements exist and where we could use these stations for 'emulating' $PM_{2.5}$ stations. Measurement data for the years 2003 and 2004 are used. Figure 5.24 shows the regression relations for each year. The number of such rural stations is very small, 9 stations for 2003 and 13 stations for 2004, leading to findings that cannot be considered to be representativeness for application on the whole European study area.

Additionally, the annual averages ratio $PM_{2.5}/PM_{10}$ at these stations is examined. (This is a simple ratio of annual $PM_{2.5}$ and PM_{10} averages, as the map would be eventually created with help of PM_{10} annual averages; however, it would be better to calculate $PM_{2.5}/PM_{10}$ on a the daily basis.) The ratio varies from 0.45 to 0.81 in the year 2003 and from 0.52 to 0.85 in the year 2004, with an average of 0.66 in 2003 and 0.70 in 2004. Furthermore, the standard deviation is 0.12 in the year 2003 and 0.11 in the year 2004, demonstrating significant uncertainties that would be introduced when $PM_{2.5}$ concentrations would be estimated from those PM_{10} measurement stations where no $PM_{2.5}$ is measured. The number of PM_{10} stations is much larger than the number of $PM_{2.5}$ stations.

It can be concluded that a map with interpolated $PM_{2.5}$ concentrations based on mainly PM_{10} measurements would therefore, in fact, lead to a map representing PM_{10} concentrations multiplied by the regression factor. Such a map cannot be considered as a representative interpolated $PM_{2.5}$ map for Europe and is not prepared in this paper.

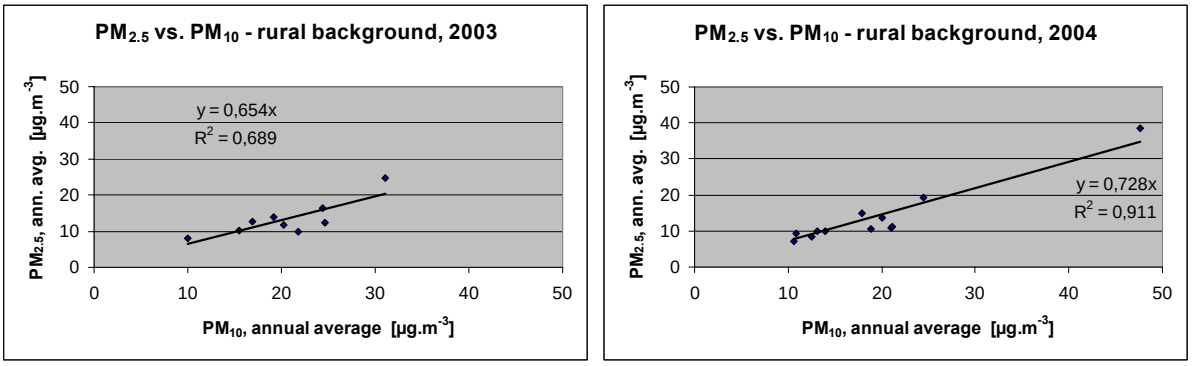

Figure 5.24 The graphs represent the results of the linear regression indicating the level of correlation between the annual averages of $PM_{2.5}$ (y-axis) and PM_{10} (x-axis) in rural areas for the years 2003 (left) and 2004 (right).

Another option is to use the EMEP model $PM_{2.5}$ output and investigate its relation with the measured $PM_{2.5}$ concentrations. Figure 5.25 shows their correlation resulting from the linear regression on data of 2004 and use that relation for preparing an interpolated $PM_{2.5}$ map.

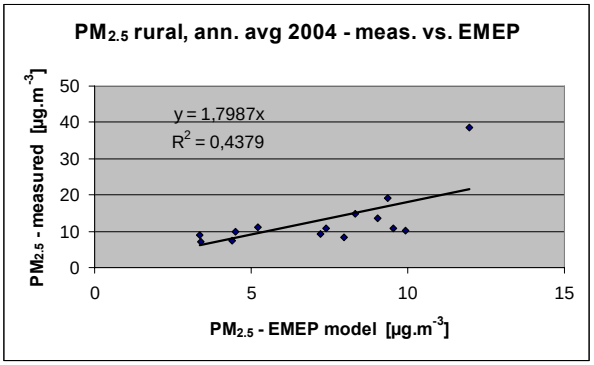

Figure 5.25 The graph represents the result of the linear regression indicating the level of correlation between the annual average of measured $PM_{2.5}$ concentrations at rural stations (y-axis) and the EMEP modelled values (x-axis) for the year 2004.

It can be concluded that using EMEP model $PM_{2.5}$ output for preparing an interpolated $PM_{2.5}$ map is not representative yet, because the number of the stations from which the interpolated rural background $PM_{2.5}$ concentration field should be derived is still very small and the correlation with the model is too low. Therefore no such map is prepared in this paper.

5.7 Urban mapping

Urban mapping concerns only the pollutants relating to human-health, i.e. PM_{10}, ozone and $PM_{2.5}$, and associated parameters. For the individual indicators, various linear regression models (as described in Section 2.2) are examined and mutually compared according to the procedure described in Section 2.5. Subsequently, both the interpolation methods using primarily monitoring data and the methods using the interpolation of residuals of linear regression models are examined (as described in Section 2.3 and 2.4). This is followed by methods that interpolate the difference between the urban stations and the interpolated rural background concentration field, the so called Delta, which then add the interpolated difference field to the rural background are examined (Section 3.2). All the interpolation methods are compared using cross-validation indicators, as described in Section 2.6. The results of the cross-validation analysis are also used for examination and estimation of uncertainty of different interpolation methods.

In the Section 5.6 it was concluded that currently there is not enough $PM_{2.5}$ measurement data for making a rural map. It concerns in general low temporal coverage on $PM_{2.5}$ measurements for both rural and urban areas. Data from 55 urban/suburban background stations measuring $PM_{2.5}$ with at least a 75% temporal data coverage, are included in AirBase for 2004, but spatial coverage is very irregular. This number of stations is not sufficient for creating a map by interpolation using primarily monitoring data. The alternative to base an urban $PM_{2.5}$ map on some urban $PM_{2.5}/PM_{10}$ ratio is yet not realistic for the same reasons as given in Section 5.6 for the rural areas. Annual averaged $PM_{2.5}$ maps based on a $PM_{2.5}/PM_{10}$ ratio should be based on the same days for both pollutants. However, yet there is low temporal coverage at stations with PM2.5 and PM10 measured on the same day. All these matters makes urban $PM_{2.5}$ mapping not very useful.

Concerning human health indicators there is no NO_x limit value defined. The first Daughter Directive defines a SO_2 limit value, but we would not have produced a SO_2 human-health exceedance maps anyway, since there are hardly any exceedances in (<1%) the EU25, as CSI004 explains. An activity we did not focus on in this project, but could be relevant in future work, is to prepare a NO_2 human health interpolated annual average exceedance indicator map as defined in the first Daughter Directive, since CSI004 shows that there are still considerable exceedances in Europe for this pollutant.

5.8 Urban areas - PM_{10}

5.8.1 Comparison of linear regression models for urban PM_{10}

Several submodels of the linear regression model equation 2.1 are examined, for both the annual average and the 36th maximum daily average PM_{10} indicators:

Submodel	Input parameters
UP.1	EMEP model output
UP.2a	EMEP model output, surf. solar radiation, rel. hum., wind speed, temper., total. precip.
UP.2b	EMEP model output, surf. solar radiation, rel. humidity, wind speed, temperature
UP.2c	EMEP model output, surf. solar radiation, rel. humidity, wind speed
UP.2d	EMEP model output, surf. solar radiation, rel. humidity, temperature

The input parameters for the stepwise selection are altitude, meteorological parameters (i.e. wind speed, surface solar radiation, temperature, relative humidity, total precipitation) and EMEP model output. The basic submodel arrived at after a stepwise regression with backward elimination of parameters (Section 2.5) is submodel UP.2a, for the annual average and for the 36th maximum daily averages. The other submodels are included in the comparison to show the decrease of R^2 after excluding one or two parameters. Submodels UP.2b, UP2.c and UP.2d are chosen because they show the smallest decrease of R^2 in the stepwise selection process.

The performance of the different linear regression models for the two indicators is compared in Table 5.21 and 5.22, which give the parameters *c, a1, ..., a7* for the different submodels of linear regression model equation 2.1.

Table 5.21 shows the results for the PM_{10} annual average concentration. The values of R^2 and RMSE for the submodels of types 1 and 2 show quite clearly that the addition of supplementary parameters substantially improves the closeness of the regression relation by an increased R^2 of about 0.15 and a decreased RMSE by approximately one tenth. However, all of these correlations are rather small: the highest R^2 is only about 0.2.

The best results with regard to R^2 and RMSE are obtained with model UP.2a. However, model UP.2d gives very similar results, with a R^2 that is only about 0.01 lower and a RMSE of only 0.05 $\mu g.m^{-3}$ higher, while it uses a smaller number of supplementary parameters of four instead of six. This leads to the selection of UP.2d, using the EMEP model output, surface solar radiation, relative humidity and temperature, as the preferred regression model.

Table 5.21 Comparison of different submodels of linear regression model equation 2.1 describing the relation between PM_{10} annual average for 2004 and different supplementary parameters in the urban areas.

lin. regr. model (2.1)	UP.1	UP.2a	UP.2b=UP.2d	UP.2c
c (constant)	19.6	124.7	190.4	139.6
a1 (altitude GTOPO)	not used	not used	not used	not used
a2 (temperature 2004)	not used	-0.80	-1.05	not used
a3 (wind speed 2004)	not used	-1.13	n. sign.	-1.33
a4 (rel. hum. 2004)	not used	-1.16	-1.94	-1.33
a5 (s. solar rad. 2004)	not used	1.67	1.86	0.81
a6 (total precipitation 2004)	not used	-0.004	not used	not used
a7 (EMEP model 2004)	0.66	0.92	1.04	0.83
R^2	**0.048**	**0.205**	**0.196**	**0.187**
adjusted R^2	**0.046**	**0.198**	**0.191**	**0.182**
RMSE [$\mu g.m^{-3}$]	**9.15**	**8.36**	**8.41**	**8.46**

Table 5.22 shows the results for the 36th maximum daily mean PM_{10} value. Submodel UP.1 shows a very low R^2, meaning that there is hardly any correlation between the measured concentrations and the EMEP model output. This is probably caused by the relative low grid resolution of 50 km on which the EMEP model output is available. The submodels UP.2a to UP.2d that use additional supplementary parameters substantially improve the closeness of the regression relation by an increased R^2 of about 0.18 and a decreased RMSE of about one tenth. Similar to the annual average, all of these correlations are only small, i.e. less that 0.20.

The different submodels for the 36th maximum daily averages show quite similar results when compared to the annual averages. The best result with regard to R^2 and RMSE is obtained with model UP.2a. And again, the model UP2.d gives only slightly smaller R^2, and a slightly increased RMSE, while it uses four parameters instead of six. This leads also for the 36th maximum daily averages to the selection of UP.2d as the preferred regression model, which uses the EMEP model output, surface solar radiation, relative humidity and temperature.

Table 5.22 Comparison of different submodels of linear regression model equation 2.1 describing the relation between PM_{10} parameter 36th maximum daily average value for 2004 and different supplementary parameters in the urban areas.

lin. regr. model (2.1)	UP.1	UP.2a	UP.2b	UP.2c	UP.2d
c (constant)	38.7	218.0	278.5	239.7	395.2
a1 (altitude GTOPO)	not used	not used	not used	not used	not used
a2 (temperature 2004)	not used	-1.58	-1.70	not used	-2.40
a3 (wind speed 2004)	not used	-3.20	-2.38	-3.64	not used
a4 (rel. hum. 2004)	not used	-1.97	-2.73	-2.210	-4.04
a5 (s. solar rad. 2004)	not used	3.05	3.23	1.316	3.65
a6 (total precipitation 2004)	not used	-0.01	not used	not used	not used
a7 (EMEP model 2004)	0.24	0.61	0.68	0.51	0.76
R^2	**0.008**	**0.189**	**0.183**	**0.169**	**0.172**
adjusted R^2	**0.007**	**0.181**	**0.176**	**0.164**	**0.167**
RMSE [µg.m^{-3}]	**16.76**	**15.10**	**15.16**	**15.28**	**15.26**

Additional to the EMEP model output, altitude and meteorological parameters, we examined as other supplementary parameter the gridded dataset with NO_X emissions from the APMoSPHERE project. This dataset covers only the EU-15 countries and Norway, limiting the linear regression model comparison to the data for these 16 countries only, i.e. for 521 urban and suburban background stations. Examined are the submodels UP.1 – UP.2d from above, together with several submodels including NO_x emission data:

UP.2e EMEP model output, s. sol. radiation, rel. humidity, wind speed, total prec., NO_x emission
UP.2f EMEP model output, s. solar radiation, rel. humidity, total precipitation, NO_x emission
UP.2g EMEP model output, surface solar radiation, relative humidity, NO_x emission
UP.2h EMEP model output, rel. humidity, NO_x emission

The input parameters for the stepwise selection are the same parameters as in the previous analysis, now including the NO_X emissions. The basic submodel arrived at after a stepwise regression with a backward elimination of parameters (Section 2.5) is submodel UP.2f for annual average and UP.2e for the 36th maximum daily average value. The submodels UP.2g and UP.2h are presented as well, to demonstrate the decrease of R^2 after excluding one or two parameters. They are chosen because they show the smallest decrease of R^2 in the stepwise selection process. The submodels UP.2a-UP.2d are presented in order to compare the submodels with and without NO_x emission.

The performance of the different linear regression models is compared in Tables 5.23 for the annual averages and in Table 5.24 for the 36th maximum daily averages. The changes in the absolute values of R^2 and RMSE for UP.2a – UP.2d in Tables 5.23 and 5.24, compared to those in Tables 5.21 and 5.22, are caused by the different area and the set of stations for which the analysis is done.

The results in Table 5.23 for the PM_{10} annual averages show that the inclusion of the NO_x emissions improves the performance of the linear regression models. The best submodels using NO_x emission, e.g. UP.2f, give a R^2 of about 0.03-0.05 higher than those at the best submodels without NO_x emission, e.g. UP.2c.

The results in Table 5.24 for the 36th maximum daily mean PM_{10} values are quite similar as for the annual average. The inclusion of NO_x emissions improves the regression relation: submodel UP.2e gives a R^2 of about 0.03 higher than the best performing submodel UP.2e without NO_x emissions.

NO_x emissions in 1 x 1 km grid resolution were used in the regression relations. The use of aggregated grid (e.g. 5 x 5 km) is considered to bring additional improvement. However, the usability of these emissions for European wide maps creation depends on their completeness.

Table 5.23 Comparison of different submodels of linear regression model equation 2.1 describing the relation between PM_{10} annual average for 2004 and different supplementary parameters including NO_x emission in the urban areas of EU-15 + Norway.

lin. regr. model 2.1	UP.1	UP.2a=UP.2b=UP.2c=UP.2d	UP.2e=UP.2f	UP.2g	UP.2h
c (constant)	19.1	156.8	161.7	156.8	261.2
a1 (altitude GTOPO)	not used	not used	not used	not used	not used
a2 (temperature 2004)	not used	n. sign.	not used	not used	not used
a3 (wind speed 2004)	not used	n. sign.	n. sign.	not used	not used
a4 (rel. hum. 2004)	not used	-1.616	-1.725	-1.615	-2.600
a5 (s. solar rad. 2004)	not used	1.108	1.232	1.083	not used
a6 (total precip. 2004)	not used	n. sign.	0.004	not used	not used
a7 (NO_x emission)	not used	not used	0.011	0.011	0.011
a8 (EMEP model 2004)	0.53	0.80	0.78	0.74	0.67
R^2	**0.048**	**0.282**	**0.332**	**0.321**	**0.283**
adjusted R^2	**0.047**	**0.277**	**0.326**	**0.315**	**0.279**
RMSE [µg.m^{-3}]	**7.77**	**6.74**	**6.50**	**6.55**	**6.73**

Table 5.24 Comparison of different submodels of linear regression model equation 2.1 describing the relation between PM_{10} parameter 36th maximum daily value for 2004 and different supplementary parameters including NO_x emission in the urban areas of EU-15 + Norway.

lin. regr. model (2.1)	UP.1	UP.2a	UP.2b=UP.2c	UP.2d	UP.2e	UP.2f	UP.2g	UP.2h
c (constant)	36.2	227.7	180.4	347.4	229.0	360.8	345.7	490.2
a1 (altitude GTOPO)	not used	not used	not used	not used	not used	not used	not used	not used
a2 (temperature 2004)	not used	n. sign.	n. sign.	not used	not used	not used	not used	not used
a3 (wind speed 2004)	not used	-2.35	-3.06	not used	-2.31	not used	not used	not used
a4 (rel. hum. 2004)	not used	-2.35	-1.75	-3.57	-2.37	-3.87	-3.552	-4.904
a5 (s. solar rad. 2004)	not used	2.35	2.26	1.60	2.31	1.98	1.551	not used
a6 (total precip. 2004)	not used	0.006	not used	not used	0.007	0.011	not used	not used
a7 (NO_x emission)	not used	not used	not used	not used	0.019	0.019	0.018	0.018
a8 (EMEP model 2004)	0.198	0.603	0.557	0.574	0.556	0.597	0.524	0.457
R^2	**0.009**	**0.273**	**0.267**	**0.236**	**0.307**	**0.293**	**0.268**	**0.244**
adjusted R^2	**0.007**	**0.266**	**0.261**	**0.232**	**0.298**	**0.286**	**0.262**	**0.240**
RMSE [µg.m^{-3}]	**14.43**	**12.35**	**12.41**	**12.66**	**12.06**	**12.18**	**12.40**	**12.59**

5.8.2 Conclusion of linear regression models for urban PM_{10}

Different submodels of linear regression model equation 2.1 were examined for the two PM_{10} indicators, the annual average and the 36th maximum daily average value for urban areas, using different supplementary data.

As the preferred submodel for both the annual average and the 36th maximum daily average value were selected submodel UP.2d, which uses EMEP model output, surface solar radiation, relative humidity and temperature. This submodel will be further examined in the spatial interpolation comparisons in the next section. Despite the rather small correlations of all examined submodels we include for illustration two other models in the comparison on their usefulness for spatial interpolation.

The expected improved of the regression relation provided by using NO_x emissions as additional parameter was examined. We used the recent NO_x emissions from the EU-project APMoSPHERE, covering the area of the EU-15 and Norway. For this area it is confirmed that NO_x emissions do improve the regression relation, however, due to its limited European coverage we do not make further use of this data source at this moment.

5.8.3 Comparison of spatial interpolation methods for urban PM_{10}

Various methods were used for spatial interpolation and were compared with each other using RMSE from cross-validation, including the methods which use the urban Delta (Section 3.2 and Horálek et al., 2005). The results are also compared with a few submodels of the linear regression model (equation 2.1) without interpolation, as examined in Section 5.8.1 and coded the same. The compared methods are as follows:

1. Linear regression models without interpolation

   UP.1 EMEP model output
   UP.2c EMEP model output, surface solar radiation, relative humidity, wind speed
   UP.2d EMEP model output, surface solar radiation, relative humidity, temperature

2. Interpolation methods using primarily monitoring data

   a. IDW
   b. Ordinary kriging (OK) – parameters of variogram selected automatically (b1) and manually fitted (b2)
   e. Lognormal kriging (LK) – parameters of variogram selected automatically (e1) and manually fitted (e2)

3. Interpolation of the residuals of linear regression models, with supplementary data

   UP.1 EMEP model output
   UP.2c EMEP model output, surface solar radiation, relative humidity, wind speed
   UP.2d EMEP model output, surface solar radiation, relative humidity, temperature

   using the interpolation methods

   a. IDW
   b. Ord. kriging (OK) – parameters of variogram selected autom. (b1) and man. fitted (b2)

4. Methods for interpolation of Delta (and its subsequent addition to the rural background field as selected in Section 5.2.7 for final mapping), using

   a. IDW
   b. Ord. kriging (OK) – parameters of variogram selected autom. (b1) and man. fitted (b2)

The cross-validation scatter plots for different methods using primarily monitoring data (i.e. only for interpolation methods of type 2) are presented in Figure 5.26 for the annual average PM_{10} and in Figure 5.27 for the 36th maximum daily average value.

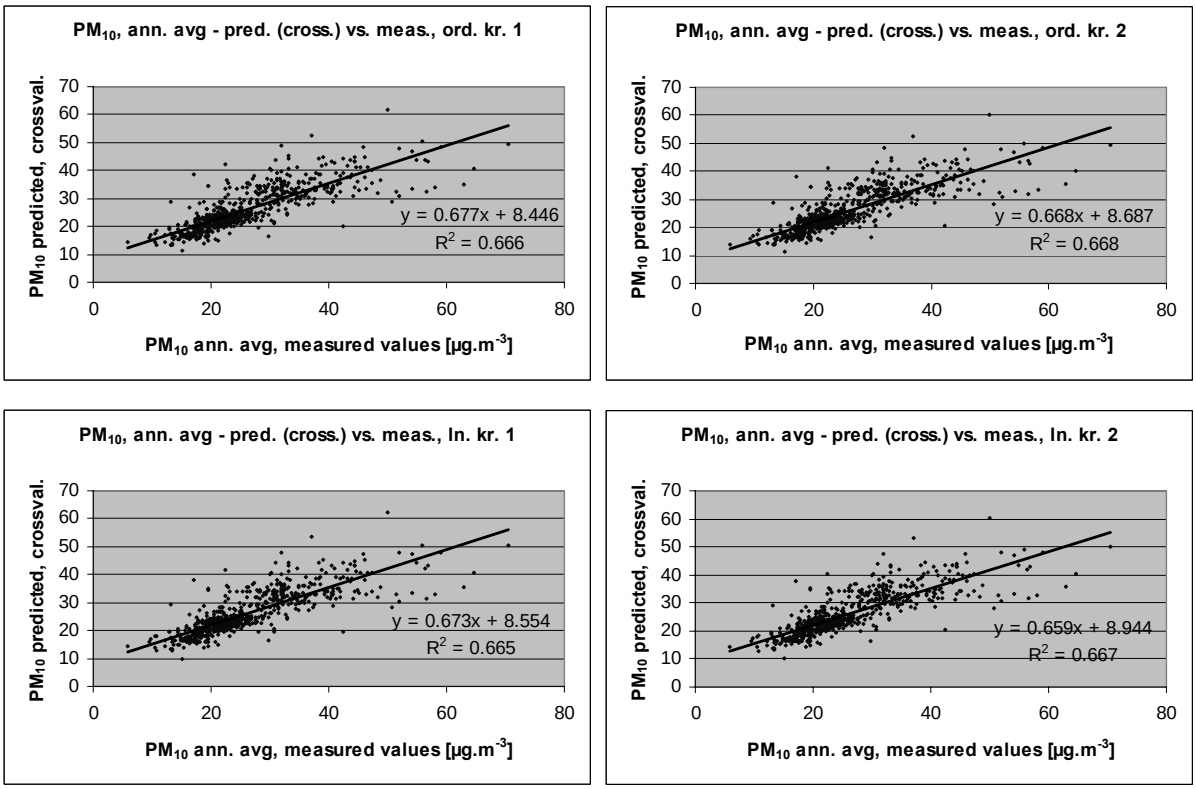

Figure 5.26 Correlation between cross-validation predicted values (y-axis) and measurements (x-axis) for the PM_{10} annual average for 2004 in urban areas, for ordinary kriging (top) and lognormal kriging (bottom), with parameters of variogram estimated automatically (left) and manually (right).

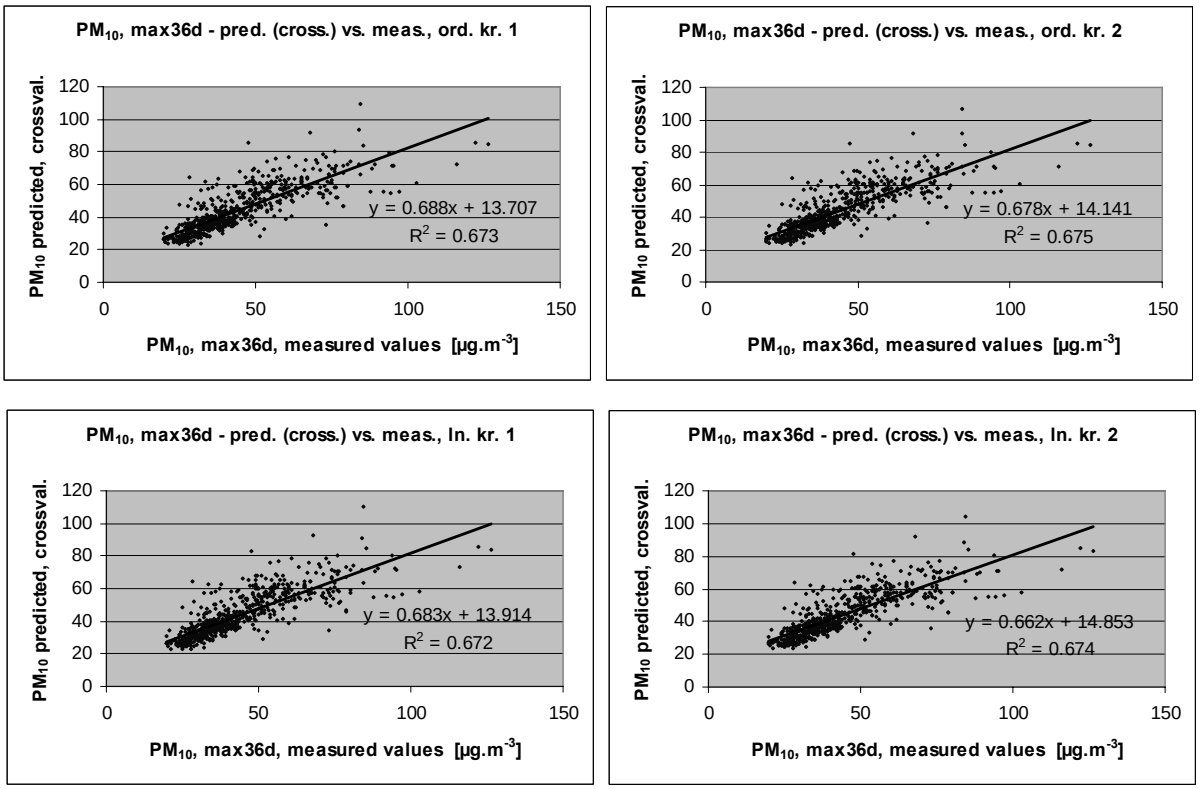

Figure 5.27 Correlation between cross-validation predicted values (y-axis) and measurements (x-axis) for the 36th maximum daily average value for 2004 in urban areas, for ordinary kriging (top) and lognormal kriging (bottom), with parameters of variogram estimated automatically (left) and manually (right).

The cross-validation analysis was done for all examined methods. The tests on the RMSE were performed for two sets of stations: one set with all 655 (sub)urban stations and a second set of 535 stations, being a subset of the first with only one station per each city. The other statistical indicators analyses are performed on the set with all stations. The comparison is carried out with the use of RMSE and other indicators of the cross-validation and is presented in Table 5.24.

The reason for using such a subset for RMSE with only one station per city needs an additional explanation. From the cities with more monitoring stations, one station is randomly selected and added to the station subset of cities with one station. The cross-validation method computes the spatial interpolation for each measured point using all the available information except from that one point (i.e. it withholds one data point and then makes a prediction at the spatial location of that point). The predicted and measured values are then compared and the procedure is repeated for all points. The use of only one station per city ensures that the predicted values of the cross-validation are computed from the stations from other cities then its own city. It guarantees a most representative cross-validation on the (sub)urban stations throughout Europe and hence simulates better the cities in Europe without measurements.

A number of specific conclusions are made

- The use of interpolation methods, both interpolations using primarily monitoring data (type 2) and interpolations of the residuals of linear regression models (type 3), give better results with regard to RMSE (and also SD, MAE, MedAE) than the methods using linear regression models without interpolation (type 1).
- In case of interpolation methods of type 2, the best results, with regard to RMSE (and also SD and R2), for both indicators and both sets of stations are obtained with ordinary kriging, method 2-b. (Lognormal kriging, i.e. 2-e is better with regard to MedAE and MPSE.)

- The methods using the urban Delta (type 4) give worse results than those using interpolation methods of type 2 and 3, based on RMSE (and also SD, MAE and MedAE).
- The best method for the PM_{10} annual averages at the subset of stations is 3-UP.2d-b, i.e. linear regression model using EMEP model output, surface solar radiation, relative humidity and temperature followed by interpolation of its residuals by ordinary kriging. It means that for the cities without measurements it is helpful to use the supplementary parameters.
- The best method for the 36th maximum daily averages at the subset of stations is 2-b, ordinary kriging. This method is also the best performing for the set of all stations for both the annual averages and the 36th maximum daily averages.

The maps created by the best method (i.e. 2-b2) are presented in Figure 5.28 for both PM_{10} indicators. The uncertainty of these maps expressed by RMSE in µg.m^{-3} can be seen in Table 5.25. The relative uncertainty of the urban PM_{10} map is about 21% for annual average and about 22% for the 36th maximum daily average.

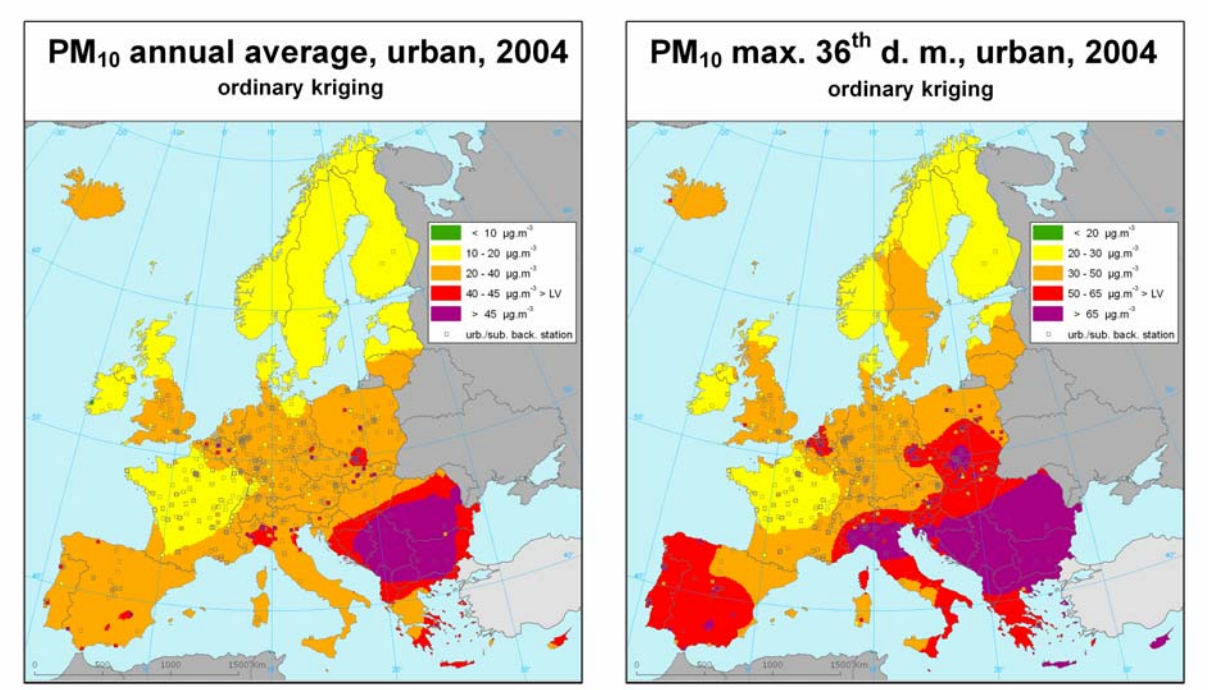

Figure 5.28 Maps showing the PM_{10} indicators annual average (left) and 36th maximum daily value (right), in µg.m^{-3}, on European scale for urban areas in 2004 in 10 x 10 km grid resolution as a result of interpolation method 2-b2, i.e. ordinary kriging. The maps are applicable only in the urban areas.

Table 5.25 Comparison of different interpolation methods showing RMSE (in µg.m^{-3}) for the PM_{10} indicators annual average and 36th maximum value, for 2004, urban areas (RMSE separately for all stations and for subset with max. one station per city).

mapping method		annual average PM_{10} [µg.m^{-3}]										36th maximum daily average [µg.m^{-3}]									
		RMSE all stat.	RMSE subset	MPE	SD (error)	min (error)	max (error)	MAE	MedAE	R^2	MPSE	RMSE all stat.	RMSE subset	MPE	SD (error)	min (error)	max (error)	MAE	MedAE	R^2	MPSE
1-UP.1	lin. regr. UP.1	9.15	9.08	0.00	9.15	-18.11	37.09	7.08	6.06	0.048		16.77	16.51	0.07	16.76	-24.80	84.40	13.03		0.008	
1-UP.2C	lin. regr. UP.2c	8.46	8.26	0.00	8.46	-18.04	28.66	6.46	5.58	0.187		15.28	14.89	0.00	15.28	-25.45	75.62	11.74	9.47	0.169	
1-UP.2d	lin. regr. UP.2d	8.41	8.26	0.00	8.41	-18.68	29.23	6.46	5.39	0.196		15.26	14.98	0.00	15.26	-24.94	76.78	11.69	9.70	0.172	
2-a	interp. IDW	5.58	5.61	0.40	5.57	-26.84	22.20	3.79	2.50	0.646		9.95	9.93	0.82	9.91	-46.04	37.04	6.73	4.39	0.649	
2-b1	interp. OK-aut	5.38	5.52	0.04	5.38	-27.68	21.45	3.58	2.33	0.666	5.18	9.52	9.77	0.11	9.52	-43.58	38.55	6.29	3.86	0.673	9.20
2-b2	interp. OK-fit	5.37	5.51	0.03	5.37	-27.59	21.27	3.57	2.27	0.668	5.45	9.49	9.70	0.09	9.49	-44.49	37.83	6.28	3.98	0.675	10.05
2-e1	interp. LK-aut	5.39	5.54	0.03	5.39	-27.45	20.89	3.57	2.24	0.665	4.78	9.52	9.81	0.08	9.53	-44.64	35.66	6.26	3.84	0.672	8.04
2-e2	interp. LK-fit	5.38	5.51	0.06	5.38	-27.26	20.74	3.57	2.22	0.667	5.22	9.50	9.71	0.14	9.49	-45.22	35.36	6.26	3.96	0.674	9.09
3-UP.2c-a	lin. regr. 2b + IDW	5.60	5.62	0.09	5.60	-26.60	22.52	3.75	2.36			10.00	10.00	0.41	9.99	-43.59	39.78	6.67	4.22		
3-UP.2c-b1	lin. regr. 2b + OK-aut	5.42	5.58	-0.03	5.42	-26.78	21.32	3.60	2.35		5.28	9.68	9.91	0.02	9.68	-44.01	41.04	6.40	4.10		9.37
3-UP.2c-b2	lin. regr. 2b + OK-fit	5.37	5.52	-0.04	5.37	-26.42	21.78	3.58	2.26		5.35	9.59	9.88	-0.02	9.59	-43.86	38.28	6.36	4.01		9.81
3-UP.2d-a	lin. regr. 2d + IDW	5.59	5.62	0.11	5.59	-26.44	23.31	3.72	2.30			10.05	10.02	0.35	10.04	-45.06	38.36	6.72	4.32		
3-UP.2d-b1	lin. regr. 2d + OK-aut	5.45	5.54	-0.02	5.45	-26.64	22.10	3.59	2.35		5.26	9.61	9.84	0.00	9.61	-46.32	36.63	6.39	4.17		9.56
3-UP.2d-b2	lin. regr. 2d + OK-fit	5.40	5.49	-0.04	5.40	-25.56	22.43	3.57	2.34		5.57	9.54	9.83	-0.04	9.54	-45.68	37.23	6.36	4.10		9.97
4-a	Delta+IDW	5.71	5.86	0.00	5.71	-29.25	20.37	3.84	2.55			10.02	9.93	0.10	10.02	-40.16	39.49	6.73	4.30		
4-b1	Delta+OK-aut	5.71	5.83	-0.05	5.71	-31.68	19.55	3.83	2.61		5.12	9.84	9.97	-0.04	9.84	-44.22	41.26	6.65	4.37		8.95
4-b2	Delta+OK-fit	5.56	5.67	-0.07	5.56	-30.19	20.88	3.73	2.40		4.87	9.67	9.80	-0.09	9.67	-42.52	35.51	6.51	4.08		8.76

5.8.4 Conclusions on the spatial interpolation for PM_{10}, urban areas

A number of conclusions can be drawn for the spatial interpolation mapping of PM_{10}:

- The best mapping method for the 36th maximum daily averages is method 2-b2 when using the complete station set and when using the subset in the cross-validation.
- The best mapping method for the annual averages is in principle 3-UP.2d-b2 when using the station subset. However, close 2nd best is method 2-b2, which is the best performing method when using all stations in the cross-validation. Furthermore, at the annual averages for the station subset the RMSE for method 3-UP.2d-b2 does not differ significantly from the one for method 2-b2.
- Considering that the use of one interpolation method for both PM_{10} indicators, using both the complete station set and the station subset is most practical, the spatial interpolation method 2-b2 is preferred to be used in the final interpolated urban mapping for PM_{10} of Chapter 8.
- On the basis of cross-validation analysis the uncertainty of the constructed maps was estimated.

5.9 Urban areas - Ozone

5.9.1 Comparison of linear regression models for urban ozone

Several linear regression models and submodels of equation 2.1 are examined, for SOMO35 and for the 26th highest daily maximum 8-hour value indicators:

Submodel	Input parameters
UO.1	EMEP model output
UO.2a	EMEP model output, altitude, wind speed, relative humidity
UO.2b	EMEP model output, wind speed, relative humidity
UO.2c	EMEP model output, altitude, relative humidity
UO.2d	EMEP model output, relative humidity
UO.3a	wind speed, relative humidity, surface solar radiation
UO.3b	wind speed, relative humidity

The input parameters for the stepwise selection are altitude, meteorological parameters (i.e. wind speed, surface solar radiation, temperature, relative humidity, total precipitation) and EMEP model output. NO_x emissions were not used because of their incomplete spatial coverage; nevertheless this is another parameter for eventual improving of the regression relation.

The basic submodel of type 2 for the SOMO35, selected after a stepwise regression with backward elimination of parameters (Section 2.5), is UO.2a. Other submodels are included in the comparison to show the decrease of R^2 after excluding one or two parameters. Submodels UO.2b, UO2.c and UO.2d are chosen because they show the smallest decrease of R^2 in the stepwise selection process.

For both examined ozone human health indicators SOMO35 and the 26th highest daily maximum 8-hour average the basic submodel of type 3 selected after the same kind of stepwise selection UO.3a, Submodel UO.3b is included for comparison as the best submodel with a smaller number of variables.

Table 5.26 shows the results for SOMO35. The values of R^2 and RMSE for the submodels of types 1 and 2 show the level of improvement of the regression relation in case supplementary parameters are used: R^2 increases by 0.04 and RMSE decreases by approximately 5%. This is a much smaller improvement than at the rural areas (Section 5.3.1).

The best results with regard to R^2 and RMSE are obtained with model UO.2a. However, model UO.2d gives a 0.01 lower R^2, while it uses only two supplementary variables instead of four. This leads to the

selection of regression model UO.2d, using the EMEP model output and relative humidity, as the preferred regression model.

Table 5.26 Comparison of different submodels of linear regression model equation 2.1 describing the relation between ozone parameter SOMO35 and different supplementary parameters in the urban areas.

lin. regr. model (4.1)	UO.1	UO.2a	UO.2b	UO.2c	UO.2d	UO.3a	UO.3b
constant	n. sign.	34369	35082	34778	36327	42244	76015
altitude GTOPO	not used	0.632	not used	0.902	not used	not used	not used
temperature 2004	not used	not used	not used	not used	not used	not used	not used
wind speed 2004	not used	-155.7	-222.2	not used	not used	-755.3	-609.6
rel. hum. 2004	not used	-348.0	-351.7	-360.3	-376.2	-410.3	-742.9
s. solar radiation 2004	not used	not used	not used	not used	not used	288.6	not used
EMEP model 2004	0.87	0.60	0.60	0.64	0.66	not used	not used
R^2	**0.494**	**0.535**	**0.533**	**0.533**	**0.526**	**0.452**	**0.422**
adjusted R^2	**0.494**	**0.533**	**0.531**	**0.531**	**0.525**	**0.450**	**0.421**
RMSE	**1584.6**	**1520.3**	**1524.6**	**1524.6**	**1535.3**	**1650.6**	**1695.4**

Table 5.27 shows the results for the 26th highest daily maximum 8-hour average value. Only submodels of type 3 were examined, because the EMEP model output is not available for this indicator. The best results are obtained with model UO.3a. Almost similar results are given by the model UO.3b, which uses a smaller number of variables, wind speed and relative humidity, and is therefore to be preferred.

Table 5.27 Comparison of different submodels of linear regression model equation 2.1 describing the relation between ozone parameter 26th highest daily maximum 8-hour average value and different supplementary parameters in the urban areas.

lin. regr. model (4.1)	UO.3a	UO.3b
constant	396.5	519.2
altitude GTOPO	not used	not used
temperature 2004	not used	not used
wind speed 2004	-6.65	-6.12
rel. hum. 2004	-2.92	-4.12
s. solar radiation 2004	1.05	not used
EMEP model 2004	not used	not used
R^2	**0.452**	**0.444**
adjusted R^2	**0.450**	**0.443**
RMSE	**11.53**	**11.62**

5.9.2 Conclusion of linear regression models for urban ozone

Different submodels of the linear regression model (equation 2.1) were examined for the two ozone indicators, SOMO35 and the 26th highest daily maximum 8-hour average value for urban areas, using different supplementary data.

As the preferred submodel we selected for SOMO35 model UO.2d, which uses EMEP model output and relative humidity, and for the 26th highest daily maximum 8-hour average value, for which no EMEP model output was available, we selected model UO.3b, which uses wind speed and relative humidity. These submodels will be further examined in the spatial interpolation comparisons of the next section.

5.9.3 Comparison of spatial interpolation methods for urban ozone

Various methods were used for spatial interpolation and were compared with each other using RMSE from cross-validation, including the methods which use the urban Delta (Section 3.2, 5.7.3 and Horálek et. al., 2005). The results are also compared with a few submodels of the linear regression model equation 2.1 without interpolation, as examined in Section 5.9.1 and coded the same. The compared methods are as follows:

1. Linear regression models without interpolation

   UO.1 EMEP model output
   UO.2d EMEP model output, relative humidity
   UO.3b wind speed, relative humidity

2. Interpolation methods using primarily monitoring data
   a. IDW
   b. Ordinary kriging (OK) – parameters of variogram selected automatically (b1) and manually fitted (b2)
   c. Ordinary cokriging (LC), using altitude – parameters of variogram selected automatically (c1) and manually fitted (c2)

3. Interpolation of the residuals of linear regression models, using the interpolation methods
   a. IDW
   b. Ord. kriging (OK) – parameterisation of variogram selected automatically (b1) and man. fitted (b2)

4. Methods for interpolation of Delta (and its addition to the rural background field as selected in Section 5.3.5 for final mapping), using
   a. IDW
   b. Ord. kriging (OK) – parameterisation of variogram selected automatically (b1) and man. fitted (b2)

The cross-validation scatterplots for SOMO35 for different interpolation methods using primarily monitoring data (i.e. only for interpolation methods of type 2) are presented in Figure 5.29.

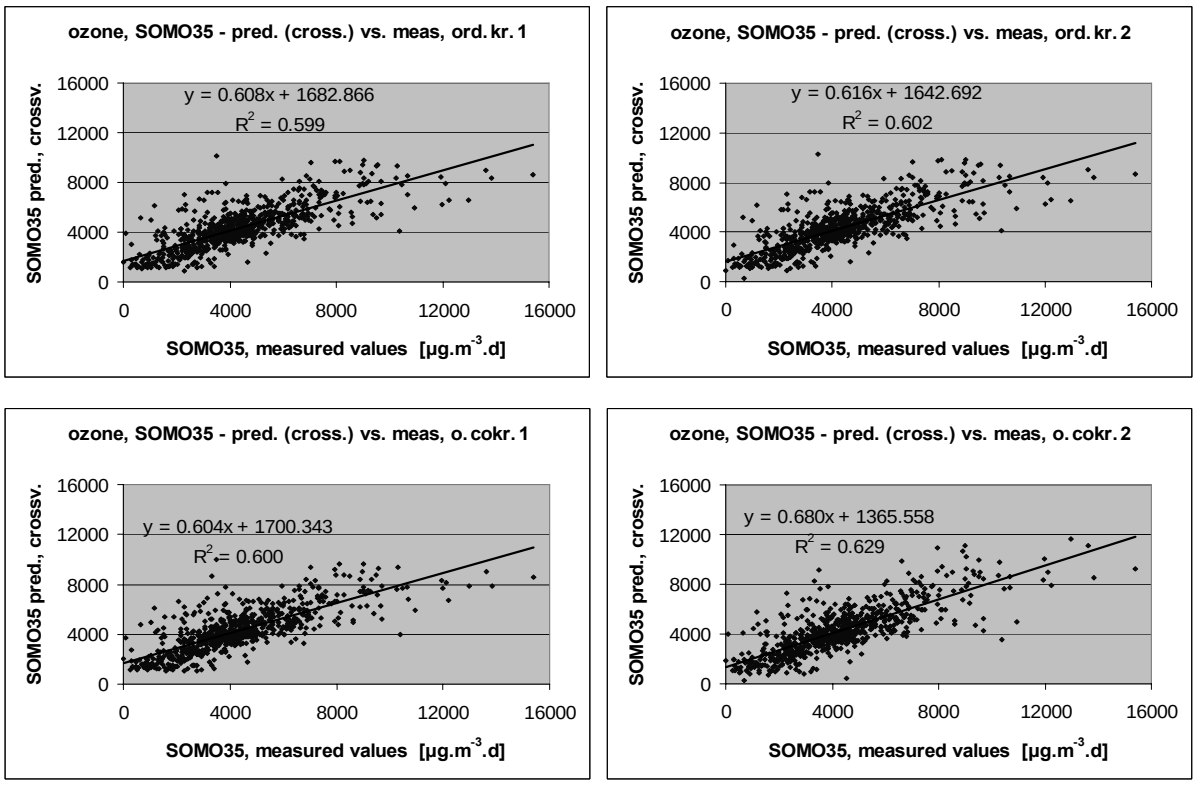

Figure 5.29 Correlation between cross-validation predicted values (y-axis) and measurements (x-axis) for SOMO35 for 2004 in urban areas, for ordinary kriging (top) and ordinary cokriging using altitude (bottom), with parameters of variogram estimated automatically (left) and manually (right).

Similar analysis is presented in Figure 5.30 for the 26th highest daily maximum 8-hour value.

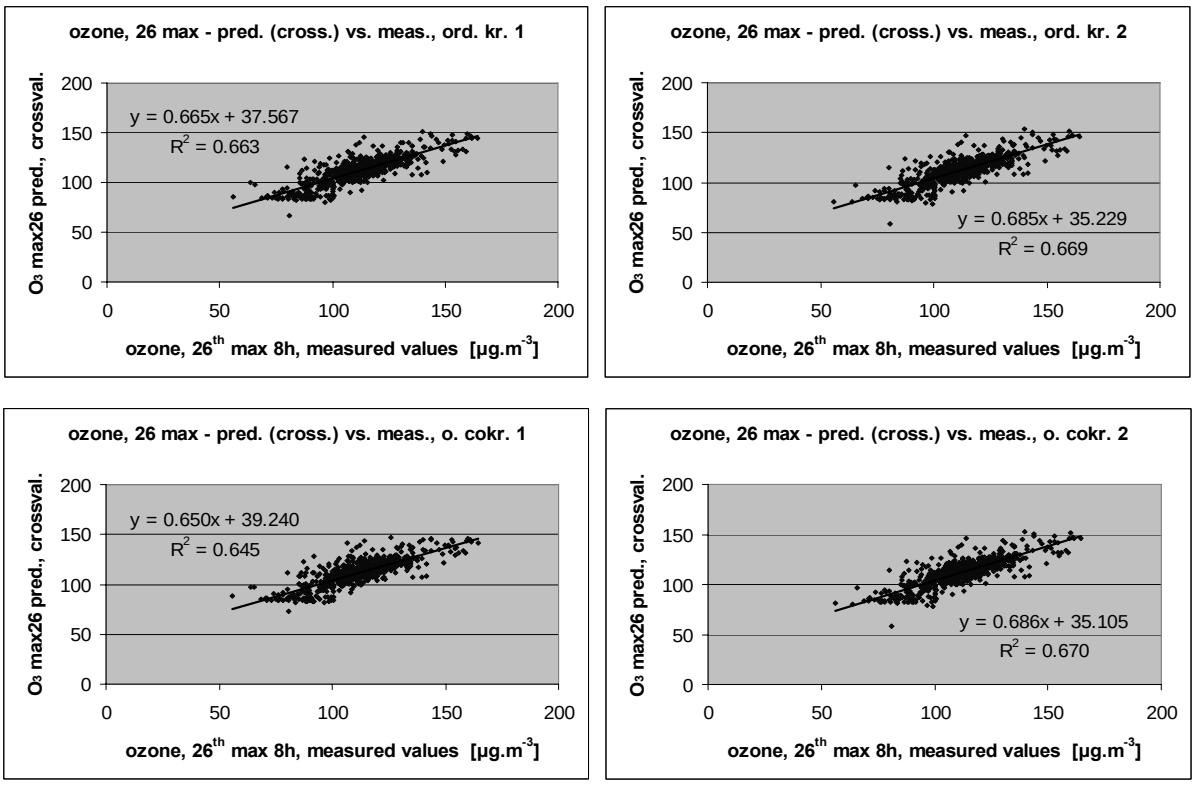

Figure 5.30 Correlation between cross-validation predicted values (y-axis) and measurements (x-axis) for the 26th highest daily maximum 8-hour value for 2004 in urban areas, for ordinary kriging (top) and ordinary cokriging using altitude (bottom), with parameters of variogram estimated automatically (left) and manually (right).

The comparison is carried out with the use of the RMSE and other statistical indicators of the cross-validations and is presented in Table 5.28.

The use of interpolation methods, both interpolations using primarily monitoring data (type 2) and interpolations of the residuals of the linear regression models (type 3), give better results with regard to RMSE and all other statistical indicators than the methods using linear regression models without interpolation (type 1).

The methods using the urban Delta (type 4) give slightly better results than those of type 3 in the case of SOMO35, but give significant worse results in the case of the 26th highest daily maximum 8-hour average value. This might be due to a more reliable (higher R^2 values, Section 5.3.1) interpolated rural background concentration field for SOMO35 than for the 26th highest daily maximum 8-hour value values. The Delta increments are not further used in this paper, because of their relative week performance. Eventual better use of Delta can be a point for future examination.

Table 5.28 shows that for both human health indicators, the SOMO35 and the 26th highest daily maximum 8-hour averages, the best method is 2-c, i.e. ordinary cokriging with altitude (based on RMSE and almost all other statistical indicators from cross-validation).

The maps used in final mapping (i.e. 2-b2 for SOMO35 and 2-c2 for the 26th highest daily maximum 8-hour averages, see Section 5.9.4) are presented in Figure 5.31, for both ozone indicators. The uncertainty of these maps expressed by RMSE in $\mu g.m^{-3}$ can be seen in Table 5.28. The relative uncertainty of the urban ozone map is about 33% for SOMO35 and about 8% for the 36th 26th highest daily maximum 8-hour value.

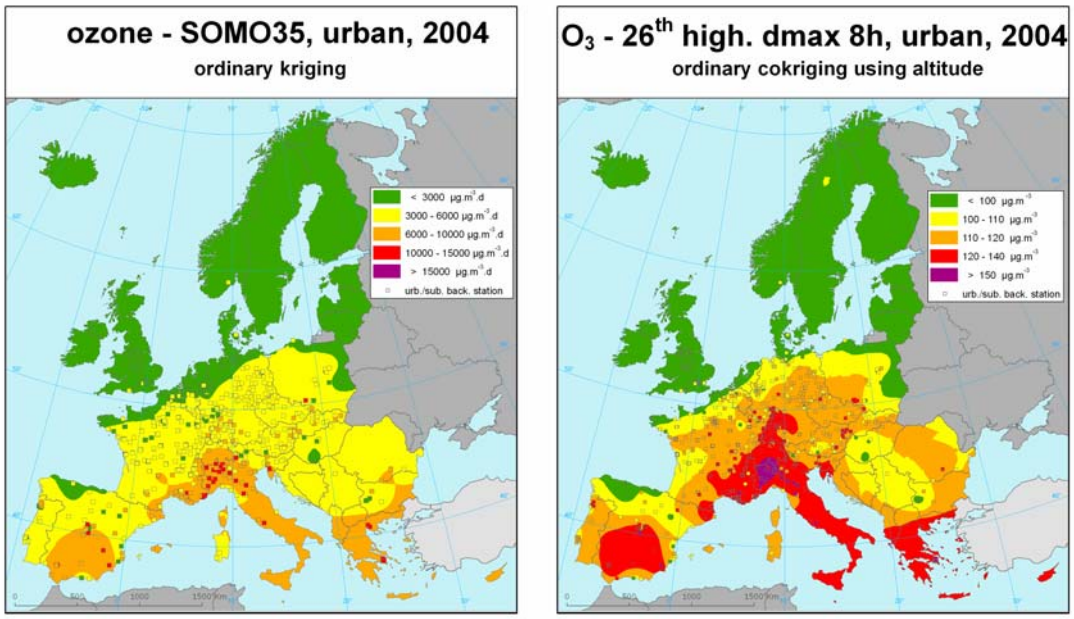

Figure 5.31 Maps showing the ozone indicators SOMO35, in µg.m^{-3}.days (left) and 26th highest maximum daily 8-hour value, in µg.m^{-3} (right) on European scale for urban areas in 2004 as a result of interpolation method 2-b2 (left) and 2-c2 (right). The maps are applicable only in the urban areas.

Table 5.28 Comparison of different interpolation methods showing RMSE (in different units) for the ozone indicators SOMO35 and 26th highest daily maximum 8-hour average value, for 2004, urban areas.

mapping method		SOMO35 [µg.m^{-3}.h]									26th highest daily maximum 8-hour value [µg.m^{-3}]								
		RMSE	MPE	SD (error)	min (error)	max (error)	MAE	MedAE	R^2	MPSE	RMSE	MPE	SD (error)	min (error)	max (error)	MAE	MedAE	R^2	MPSE
1-UO.1	lin. regr. UO.1	1585	19	1583	-5732	9279	1115	780	0.494										
1-UO.2d	lin. regr. UO.2d	1535	0	1534	-6381	8672	1060	730	0.526										
1-UO.3b	lin. regr. UO.3b	1695	0	1694	-7963	8640	1196	820	0.422		11.62	0.00	11.61	-54.13	38.17	8.62	6.48	0.444	
2-a	interp. IDW	1416	-50	1415	-6506	6598	988	692	0.602		9.29	0.00	9.29	-31.70	36.44	6.86	5.18	0.656	
2-b1	interp. OK-aut	1419	-1	1419	-6774	6664	983	694	0.599	1208	9.18	0.05	9.18	-32.00	36.56	6.79	5.20	0.663	8.31
2-b2	interp. OK-fit	1413	-6	1413	-6708	6811	981	692	0.602	1108	9.10	-0.04	9.10	-32.56	35.68	6.77	5.12	0.669	6.83
2-c1	interp. OC-aut (alt.)	1417	-1	1417	-6789	6512	993	689	0.600	1183	9.43	0.06	9.43	-33.43	36.02	6.98	5.28	0.645	8.11
2-c2	interp. OC-fit (alt.)	1372	-10	1371	-6854	5665	965	660	0.629	907	9.09	-0.03	9.09	-32.87	35.56	6.76	5.14	0.670	6.87
3-UO.1-a	lin. regr. 1 + IDW	1478	-54	1477	-7561	6667	1023	701											
3-UO.1-b1	lin. regr. 1 + OK-aut	1500	0	1500	-8165	6189	1035	698		1346									
3-UO.1-b2	lin. regr. 1 + OK-fit	1464	-6	1464	-6967	6181	1018	742		1326									
3-UO.2d-a	lin. regr. 2a + IDW	1454	-72	1452	-7088	6675	1003	709											
3-UO.2d-b1	lin. regr. 2a + OK-aut	1476	-3	1476	-7723	6104	1015	683		1315									
3-UO.2d-b2	lin. regr. 2a + OK-fit	1443	-14	1443	-6904	6255	1002	707		1267									
3-UO.3b-a	lin. regr. 3b + IDW	1457	-111	1453	-6413	6469	1023	740			9.33	-0.46	9.32	-33.45	36.21	6.92	5.39		
3-UO.3b-b1	lin. regr. 3b + OK-aut	1484	-7	1484	-6878	6121	1042	732		1311	9.40	0.03	9.40	-31.05	39.91	7.04	5.31		8.80
3-UO.3b-b2	lin. regr. 3b + OK-fit	1459	-34	1459	-6937	5992	1032	751		1306	9.22	-0.05	9.22	-32.01	37.68	6.91	5.37		8.55
4-a	Delta IDW	1452	-40	1451	-6419	5849	1020	698			9.82	-0.49	9.81	-57.92	35.73	7.19	5.51		
4-b1	Delta OK-aut	1475	5	1475	-6863	6449	1019	661		1359	10.35	-0.13	10.35	-60.25	37.46	7.52	5.67		9.28
4-b2	Delta OK-fit	1421	-6	1421	-6502	4984	1000	698		1212	9.62	-0.19	9.62	-62.44	33.90	7.01	5.15		7.79

5.9.4 Conclusions on the spatial interpolation for ozone, urban areas

Various methods were used for spatial interpolation and were mutually compared using RMSE and other statistical indicators from cross-validation for both examined ozone indicators SOMO35 and the 26th highest daily maximum 8-hour averages.

The best results were obtained for both human health-related ozone indicators by method 2-c, ordinary cokriging using altitude. This method is used for the final mapping of the 26th highest daily maximum 8-hour average values (Chapter 8). However, for SOMO35 the final urban maps and tables were created by its very close "second best" method 2-b, i.e. ordinary kriging, because they were already constructed before the additional test on method 2-c took place.

6 Comparison of exceedance mapping based on daily and annual statistics

A matter of extra interest to the mapping methodologies applied in this report is how interpolations on different temporal resolutions may affect the ultimate conclusions and maps of exceedances for Europe. It is important to investigate these exceedances in time and space for temporal resolutions that coincide with the actual exceedance legislation. For the case of PM_{10}, which has a daily mean limit value, this means carrying out the interpolation based on daily mean concentration fields and to compare their sums and distributions with the exceedances based on annual resolutions, i.e. the annual statistics used in the interpolations in the other chapters of this report. This will allow a comparison between the use of temporal resolutions of daily means versus the annual statistics for the assessment indicators of annual mean, 36^{th} maximum daily mean and number of exceedance days. One practical drawback of interpolation using daily means is that the calculation of the 365 fields required is much more demanding, and impossible if automated routines are not in place, and can therefore lead to preferred assessments based on annual statistics. The different outcomes of the study in this chapter can become important determinants for assessing the uncertainties in the use of annual statistical data versus daily means and can contribute to refine calculation methods of exceedances proposed for legislation.

In this chapter the interpolation methodology already applied to produce maps for ozone and PM_{10} based on annual statistics, i.e. residual kriging of the regression model, is now applied to daily concentration fields of PM_{10}. The aim of this study is to apply the methodology on short time scales, i.e. daily mean concentrations instead of annual data, to determine if the interpolation is best carried out on a daily or annual basis. Three PM_{10} indicators are investigated for the year 2003, being

1. Annual mean PM_{10} concentration
2. 36^{th} highest daily mean PM_{10} concentration
3. The number of exceedance (NOE) days of PM_{10}, i.e. days when daily mean $PM_{10} > 50\ \mu g \cdot m^{-3}$

Conceptually differences in calculated fields should occur for the following reasons:

- The regression and residual kriging parameters will be defined on a daily basis.
- The number of stations available on a particular day will vary. Stations with coverage < 75% on an annual basis can contribute on a daily basis.

The methodology differs slightly from that applied in the previous chapters and reports in the following ways:

- The entire process is scripted using MATLAB software, as opposed to ESRI based software.
- Regression is carried out using the Unified EMEP model only, i.e. no other parameters such as altitude are included.
- When the regression coefficient is very low, i.e. $R^2 < 0.1$, for a daily mean calculation then the model field is adjusted by the mean bias only, i.e. the regression slope is fixed at 1. This is to avoid unrealistic results when correlation is poor.
- The kriging parameters of sill, nugget and range are set for each day based on minimising the cross validation RMSE for each day. This is carried out by searching the parameter space of Nugget:sill ratio (0 – 1) and range (100 – 1000 km). Previously this optimisation was carried out manually. The sill value is automatically set by fitting the semivariogram with a spherical model (Denby et al. (2005), Section 2.5.1).
- The number of stations used is slightly different to previous assessments since daily mean data was not available at all of the stations used in Horálek et al. (2005)
- Only rural background stations are included and the mapping resolution is 25 x 25 km, as opposed to the 10 x 10 km resolution used in previous studies.

- The number of nearest stations used for each individual interpolation on the grid is 20 stations, as opposed to 50.

To avoid inconsistencies associated with the above points when comparing annual and daily interpolations the interpolations based on annual statistics are recalculated using the same stations, method and resolution as used for the daily means.

In this chapter we will first examine the statistical, regression and kriging parameters on a day-by-day basis to see how these vary with time (Section 6.1). We will then go on to look at the results for the three different PM_{10} indicators mentioned above (Sections 6.2 – 6.4), including the spatial uncertainty (Section 6.5), and conclude with a discussion of the results and on uncertainty (Section 6.6).

Throughout the comparison use is made of the cross validation RMSE to assess the quality of the interpolations, as has been previously done.

6.1 Daily variation of interpolation parameters

For each day the daily mean observed and modelled data are analysed and displayed in Figures 6.1-6.5. The analysis includes the following parameters

1. Daily mean of observed and modelled concentrations
2. Daily standard deviation (SD) of observed and modelled concentrations
3. Regression parameters of intercept, slope and regression coefficient (R^2)
4. Kriging parameters of range and nugget:sill ratio
5. Cross validation RMSE for the
    a. EMEP model
    b. Model regression
    c. Kriging only
    d. Residual kriging

6.1.1 Station availability

For the year 2003, 203 PM_{10} stations were available from the AirBase database with data coverage > 25%. Of these, only 151 stations with a coverage > 75% are used in the annual statistics. On a daily basis however the number of stations used for the interpolation varies. This is shown in Figure 6.1. The number of stations used each day is, on average, 166.

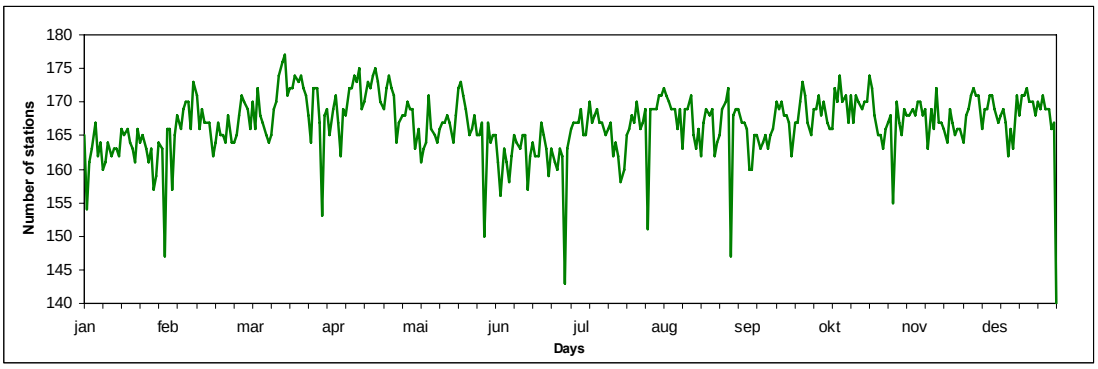

Figure 6.1 Plot showing the number of stations used for the daily interpolations, for the year 2003.The number of stations with coverage > 75% is 151. Number of stations with coverage>25% is 203. Average number of stations used each day is 166.

6.1.2 Daily mean and standard deviation comparison

The daily mean (mean of all available stations for that day) is plotted in Figure 6.2-top for both the observed and modelled (interpolated to monitoring sites) concentrations. There is a clear bias between monitoring and modelling with an average model bias of -12.2 $\mu g \cdot m^{-3}$, or a relative bias of around –50%. The EMEP model is clearly underestimating PM_{10} concentrations throughout the model domain but the daily variation is well correlated, R^2=0.64, suggesting that there are missing sources (e.g. secondary particle formation, soil dust, etc.) but the effect of meteorology is well represented.

The daily SD (SD of all available stations for each day) is plotted in Figure 6.2-bottom for both the observed and modelled (interpolated to monitoring sites) concentrations. The SD shows a similar bias to the mean concentrations, however when the normalised SD is calculated then both model and observations show very similar relative variance, of 59 % and 65 % respectively. This indicates that the EMEP model is capturing much of the variation inherent in the system even though concentrations are too low.

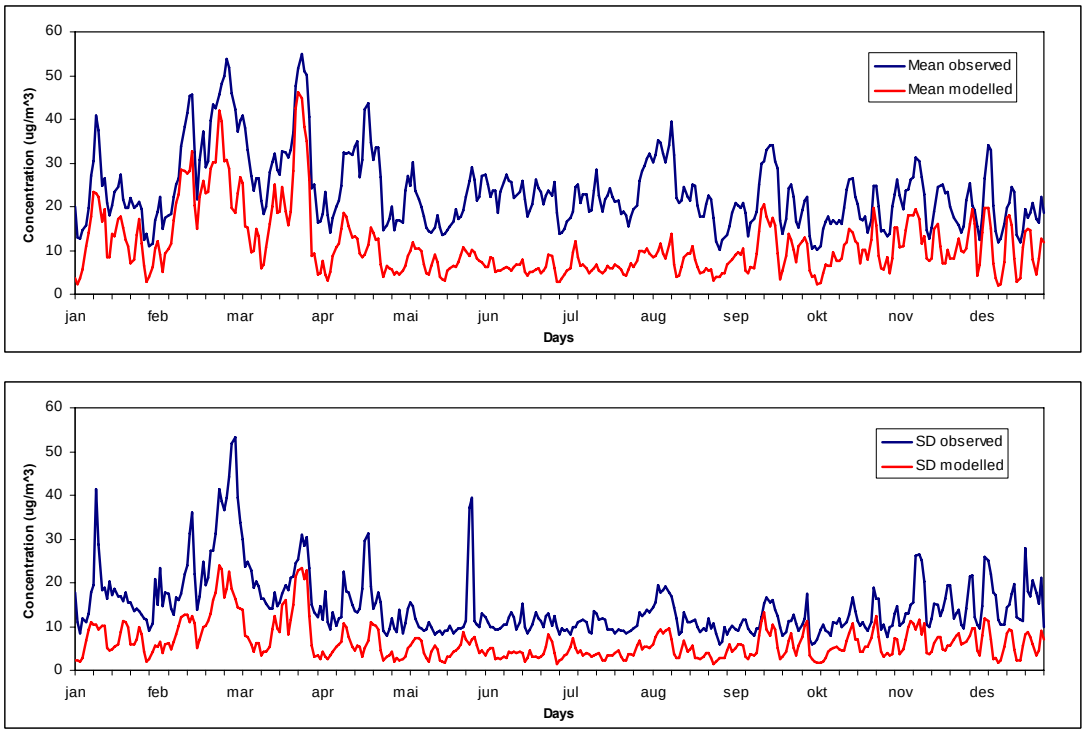

Figure 6.2 Plot of the daily mean concentrations (top) and SD (bottom) for all stations used in the daily interpolation, blue, along with the corresponding model concentrations, red, for the year 2003.

6.1.3 Regression parameters

For each day the model is fitted using linear regression with the resulting regression parameters of intercept, slope and correlation coefficient (R^2). Note that, to avoid spurious regressions when correlation is poor, the linear regression model was substituted by a simple bias correction when $R^2 <$ 0.1. These parameters are plotted in Figure 6.3. Only occasionally does the intercept fall below 0, with an average for the entire period of 12.0 $\mu g \cdot m^{-3}$, compared to the model bias of –12.2 $\mu g \cdot m^{-3}$. This reflects the general bias already known in the EMEP model in regard to PM_{10}.

The slope of the linear regression varies from day to day but is rarely below 0.5 or above 2.0. The correlation coefficient is larger than 0.1 for 63% of the time and so normal linear regression is applied for the majority of cases. The average slope of all the days is 1.10.

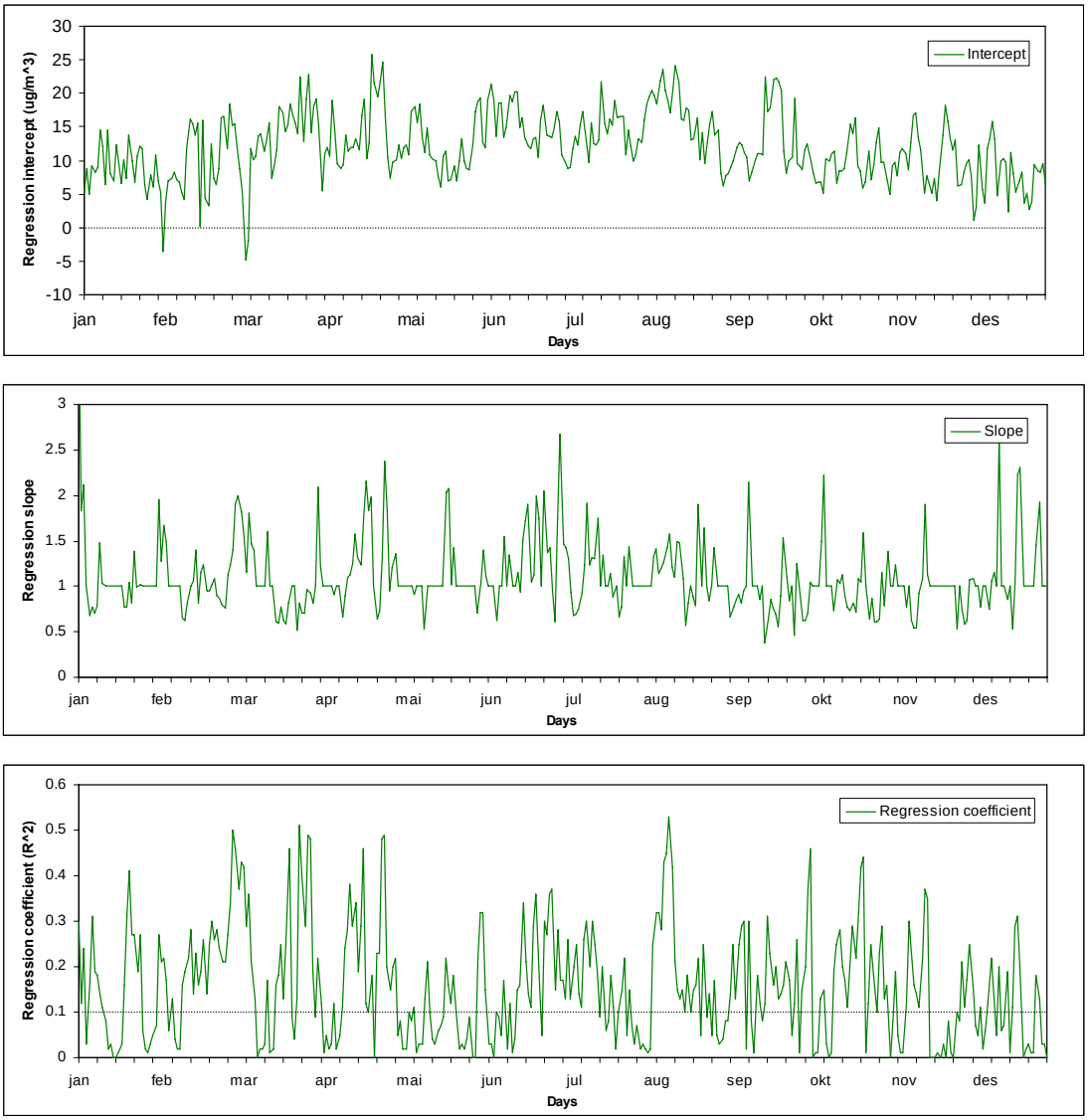

Figure 6.3 Plot showing the daily variation of the regression parameters used in the linear regression model fit of the modelled concentrations to the observed concentrations for the year 2003. Intercept (top), slope (middle) and regression correlation coefficient (bottom).

6.1.4 Kriging parameters

For each day the residual, observed concentration minus regression model concentration, is interpolated to create the final interpolation map. For comparison purposes the direct kriging of the observed concentrations is also carried out. The kriging parameters are determined by an automatic routine that minimises the cross validation RMSE in regard to range and nugget:sill ratio. This routine tests range values, from 100 km to 1000 km in steps of 100 km, as well as nugget:sill ratios, from 0 to 1 in steps of 0.1, to find the parameters that minimise the cross validation RMSE. In addition to this routine it is also possible to directly fit the variograms with a spherical model for which the range is fixed at 300 km, a value found to be optimal (see Section 6.2) for annual mean interpolations. The sill is specified in both cases by this fit.

The nugget:sill ratio and range, Figure 6.4 top and bottom, indicate the dependence of spatial variance on the lag distance. Short ranges indicate small scale spatial variance and small nugget:sill ratios indicate strong local covariance. If the variogram model has a high nugget:sill ratio then this means there is little spatial covariance between observations. If the range is very small, independent of the nugget:sill ratio, then there is also very little spatial covariance over the region. When this is the case

the kriging methodology does little more than produce the spatial average of the stations used for the kriging interpolation at that point.

From Figure 6.4-top it can be seen that there are a significant number of days with nugget:sill ratios of intermediate values, indicating that kriging is indeed providing spatial interpolations. It is interesting to note that the nugget:sill ratios for residual and pure kriging follow very similar temporal developments. This indicates, as will be discussed later, that the spatial covariance of the residual and the observations are quite similar.

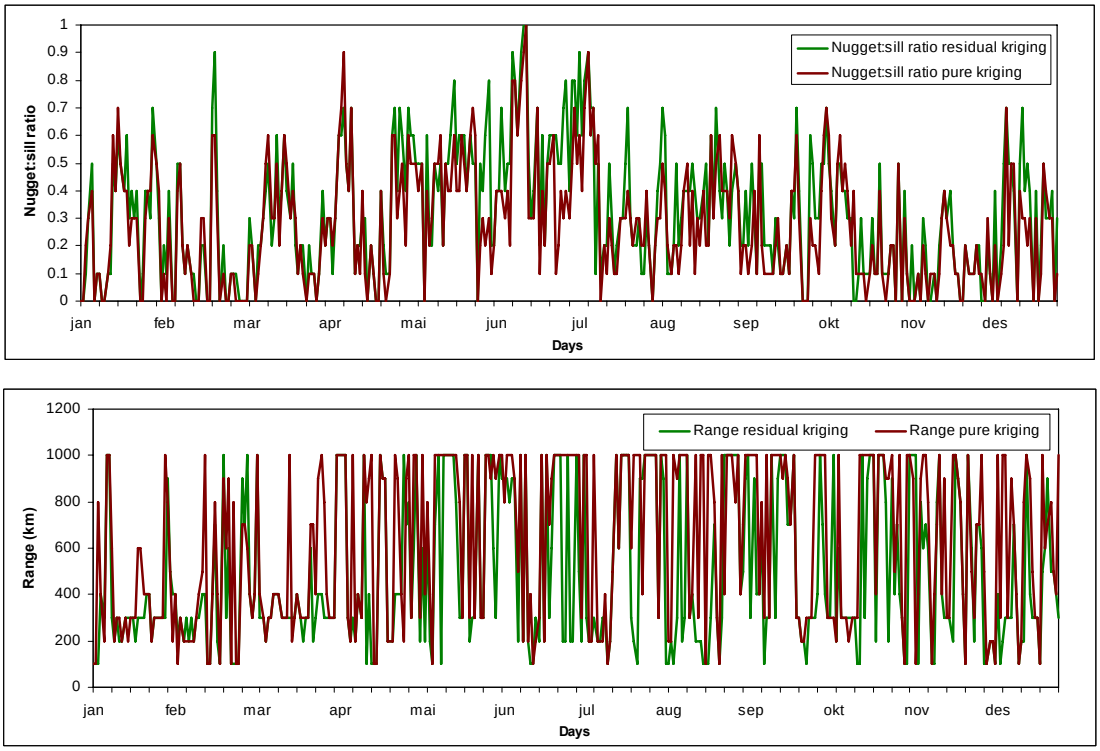

Figure 6.4 Plots of the kriging parameters determined on a daily basis: nugget:sill ratio (top) and range (bottom). The parameters are determined by minimising the cross validation RMSE for each day. Shown are the kriging parameters for both residual kriging, green, and pure kriging (direct kriging of observations), brown.

6.1.5 Cross validation RMSE

The RMSE has been calculated on a daily basis for the 4 cases of model, regression model, pure kriging and residual kriging. The resulting graph is shown in Figure 6.5 (top), along with a cut out for the month of April (Figure 6.5, bottom) to show the results in more detail. Included in the graph is also the observed SD for reference. This is included since any interpolation should improve upon this value as it indicates the RMSE of the simplest model available, that being a model where the entire concentration field is equal to the mean of the observations.

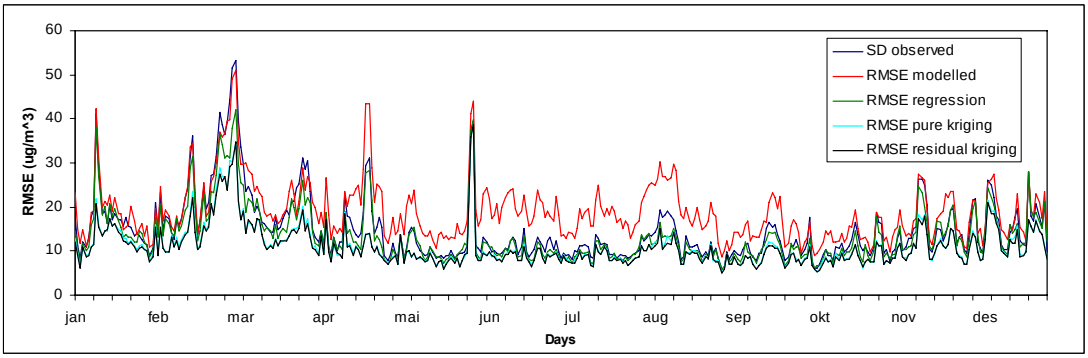

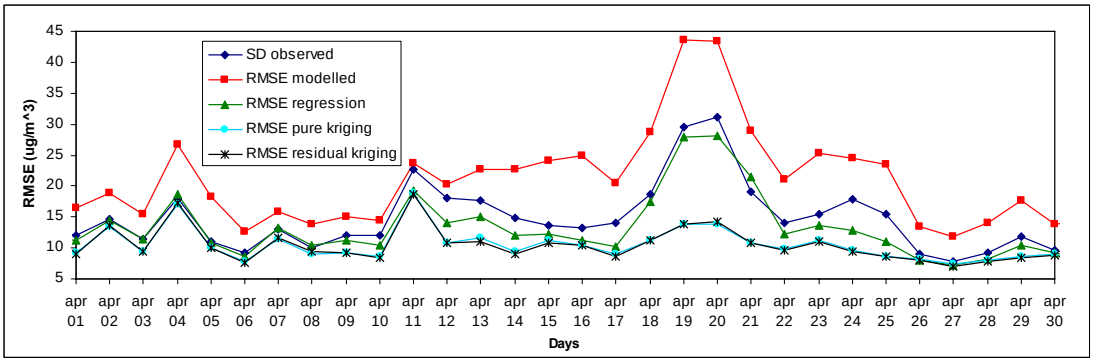

Figure 6.5 Plots for the entire year (top) and for April only (bottom) of the cross validation RMSE determined on a daily basis for model, regression model, pure kriging and residual kriging. Included is the observed SD for comparison.

The modelled RMSE is clearly the largest, mainly due to the bias in the EMEP model for PM_{10}. Regression removes this bias and for the most part improves on the observed SD. However, pure kriging generally produces RMSEs that can be significantly less than the regression models. There is only a minimal improvement when kriging of the residual is applied.

The results are summarised in Table 6.1 below, which gives the total RMSE for all stations and all days. These values indicate that kriging is dominant in providing the best interpolation on the daily scale. The improvement obtained through residual kriging is small.

Table 6.1 Summary table showing the total cross validation RMSE on a daily basis. Normalisation of RMSE (NRMSE) is carried out using the total mean observed concentration = 23.48 $\mu g \cdot m^{-3}$

Interpolation method	Cross validation RMSE (ug/m3)	Cross validation NRMSE (%)
Observed SD	16.4	70
EMEP model	20.0	85
Regression model	14.8	63
Pure kriging	12.1	52
Residual kriging	11.8	50

Since the interpolation, when using regression or kriging, is generally unbiased the RMSE given in Table 6.1 can be directly interpreted in terms of the global uncertainty in the interpolation, expressed in terms of standard deviation when a Gaussian distribution is assumed. Even when using the best interpolation method the normalised RMSE (NRMSE) is still 50% indicating that the global uncertainty in the daily mean concentration fields of rural background PM_{10} is quite high.

6.2 Comparison of annual mean fields using daily and annual statistics

We will now compare the calculated annual mean fields derived from daily and annual statistics using residual kriging of the model regression. The two fields are calculated in essentially the same manner except that for daily statistics the resultant field is given by the mean of the interpolated fields whilst for annual statistics the resultant field is the interpolation of the observed means.

Figure 6.6 shows the annual field, the daily field and the difference field (annual – daily) respectively. Differences over most of Europe are of the same order or smaller than the estimated uncertainty, based on the RMSE shown in Table 6.2. However, it should be noted that the comparison is complicated by the RMSE minimisation methodology applied to determine the kriging parameters. This minimisation is applied to the annual means only once and the kriging parameters obtained strongly influence the resulting interpolation. To avoid this complication the map shown in Figure 6.6 (top-left) was determined using the average nugget:sill ratio and range taken from the daily fits, i.e. 0.31 and 250 km respectively. If this was not done then the automatic RMSE minimisation routine would have provided a nugget:sill ratio of 0 and a range of 100 km resulting in a significantly different plot but with an insignificant improvement in RMSE.

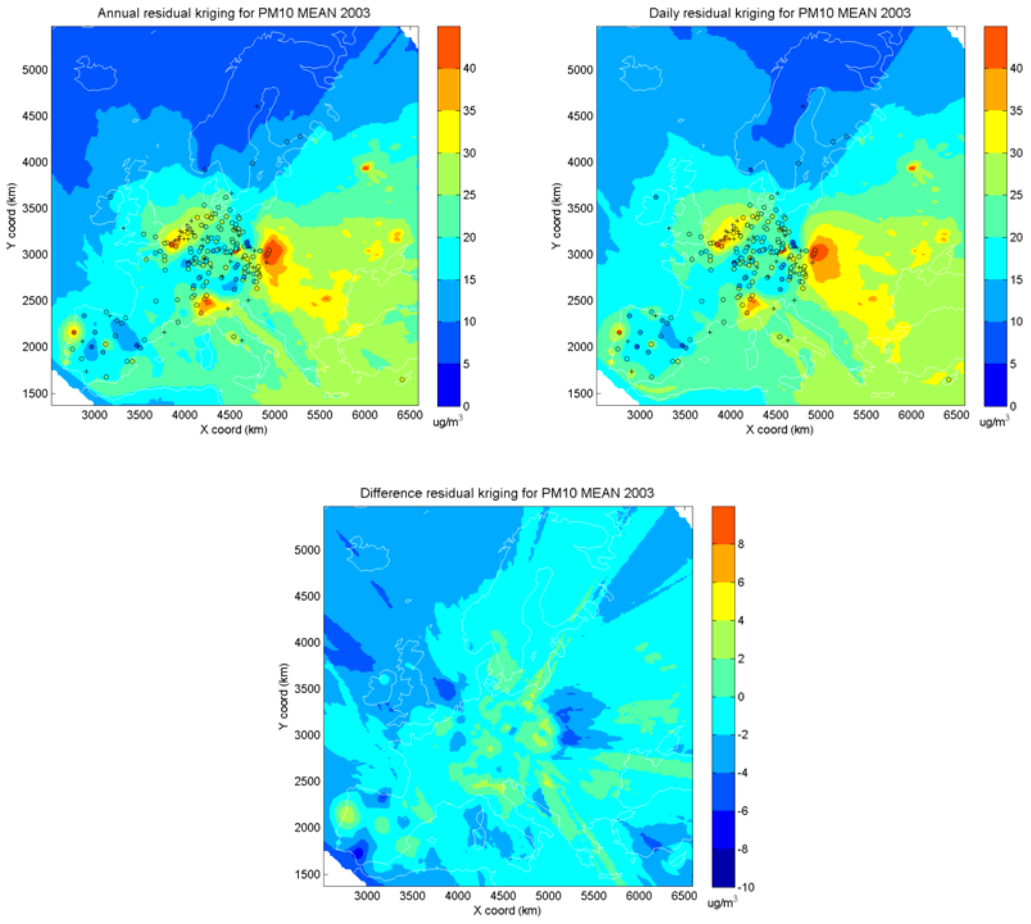

Figure 6.6 Showing the interpolated field for annual mean PM_{10} ($\mu g \cdot m^{-3}$) in 2003 based on annual statistics (top-left), daily statistics (top-right) and the difference (annual – daily) between the 2 fields (bottom). The interpolation method used is the residual kriging of model regression and the grid resolution of the interpolation is 25 x 25 km. Also included are the stations used in the interpolations. Stations with coverage > 75%, used in the annual interpolation, are shown with values as circles. Other stations used in the daily interpolation with coverage >25% are shown as crosses.

Table 6.2 summarises the results in terms of the cross validation RMSE and NRMSE. The annual mean field produced using residual kriging after regression produces the lowest RMSE. The RMSE is slightly lower when using daily statistics for all cases.

Table 6.2 RMSE of annual and daily statistics. The NRMSE is calculated using the annual limit value = 40 μg·m^{-3} to indicate the relative uncertainty at this value.

	Annual		Daily	
Interpolation method	RMSE (ug/m3)	NRMSE (%)	RMSE (ug/m3)	NRMSE (%)
Observed SD	9.26	23	9.26	23
EMEP model	14.4	36	14.4	36
Regression model	8.31	21	8.26	21
Pure kriging	7.07	18	6.93	17
Residual kriging	6.74	17	6.56	16

Conclusion

Though there are some differences between the annual mean concentration fields for PM_{10} produced using annual and daily statistics, these differences are of the same order, or smaller, than the estimated uncertainty in the methods when appropriate kriging parameters are used for the annual interpolation. Thus the small improvement obtained using daily data must be weighed against the extra data handling requirements to achieve them. However, use of daily interpolations must be seen as a more robust method in terms of estimating the appropriate kriging parameters than the use of a single interpolation for the annual statistics. In addition the inclusion of more stations, on a daily basis, can only help to improve the resulting mean fields.

6.3 Comparison of percentile fields using daily and annual statistics

We will now compare the calculated annual percentile fields derived from daily and annual statistics using residual kriging of the model regression. The two fields are calculated in essentially the same manner except that for daily statistics the resultant field is given by the 36th highest daily mean of the interpolated fields whilst for annual statistics the resultant field is the interpolation of the observed 36th highest daily mean.

Figure 6.7 shows the annual percentile field, the daily percentile field and the difference field (annual – daily) respectively. Differences over most of Europe are of the same order or smaller than the estimated uncertainty, based on the RMSE shown in Table 6.3. However, as in the case of the annual mean, the comparison is sensitive to the choice of kriging parameters. In a similar fashion the top-left map of Figure 6.7 was determined using the average nugget:sill ratio and range taken from the daily fits, i.e. 0.31 and 250 km respectively. If this was not done then the automatic RMSE minimisation routine would have provided a nugget:sill ratio of 0 and a range of 100 km resulting in a quite different plot and a more substantial difference between the daily and annual fields.

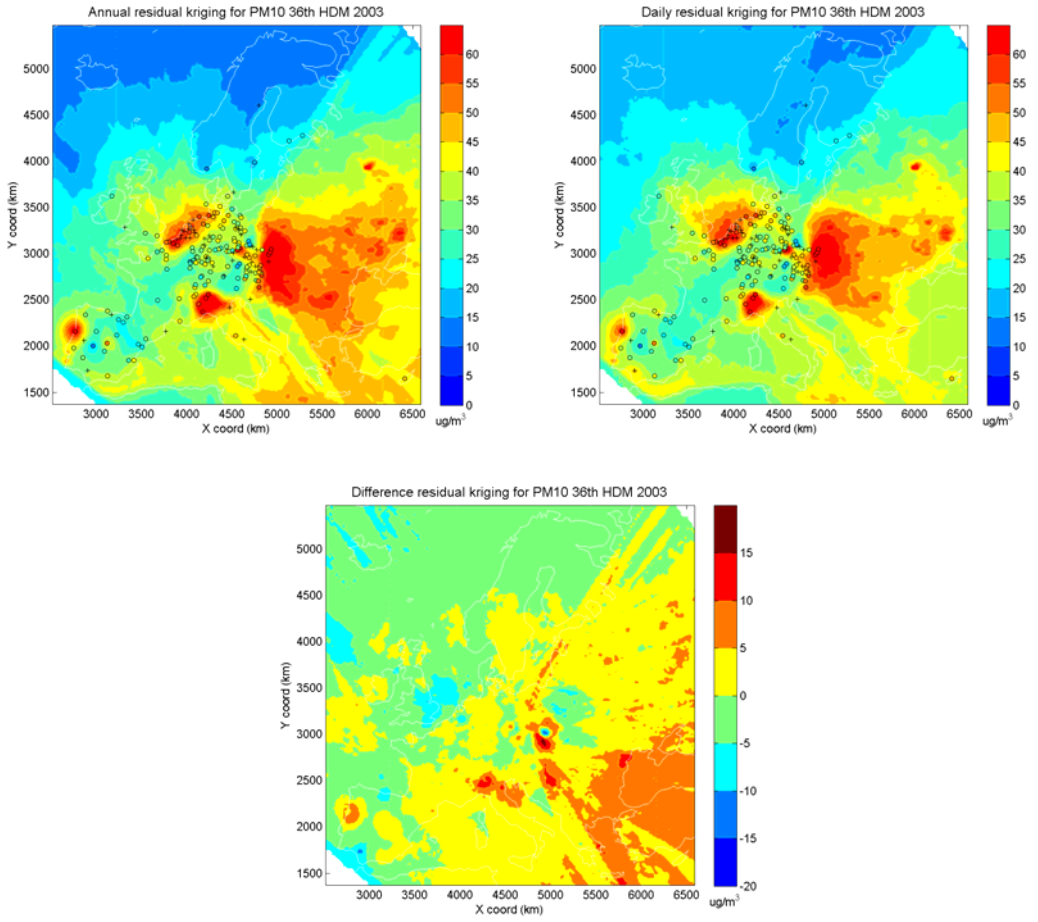

Figure 6.7 Showing the interpolated field for the 36th highest daily mean concentration of PM_{10} ($\mu g \cdot m^{-3}$) in 2003 based on annual statistics (top-left), daily statistics (top-right) and the difference (annual – daily) between the 2 fields (bottom). The interpolation method used is the residual kriging of model regression and the grid resolution of the interpolation is 25 x 25 km. Stations with coverage > 75%, used in the annual interpolation, are shown with values as circles. Other stations used in the daily interpolation with coverage >25% are shown as crosses.

Table 6.3 summarises the results in terms of the cross validation RMSE and NRMSE, where the RMSE has been normalised with the daily limit value for human health of 50 $\mu g \cdot m^{-3}$. The percentile field produced using residual kriging after regression produces the lowest RMSE. The RMSE is slightly lower when using daily statistics for all cases.

Table 6.3 RMSE of annual and daily statistics for the 36th highest daily mean. The NRMSE is normalised using the limit value of 50 ug/m3 to indicate the relative uncertainty at the threshold value.

	Annual		Daily	
Interpolation method	RMSE (ug/m3)	NRMSE (%)	RMSE (ug/m3)	NRMSE (%)
Observed SD	17.4	35	17.4	35
EMEP model	22.8	46	22.8	46
Regression model	16.0	32	16.1	32
Pure kriging	13.2	26	12.6	25
Residual kriging	12.6	25	12.0	24

Conclusion

Though there are some differences between the percentile fields for PM_{10} produced using annual and daily statistics, these differences are of the same order, or smaller, than the estimated uncertainty in the methods when appropriate kriging parameters are used for the annual interpolation. However, use of daily interpolations must be seen as a more robust method in terms of estimating these kriging parameters than the use of a single interpolation for the annual statistics. In addition the inclusion of more stations, on a daily basis, can only help improve the resulting percentile fields.

6.4 Comparison of number of exceedance days fields using daily and annual statistics

We will now compare the calculated number of exceedance days (NOE) derived from the daily and annual statistics using residual kriging of the model regression. The NOE and the 36^{th} highest daily mean are two methods for describing the exceedance of limit values but they differ in that the percentile field is more continuous, having no cut-off value, whilst the NOE on the other hand is calculated using such a threshold value. This tends to lead to a more discontinuous field.

The interpolation using daily and annual statistics differ in that for daily statistics each daily mean concentration field is assessed as to whether it has exceeded the limit value of 50 $\mu g \cdot m^{-3}$. The exceedance field is then summed over the entire year. When using annual statistics the number of observed exceedance days, in combination with those calculated with the EMEP model and regression, are interpolated. This leads to complications since the EMEP model, due to its bias, rarely exceeds the threshold value leading to little improvement through regression. In addition, because there are many regions with no exceedance days, the residual kriging or pure kriging interpolations can lead to negative values of the exceedance days when the interpolation is carried out based on annual statistics.

Figure 6.8 shows the annual based NOE field, the daily based NOE field and the difference field (annual – daily) respectively. Differences between the two methods can be quite large but are of the order of the estimated uncertainty, based on the RMSE shown in Table 6.5 and the uncertainty maps given in Figure 6.10. It is important to note that even the best RMSE for the NOE days is still 20 days indicating a large uncertainty in the spatial mapping of this parameter.

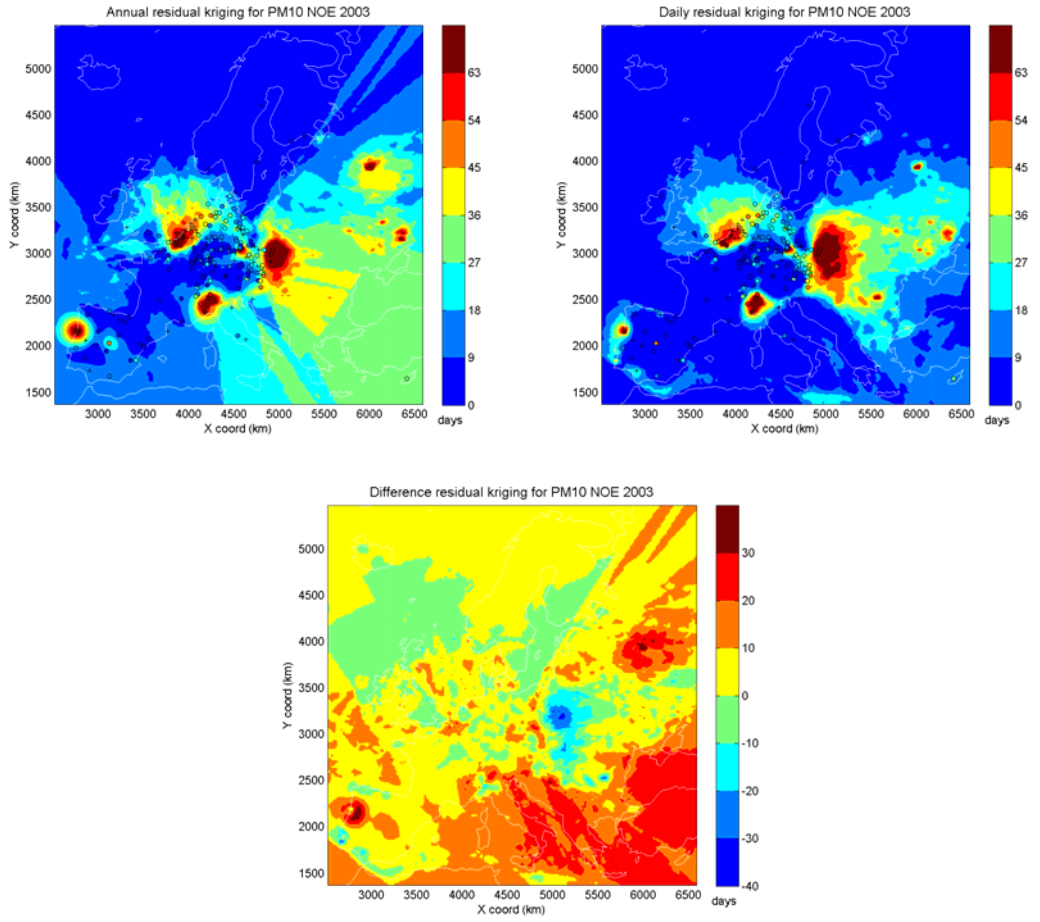

Figure 6.8 Showing the interpolated field for NOE days for PM_{10} (days) in 2003 based on annual statistics (top-left), daily statistics (top-right) and the difference (annual – daily) between the 2 fields (bottom). The interpolation method used is the residual kriging of model regression and the grid resolution of the interpolation is 25 x 25 km. Stations with coverage > 75%, used in the annual interpolation, are shown with values as circles. Other stations used in the daily interpolation with coverage >25% are shown as crosses.

Table 6.4 summarises the results in terms of the cross validation RMSE and NRMSE, normalised with the threshold value of 36 days. The NOE field produced using residual kriging after regression produces the lowest RMSE. In this case, as opposed to the mean and percentile fields, the RMSE is slightly lower when using annual statistics, though it cannot be considered to be significant. Also improvement of the RMSE of NOE through regression with the Unified EMEP model is less than that found in the annual mean and percentile calculations, Table 6.3. Residual kriging is only a small improvement on the pure kriging method. This is true for both the annual and daily statistics.

Conceptually it is expected that the best method for creating NOE day fields is by the use of daily statistics, as has been found for the annual mean and percentile calculations, see Tables 6.2 and 6.3. The cross validation RMSE is, however, not improved using daily statistics when interpolating the NOE, Table 6.4. However it is important to note that there is a direct spatial correspondence between the percentile and NOE maps produced when daily statistics are used. This guarantees that the contour representing the limit value, for the case of percentile maps, and the contour representing the number of allowed exceedance days, for the NOE maps, is concurrent in space. This is not the case when interpolating the percentiles and NOE using annual statistics, since the two indicators are interpolated independently of each other. This can be seen when comparing the annual based percentile and NOE interpolations, Figures 6.7-top-left and 6.8-top-left, where the limit value contour of 50 $\mu g \cdot m^{-3}$ is not spatially coincident with the 36 NOE days contour.

Table 6.4 RMSE of annual and daily statistics for the number of exceedance days. The NRMSE is normalised with the limit threshold of 36 days to indicate the relative uncertainty around this threshold.

	Annual		Daily	
Interpolation method	RMSE (days)	NRMSE (%)	RMSE (days)	NRMSE (%)
Observed SD	29.2	81	29.2	81
EMEP model	32.6	91	32.6	91
Regression model	26.1	73	27.8	77
Pure kriging	21.1	59	21.8	61
Residual kriging	20.8	57	21.0	58

Conclusion

The differences between the NOE fields for PM_{10} produced using annual and daily statistics, are of the same order as the estimated uncertainty in the methods and as such it cannot be considered as significant. Even though the cross validation RMSE is almost the same for the annual interpolation the use of daily interpolations must be seen as a more robust method for mapping NOE for the following reasons:

- It is more robust in estimating the appropriate kriging parameters than the use of a single interpolation for the annual statistics
- There is consistency with the percentile maps
- The number of observations used is higher
- Kriging of a non-continuous function, as is the case of NOE using annual statistics, is not preferred

6.5 Uncertainty analysis and mapping

A discussion concerning the uncertainty in the two different methods is required. Throughout this chapter and this report the cross validation RMSE has been used to indicate the quality of the interpolation. This is a useful and well established parameter, though several other parameters may also have been used. This parameter, however, does not give spatial information on the uncertainty of the maps but provides a more global indication of the mapping quality. To indicate the spatial uncertainty use can be made of the variance field produced from the residual kriging interpolation, whether it is based on annual or daily statistics. The spatial uncertainty can be represented by the square root of this variance which is indicative, if a normal distribution is assumed, of the standard deviation (SD_{krig}).

The sill values of the residual kriging interpolation, determined automatically by fitting a spherical model to the residual semivariogram, should thus be close to, but most likely slightly larger than, the regression model RMSE. This is because the regression model RMSE is equivalent to the residual standard deviation (SD_{res}) and the sill represents variances that are generally larger than this value, given that smaller variances are found for shorter lag distances. This is found to be the case, as shown in Table 6.5 for the interpolation based on annual statistics. The cross validation RMSE should then be less than the sill value since it represents stations both close to and far from other stations. This is indeed the case, as shown in Table 6.5.

Table 6.5 Cross validation RMSE for residual kriging, regression model RMSE and SQRT(sill) for the annual based residual interpolations.

Interpolation indicator	Cross validation RMSE	Regression model RMSE (SD_{res})	SQRT(sill)
Mean ($\mu g \cdot m^{-3}$)	6.7	8.3	8.4
Percentile ($\mu g \cdot m^{-3}$)	12.6	16.0	16.3
NOE days (days)	20.4	26.1	26.3

The use of the single globally valid semivariogram model in the kriging interpolation also leads to a rather homogenous spatial view of the uncertainty, particularly far from stations, since it then becomes independent of local concentrations levels. This is likely not to be an appropriate representation of the true spatial uncertainty in the maps.

Despite this, the residual kriging standard deviation field (SD_{krig}) may be used to indicate the spatial uncertainty for the annual based statistics but this becomes more complicated when using daily statistics and when estimating the NOE days, as will be further discussed in Section 6.5.1 and 6.5.2.

6.5.1 Uncertainty in the annual mean when using daily statistics

To estimate the total variance for the annual mean, when it is based on the sum of daily mean values, it is not sufficient to simply 'add up' the daily variance fields calculated from the residual kriging, since there is a certain amount of correlation between concentration fields from day to day. A more extensive analysis is thus required. To estimate the total variance the temporal covariance matrix must be calculated since it is this that represents the correlations between all the days of the year. Mathematically it is useful to decompose the total variance into the sum of the variances and covariances, noting that in terms of the covariance matrix the variances are the diagonal terms and the covariances are the off diagonal terms. If we wish to calculate the total variance of the mean of a parameter *X,* based on the individual variances *Var(X)* then the variance can be written as

$$Var\left(\frac{1}{n}\sum_{i=1}^{n} X_i\right) = \frac{1}{n^2}\sum_{i=1}^{n} Var(X_i) + \frac{1}{n^2}\sum_{i=1}^{n}\sum_{j=1, j\neq i}^{n} Cov(X_i, X_j) \qquad (6.1)$$

$$= \frac{1}{n}\sum_{i=1}^{n} Var(X_i)\left[\frac{1}{n} + \frac{\frac{1}{n^2}\sum_{i}^{n}\sum_{j\neq i}^{n} Cov(X_i, X_j)}{\frac{1}{n}\sum_{i=1}^{n} Var(X_i)}\right] \qquad (6.2)$$

$$= \frac{1}{n}\sum_{i=1}^{n} Var(X_i)[F_{cv}]$$

The first term on the right hand side of equation 6.1 represents the on-diagonal terms of the covariance matrix and the second term the contribution from the off-diagonal terms. When there is no correlation between the elements of *X*, in this case days of the year, then this second term is 0 and the variance of the mean can simply be determined by the first term on the right hand side. In that case it would be possible to use the daily determined kriging variance to represent *Var(X)* and simply divide by n^2, where *n* is the number of days. However, there is quite high correlation in the concentration fields and this must be accounted for by estimating the other covariance terms.

The above equation is rewritten, equation 6.2, to simplify interpretation. In its final form the total variance is simply the mean variance of all the days multiplied by a covariance factor F_{cv}. This factor represents approximately the ratio of the mean off-diagonal terms with the mean on-diagonal terms. Thus when the days are completely correlated with one another this factor approaches 1. When they are totally uncorrelated they approach n^{-1}. Writing the equations in this form allows us to estimate F_{cv}

by creating the temporal covariance matrix, and using the daily kriged variance fields to represent $Var(X_i)$. The individual elements of the covariance matrix are estimated by calculating the variance between the interpolated fields from day to day. In this case the covariance matrix elements are calculated using the residual kriging fields at the positions of the observational stations, instead of the entire model domain, since these are likely to give the most representative results. The covariance matrix created thus contains 365 x 365 elements, representing the covariance of every day with every other day of the year.

Making the calculation in equation 6.2 gives $F_{cv} = 0.239$ indicating a substantial contribution to the total variance from the covariance terms. This factor is then used to scale the sum of the kriged variance estimates, taken from the daily interpolations, to estimate the total variance of the daily averaged fields. The results of this calculation, along with the kriged standard deviation field calculated using annual statistics, are shown in Figure 6.9. The uncertainty calculated in this way is generally slightly lower for the daily statistical method, but only by a value of around 1 $\mu g \cdot m^{-3}$. It is possible to see reduced uncertainty, in the daily based method, at stations that are not represented in the annual calculations.

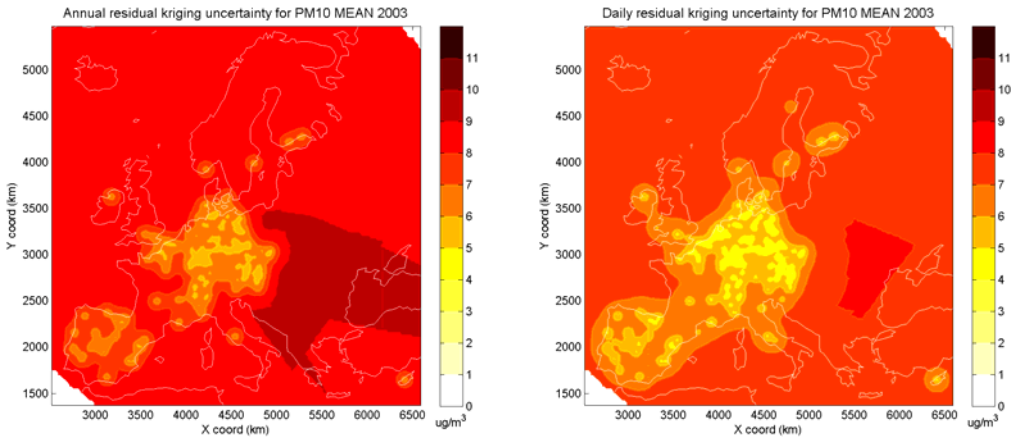

Figure 6.9 Showing the uncertainty maps (SD_{krig}) for the annual mean PM_{10} concentrations based on (left) annual statistics and (right) daily statistics. See text for detailed description of their derivation. The annual mean concentration maps related to these can be found in Figure 6.6.

6.5.2 Uncertainty in the exceedance fields when using daily statistics

In order to compare the spatial uncertainty in the number of exceedance (NOE) days another, in this case more pragmatic, approach is required. From a statistical perspective the expected number of exceedances is the sum of the probability of exceedance for every individual day. It is in principle possible to calculate the probability of exceedance for every day if we know the probability density distribution of the daily mean concentration. If the probability density function is represented by a normal distribution we can use the residual kriging variance to represent the standard deviation and thus calculate the probability of exceedance for each day. If this is done in this fashion, then the final uncertainty in the NOE days will tend to be small, since it assumes each probability to be uncorrelated (which we have shown is not the case) and it does not take into account the question of representativeness and bias.

Instead, the uncertainty in the expected number of exceedance days is calculated by adding up the individual probabilities of exceedance, as described above, but in addition adding and subtracting the annual mean variance, as shown in Figure 6.9, to represent the representativeness and model error. The uncertainty in NOE days is then interpreted as being the maximum deviation, in number of days, from the plus and minus calculations. For example, at one spatial point the annual standard deviation is calculated to be 5 $\mu g \cdot m^{-3}$ and the expected NOE days at that point is calculated to be 20 days. By adding and subtracting 5 $\mu g \cdot m^{-3}$ from the daily mean concentrations used in the probability calculation it is found that adding gives 29 exceedances and subtracting gives 15 exceedances. The uncertainty in the NOE days is then given as 9 days. Using this methodology accounts for the threshold nature of

exceedances, giving low uncertainty in NOE days when the daily mean values are well below the limit and giving high uncertainty in NOE days when the annual mean bias is uncertain and the daily mean values are close to the limit value.

The results of this calculation, as well as the kriged standard deviation field for NOE days calculated using annual statistics, are shown in Figure 6.10. The annual uncertainty map gives a much more homogenous interpretation of the uncertainty, showing reduced uncertainty only in regions near observations. Such kriging is not actually suitable for mapping of this type when a threshold value is involved, and overestimates the uncertainty in areas where low numbers of exceedances occur. The daily based uncertainty map, on the other hand, shows low uncertainty in areas with low numbers of exceedances and in regions close to observations. High uncertainty is estimated in areas without observations and with large numbers of exceedances.

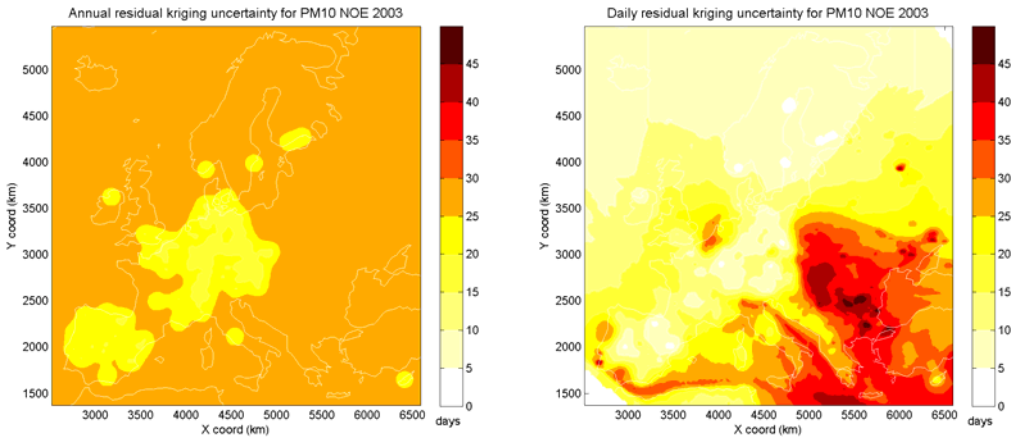

Figure 6.10 Showing the uncertainty maps (SD_{krig}) for the NOE days for PM_{10} based on (left) annual statistics and (right) daily statistics. See text for detailed description of their derivation. The NOE maps related to these can be found in Figure 6.8.

6.5.3 Comments on the kriging semivariogram

The question also arises as to the applicability of the kriging assumptions and semivariogram models. One of the assumptions is that there is spatial correlation, as a function of lag distance, of the parameter to be interpolated. This is at the heart of the variance models used in the kriging methodology. Though this methodology has been fruitful in many geosciences, its application for air quality mapping is still open to debate. Investigation of the empirical semivariograms used in this study indicates a limited dependence of the variance with lag distance, Figure 6.11, though this may vary from year to year. This brings into discussion the spatial representativeness of the observations since even at small distances the variance of the observations is quite high. Even if kriging methods are applied, the form of the semivariogram model should also be assessed. In this report the spherical model has been applied, based on initial sensitivity tests carried out in Horálek et al. (2005), but investigation of the daily mean variograms used in this study implies that other models, such as power law models, may give better fits to the data on a daily basis. Alternative methods (e.g. Blond et al., 2003) for determining the spatial variation of the covariance field may be more appropriate than the lag distance dependent method used in kriging. Such methods establish spatial covariance relationships based on analysis of a set of temporal data and creating functional relationships with model calculations.

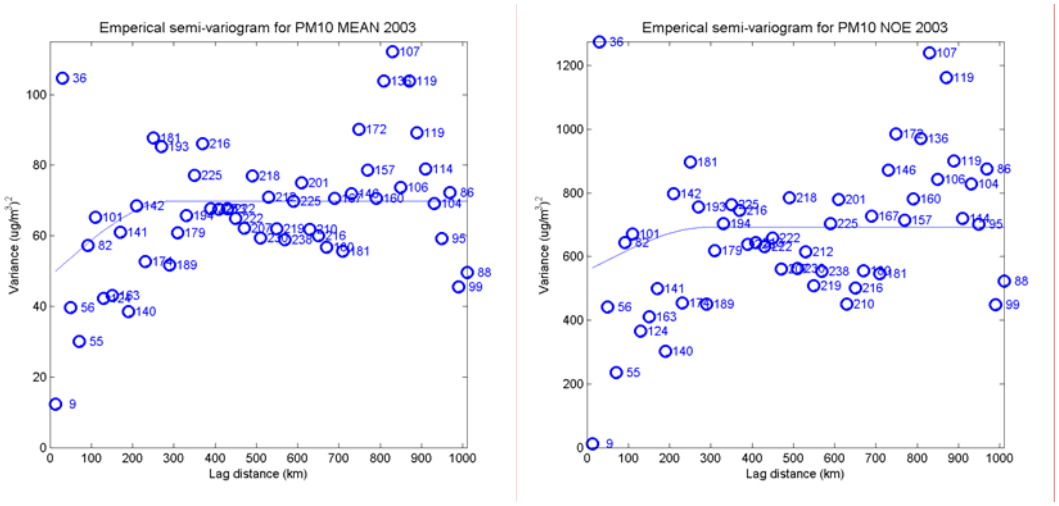

Figure 6.11 Showing the annual statistics residual semivariogram, and estimated sill (solid line), for annual mean PM_{10} (left) and NOE days PM_{10} (right), for the year 2003. The numbers indicate the number of station pairs used to calculate the variance.

6.5.4 Conclusions on uncertainty mapping

The estimated uncertainty in the annual mean rural PM_{10} values, of 8 $\mu g \cdot m^{-3}$ or less (Figure 6.9), should be considered quite reasonable, considering that spatial representativeness may contribute significantly to this value. Uncertainty in the percentile concentration and NOE days however, must be considered to be quite high, especially in areas where no measurements are available. The spatial variation of uncertainty in NOE days is also highly variable due to its threshold nature (Figure 6.10). In many areas of Europe the uncertainty in NOE is too large to make the assessment useful for policy implementation. However, it must be noted again that representativeness is an important aspect of this uncertainty. The maps produced should indicate the mean concentration, or NOE, in a 25 x 25 km grid. Clearly there is a large variability within such a grid, as is indicated in Figure 6.11 and the uncertainty discussed here will include that. This means, for example, that a significant part of the uncertainty in the NOE will not lie with the interpolation itself but with the variation of the observed concentration within the gridded region. More effort is thus required to assess this particular aspect of the interpolation uncertainty.

Further to this it should be noted that the use of kriging, or residual kriging, to interpolate NOE days using annual statistics is not recommended as it does not deal well with the threshold nature of this parameter and does not provide uncertainty maps that give a suitable spatial representation. If annual statistics are to be used to map exceedances then the 36th percentile concentration field is recommended, though this does not provide all the information that may be required for assessment. The use of daily means, on which the NOE and percentiles are based, is recommended when spatially interpolating the NOE days.

6.6 Discussion and conclusions concerning the use of daily and annual statistics

A number of points regarding the interpolations carried out in this chapter require discussion. Firstly it is worth pointing out the advantages of using daily statistics. These are:

1. The number of observation days used is larger when using daily statistics than annual statistics when a limit on the allowable coverage is applied.
2. The quality of the maps is as good as, and generally better than, maps produced using annual statistics, based on the cross validation RMSE.
3. There is consistency between the percentile and NOE fields.

4. The maps are more robust in regard to the use of automatic routines for defining interpolation parameters used in the kriging interpolation.
5. Future improvements in the interpolation based on multiple regression with meteorological parameters will probably be better represented on a daily basis.

The following disadvantages also exist:

1. The data and calculation requirements are significantly higher for the daily than for the annual statistics
2. The reduction in uncertainty may be small in regard to other possible improvements in the interpolation methodology that would be less data intensive
3. The interpretation of uncertainty mapping is more complex

Thus, there is no scientific reason for not carrying out the interpolation on a daily basis, however time and data constraints may be defining.

7 Uncertainty analyses on spatial interpolation

7.1 Introduction

One of the intensions of this year's project was to report in more detail on a transparent quantification of uncertainties and errors. Sources of uncertainties and errors can be the measurements, the resolution and the interpolations. We focussed in this paper specifically on the interpolation uncertainties and errors. The following three approaches were considered:

1. Cross-validation of errors between parameters by using the root-mean square error (RMSE) and other cross-validation parameters (Chapter 5)
2. Actual measurements compared to the interpolated and/or modelled values (using scatterplots), based on cross-validation (Chapter 5) and non cross-validation approach (Section 7.2)
3. Spatial maps of the errors in the interpolation maps: maps with prediction standard error or standard deviations (SD), (Section 6.5 and 7.3). As already mentioned in Chapter 6, this appears to be a complex issue. In this chapter additional attempts are presented specifically in context to the interpolations of Chapter 5.

The cross-validation parameter root-mean square error (RMSE) and other cross-validation parameters are discussed throughout the paper in the chapters on the spatial interpolation comparisons. Chapter 6 already explored and to some extent explained the uncertainties of the interpolations based on daily averages versus annual averages from measurements. Chapter 5 focuses in some more detail with additional statistical parameters on the analysis of uncertainties of the interpolation methods of the types 2 and 3 used to derive both rural and/or urban maps for 2004 of the air pollution indicators of PM_{10}, ozone, NO_x and SO_2. It presents the scatterplots comparing the measured and interpolated values using cross-validation.

In addition to this, Section 7.2 will present for some pollutants a simple and not cross-validating comparison of measured and interpolated values. Finally, in Section 7.3 a first version of the uncertainty maps are presented.

The results of the uncertainty analyses could contribute to improve updates of EEA's relevant air quality related Core Set Indicators (CSI004 and CSI005) and forthcoming EEA Air Pollution reports. They also can become important determinants for defining limit or target values and thresholds, including refinement of calculation methods of their exceedances proposed for legislation.

7.2 Comparison of measured and interpolated values

In addition to the more complex cross-validation analysis, a simple comparison between the measured and interpolated values is made for human health pollutant indicators. This comparison differs from the cross-validation scatter plots in two ways:

First, the interpolation is constructed from all stations, thus the comparison is just for the sites with measurement data, whereas in the cross-validation the values are predicted for locations without measurement data. In case of a so-called exact interpolation method, i.e. a method in which the resulting interpolation values goes through the measured values, the scatter plot taken at the sites of the measuring stations should be of the form $y = x$. However, at sites without measurement data such method can be worse than the methods that smooth the interpolation field and do not hold all the measured values. (One of so-called exact interpolation methods is IDW, i.e the interpolation field goes through the measured values. Contrary to that, kriging in general smooths the interpolation field. Nevertheless, from the Chapter 5 is clear that IDW gives worse results for the whole map.)

The second difference is that the interpolated value is the average of a 10 x 10 km grid, whereas in cross-validation it concerns the predicted value at the exact point of the monitoring station. Thus the scatter plot is not of the form $y = x$ even in case of so-called exact interpolation methods.

The results of this Section 7.2 have to be considered together with the cross-validation results, as presented in Chapter 5: Scatter plots of Chapter 5 show the uncertainty in the places without measurement (caused only by the interpolation method, without taken into account the uncertainty caused by the grid resolution), whereas the scatter plots presented here show the uncertainty in the places of measurement (caused both by the interpolation method and the grid resolution).

Only the methods used in final mapping are presented, i.e. one method per parameter and the type of area (i.e. rural and urban).

In Figure 7.1 the scatter plots for the PM_{10} indicators are presented, for rural areas. In comparing these graphs with cross-validation scatter plots presented in Section 5.2.6 (i.e. with Figures 5.4 and 5.5) one has to bear in mind that the different methods are compared. In Section 5.2.6 the methods using primarily monitoring data only are examined, whereas here the method using the interpolation of residuals is presented.

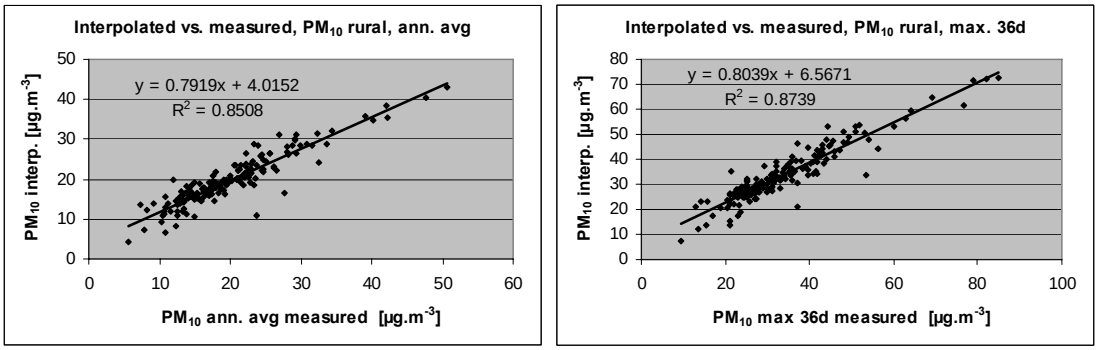

Figure 7.1 Correlation between predicted values (y-axis) and measurements (x-axis) for the PM_{10} annual averages (left) and the 36th maximum daily average values (right) for 2004 in rural areas, for the linear regression model using EMEP model output, altitude, surface solar radiation and wind speed, followed by interpolation of its residuals by ordinary kriging (method 3-P.2b-b2).

In Figure 7.2 the scatter plots for the PM_{10} indicators are presented, for urban areas. These graphs can be directly compared with the Figures 5.26 and 5.27 (top, right), where the same method is presented as here, i.e. ordinary kriging (2-b2). Higher R^2 in the Figure 7.2 shows that the uncertainty in the places of measurement is lower than the uncertainty in the places without measurement, as expected (nevertheless uncertainty caused by grid resolution, which is not taken into account in Figures 5.26 and 5.27).

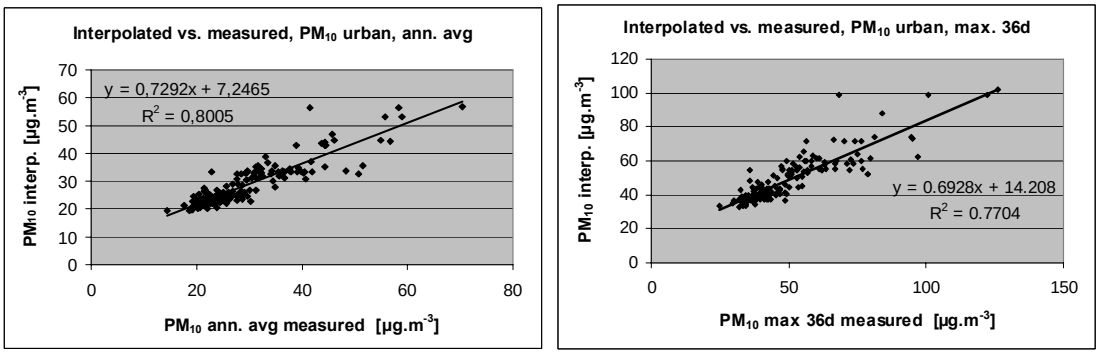

Figure 7.2 Correlation between predicted values (y-axis) and measurements (x-axis) for the PM_{10} annual averages (left) and the 36th maximum daily average values (right) for 2004 in urban areas, for the interpolation method ordinary kriging (method 2-b2).

In Figure 7.3 the results for the human health ozone indicators are presented, for rural areas.

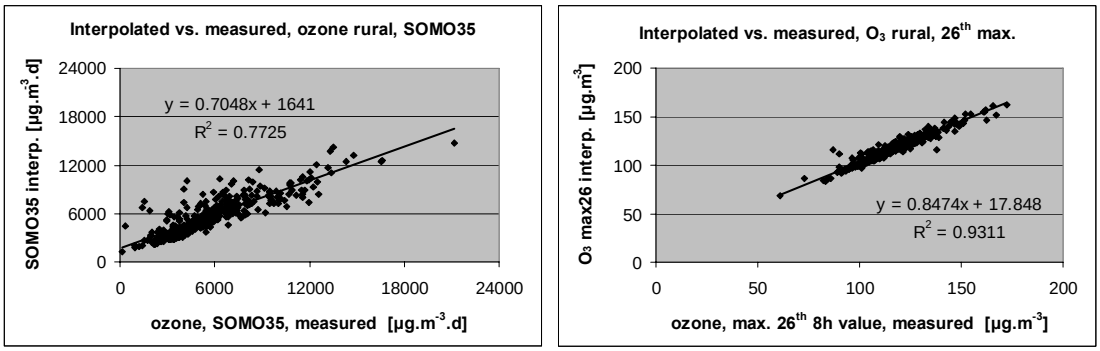

Figure 7.3 Correlation between predicted values (y-axis) and measurements (x-axis) for SOMO35 (left) and the 26th highest daily maximum 8-hour values (right) for 2004 in rural areas. The interpolation method used for SOMO35 is linear regression model using EMEP model output, altitude and surf. solar radiation followed by interpolation of its residuals by ordinary kriging (method 3-O.2c-b2). For the 26th highest daily maximum 8-hour values is used the ordinary cokriging using altitude (method 2-c2).

The left graph showing SOMO35 results can be related with cross-validation scatter plots presented in Figure 5.9, although these are based on different methods. The right graph showing 26th highest daily maximum 8-hour values results can be directly compared with the Figure 5.10 (bottom, right), both presenting ordinary cokriging using altitude (2-c2). Higher R^2 in the Figure 7.3 shows that the uncertainty in the places of measurement is lower than the uncertainty in the places without measurement, as expected. From the comparison of parameters of linear regression $y = a.x + c$ in the Figure 7.3 and 5.10 can be seen that the interpolation is more smoothed in the places without measurement, as expected (a is lower and c is higher in Figure 5.10).

Higher R^2 in case of 26th highest daily maximum 8-hour values in comparing with SOMO35 is caused by the kriging parameter value chosen, i.e. a low value of the nugget in case of 26th highest daily maximum 8-hour values. By this parameter setting is caused that the interpolation is in this case almost "exact", i.e. it almost respects the measured values. (Kriging respects the measured values in case of nugget parameter setting equal to zero.) However, the relevant cross-validation scatter plot in Figure 5.10 (bottom, right) shows clearly that the "exact" method is not necessarily better: R^2 in the places without measurement (as simulated by cross-validation) is only 0.55 (i.e. less than the relevant value of R^2 for SOMO35, see Figure 5.9, bottom right).

In Figure 7.4 the results for the human health ozone indicators are presented, for urban areas.

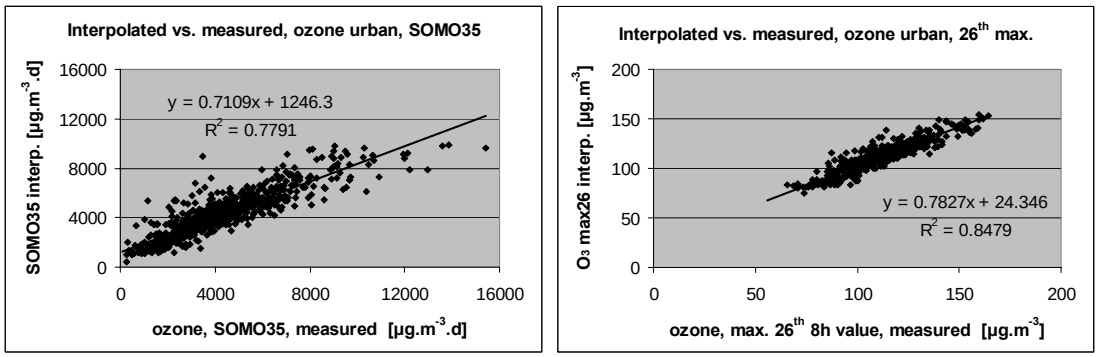

Figure 7.4 Correlation between predicted values (y-axis) and measurements (x-axis) for SOMO35 (left) and and the 26th highest daily maximum 8-hour values (right) for 2004 in urban areas. The interpolation method used for SOMO35 is ordinary kriging (method 2-b2), while for the 26th highest daily maximum 8-hour values it is ordinary cokriging using altitude (method 2-c2).

The left graph showing SOMO35 results can be directly compared with the Figure 5.29 (top, right), as the same method is presented in these two graphs, i.e. ordinary kriging (2-b2). The right graph showing 26th highest daily maximum 8-hour values results can be directly compared with the Figure 5.30 (bottom, right), both presenting ordinary cokriging using altitude (2-c2).

All cases discussed in this section are geostatistical methods, all with two different sources of uncertainty at the points of measurement:

1. uncertainty given by the method; geostatistical methods mostly smooth the values (except when the nugget is set to zero)
2. spatial uncertainty; the point value of the measurement station is compared with the average predicted value on a 10 x 10 km grid cell.

Thus the high correlation, for example, at the 26th highest daily maximum 8-hour value for rural areas (Figure 7.3) is caused by the chosen parameter value, i.e. low nugget. In fact the RMSE should in principle represent the nugget variance. The distinguishing of these two sources of uncertainty and the investigation of possible maps to reduce them is a task for the future.

7.3 Uncertainty maps

In addition to the cross-validation analysis of uncertainties, geostatistical methods (i.e. various types of kriging) enable spatial assessment of uncertainties. In fact, uncertainty maps can be obtained directly from the kriging methodology. The way of constructing the maps is presented in more details by Cressie (1993).

In most cases more complex mapping methods give higher uncertainties in the uncertainty estimates. Therefore we started the uncertainty mapping by using simpler interpolation methods using primarily monitoring data only. Three uncertainty maps are presented, two of them for rural and one for urban area.

Figure 7.5 shows uncertainty maps for the 26th highest daily maximum ozone values for the rural and the urban areas. These uncertainty maps relate to the concentration maps presented in Figure 5.14, left (rural areas) and 5.31, right (urban areas). Both the maps are created by ordinary cokriging using altitude, i.e. method 2-c2.

Compared to the urban map, the rural map shows higher uncertainty values caused by a lower number of measurement stations combined with higher concentration values. The circles around the stations in the rural map are caused by the parameter value chosen, i.e. a low value for the nugget, assuming spatially little uncorrelated noise and error effects at measurements.

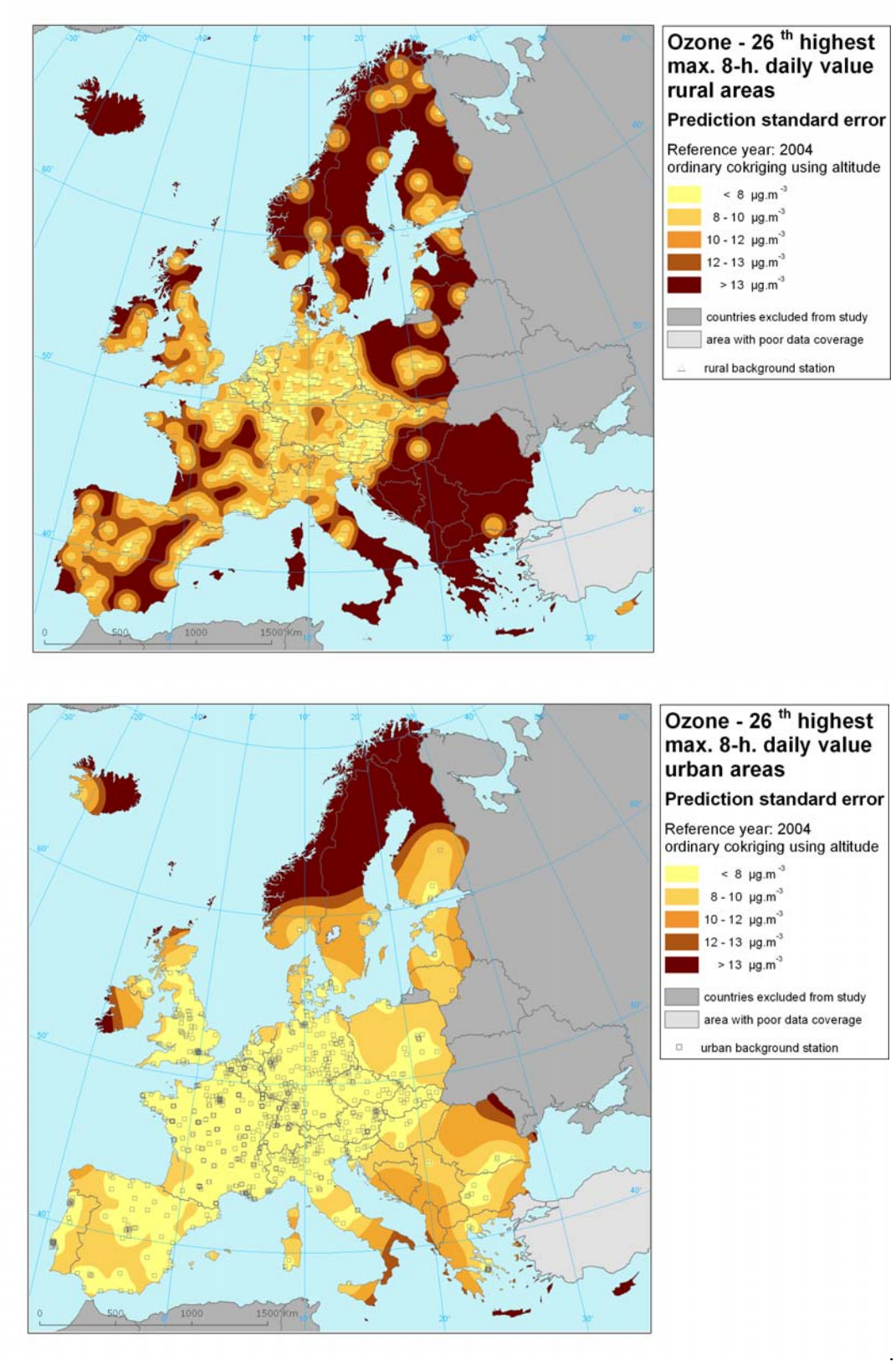

Figure 7.5 Uncertainty maps for the 26th highest daily maximum 8-hour ozone values for rural areas (top) and urban areas (bottom).

Figure 7.6 shows the spatial uncertainty map of the AOT40 for crops map as constructed with ordinary kriging using altitude. It is evident that the uncertainty is higher in regions with limited coverage of rural background measurement stations.

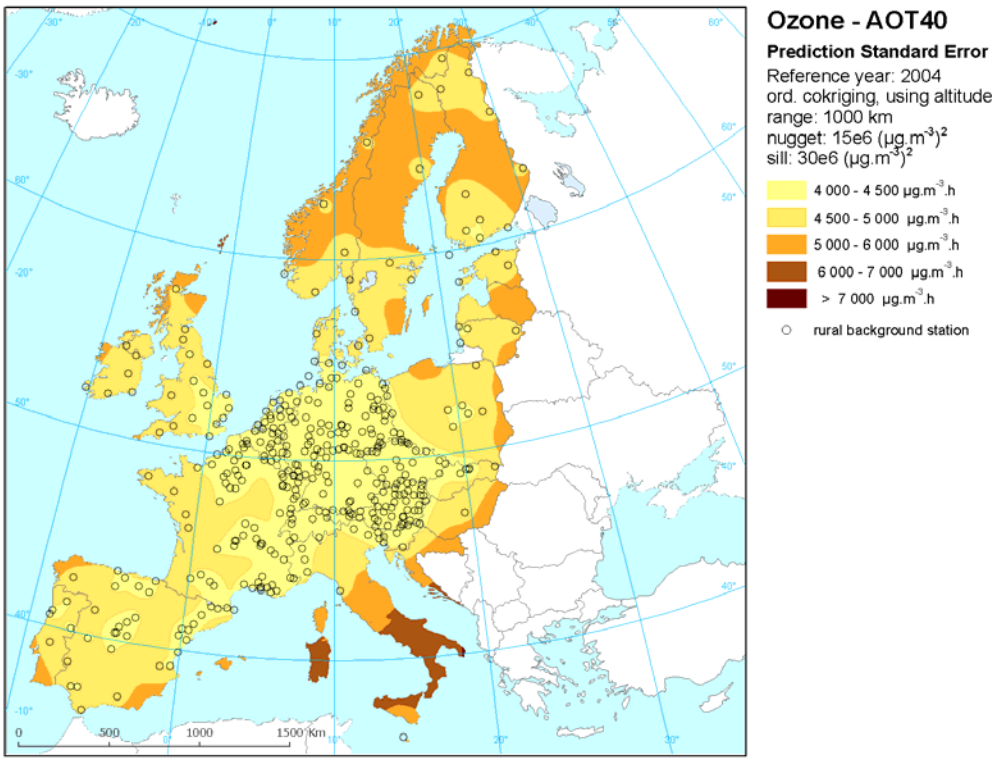

Figure 7.6 Uncertainty map for the ozone indicator AOT40 for crops for rural areas .

The concentrations map and the uncertainties map can be combined into a map of exceedances. This map indicates the probability of exceeding the air pollution limit value in particular areas. One of the possibilities to do that is directly via so-called indicator kriging (for details, see Cressie, 1993). Figure 7.7 shows such map of the probability of exceeding the limit value (120 µg.m^{-3}) for the 26th highest daily maximum 8-hour values, separately for the rural and urban areas.

Only first attempts are presented here on the construction of uncertainty maps and maps probability of limit value exceedances. The quality of these maps is not investigated yet and has to be tested before they can be qualified as more formal products to be used in assessments and such.

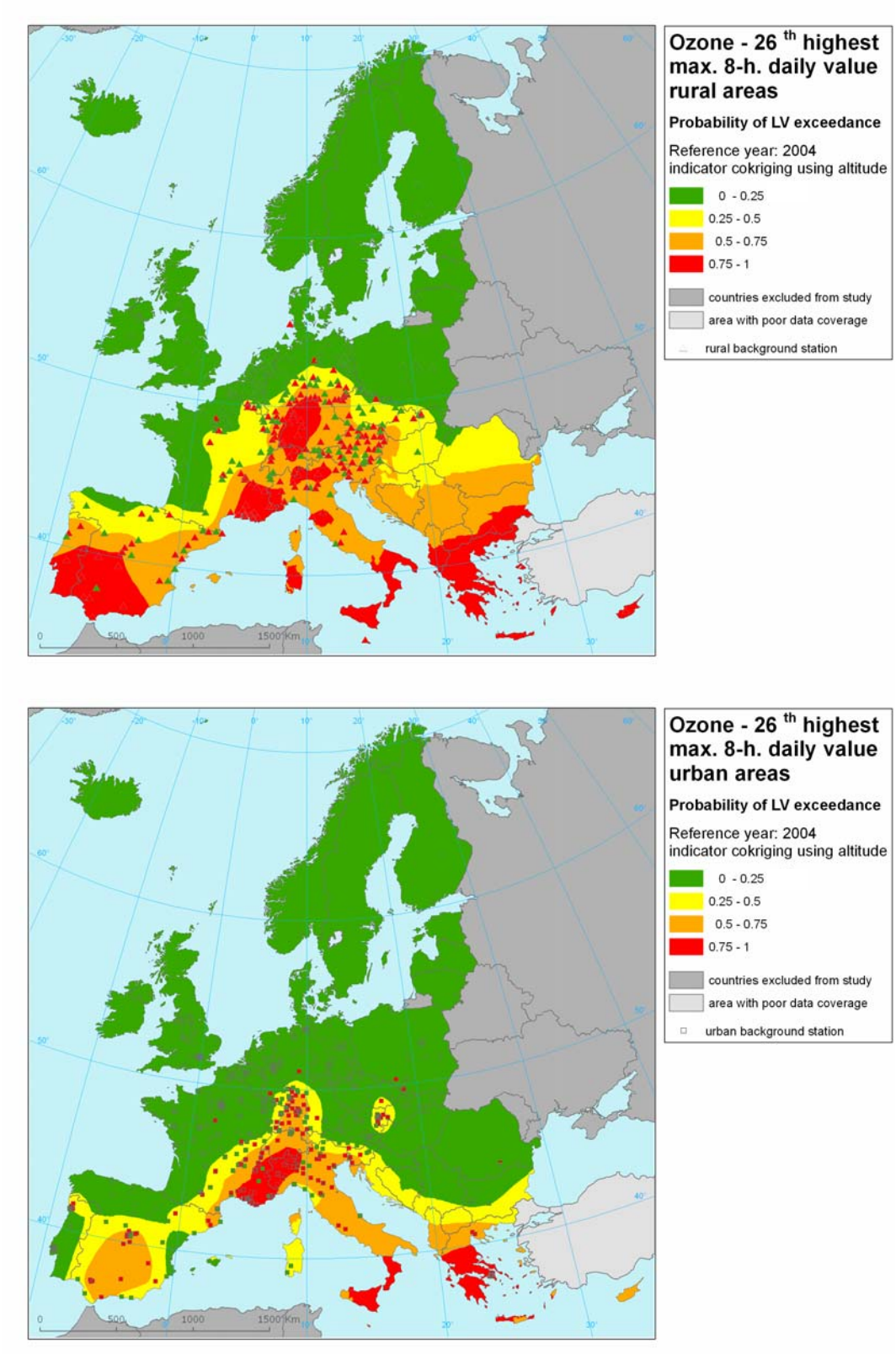

Figure 7.7 Probability maps of the limit value exceedances for ozone parameter 26th highest daily maximum 8-hour ozone values for rural areas (top) and urban areas (bottom).

8 Using the maps in impact assessments

8.1 Introduction

The procedures as described in the previous chapters have been used to produce a final set of maps for 2004. These maps have been combined with the population and land cover maps (see Chapter 4 for details on these data sets) in order to estimate the exposure of population and vegetation/ecosystems to air pollutants. All concentration maps, information on the applied method and country-specific exposure tables are presented in the Annex.

8.2 Population exposure and health impacts

8.2.1 Health impact of particulate matter

Epidemiological studies have reported statistical associations between short-term, and to a limited extent also long-term, exposure to increased ambient particulate matter (PM) concentrations (PM_{10}, sometimes also $PM_{2.5}$ and ultra-fine PM) and increased morbidity and premature mortality. Whether these associations are causal and which PM properties and/or mechanisms (PM_{10}, $PM_{2.5}$, ultrafine-mode particles, physical properties, chemical or biological components) are responsible for these health effects, is still unclear. It is currently assumed that there is no threshold below which health effects of PM are unlikely to occur. The recent update of the World Health Organisation Air Quality Guidelines for PM (WHO, 2006) proposed that, despite the apparent lack of a threshold value, guidelines should be set to minimise the risk of adverse effects of both short-term and long-term exposure to PM. These values were set as 20 $\mu g\ m^{-3}$ for an annual mean and 50 $\mu g\ m^{-3}$ as a daily mean for PM_{10}, with corresponding values of 10 $\mu g\ m^{-3}$ and 25 $\mu g\ m^{-3}$ for $PM_{2.5}$. It is often assumed that $PM_{2.5}$ is more toxic than PM_{10} because it penetrates deeper into the lungs; however, the health effects of the 'coarse' particles ($PM_{2.5-10}$) should not be neglected (Brunekreef and Forsberg 2005; Sandström et al., 2005). The European Commission has proposed to use $PM_{2.5}$ as an additional indicator because it reflects better the anthropogenic fine particle emissions and it is assumed to contribute significantly to the health effects of ambient PM exposure.

Whilst evidence is growing that finer particle size fractions are perhaps more important, ambient air quality measurements and emission data at present are often only available for PM_{10}, i.e. particles of average 10 μm diameter and below, including those smaller than 2.5μm. As discussed above, monitoring information is too limited to prepare a $PM_{2.5}$ concentration map over Europe. Therefore this chapter focuses on exposure to PM_{10} and its associated health impacts. According to the recommendations of the WHO, the annual mean concentration is an important indicator to take into account the premature mortality associated with long-term exposure.

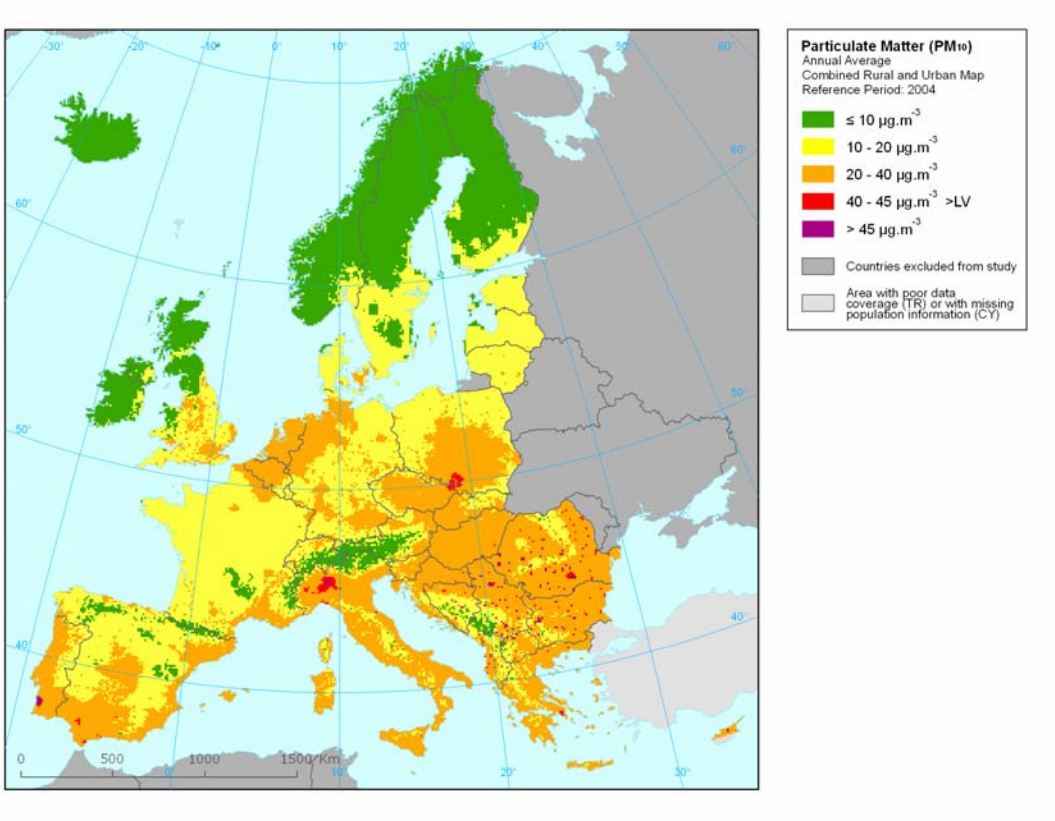

Figure 8.1 Annual mean PM10 concentrations (µg·m^{-3}), 2004.

The final concentration map of PM_{10} annual mean concentrations is given in Figure 8.1. Increased PM_{10} concentrations are seen in the urbanized areas, relatively low concentrations are observed in France. It can not be excluded that these low levels are caused by the low correction factor applied in the French networks for correcting the data of non-reference measuring configurations (de Leeuw, 2005).

For those countries for which information is available in the JRC population database (see Section 4.9), the population weighted averaged concentrations are given in Table A1 of the Annex. Note that in preparing the final PM_{10}-map (Figure 8.1) for those countries missing in the JRC population database, LandScan data (Section 4.9) has been used. The systematic difference observed between the two population databases hampers the comparability between countries. It was therefore decided to limit the exposure estimates to the countries included in the JRC database, see the Annex for further details. The EU27 with exception of Cyprus are covered.

There might be large gradients in PM_{10} concentration within a country. The weighted concentration does not give information on the (low) number of people exposed to the higher levels. Table A1 in the Annex and Figure 8.2 present the population frequency distribution for a limited number of exposure classes. A small fraction (2 %) is exposed to PM_{10} levels below 10 µg.m^{-3}. Up to a quarter is exposed to PM_{10} concentrations below the stage-2 indicative limit value of 20 µg.m^{-3}. It can be seen that the largest number of European inhabitants (i.e. two thirds) lived in 2004 in areas with PM10 levels between 20 and 40 µg.m^{-3}. According to the presented mapping methodology, 6 % of the European population lived in areas above the limit value for the PM_{10} annual average of 40 µg.m^{-3}. However, this European number of 6 % was probably higher, because of the underestimation of high values at all interpolation methods in areas without measurements (Section 7.2). Furthermore, three countries had even more than 25 % of the population living above the limit value (Bulgaria, Greece and Romania), whereas in various other countries, including Germany, the Netherlands, there appears to be no exceedances of the limit values. For a few countries, e.g., Slovakia and Belgium, no areas above the limit value are identified, although some measuring stations show exceedances. This is caused by the

grid resolution of the map and particularly by the interpolation methodology (Section 7.2). Exceedances may occur at hot spot situation but they are not resolved in the interpolation procedures.

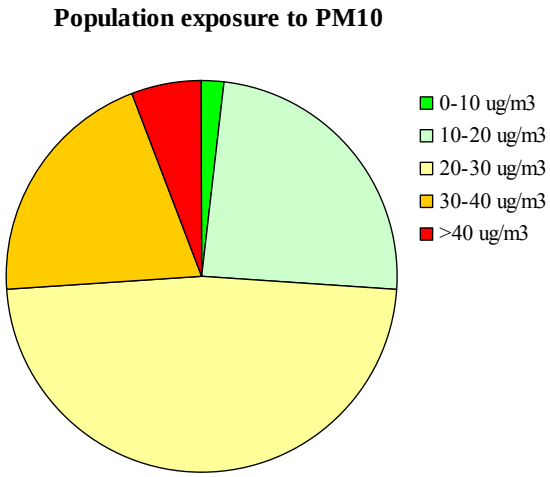

Figure 8.2 Population exposure to PM_{10} concentration, annual mean (reference year 2004).

The country-wide population weighted mean values calculated here can be compared with the information in the Eurostat Structural Indicator "Urban population exposure to air pollution by particulate matter" (Eurostat, 2007). In this indicator the population weighted mean values are calculated for all the urban agglomeration as defined by each Member States under the Air Quality Framework Directive and related daughter directives (EC, 1996; 1999, 2000, 2002, 2004). The number of inhabitants in an agglomeration has been provided by the Member States. For each agglomeration the PM_{10} concentration is obtained by averaging the data of all available (sub)urban background stations in AirBase. In contrast to the map in Figure 8.1, the Structural Indicator (SI) is based on monitoring data only. Figure 8.3 shows the relation between the urban-only (SI) and total population (this report) estimates. The correlation between the two sets is high (R^2 = 0.88); the urban value is about 30 % higher than the country-wide averaged value.

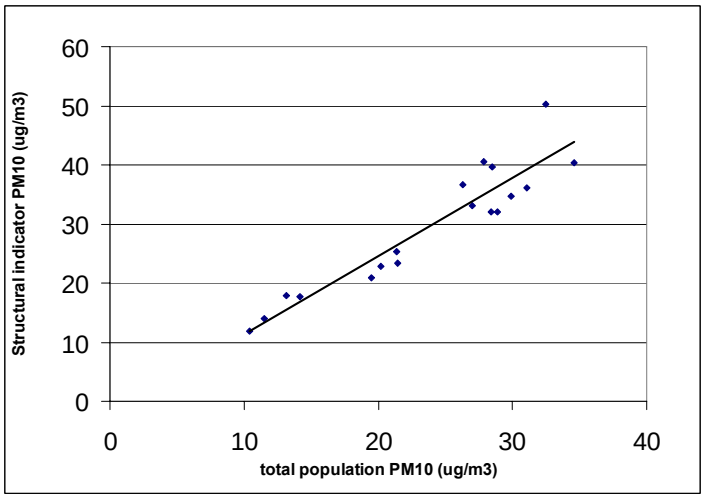

Figure 8.3 Comparison between the population weighted PM_{10} concentration (annual mean) obtained from the Structural Indicator (for urban population only) and the weighted PM_{10} concentration using the total population (this report).

In the health impact assessment, (premature) mortality has been selected as the endpoint since it represents the major impact in economic terms and the baseline rate is well-documented. The health effects of a long-term exposure to particulate matter have been studied widely. From these analyses concentration-response relations have been obtained. In the impact assessment studies of, among others, CAFE, the risk coefficients from the American Cancer Society Study (Pope et al., 2002) are used to estimate the mortality effect from long-term exposure to PM. In this study a relative risk (RR) of 6 % increase in mortality rate (all causes) per 10 $\mu g.m^{-3}$ increase in $PM_{2.5}$ is estimated. In a European study covering Austria, France and Switzerland, Künzli et al. (2000) estimated a RR of 4.3 % per 10 $\mu g.m^{-3}$ PM_{10} for total mortality (excluding violent death). This meta-analysis estimate is the weighted average from two American cohort studies, also including the study by Dockery et al. (1993). Both Pope et al. and Künzli et al. use the age group of 30 years and older to estimate the RR in the age group 30 years and more. As we are not yet able to construct monitoring based $PM_{2.5}$ maps over Europe (see Sections 5.6 and 5.7) we have used here the RR from Künzli et al. (2000). Note that as the empirical ratio between $PM_{2.5}$ and PM_{10} is in the range 0.53 to 0.83 (Putaud et al., 2003; EEA, 2007) both relative risks are comparable. In urban areas, close to sources, the $PM_{2.5}/PM_{10}$ ratio tends to be at the lower end and the relative risk-factor from Künzli et al. may result in slightly higher numbers than the RR-factor from Pope et al.

According to WHO there is no evidence for a no-effect level of PM: even at low concentrations health impacts may be expected. In estimating the impact of anthropogenic air pollution, a natural background concentration has to be subtracted from the interpolated PM_{10} concentrations. A similar approach is taken in assessments built on transport models (for example within the CAFE process): in the model only anthropogenic sources are included. The natural background over Europe is unknown and it will show large variations: high close to the coastline (sea-salt contribution) but also high inland because of contributions of resuspended soil or from secondary aerosol originating from biogenic organics. Here we have applied two scenarios assuming a constant European-wide natural background of 5 and 10 $\mu g.m^{-3}$, respectively. As Figure 8.1 indicates, a non-anthropogenic background of 10 $\mu g.m^{-3}$ is a clear overestimation for the NW part of Europe.

Country-specific data on population, age distribution and baseline mortality has been taken from the UN Population Division (UN, 2005) and the WHO Burden of Disease project (WHO, 2004). The health impact assessment is performed according to standard population attributive risk principles.

The estimated number of premature deaths attributable to long-term exposure to PM_{10} is given in Table 8.1. In the EU24 countries[1] the estimated number is 246,000 – 327,000 depending on the choice of the natural background concentration. In the CAFE Thematic Strategy an estimate of 348,000 premature deaths for EU25 (reference year 2000) is given. In view of the differences in reference year and in methodology this corresponds with our estimate assuming a 5 $\mu g.m^{-3}$ natural background. It is encouraging that the model-based approach of CAFÉ and the monitoring-based approach used here give similar estimates. Künzli et al. (2000) report for Austria and France 5,600 and 31,700 premature deaths, respectively. Our outcomes are approximately 4,500 and 27,700 premature deaths, respectively. This difference is largely caused by the differences in concentration and assumed reference concentration.

[1] Note that Cyprus could not been included in the health impact assessment of PM_{10} and ozone as Cyprus is not included in the JRC population database, see Section 4.9.

Table 8.1 Estimates of premature deaths attributable to the exposure to PM_{10} and ozone (cases per year). For PM_{10} results assuming a reference concentration of 5 and 10 $\mu g.m^{-3}$ are given.

Country	Population (thousands) 2004	PM10		Ozone
		5 $\mu g.m^{-3}$	10 $\mu g.m^{-3}$	
Austria	8171	4525	3254	334
Belgium	10400	10311	8420	234
Bulgaria	7780	12234	10476	491
Croatia	4540	5238	4307	226
Czech Republic	10229	9366	7443	413
Denmark	5414	2887	1776	132
Estonia	1335	605	282	29
Finland	5235	1223	405	90
France	60257	27711	18323	1698
Germany	82645	53257	37475	2566
Greece	11098	13003	10915	767
Hungary	10124	11573	9358	465
Ireland	4080	712	184	40
Italy	58033	60226	49817	3488
Latvia	2318	1401	790	56
Lithuania	3443	1925	1192	84
Luxembourg	459	176	110	11
Malta	400	328	277	16
Netherlands	16226	13223	10568	262
Poland	38559	26380	20370	1055
Portugal	10441	9302	7506	421
Romania	21790	27225	22938	1100
San Marino	29	24	19	2
Slovakia	5401	4273	3335	230
Slovenia	1967	1568	1238	87
Spain	42646	33495	26617	1737
Sweden	9008	3009	1329	203
United Kingdom	59479	36536	24994	815
Total	**491510**	**371743**	**283716**	**17054**
Confidence interval [(1)]		**229287 - 516491**	**174424 - 395532**	**5694 - 22720**

[(1)] Confidence interval resulting from uncertainties in the relative risk factors. (PM_{10}: Künzli et al. (2000); ozone: WHO (2006)).

8.2.2 Health impact of ozone

Epidemiological studies show that enhanced ozone levels during summer smog episodes appear to be associated with increased premature mortality and morbidity, lung function decline, airway irritation, worsening of asthma, and airway and lung tissue damage and inflammation. Many of these effects have also been found in controlled toxicological studies. In 2000 the WHO recommended an Air Quality Guideline for ozone (WHO 2000) of a daily maximum 8-hour mean value of 120 $\mu g/m^3$, which has been adopted by the EU not to be exceeded on more than 25 days per year. Looking at the current epidemiological evidence for health effects of ozone, with often effects seen at much lower levels, it has been recognized that the WHO 2000 guideline may offer inadequate protection of public health from acute and maybe also from repeated and long-term exposures (although the evidence for effects from long-term exposure is still insufficient to consider a separate guideline). Therefore, the WHO has recently updated the Air Quality Guidelines for ozone (WHO, 2006). The new guideline is a daily maximum 8-hour mean value of 100 $\mu g/m^3$, assuming that this concentration will provide further protection of public health, though some health effects may occur below this level.

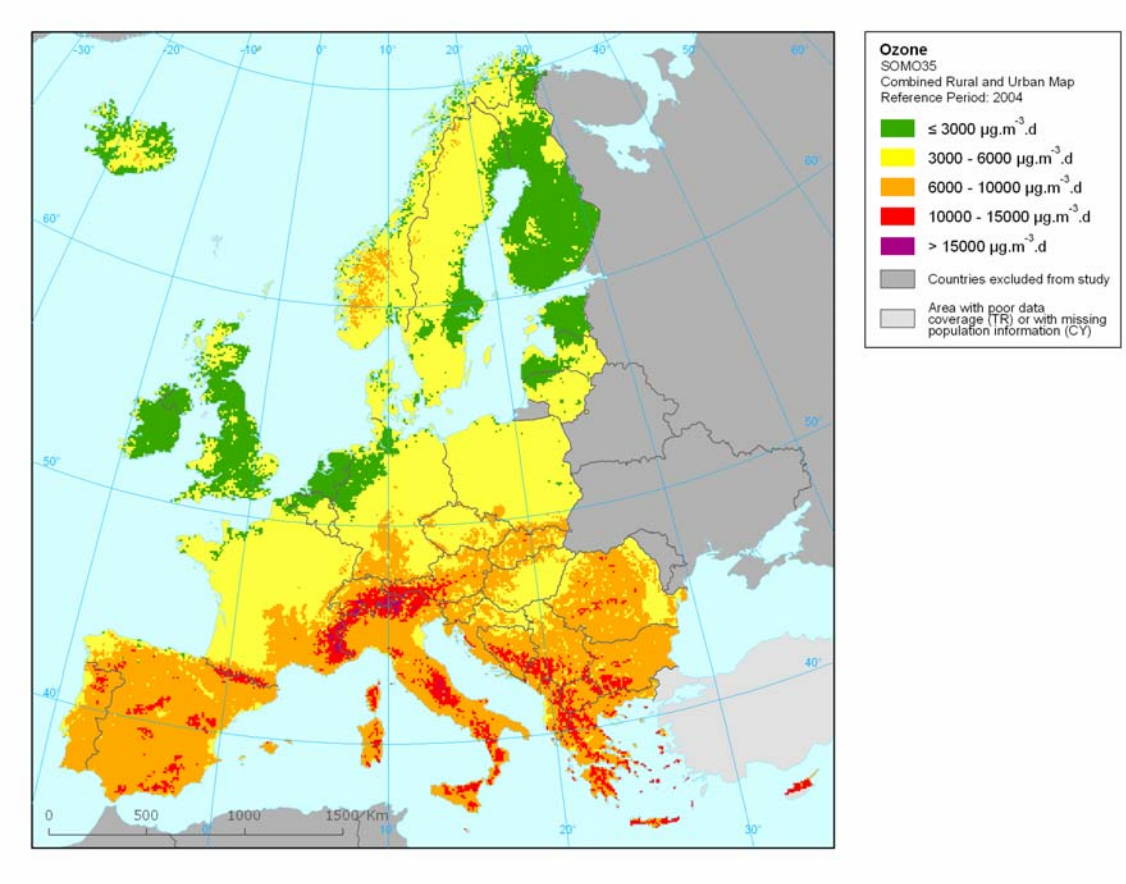

Figure 8.4 Ozone concentrations expressed as SOMO35, unit: µg.m^{-3}.day.

The WHO recommends a daily maximum 8-hour mean concentration as the principal benchmark for assessing impact on mortality, with assessment over a full year. The WHO stated that it was not possible to identify a threshold for the effects of ozone on mortality. At the same time, it was acknowledged that there were increasing uncertainties concerning the shape of concentration-response function for the associations between effects and ozone levels at very low concentrations. The WHO noted that for the integrated assessment modeling, these uncertainties should be kept in mind when selecting an indicator for ozone-related mortality. Therefore, current evidence is insufficient to derive a level for this 8-hour mean below which ozone has no effect on mortality. However, the practical use of a cut-off for integrated assessment modeling at 35 ppb, considered as a daily maximum 8-hour mean ozone concentration, was recommended for the IIASA modeling exercise for the European CAFE programme (IIASA, 2005). For days with ozone concentration above 35 ppb as maximum 8-hour mean, only the increment exceeding 35 ppb has been used to calculate effects. No effects of ozone on health would then be calculated on days below 35 ppb as maximum 8-hour mean. Effectively, this meant that the exposure parameter was the sum of excess of daily maximum 8-h means over the cut-off of 35 ppb calculated for all days in a year. This parameter, the SOMO35 (sum of means over 35 ppb), is a measure of accumulated high exposure and is mapped for Europe in Figure 8.4. The cut-off recommendation was based on the application of a very conservative approach to integrated assessment modeling and took account of the uncertainties in the slanted shape of the concentration-response function at low ozone concentrations. It also reflected the seasonal cycle and geographical distribution of background ozone concentrations, as well as the range of concentrations for which models provided reliable estimates. It was considered highly likely that the overall health impact of ozone were underestimated by this approach.

Population weighted concentration data for this ozone indicator SOMO35 is presented in Table A2 of the Annex. It can be seen that almost half of the European population lived in areas above 3,000 and below 6,000 µg.m^{-3}.days and about a quarter of the population lived in areas below 3,000 µg.m^{-3}.days

and the other quarter of inhabitants in areas above 6,000 µg.m^{-3}.days. The population weighted average SOMO35 concentration in Europe is about 4,460 µg.m^{-3}.days. The EU has neither defined a limit or target value nor a long-term objective for SOMO35. However, a regression between observed SOMO35 and 26th highest daily maximum ozone values at urban background stations shows that the target value of 120 µg.m^{-3} corresponds with a SOMO35 in the range of 4,500 to 6,500 (µg.m^{-3}.day).

Figure 8.5 gives a comparison between the country-wide population weighted ozone concentrations with the data presented in the Structural Indicator "Urban population exposure to air pollution by ozone". As is the case for the PM-structural indictor, a fair – but slightly worse – correlation is found.

Following the recommendation of the WHO (WHO, 2006), a relative risk for all-cause mortality of 1.003 (confidence interval 1.001 to 1.004) for a 10 µg.m^{-3} increase in the daily maximum 8-hour mean is used in the health impact assessment. The estimates of premature deaths attributable to the exposure to ozone are presented in Table 8.1. Total number for the EU25 (not including Cyprus) is about 17,000. In the CAFÉ calculations (IIASA, 2005) a total of 21,000 has been estimated for the year 2000. Our slightly lower number will not be caused by differences in concentrations (in contrast to many other pollutants, ozone hardly shows a decreasing trend over the recent years) but it is due to the treatment of the urban background concentrations. The CAFE calculations are based on regional scale ozone calculations on a 50 x 50 km grid, not resolving urban areas; as urban levels are systematically lower then rural concentrations, CAFÉ may overestimate the attributable deaths. We have included the measured urban background concentration in the interpolation scheme and health impact assessment.

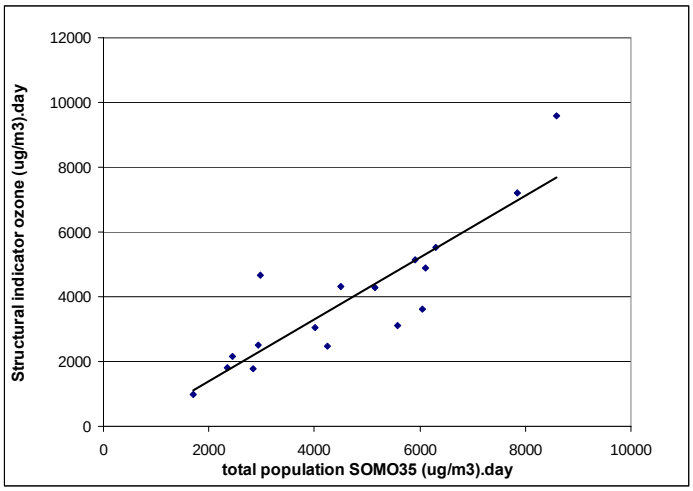

Figure 8.5 Comparison between the population weighted ozone concentrations (expressed as SOMO35) obtained from the Structural Indicator (for urban population only) and the weighted ozone SOMO35 concentration using the total population (this report).

8.2.3 Other pollutants

In the first and second Daughter Directive, limit values for the protection of human health have also been set for SO_2, NO_2, Pb, CO, and benzene. Exceedance maps and estimates of population exposure have not been made for these pollutants. For SO_2, Pb, CO, and benzene no frequent or widespread exceedances of the limit values are expected. According to an overview of the air quality reports on 2004 under the Air Quality Framework Directive (Van de Hout, 2006) exceedances have been observed in 0.4 %, 1.1 % and 2.5 % of all zones in the EU25 for Pb, CO and benzene, respectively. In most cases this will concern traffic or industrial hotspots within the zone; the current interpolation methodologies are not suitable for these hotspot situations with a typical spatial scale of less then several hundred meters. For SO_2 slightly more zones in exceedance can be identified: the hourly limit value is exceeded in 3.1 % of the zones, the daily limit values in 2.3 %. In the Core Set Indicator on urban air quality it has been estimated that less then 1 % of the urban population is exposed to SO_2 levels above the limit value.

With respect to NO_2, a more frequent violation of the limit values, especially the annual mean, is observed: in 23 % of the zones exceedances are reported (van den Hout, 2006), 23 % of the urban population is exposed to levels above the limit value for annual mean. The health effects of NO_2 exposure are less clear than those from particulate matter and ozone. Epidemiological studies show that health effects like increased mortality and morbidity are associated with ambient NO_2 levels; however, it is possible that NO_2 in these studies has not acted as a causal agent because NO_2 is highly correlated with other pollutants and could possibly act as a surrogate or indicator of the combustion-generated particulate air pollution. In its 2006-update of the air quality guidelines, the WHO therefore concludes that there is not sufficient evidence to justify a change (lowering) of the annual mean NO_2 guideline value. Therefore no separate health impact assessment for NO_2 has been made; its effects will probably be largely included in the PM assessment.

8.3 Exposure of vegetation

In the EU air quality legislation limit or target values for the protection of vegetation and ecosystems have been set for SO_2, and NO_x (first Daughter Directive) and for ozone (third Daughter Directive). For these pollutants, interpolated maps have been made in order to estimate the exceedance area. In the preparation of these maps only rural background stations have been included.

8.3.2 Ozone

In the ozone directive a target value (TV) and a long-term objective (LTO) for the protection of vegetation have been defined. TV and LTO are defined as AOT40, calculated from 1-hour values (daylight hours only, defined as the period between 8:00 and 20:00 CET) from May to July. The TV for 2010 is 18,000 $\mu g.m^{-3}.h$; the LTO is 6,000 $\mu g.m^{-3}.h$. The term *vegetation* is not further defined in the ozone directive. The UNECE Working group on Effects describes in its Mapping Manual (UNECE, 2004) also the AOT40 as the main indicator for quantifying vegetation damage. The Mapping Manual defines critical loads for crops, forests and semi-natural vegetation in terms of different levels of AOT40, calculated over different time windows. Comparing the definitions in the Mapping Manual and those in the ozone directive suggests that we have to interpret the term *vegetation* in the ozone directive as agricultural crops.

The exposure of agricultural crops has been evaluated here on basis of the AOT40 for vegetation as defined in the ozone directive. In addition, exposure of forests has been estimated on the basis of the corresponding definition in the Mapping Manual: critical level of 10 $mg.m^{-3}.h$ (corresponding to 5 ppm.h), accumulation over the full vegetation period, April 1 – September 30.

Agricultural crops

The rural map for ozone, AOT40 for vegetation, is given in Figure 8.6. This map has been combined with the land cover CLC2000 map. Exposure of agricultural area (defined as the land cover level-1 class *2 Agricultural areas* encompassing the level-2 classes *2.1 Arable land, 2.2 Permanent crops, 2.3 Pastures and 2.4 Heterogeneous agricultural areas)* has been calculated at the country-level. Table 8.2 gives the agricultural area where the target value and long-term objective for ozone are exceeded.

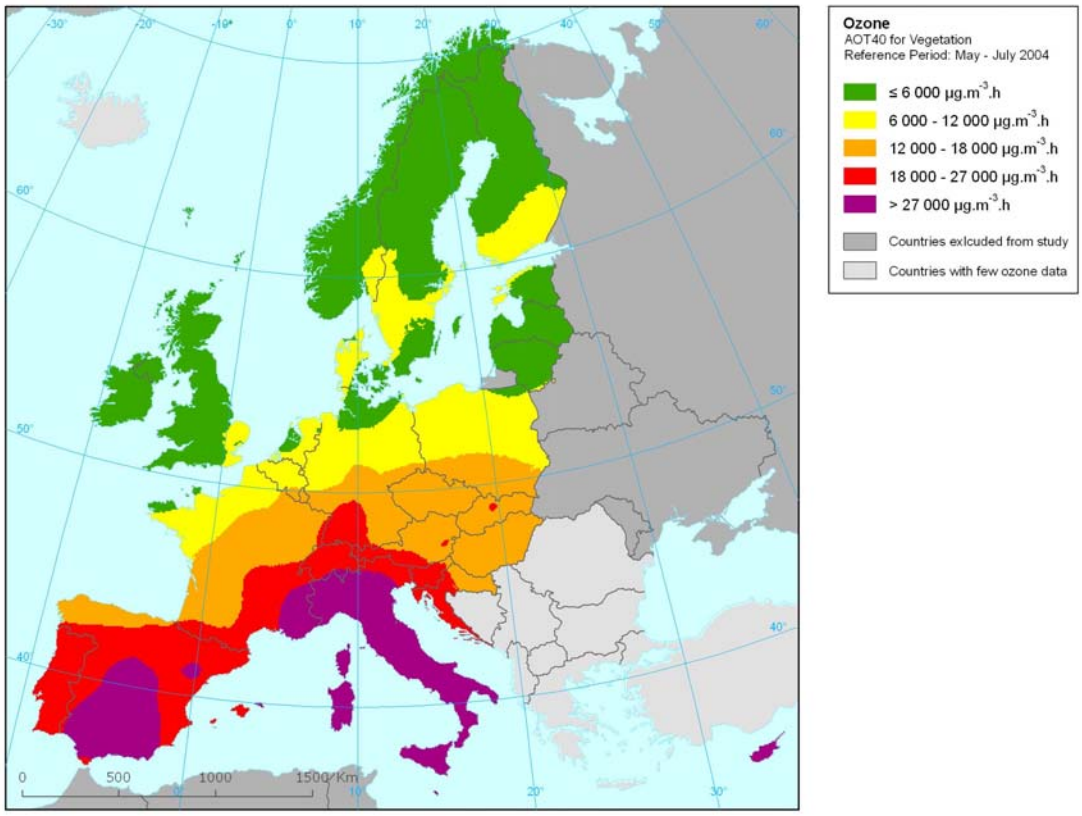

Figure 8.6 Rural concentration map of ozone, AOT40 for vegetation, 2004.

Table 8.2 Agricultural area (km^2) where the Long-term objective (LTO) and target value (TV) are exceeded, and forest area (km^2) where the critical level (CL) and reporting value (RV) for ozone are exceeded.

Country	Agricultural area [km^2]			Forest area [km^2]		
	total area (1)	above LTO	above TV	total area (2)	above CL (4)	above RV (5)
Andorra	14	14	14	61	61	61
Austria	27451	27451	3224	37598	37598	37598
Belgium	17654	17654	0	6095	6095	4766
Croatia	24168	24168	11509	20155	20155	20155
Cyprus	4269	4269	4269	1541	1541	1541
Czech Republic	45570	45570	0	25471	25471	25471
Denmark	32232	21151	0	3702	3702	0
Estonia	14680	1960	0	20781	20781	0
Finland	28893	15430	0	193300	193132	0
France	328400	321917	67089	144868	144868	133985
Germany	213603	184150	22665	103785	103785	81435
Hungary	63108	63108	0	17321	17321	17321
Ireland	46396	0	0	2908	0	0
Italy	155704	155704	155704	78801	78801	78801
Latvia	28324	0	0	26945	25313	0
Liechtenstein	41	41	41	61	61	61
Lithuania	40002	532	0	18671	13486	0
Luxembourg	1410	1410	0	910	910	910
Malta	122	122	122	2	2	2
Monaco	0	0	0	0	0	0
Netherlands	24920	19828	0	3105	3105	0
Poland	200543	194625	0	91776	91776	52046
Portugal	42553	42553	42553	24301	24301	24301
San Marino	43	43	43	5	5	5
Slovakia	24383	24383	199	19270	19270	19270
Slovenia	7133	7133	5573	11479	11479	11479
Spain	252381	252381	235882	91795	91795	91795
Sweden	38640	16453	0	249898	249898	0
United Kingdom	141878	16286	0	19693	5399	0
Total	**1804515**	**1458336**	**548887**	**1214297**	**1190110**	**601002**
Northern (3)	182770	55526	0	513298	506312	0
North-western	492992	309429	29262	122288	105087	84629
Central & eastern	574697	539326	26129	295281	295281	233202
Southern	554052	554052	493496	283430	283430	283171

(1) Total agricultural area.
(2) Total forest area.
(3) See footnote at Agricultural crops of Section 8.3.2 for definition of the European regions.
(4) Area where the critical level of ozone (10 $mg.m^{-1}.h$) is exceeded.
(5) Area where the "reporting" level of ozone (20 $mg.m^{-1}.h$, see text for explanation) is exceeded.

A frequency distribution of exposure classes for 4 European sub-regions[2] is presented in Figure 8.7. More detailed information is presented in the Annex.

Table and Figure illustrate that more than 30 % of all agricultural land is exposed to ozone exceeding the target value of 18 $mg.m^{-3}.h$ and more than 80 % is exposed to levels in excess of the long-term objective of 6 $mg.m^{-3}.h$. In southern countries about 90 % is exceeding the target values (Spain, Portugal, Italy and some small countries). In northern Europe the ozone levels are below the target value for nearly 70 % of the agricultural area.

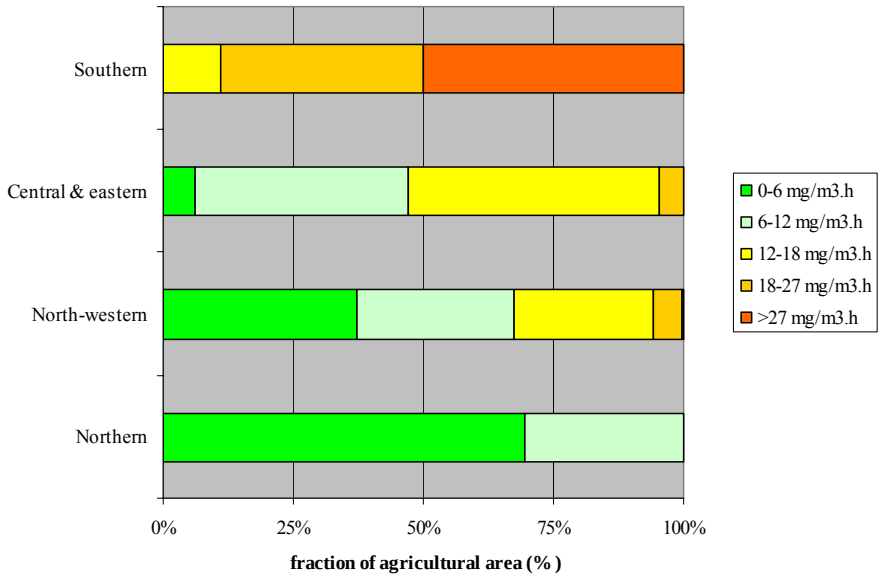

Figure 8.7 Exposure of agricultural area in Europe to ozone (AOT40 for vegetation).

Forest

The ozone directive does not give a target value or a long-term objective for the protection of forest. However, Annex III - which defines the information to be submitted to the Commission - mentions a level of 20 $mg.m^{-3}.h$. In this paper we will use this level (indicated as: reporting value or RV) as reference in combination with the critical level (CL) of 10 $mg.m^{-3}.h$ as defined in the Mapping Manual.

The rural ozone map for ozone, AOT40 for forest, is given in Figure 8.9. The gradients in this map are very similar to those in the map of AOT40 for vegetation: increasing concentrations from north to south. Table 8.2 gives the forest area where the critical level for ozone is exceeded. Similar to the finding in CAFE, we observe that in many countries, except for the UK and some of the northern countries, all forest area is exposed to levels above the critical level. The reporting level is exceeded in 50 % of the European forest area. The frequency distribution of forest exposure is given in Figure 8.8.

[2] Northern Europe: Norway, Sweden, Finland, Estonia, Lithuania, Latvia, Denmark and Iceland
North-western Europe: United Kingdom, Ireland, the Netherlands, Belgium, Luxembourg, France north of 45 degrees latitude
Central and Eastern Europe: Germany, Poland, Czech Republic, Slovakia, Hungary, Austria, Switzerland, Liechtenstein
Southern Europe: France south of 45 degrees latitude, Portugal, Spain, Andorra, Monaco, Italy, San Marino, Slovenia, Croatia, Greece, Cyprus, Malta

It is clear that in northern Europe the reporting level of 20 mg.m^{-3}.h is not exceeded but in southern Europe it is exceeded everywhere.

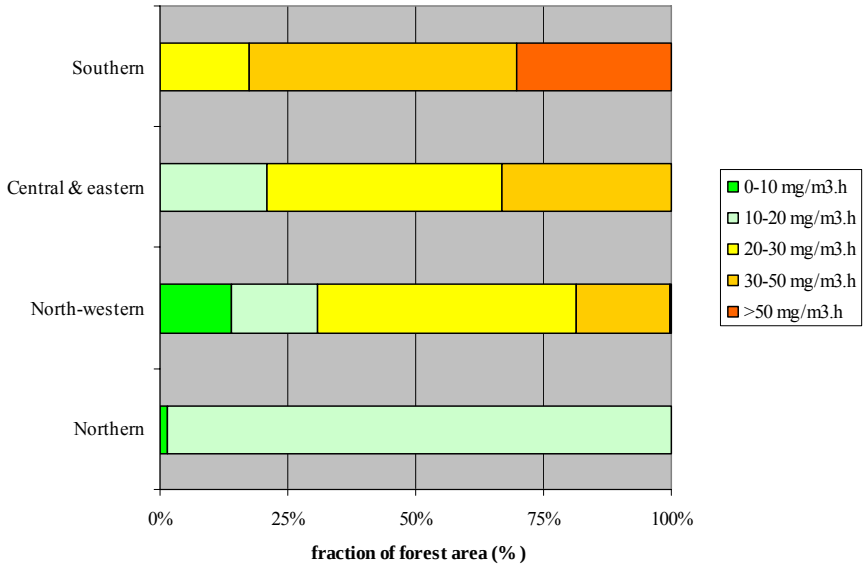

Figure 8.8 Exposure of agricultural area in Europe to ozone (AOT40 for forest).

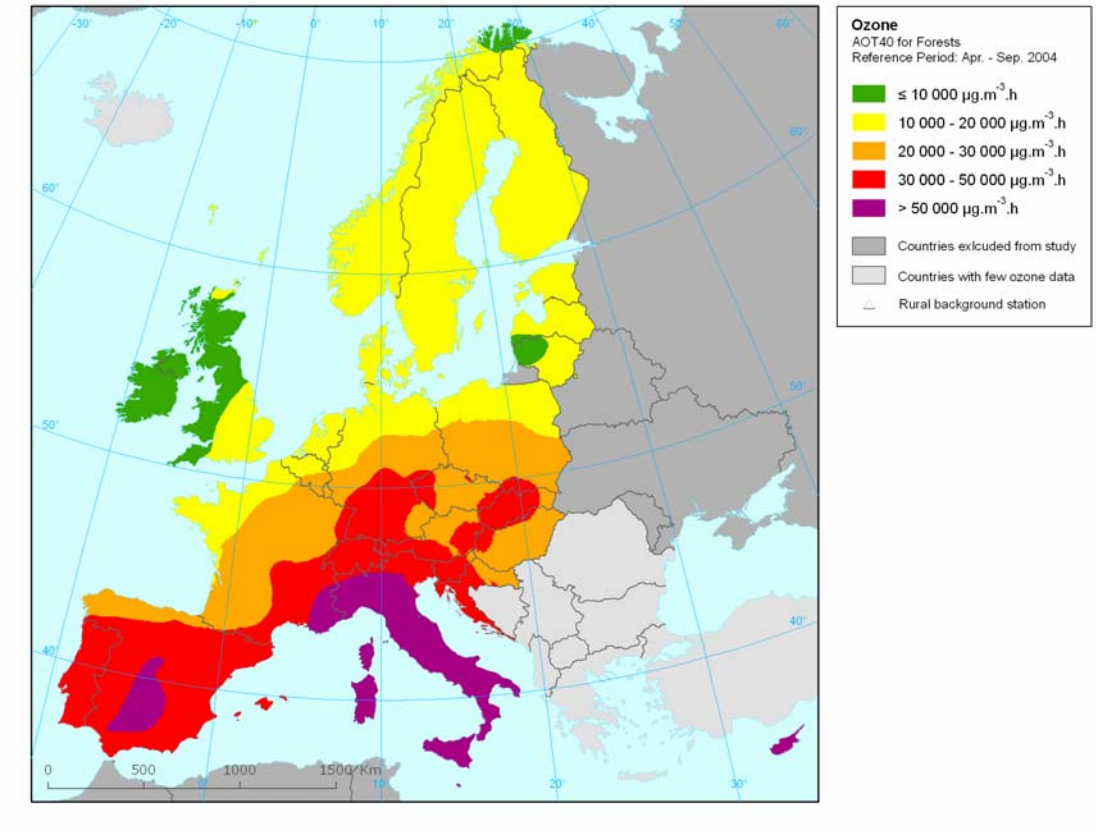

Figure 8.9 Rural concentration map of ozone, AOT40 for forest, 2004.

8.3.3. SO_2 and NO_x

In the first Daughter Directive the SO_2 limit value for protection of ecosystems is 20 μg.m^{-3} both for the annual mean as for the winter period. An initial assessment suggested that the interpolated map of annual average SO_2 based on the 2004 measurements would show no ecosystem exceedances of significance throughout Europe. In other words, the annual mean limit value set in the Directive is not exceeded in Europe except for some small areas in the most eastern parts, see also Figure 5.23.

Also, no indicator map was produced for average SO_2 concentrations in the winter season (1 October – 31 March next year). Although the winter mean will be systematically higher than the annual average, we expected a similar compliance with the limit value over Europe as for the limit value for the annual mean. However, because of the higher winter values, this could be subject of future activities.

The rural NO_x map shows a few regions where the NO_x limit value for the protection of vegetation is exceeded. These areas are located in the Benelux, in the Rhone Valley and northern Italy. The highest concentrations are observed in the Po Valley. We were not able to estimate the relevant exceedance areas for the following reason. In the first Daughter Directive term "ecosystem" and "vegetation" are not further defined. Judging the considerations for macro-scale siting of monitoring points targeted for the protection of ecosystems or vegetation, it is assumed that the limit value defined for NO_x is related to natural vegetation and the one for SO_2 is for natural ecosystems. Unfortunately, the CLC2000 land cover classification does not provide a clear-cut match to these receptors. We intended to make use of the NATURA2000 dataset for an analysis of designated areas (SACs, the Special Areas of Conservation and SCI, the Sites of Community Importance) in which the annual averages of NO_x and SO_2 concentrations would exceed the limit values. However, this dataset was not yet available and we recommend doing this analysis as soon as it becomes available, probably in early 2008.

9 Conclusions and recommendations

This report presents a continuation of the activities initiated in 2005, Denby et al. (2005) and Horálek et al. (2005), to develop and assess interpolation methodologies for producing air quality maps on the European scale and their implementation in population and ecosystem risk assessment. In these previous reports, monitoring and supplementary data from the years 2000 to 2003 were used to develop and assess methodologies for the production of spatial maps of selected PM10 and ozone indicators. In this paper these same methodologies are applied to the 2004 datasets for the same pollutants and reassessed. In addition a number of other supplementary data sources are included and the number of pollutants, and related indicators, assessed is increased to include NO_X and SO_2. Further to this extension of data sources and pollutants, attention is also given to the question of uncertainty in the assessment maps and a study concerning the temporal resolution of the assessment is performed.

The current work focuses on ground-based measurements as primary information, using modelling and other data as secondary, supplementary sources. This is in contrast to the work supporting the recent development of the European Thematic Strategy on Air Pollution, which gives prominence to modelling as primary source of information, using monitoring data to calibrate the model. While some of the methods and data sources are similar, to some extent the two methods can be regarded as complementary.

The maps of air quality are produced at a resolution of 10 x 10 km, covering all of Europe, and include both rural and (sub)urban monitoring data. The monitoring data, also referred to as primary data, is retrieved from the AirBase database. Spatially resolved supplementary data, i.e. other data sources than the primary monitoring data, are used in the interpolation methodologies to improve the spatial assessment.

This chapter provides a summary of the results of this study, with reference to the previous results, as well as providing recommendations on a number of points including:

- Recommended interpolation methods for producing spatial maps for the various pollutants, indicators and scales (rural and urban)
- Considerations for the adoption of operational spatial interpolation methods
- Applications to risk assessment
- Recommendations on further work and focus

9.1 Summary of the interpolation methodologies and applications

9.1.1 Methodologies assessed

As in Horálek et al. (2005) the focus of the spatial interpolation methods in this study is on the following three methods:

1. Multiple linear regression models relating monitoring data to spatially resolved supplementary data
2. Spatial interpolation methods using primarily monitoring data
3. Multiple linear regression models plus the spatial interpolation of their residuals

Within these 3 methodologies are subgroups of methods and various combinations of supplementary data. For the spatial interpolation, for instance, 4 different methodologies are employed. These are inverse distance weighting (IDW), Ordinary Kriging (OK), Ordinary Cokriging (OC) and lognormal kriging/cokriging (LK/LC).

The methodologies are applied separately to rural and urban maps and these are combined using a population weighted algorithm to produce combined maps of Europe at a resolution of 10 x 10 km.

One variation of the spatial interpolation methods (2) that is applied solely to the urban interpolations is interpolation of the urban DELTA, the DELTA being the difference between urban observations and interpolated rural fields.

9.1.2 Pollutants and indicators assessed

These methods are assessed for the following pollutants and their relevant indicators

- PM_{10} – annual average
  – 36th maximum daily average value
- $PM_{2.5}$ – annual average
- Ozone – SOMO35
  – 26th highest daily maximum 8-hour average value
  – AOT40 for crops
  – AOT40 for forests
- SO_2 – annual average
- NO_x – annual average

9.1.3 Monitoring and supplementary data used

Monitoring data is provided for the above pollutants and their indicators directly from the AirBase and EMEP databases. Station types classified as rural background or (sub)urban background are used.

In addition to the primary monitoring datasets the following types of supplementary data are also used

- Unified EMEP model calculations
- Altitude
- Annual mean meteorological fields
- Climatological fields

9.1.4 Assessment and selection of the interpolation methodologies

There are two elements to the assessment and recommendation of suitable interpolation methodologies tested in this study. The first involves the objective assessment of the interpolation quality and the second refers to the selection of a robust methodology for operational purposes.

Central to the objective assessment is the use of cross-validation to provide an independent comparison between the interpolated and measured data. The cross-validation method computes the spatial interpolation for each measurement point using all the available information except for that one point. The interpolated and measured values at that point are then compared and the procedure is repeated for all points. A number of statistical parameters, see Section 2.6, are used to objectively assess the quality of the interpolations. The root mean square error (RMSE) is used as the primary error indicator throughout the study.

In addition to the objective assessment obtained through the cross validation method there are also a number of other considerations when determining the best methodology for operational use. These aspects are discussed further in Section 9.7.

9.2 Summary of the rural interpolation results

In this and the following section the selected methodologies for the various pollutants and indicators will be summarised. Details concerning the process are contained within the body of this document, particularly Chapter 5, and the results are summarized in the Table 9.1. A number of general conclusions can be drawn at this point, that cover all the pollutants and indicators.

1. Kriging methods always show themselves to be better spatial interpolators than inverse distance weighting. This was found to be true in the previous study as well. IDW methods can be ignored in future work.
2. Lognormal kriging regularly gives better results than ordinary kriging, particularly for PM10, and should be more closely evaluated in future work. This was also concluded in the previous study.

3. The use of concurrent meteorological data, rather than climatological data, tested in this study for 2004 always provided improved results. It is recommended to use the concurrent meteorological data if it is available.
4. There is a degree of interannual variation in the optimal methodology and supplementary data sources. Recommendations on the operational methodology cannot be based solely on a single year's analysis.
5. Methodologies based on linear regression models, using supplementary data, are generally preferred to pure interpolation methods as the pure interpolation methods give highly uncertain results far from monitoring sites.

9.2.1 PM_{10}

Based on the objective assessment, two methodologies are selected as providing the best interpolation of PM_{10}, for both the annual mean and the 36th percentile. These are, in order of preference:

1. Multiple linear regression and spatial interpolation of the residual using ordinary kriging. Supplementary data includes: EMEP model, altitude, solar radiation and wind speed
2. Lognormal cokriging with altitude as the supplementary data source.

Both of these methods are shown to give the best interpolations, based on the RMSE, consistently for the 5 year period analysed to date. The second of these two methods is by far the simplest and relies only on altitude as a supplementary source. The first method requires more data, concurrent meteorological and CTM data, from the analysis year. Both methods give average uncertainties of around 25%, based on the normalised SD of the residuals.

The advantage of the cokriging method is that there is no reliance on data sources other than the monitoring data. The disadvantage of the method is that the interpolation has high uncertainty in areas where no monitoring stations are available. This is unlike the residual method that can rely on the supplementary data to provide better estimates in regions far from observations. The residual method also provides the possibility for future improvement in the interpolation with improved resolution and process descriptions in Chemical Transport Models (CTMs). As a result the linear regression with residual kriging method is recommended, but the cokriging method must be considered a very good option if supplementary data is not available.

9.2.2 Ozone

For the case of ozone, with 4 different indicators, there are a variety of methods that provide a similar quality of interpolation. Based on the objective assessment, two methodologies are selected as being the most consistent for the ozone indicators SOMO35, AOT40(crops), AOT40(forests) and the 26th percentile of the running 8 hour mean. These are, in order of preference:

1. Multiple linear regression and spatial interpolation of the residual using ordinary kriging. Supplementary data includes: EMEP model, altitude, solar radiation and humidity
2. Cokriging with altitude as the supplementary data source.

Though the optimal method, method with minimum RMSE, varied for the different indicators the first method above is seen as being robust for all indicators and giving consistent results for the 5 year period analysed to date. As an alternative to the above method, as in the case of PM_{10}, the second interpolation method can be applied as a simplified method. The advantages and disadvantages of these two methods are discussed above.

Average uncertainties for this method, based on the normalized SD of the cross-validation, vary for the indicator. For the SOMO35 and AOT indicators this is around 35%, for the 26th percentile this is estimated at around 10%.

9.2.3 NO_x

For the case of NO_x only the annual mean for the year 2004 is analysed using a limited number of methodologies, Section 5.4. Based on this analysis no robust conclusions concerning the methodologies can be made but the following 2 methodologies are found to produce the best interpolations.

1. Multiple linear regression and spatial interpolation of the residual using ordinary kriging. Supplementary data includes: EMEP model and altitude.
2. Ordinary kriging or cokriging with altitude as the supplementary data source.

This result reflects the previous results for both PM_{10} and ozone in regard to the best methodologies. Once more the preference would be given to the linear regression and spatial interpolation of the residual method since it provides better spatial coverage than the pure interpolation methods. The average uncertainty for this method and pollutant, based on the normalised SD of the cross-validation, is around 58%.

9.2.4 SO_2

As for the case of NO_x limited testing of methodologies has been carried out for SO_2, Section 5.5, and only the annual mean concentration for 2004 has been assessed. Based on this analysis no robust conclusions concerning the methodologies can be made but the following 2 methodologies are found to produce the best interpolations.

1. Linear regression and spatial interpolation of the residual using ordinary kriging. Supplementary data includes: EMEP model.
2. Lognormal kriging.

Once more the preference would be given to the linear regression and spatial interpolation of the residual method since it provides better spatial coverage than the pure interpolation methods. The average uncertainty for this method and pollutant, based on the normalised SD of the cross-validation, is around 60%.

9.2.5 $PM_{2.5}$

An analysis of the possibility for carrying out interpolations of $PM_{2.5}$ has been carried out. However, the current limited number of $PM_{2.5}$ rural monitoring sites, only 13 for 2004, inhibits an effective or testable interpolation methodology. This will need to be readdressed when improved coverage of $PM_{2.5}$ sites is available.

9.3 Summary of the urban interpolation results

The methodologies tested for urban interpolation are slightly different to those implemented for the rural interpolations, for instance cokriging is not carried out, but interpolation of the urban DELTA is an additional methodology. Only the pollutants PM_{10}, ozone and $PM_{2.5}$ are treated here. The following conclusions can be drawn.

9.3.1 PM_{10}

Based on the objective assessment, one methodology is selected as providing the best interpolation of PM_{10}, for both the annual mean and the 36th percentile, Section 5.8. This is:

1. Ordinary kriging or lognormal kriging.

Though a number of other methods are tested, ordinary kriging or lognormal kriging gave results of similar or better quality to the more complex methods such as the multiple linear regression and residual methods or the urban DELTA interpolation method. Average uncertainties for this method are around 20-25%, based on the normalised SD of the cross-validation. The 2004 results here are also consistent with previous results though 2003 indicated that the urban DELTA method was superior.

There is no doubt an interannual variation in the best method to be applied and this will need to be further assessed in future work.

9.3.2 Ozone

Based on the objective assessment, one methodology is selected as providing the best interpolation of ozone, for both the SOMO35 and the 26th percentile of the maximum daily 8 hour running mean, Section 5.9. This is:

1. Cokriging with altitude as the supplementary data source.

Though a number of other methods are tested, cokriging gave results of similar or better quality to the more complex methods such as the multiple linear regression and residual methods or the urban DELTA interpolation method.

Only the year 2004 has been tested for urban ozone interpolation and so this result will need to be further assessed in future work.

9.3.3 $PM_{2.5}$

As in the rural interpolation of $PM_{2.5}$ analysis of the possibility for carrying out interpolations of $PM_{2.5}$ for urban areas has been carried out, Section 5.7. However, the current limited number of $PM_{2.5}$ urban background monitoring sites, 55 for 2004, inhibits an effective or testable interpolation methodology. This will need to be readdressed when improved coverage of $PM_{2.5}$ sites is available.

9.4 Summary of the use of daily or annual statistics

In Chapter 6 a study is carried out to assess the need and applicability of the interpolation methods for higher temporal resolutions in the interpolations. This was applied to PM_{10} data for the year 2003, using the linear regression and interpolation of the residual method, where interpolations of daily mean values is compared with the annual statistics to determine annual mean concentrations, 36th percentile of the daily mean and the number of exceedance (NOE) days. The following conclusions are made:

1. Maps of annual mean, 36th percentile and NOE are similar, but not the same, for both temporal resolutions. The differences are of the order of the estimated uncertainties in the methodologies.
2. The maps showing NOE are completely consistent with the 36th percentile maps when using daily interpolations. When using annual statistics these can be different, the extent of which will likely vary from year to year.
3. There are a number of advantages in using daily mean data over annual statistical data including:
    a. The number of observation days used is larger when using daily statistics than annual statistics when a limit on the allowable coverage is applied, e.g. >75%.
    b. The quality of the maps is as good as, and generally better than, maps produced using annual statistics, based on the cross-validation RMSE.
    c. There is absolute consistency between the percentile and NOE fields.
    d. The maps are more robust in regard to the use of automatic routines for defining interpolation parameters used in the kriging interpolation.
    e. Future improvements in the interpolation based on multiple regressions with meteorological parameters will probably be better represented on a daily basis. This is supported by Koelemeijer et al. (2006b).
4. There are a number of disadvantages in using daily mean data over annual statistical data including:
    a. The data and calculation requirements are significantly higher for the daily than for the annual statistics
    b. The reduction in uncertainty may be small in regard to other possible improvements in the interpolation methodology that would be less data intensive
    c. The interpretation of uncertainty mapping is more complex

The advantages above relate mainly to the scientific content of the results, the disadvantages to the increased calculations for the implementation of the interpolations. These must be weighed against each other when selecting an operational system.

9.5 Summary of the uncertainty analysis

In Chapters 5, 6.5 and Chapter 7 uncertainties in the interpolation methods are discussed and a selection of maps is displayed. Uncertainties in the interpolated maps can be due to a number of uncertainty factors in the input data and techniques itself, which are used in the interpolation, such as:

- Uncertainties in the supplementary data used
- Uncertainties in the linear regression models
- Uncertainties in the kriging method and its parameters
- Uncertainties in the representativeness of the monitoring stations
- Uncertainties related to the air quality measurement instruments and procedures
- Uncertainties in the spatial representativeness of the modelling data

Uncertainty related to the interpolation methods were evaluated using cross-validation (by RMSE and several other indicators). In addition, three aspects of uncertainty on the output side, i.e. the resulting maps itself, have been addressed to a limited extent in the current study. These are:

1. Spatial representativeness
2. Kriging interpolation variance
3. Exceedance uncertainty

9.5.1 Spatial representativeness

The spatial interpolation carried out in this study produces maps with a resolution of 10 x 10 km. The maps are thus intended to represent average concentrations or indicators for a 10 x 10 km grid square. Even if the interpolation was perfect measurements made within a grid square will vary in regard to this mean, dependent on the pollutant, e.g. the spatial representativeness of ozone is expected to be larger than that for NO_2.

The spatial representativeness is difficult to assess directly but can be indicated through the nugget variance, be it residual or pure kriging, as this represents the expected variance over small spatial scales. This variance, however, also includes other uncertainties when regression analysis is involved. The spatial representativeness can also be assessed (Section 7.2) by comparing the interpolated grid concentrations with the actual observed concentrations. The SD of these should be indicative of the spatial representativeness uncertainty.

It should also be noted that the kriging interpolation methods tend to smooth out the interpolation. E.g. an interpolated grid concentration at the same spatial position as a single high measurement concentration surrounded by lower concentrations will have a lower interpolated concentration at the grid. This is a result of the choice of kriging parameters, such as nugget and range, and cannot be avoided in the interpolation procedure unless exact interpolation methods are used.

In this study no quantitative estimate has been made in regard to the spatial representativeness and this needs to be addressed in future work.

9.5.2 Kriging variance

A number of maps have been produced that indicate the kriging variance field for both residual kriging and pure kriging methods. These provide the most obvious route to uncertainty mapping when kriging is used as an interpolator. They are, however, directly dependent on the choice of kriging parameters such as the nugget, the sill, the range, the variogram model (Section 2.3.5) and the number of stations included. Choices of these parameters will affect the variance field as well as the interpolated field.

One of the major problems with using kriging variance as a spatial field, and kriging in general, is that it is assumed that the form of the variance is the same everywhere, independent of the concentration levels. This can lead to over or underestimates in areas of high or low concentrations.

9.5.3 Uncertainty in the number of exceedances

When the interpolations are temporally resolved at a level equivalent to the exceedance time scale (Chapter 6) then it is possible to use alternative methods for estimating the number of exceedances, as well as the percentiles. This can be done by estimating uncertainty on a daily basis, for the case of PM_{10}, and then estimating spatial uncertainty using for example the kriging variance. By taking the percentile 67% bands, i.e. ± SD, for each day it is then possible to calculate the uncertainty in the total number of exceedances. This provides a much more adequate explanation of the exceedance uncertainty than does simply taking the annual kriging variance fields.

9.6 Summary of the risk assessment

By overlaying the air quality maps with population density and land use data it is possible to compute population and vegetation at risk tables, for individual countries and for Europe as a whole, both in absolute numbers and in percentages.

9.6.1 Population exposure

By overlaying the air quality maps with population density estimates can be made of population exposure and estimates of premature deaths. To demonstrate this application a number of assessments are made for PM_{10} and ozone with the following summary:

- The number of Europeans exposed to annual mean concentrations of PM_{10} above the European limit value of 40 $\mu g.m^{-3}$ is 6% of the total population
- The estimated number of premature deaths calculated using 2004 as the reference year is between 246 000 and 327 000 in the EU25 without Cyprus, depending on the choice of natural background concentration.

9.6.2 Vegetation exposure

For ecosystems, the following findings are important

- More than 30 % of all agricultural land may be exposed to ozone exceeding the target value of 18 $mg.m^{-3}.h$ and more than 80 % may be exposed to levels in excess of the long-term objective of 6 $mg.m^{-3}.h$. In southern countries about 90 % is estimated to exceed the target values, while in northern Europe the estimated ozone levels are below the target value for nearly 70% of the agricultural area.
- For forests, in Northern Europe the critical, ozone reporting level of 20 $mg.m^{-3}.h$ is not exceeded in our calculations, but in Southern Europe this level is exceeded everywhere.
- The rural NO_x map shows a few regions where the NOx limit value for the protection of vegetation is exceeded (the Benelux, the Rhone Valley and Northern Italy).
- No significant exceedances for SO_2 were expected as the interpolated map of annual average SO_2 confirms.

Significant uncertainties exist in these calculations but these have yet to be assessed. These calculations also contain discrepancies that will need to be resolved in the future. For instance several countries show monitoring data above the exceedance levels but there are no exceedances in the interpolation. This is a result of the interpolation methodology that tends to smooth out observations and, as mentioned in Section 9.5, represents the average concentrations in a 10 x 10 km grid.

9.7 Considerations when recommending operational air quality mapping and risk assessment procedures

In this section considerations when recommending methodologies for operational mapping are given. Though this is not discussed in detail in the report these aspects are regularly referred to when recommending 'best' methods. These preliminary recommendations will further help steer the required discussions for future development.

Operational methods need to produce the best spatial assessment possible given the available data and within a feasible budget and time frame. For this reason several levels can be considered, dependent on the data availability and the application. Applications will include:

1. Air quality assessment on the European scale for policy and public information dissemination
2. Air quality indicators for risk assessment of ecosystems and human health
3. Real time air quality mapping for public information and dissemination
4. Mapping of inter-annual trends

Aspects to be considered in the selection of an operational methodology include:

- Quality of the interpolation
- Robustness and continuity from year to year
- Homogeneity between pollutants and indicators
- Physical basis for the supplementary data inclusion
- Availability and reliability of the data
- The application requirements of the assessment
- Quality of the spatial coverage
- Technological platform

Based on general considerations it is recommended to:

1. Adopt a set of methodologies that are applicable to most pollutants and their indicators.
2. Adopt methodologies that are physically reasonable and consistent within our understanding of the processes.
3. Adopt a prioritisation of methodologies starting from the 'best', most likely the most complex in input data requirements, to the least input demanding methodologies.
4. Always provide a backup methodology when data is delayed or not available. E.g. climatological data may be used instead of concurrent meteorological data.

A more rigorous discussion of these considerations is required before operational methods can be recommended.

9.8 Recommendations for further work

9.8.1 Further discussions concerning methodologies, additional indicators, uncertainty and applications

Selection of 'best' methodology

A discussion, e.g. through an expert meeting or group, should be held to determine which criteria are involved when selecting the 'best' method for preparing interpolated European indicator maps, keeping in mind the involved complexity, resources, time, data availability (temporal, spatial and update resolution, release date), errors and uncertainties in data sources, data assimilations, calculations, general pragmatism, history of indicator assessments. Also personal and organisation/institutional preferences may play a role.

Selection of additional pollutants or indicators

While we feel that we have addressed the substances and indicators with the highest policy relevance in the current study, the tools are available to expand the analysis to indicators which may have somewhat lower priority, but are still relevant for European air pollution assessments.

Presentation of uncertainty

Though the uncertainty can be mathematically calculated there still remains the question of communication of this parameter and its use in the applications addressed. Since this is fairly fresh ground

for air quality assessment a more informed and wider discussion is still required on this aspect of the assessment.

Application for other ETC/ACC mapping activities
Close co-operation with the other mapping tasks of ETC should be encouraged. Invitations to other task leaders involved in mapping should be made, where relevant, to meetings within this task. The reciprocal is also true.

In the following sections, these four aspects of potential future work are elaborated.

9.8.2 Further analysis needs for the spatial assessment methodologies

Reduction of interpolation methods
In the current studies a fairly broad selection of interpolation methods and supplementary data has been selected and tested. Based on these results the number of methods studied should be reduced and these should be studied in detail.

Alternative chemical transport models
Currently the Unified EMEP model is used as supplementary data for the interpolations. It has been shown to help improve the interpolations. The EMEP model currently has a spatial resolution of 50 x 50 km. It should be considered to use alternative chemical transport models of higher resolution for the interpolations.

Pressure instead of altitude
Altitude is major supplementary data input for the interpolations but it is considered not to be the best. It is advised instead to use the pressure, since air pollutants have a correlated behaviour with surface level atmospheric pressure, including interaction between this layer and the above air layers. The aspects of lognormal correlation also play a role here. The use of lognormal transformed air pollutant measurements is one of the subjects examined in this project but it ignored the role air pressure plays in it. It is recommended to examine the best application of pressure, altitude and logarithmic transformation.

Temporal resolution of the interpolations
In this report a study of the use of higher temporal resolutions has been carried out for PM_{10}, using daily means for 2003. It was concluded to be a more robust method. The same methodology can be applied to ozone percentiles and other year's data. With an eye on real time applications these methods should continued to be assessed.

Alternative techniques
The current study limits its application to kriging and residual kriging. In other work carried out in the Air4EU project alternative methods for combining kriged and regression fields were explored (Denby, unpublished work). This involved combining the kriged and regression fields using Bayesian statistics to produce the most likely field. This allows a much clearer interpretation of uncertainty and how to combine the two different fields. This methodology was shown to have similar, but slightly larger, cross-validation RMSE than the residual method but should be explored further. In many ways it is simpler, and more reasonable, to apply than the residual method.

Usage of satellite data as supplementary data
In the current study, we have intentionally used only ground-based measurements and supplementary data to develop air quality maps. Increasingly, satellite data, e.g. for NO_x and possibly also for ozone, SO_2 and aerosols/PM, are becoming available. They combine positive aspects such as high resolution over large spatial scales with negative aspects such as irregular coverage over time and the indirect relationship with actual air quality. The potential benefits of using the high spatial resolution of remote sensing information to improve interpolation methods could be explored.

9.8.3 Further pollutants and indicators

NO_2 maps

The 1st Daughter Directive defines human health limit values for NO_2: the 19th highest hourly NO_2 concentration of 200 $\mu g.m^{-3}$ and a limit value of the annual average of 40 $\mu g.m^{-3}$. A human health NO_2 exceedance map could be prepared as future activity. However, it is possible that NO_2 is highly correlated with other pollutants and could possibly act as a surrogate or indicator of the combustion-generated

particulate air pollution. Due to the small scale spatial characteristics of the NO_2 field, i.e. exceedances on hotspots, no separate health impact assessment for NO_2 has been made; its effects will probably be largely included in the PM assessment.

SO_2 maps
No indicator map has been produced for the winter season average (1 Oct. – 31 March) for SO_2 with ecosystem exceedances as defined in the 1st Daughter Directive. The exceedance are expected to be systematically higher then the annual average. We overlooked this indicator and due to lack of time we were not able to investigate this any further. This could be a subject of future activities.

Ozone percentiles
Carry out mapping of the 26th highest daily maximum 8 hour running mean ozone, in accordance with directives, including EMEP model output (Must be ordered on time).

9.8.4 Uncertainty assessment and mapping

A preliminary study of uncertainty has been carried out in this report based on the statistical assessment, e.g. cross-validation RMSE, of the interpolations and on the kriging variance for spatial mapping. However, this aspect of the mapping is far from concluded. There are a number of points in regard to uncertainty mapping that still need to be addressed in 2007.

Regression analysis
The uncertainty mapping to date has been based solely on the residual kriging. The regression analysis also introduces uncertainties in the results that are not accounted for in this analysis. Statistical methods, such as the cross-validation used for kriging, or others such as boot-strapping and jack-knife methods, may also be applied to assess the importance of the regression analysis in the total uncertainty.

Supplementary data
No analysis has yet been made on the uncertainty of the supplementary data and its influence on the interpolations. This is particularly true for chemical transport and meteorological model input.

Spatial representativeness
Uncertainty in the spatial representativeness of the monitoring data has not been directly addressed to a significant extent in the studies to date. These are indirectly implied through the nugget variance used in the spatial interpolation and are indicated in the residual kriging standard deviation maps. However this aspect should be directly addressed in future work.

Monitoring data
There is still uncertainty attached to the monitoring data, particularly with compounds such as PM_{10} and the application of non-homogeneous correction factors. This will need to be addressed. Currently all data, including metadata, from AirBase is taken as is. A more critical view of this data may be required. This is part of the current emerging process of improved quality assurance and quality control of the AirBase data.

Kriging parameters
The current methodology of using the kriging parameters that minimize the cross-validation RMSE needs to be assessed in terms of uncertainty. This optimization procedure, which is manually carried out and not entirely objective, should be assessed further to see its influence on the mapping uncertainty. This is important since these kriging parameters actually define the spatial uncertainty.

Risk assessment
Uncertainties in the interpolation methodologies will propagate through to uncertainty in the risk assessment. This needs also to be assessed. One suggested method includes using different interpolation methodologies in the final risk assessment to see its sensitivity to the selection of themethod. Another may involve using the 5% and 95% interpolation fields for assessing the uncertainty in the risk assessment.

Sub-grid variability for exposure calculations
For a more realistic assessment of population exposure the spatial variability within a grid is also required. To assess this, the spatial representativeness needs to be determined, independent of the total uncertainty of the interpolation method.

Probability maps
These maps are directly dependent on the uncertainty fields and the first preliminary versions of these have been made in this study. Further assessment of their role and application within the mapping work is still required.

9.8.5 Further applications of the assessments

Application to real time mapping
The current work focuses on indicators providing annual averaged information for European air quality. The applicability of (or parts of) the methods for near-real time or even forecast reports of air quality is not the primary scope of this project, but might be a focus of future work. We can image that at some point in the future interpolation techniques and methodologies of this project could become applicable in a way for EEA's near-real time projects. This can take place on a basis of pre-calculations that include knowledge on conditional and multi-annual air pollutant profiles. These pre-calculated results can be on stand-by for on the fly interpolations of European maps using freshly reported measurements. They might improve the current near-time web interpolated maps.

NATURA2000
It would be interesting to overlay the air quality exceedance maps for vegetation and ecosystem related indicators with the NATURA2000 maps as soon as these would become available.

Validation of satellite data
The current work has intentionally focused on ground-based measurements and ground-based supplementary data. Above, it was suggested that remote sensing data could be considered as supplementary sources of information for the improvement of interpolation methods because of their large and high resolution spatial coverage. Conversely, the interpolated ground-based air quality patterns described in the current report could be used in the calibration of remote sensing data.

Table 9.1: Comparison of different interpolation techniques for different air quality indicators. The linear regression models were examined specifically of their use in the spatial interpolation methods.

Pollutant	Area	Indicator	Type	Best methods	Used mapping method [Section: Method]	Remarks
PM_{10}	Rural	Annual average concentration	Linear regression methods	Actual meteorological plus GTOPO altitude data plus EMEP output (1-P.2) gives best results; EMEP data alone gives better results than supplementary data alone; logarithmic transformation gives improved results.		Advantage of using actual meteorological data is much larger than for ozone
			Spatial interpolation methods	Interpolation of primarily monitoring data including altitude with lognormal kriging gives best fit (2-d); 2nd best is ordinary kriging of residuals of linear regression EMEP model plus altitude and meteorology (3-P.2b-b)	5.2.7: 3-P.2b-b2	2nd best solution as to fit preferred because of better coverage of areas without measurements, continuity with earlier work and its performance close to best results
		36th max. daily mean	Same as annual average	Same as annual average	5.2.7: 3-P.2b-b2	The same method can be applied for PM10 regardless of the indicator without significant loss of accuracy
	Urban	Annual average concentration	Linear regression methods	EMEP output plus s. solar radiation, relative humidity and temperature (1-UP.2) gives the best results		Poorer results than with spatial interpolation
			Spatial interpolation methods	For the subset of cities with only one station ordinary kriging of residuals of linear regression using EMEP plus meteorology (3-UP.2d-b) is best, with close 2nd best interpolation of primarily monitoring data using ordinary kriging (2-b); For all stations interpolation of primarily monitoring data with ordinary kriging (2-b) is best.	5.8.4: 2-b2	2nd best is preferred here: It is very close to best; it is used (as best) at urban indicator PM_{10} 36th max daily mean as well, and it is simpler and easier to generate. EMEP-method most suitable for cities with no measurements
		36th max. daily mean	Linear regression methods	Same as for annual average		Poorer results than with spatial interpolation
			Spatial interpolation methods	Interpolation of primarily monitoring data with ordinary kriging (2-b) gives best results for all stations as well as for the subset of cities with only one station	5.8.4: 2-b2	

(Table 9.1 cont.)

O_3	Rural	SOMO35	Linear regression methods	Actual meteorology plus altitude data plus EMEP output (1-O.2) gives best results		Advantage over method with only supp. data is only small
			Spatial interpolation methods	Linear regression with altitude, s. solar radiation and relative humidity plus ordinary kriging of residuals (3-O.3b-b), as well as same results with altitude, s. solar radiation and EMEP (3-O.2c-b) give similar, best results. Interpolation of primarily monitoring data, including altitude with ordinary cokriging (2-c) gives also similar best result	5.3.5: 3-O.2c-b2	EMEP plus suppl. data is applied because of continuity with earlier work
		26^{th} highest maximum 8-hour	Linear regression methods	Actual meteorology plus altitude data (1-O.3) gives best results		For 26^{th} highest daily max. 8-hour averages no EMEP-results available, results inferior to SOMO35
			Spatial interpolation methods	Interpolation of primarily monitoring data, including altitude with ordinary cokriging (2-c) gives best result	5.3.5: 2-c2	Spatial methods better than linear regression
		AOT40 for crops/ forests	Linear regression methods	Actual meteorology plus altitude data plus EMEP output (1-O.2) gives best results, similar to SOMO35		Same method can be applied as SOMO35
			Spatial interpolation methods	Crops: Linear regression with altitude, s. solar radiation and relative humidity plus EMEP using ordinary kriging of residuals (3-O.2a-b) gives best result; Method 2-c (as best for forests) shows a fit of about 6% worse than 3-O.2a-b. Forests: Interpolation of primarily monitoring data, including altitude with ordinary cokriging (2-c) gives best results,	Crops and Forests: 5.3.5: 2-c2	Spatial methods better than linear regression; Method 2-c2 used because of (i) methodological consistency and compatibility between the two AOT40 indicators, and (ii) it is in continuity with the crops indicator assessments made in previous years on past years (1996-2003)
	Urban	SOMO35	Linear regression methods	EMEP plus relative humidity (1-UO.2d) gives best result		

(Table 9.1 cont.)

			Spatial interpolation methods	Best results with ordinary cokriging with altitude (2-c), very close 2nd best ordinary kriging (2-b)	5.9.4: 2-b2	2nd best used because of lack of time and marginal difference with best method
		26th highest maximum 8-hour	Linear regression methods	Wind speed plus relative humidity (1-UO.3b)		No EMEP results available for this indicator
			Spatial interpolation methods	Same as SOMO35	5.9.4: 2-c2	
NO_x	Rural	Annual average concentration	Linear regression methods	Use of EMEP output and/or altitude give poor results		NO_2->NO_x correction applied to increase data source size
			Spatial interpolation methods	Interpolation of primarily monitoring data with lognormal cokriging plus altitude gives best results (2-d); 2nd best is ordinary kriging of residuals plus EMEP and altitude (3-N.2-b)	5.3.4: 3-N.2-b2	2nd best preferred because of coverage of areas without measurements
SO_2	Rural	Annual average concentration	Linear regression methods	Using EMEP output gives poor results		
			Spatial interpolation methods	Ordinary kriging of residuals of linear regression plus EMEP (3-S.1-b)	5.4.2: 3-S.1-b2	
$PM_{2.5}$	Not pursued because of data scarcity; linking to PM_{10} or EMEP model $PM_{2.5}$ output gives poor fit					

References

AirBase, European air quality database, http://airbase.eionet.europa.eu/

Cressie, N. (1993). Statistics for spatial data. Wiley series, New York.

Blond, N., L. Bel, and R. Vautard (2003). Three-dimensional ozone data analysis with an air quality model over the Paris area, J. Geophys. Res., 108(D23), 4744.

Brabec, M., Horálek, J., Fiala, J. (2005). Statistical Approach to Pooling Empirical Data and Air Pollution Physical Modeling Output. Meteorological Journal 8, 177-186.

Briggs, D. et al. (2005). APHOSPHERE – Air Pollution Modelling for Support to Policy on Health and Environmental Risks in Europe. http://www.apmosphere.org/

Brunekreef B, Forsberg B. (2005). Epidemiological evidence of effects of coarse airborne particles on health. Eur Respir J., Aug;26(2):309-18.

Denby, B., Horálek, J., Walker, S. E., Eben, K., Fiala, J. (2005). Interpolation and assimilation methods for European scale air quality assessment and mapping. Part I: Review and recommendations. ETC/ACC Technical paper 2005/7.
http://air-climate.eionet.europa.eu/docs/ETCACC_TechnPaper_2005_7_SpatAQ_Interpol_Part_I.pdf

De Leeuw F. (2005). PM10 measurement methods and correction factors in AirBase 2004 status report ETC/ACC Technical Paper 2005/6.
http://air-climate.eionet.europa.eu/reports/ETCACC_TechnPaper_2005_6_PM10_CorrFactors2004

Dockery, D.W., Pope, C.A., Xu, X., Spengler, J. D., Ware, J.H., Fay, M.E. (1993). An association between air pollution and mortality in six U.S. cities. New England Journal of Medicine Volume 329 (Issue 24): 1753-9.

EC (1996). "Air Quality Framework Directive", Council Directive 96/62/EC on ambient air quality assessment and management, Official Journal of the European Communities (OJ) L 296, 21.11.1996, 55-63. http://eur-lex.europa.eu/LexUriServ/site/en/consleg/1996/L/01996L0062-20031120-en.pdf

EC (1997). "Exchange of Information", Council Decision 97/101/EC establishing a reciprocal exchange of information and data from networks and individual stations measuring ambient air pollution within the Member States, OJ L35, 05/02/1997, 14-22.
http://air-climate.eionet.europa.eu/country_tools/aq/aq-dem/docs/97_101_EC.doc

EC (1999). "First Daughter Directive", Council Directive 1999/30/EC relating to limit values for sulphur dioxide, nitrogen dioxide and oxides of nitrogen, particulate matter, and lead in ambient, OJ L 163, 29.06.1999, 41-60.
http://eur-lex.europa.eu/LexUriServ/site/en/oj/1999/l_163/l_16319990629en00410060.pdf

EC (2000). "Second Daughter Directive", Directive 2000/69/EC of the European Parliament and the Council relating to limit values for benzene and carbon monoxide in ambient air, OJ L313, 13.12.2000, p.12-21. http://eur-lex.europa.eu/LexUriServ/LexUriServ.do?uri=OJ:L:2000:313:0012:0021:EN:PDF

EC (2001). "Amended Annexes", Commission Decision 2001/752/EC amending the Annexes to Council Decision 97/101/EC establishing a reciprocal exchange of information and data from networks and individual stations measuring ambient air pollution within the Member States, OJ L282, 26/10/2001, 69-76. http://air-climate.eionet.europa.eu/country_tools/aq/aq-dem/docs/2001_752_EC.pdf

EC (2002). "Third Daughter Directive", Council Directive 2002/3/EC of the European Parliament and the Council relating to ozone in ambient air, OJ L 67, 09.03.2002, 14-30.
http://eur-lex.europa.eu/pri/en/oj/dat/2002/l_067/l_06720020309en00140030.pdf

EC (2004). "Questionnaire", Decision 2004/461/EC laying down a questionnaire to be used for annual reporting on ambient air quality assessment under Council Directives 96/62/EC and 1999/30/EC and under Directives 2000/69/EC and 2002/3/EC of the European Parliament and of the Council, OJ L 319, 30/04/2004, 45-64.

EEA (2006). Air pollution by ozone in Europe in summer 2005. EEA Technical Report 3/2006. http://reports.eea.europa.eu/technical_report_2006_3/en/technical_report_3_2006.pdf

EEA (2007). Air pollution in Europe 1990 – 2004. EEA Report No. x/200x. (In prep.)

Eurostat (2007). URL: http://europa.eu.int/comm/eurostat/structuralindicators

Fagerli, H., Simpson, D., Tsyro, S. (2004). Unified EMEP model: Updates. In: EMEP Report 1/2004. MSC-W, Oslo, Norway. www.emep.int/publ/reports/2004/Status_report_int_del1.pdf

Horálek, J., Kurfürst, P., Denby, P., de Smet, P., de Leeuw, F., Brabec, M., Fiala, J. (2005). Interpolation and assimilation methods for European scale air quality assessment and mapping. Part II: Development and testing new methodologies. ETC/ACC Technical paper 2005/8.
http://air-climate.eionet.europa.eu/docs/ETCACC_TechnPaper_2005_8_SpatAQ_Part_II.pdf

IIASA (2005). CAFE Scenario Analysis Report Nr. 6, "A final set of scenarios for the Clean Air For Europe (CAFE) programme". http://ec.europa.eu/environment/air/cafe/activities/pdf/cafe_scenario_report_6.pdf

Koelemeijer, R.B.A., Schaap, M., Timmermans, R.M.A, Homan, C.D., Matthijsen, J., Van de Kassteele, J. and Builtjes, P.J.H. (2006a), Monitoring aerosol concentrations and optical thickness over Europe, PARMA final report, MNP report 555034001/2006, Netherlands. http://www.mnp.nl

Koelemeijer R.B.A., Homan C.D., Matthijsen J. (2006b). Comparison of spatial and temporal variations of aerosol optical thickness and particulate matter over Europe. Atmospheric Environment 2006:40; 5304-5315.

Künzli N., Kaiser R., Medina S., Studnicka M., Chanel O., Filliger P., Herry M., Horak F., Jr., Puybonnieux-Texier V., Quenel P., Schneider J., Seethaler R., Vergnaud J.C., Sommer H. (2000). Public-health impact of outdoor and traffic-related air pollution: a European assessment. Lancet 2000;356(9232):795-801.

New, M., Lister, D., Hulme, M., Makin, I. (2002). A high-resolution data set of surface climate over global land areas. Climate Research, Vol. 21, pp. 1-25. http://www.cru.uea.ac.uk/cru/data/hrg.htm/

Pope C.A., Burnett R.T., Thun M.J., Calle E.E., Krewski D., Ito K., Thurston G.D. (2002). Lung Cancer, Cardiopulmonary Mortality, and Long-term Exposure to Fine Particulate Air Pollution. Journal for the American Medical Association 2002;287:1132-1141.

Putaud, J.-P., van Dingenen, R., Baltensperger, U., Bruggemann, E., Charron, A., Facchini, M.C., Decesari, S., Fuzzi, S., Gehrig, R., Hansson, H.-C., Harrison, R.M., Jones, A.M., Laj, P., Lorbeer, G., Maenhunt, W., Mihalopoulos, N., Muller, K., Palmgren, F., Querol, X., Rodriguez, S., Schneider, J., Spindler, G., ten Brink, H., Tunved, P., Torseth, K., Wehner, B., Weingartner, E., Wiedensohler, A., Wahlin, P., Raes, F., 2003. A European aerosol phenomenology. EUR 20411 EN. Joint Research Centre, European Commission, Ispra, Italy.

Rao, C. R. (1973). Linear statistical inference and its applications. Wiley. New York.

Sandnes Lenschow, H., Tsyro, S. (2002). Meteorological input data for EMEP/MSC-W air pollution models. EMEP MSC-W Note 2/2000.

Sandström T, Nowak D, van Bree L. (2005). Health effects of coarse particles in ambient air: messages for research and decision-making. Eur Respir J., Aug;26(2):187-8.

Simpson, D., Fagerli, H., Jonson, J. E., Tsyro, S., Wind, P., Tuovinen, J.-P. (2003). Transboundary acidification and eutrophication and ground level ozone in Europe: Unified EMEP model description. EMEP Status Report 1/03 Part I. MNP, Oslo, Norway.
www.emep.int/publ/reports/2003/emep_report_1_part1_2003.pdf

Tarassón, L., Fagerli, H., Klein, H., Simpson, D., Benedictow, A., Vestreng, V., Rigler, E., Emberson, L., Posch, M., Spranger, T. (2006). Transboundary acidification, eutrophication and ground level ozone in Europe since 1990 to 2004. EMEP Status Report 1/06. MSC-W, Oslo, Norway.
http://webdab.emep.int/Unified_Model_Results/ and
http://projects.dnmi.no/~emep/publ/reports/2004/Status_report_int_del1.pdf

Van de Hout, K.D. (2006). Overview of air quality reports on 2004 by Member States under the European air quality directives– Part 1: Main report. (To be published)

Van de Kassteele, J. (2006). Statistical air quality mapping. Doctoral Thesis Wageningen University.

Vestreng, V., Adams, M., Goodwin, J. (2004). Inventory Review 2004 Emission Data reported to CLRTAP and under the NEC Directive. MSC-W Technical Report 1/04. EMEP/EEA Joint Review Report. www.emep.int/publ/reports/2004/emep_technical_1_2004.pdf

Vestreng, V., Breivik, K., Adams, M., Wagner, A., Goodwin, J., Rozovskaya, O., Pacyna, J. M. (2005). Emission Data reported to LRTAP Convention and NEC Directive. Initial review for HMs and POPs. MSC-W. Technical Report 1/05. Oslo, Norway.
www.emep.int/publ/reports/2005/emep_technical_1_2005.pdf

Wackernagel, H. (2003). Multivariate geostatistics: An introduction with applications. 3rd ed., Springer, Berlin.

ECMWF: Meteorological Archival and Retrieval System (MARS). It is the main repository of meteorological data at ECMWF (European Centre for Medium-Range Weather Forecasts; http://www.ecmwf.int/).

UN (2005). United Nations, Department of Economic and Social Affairs, Population Division (2005). *World Population Prospects: The 2004 Revision*. *CD-ROM Edition - Extended Dataset* (United Nations publications, Sales No. E.05.XIII.12).

UNECE (2004). United Nations – Economic Commission for Europe, LRTAP Convention. Mapping Manual 2004. Manual on methodologies and criteria for Modelling and Mapping Critical Loads ands Levels and Air Pollution Effects, Risks and Trends.
http://www.oekodata.com/icpmapping/htm/manual/manual_eng.htm

WHO (2000) Air Quality Guidelines for Europe. WHO regional Publications, European Series No. 91. WHO Regional Office for Europe, Copenhagen, Denmark.

WHO (2004). Global Burden of Disease project. URL: http://www.who.int/topics/global_burden_of_disease/en/

WHO (2006). Air quality guidelines. Global update 2005. Particulate matter, ozone, nitrogen dioxide and sulfur dioxide. http://www.euro.who.int/InformationSources/Publications/Catalogue/20070323_1

Yttri, K.E. and Aas, W. (eds.) (2006). Yttri, K.E., Aas, W., Forster, C., Tørseth, K., Tsyro, S., Tarrasón, L., Simpson, D., Vestreng, V., Lazaridis, M., Kopanakis, I., Aleksandropoulou, V., Gehrig, R., Adams, M., Woodfield, M., Putaud, J.P. and Schultz, M. Transboundary Particulate Matter in Europe: Status Report 2006. EMEP Status Report 4/2006. Joint CCC & MSC-W Report 2006. http://www.nilu.no/index.cfm?ac=publications&folder_id=4309&publication_id=17233&view=rep&lanid=3

Annex. Final maps and summarizing tables for the year 2004

Introduction

Concentration maps

The methods of linear regression models plus interpolation of their residuals, as described in Section 2.4, are applied for the rural mapping, in case of many indicators. They may result in negative values at some locations in the rural maps. In these cases the negative numbers are set to zero for SOMO35, or to 0.5 for other indicator maps.

The final concentration maps are created on the basis of rural and urban maps, as discussed in Section 5. The rural and urban maps have to be merged into one combined air pollution concentration map. The combination is performed with the use of the population density grid. The basic principle of this merging is described in Section 3.3 and several details of the applied methodology are discussed here.

The separate mapping of rural and urban areas and their subsequent merging is based on the presumption that at locations not too far away from each other, rural air pollution levels are lower (in case of PM_{10}), or higher (in case of ozone) than urban air pollution. This holds in general. However, the comparison of rural and urban maps shows that this is not the case for several small areas. It is mainly caused by irregular distribution of measuring stations within the network, especially by the lack of rural stations.

In Horálek et al. (2005) this supposed inconsistency was corrected in a simple way by modifying concentrations at these particular areas of the rural map according to the urban map. In this report a more advanced approach is applied, in which for a given pollutant an auxiliary field is computed on the basis of data from all background stations, both rural and (sub)urban. In the areas where the rural map shows higher levels of air pollution (in case of PM_{10}), or lower levels (in case of ozone) than the urban map, both rural and urban maps are modified according to the auxiliary field computed from all stations.

The final merging of the resulting urban and rural maps is carried out by the application of the methodology described in Section 3.3, which uses the population density field. The value of the parameters α_1 and α_2 in the equation 3.2 are set as $\alpha_1 = 100$ inhbs.km^{-2} and $\alpha_2 = 500$ inhbs.km^{-2} on the basis of the analysis presented in Horálek et al. (2005).

The final maps were created using the EEA standard projection ETRS-LAEA5210, with map extent 1c. The aggregated grid resolution of the maps is 10 x 10 km, using a EEA reference grid , for the majority of the pollutants. The exceptions are the maps of AOT40 for crops and for forests. The aggregated grid resolution of these maps is 2 x 2 km. Each map presents not only the interpolated field but also the measured concentrations at the rural background stations (triangles) and at urban and suburban background stations (squares).

Additional to the concentration maps for PM_{10} and ozone (Maps A1 – A6), also maps demonstrating the spatial match of pollutant concentrations with population, agricultural areas and forests are presented (Maps A10 – A21). Several maps with health-related indicators (Maps A1 – A3) are overlaid with a transparent version of Map A9 with the population density at a 100 x 100 m grid resolution. The overlay consists of simply putting the population density Map A9 literally like a transparency sheet on top of the maps with the interpolated air quality concentration fields.

The AOT40 maps (A5 and A6), for both agricultural areas and forests are combined with the CLC2000 at 500 x 500 m resolution (CLC2000) to generate maps for the agriculture areas and forests at risk due to ozone exposure. The maps of the agriculture areas at risk were created for the land cover level-1 class *2 Agricultural areas* (Map A13) and in more detail for its level-2 classes *2.1 Arable land*, *2.2 Permanent crops*, *2.3 Pastures* and *2.4 Heterogeneous agricultural areas* (Maps A14 – A17). The maps with forests at risk are created for the level-2 class *3.1 Forest*s (Map A18) and in more detail for the level-3 classes *3.1.1 Broad-leaved forest*, *3.1.2 Coniferous forest* and *3.1.3 Mixed forest* (Maps A19 – A21).

Exposure tables

Population exposure (Tables A1 – A2)*:* Note that in the population density map the missing countries of the JRC population database were filled with ORNL LandScan population data (Section 4.9) to enable the combination of the rural and urban areas in these countries as well. However, the calculation of a population-weighted average in the other countries requires a proper comparability of the LandScan data with the JRC data. Some preliminary comparisons between the ORNL Landscan and the JRC datasets for countries covered by both datasets demonstrated significant differences, leading to the decision not to use the LandScan data straightforward for deriving the tables for the 'missing' countries. The Landscan data would require more detailed analyses, including adjustments to make it equivalent to the JRC source, going beyond the limits of the project resources and therefore not yet done. JRC population density information is not available for the countries: AD, AL, BA, CH, CS, CY, IS, MK, NO, TR.

For each country and for Europe the fraction of the population in the various exposure classes of the maps are given in the tables. In addition the population-weighted concentration is computed according to the equation:

$$\hat{c} = \frac{\sum_{i=1}^{N} c_i p_i}{\sum_{i=1}^{N} p_i} \qquad \text{(A.1)}$$

where $\hat{c}$ is the average concentration per inhabitant in the country,

p_i is the population in the i-th grid cell,

N is the number of grid cells in the country or in Europe as a whole,

c_i is concentration in the i-th grid cell.

The population map is based on the population census of 2001; these data may deviate from the population numbers in the reference year 2004. In the tables the 2004 population (UN, 2005) are given. It is expected that the upscaling from 2001 to 2004 has a marginal effect on the frequency distributions and population weighted mean concentrations.

Vegetation and ecosystem exposure (Tables A3 – A11)*:* Starting point for the exposure estimates for vegetation and ecosystem are the respective concentration maps (Map A5, AOT40 for crops, Map A6; AOT40 for forest) and the CLC2000 land cover data base described in Section 4.8. Exposure tables have been calculated for the land cover level-1 class *2 Agricultural areas* (Table A3) and in more detail for its level-2 classes *2.1 Arable land*, *2.2 Permanent crops*, *2.3 Pastures* and *2.4 Heterogeneous agricultural areas* (Tables A4 – A7). The forest exposure tables are calculated for the level-2 class *3.1 Forest*s (Table A8) and in more detail for the level-3 classes *3.1.1 Broad-leaved forest*, *3.1.2 Coniferous forest* and *3.1.3 Mixed forest* (Tables A9 – A11).

To reduce the computational time involved with the large number of grid cell calculations to reach the results on country level as presented in the tables and discussed in the next section, the resolution of the land cover grid was reduced to 500 x 500 m. The AOT40 maps in a 2 x 2 km grid resolution both for vegetation and for forests are combined with the CLC2000 land cover at 500 x 500 m grid resolution (Section 4.8) to generate the maps of the crops and vegetation at risk.

A number of countries are not included in the tables, either because there is only limited ozone data available (AL, BA, BG, GR, MK, RO) or because of missing land cover information (CH, CS, IS, NO, TR).

At the map descriptions are the countries indicated by their ISO 3166-1:1997 alpha-2 code.

Maps and Tables

Map A1 Combined rural and urban concentration map of PM_{10} – annual average.

Map A2 Combined rural and urban concentration map of PM_{10} – 36^{th} maximum daily average value.

Map A3 Combined rural and urban concentration map of ozone – SOMO35.

Map A4 Combined rural and urban concentration map of ozone – 26^{th} highest daily max. 8-hour value.

Map A5 Rural concentration map of ozone – AOT40 for crops.

Map A6 Rural concentration map of ozone – AOT40 for forests.

Map A7 Rural concentration map of NO_x.

Map A8 Rural concentration map of SO_2.

Map A9 Population density map of Europe at 100 x 100 m grid resolution.

Map A10 Combined rural and urban concentration map of PM_{10} – annual average, overlaid with the population density grid.

Map A11 Combined rural and urban concentration map of PM_{10} – 36^{th} maximum daily average value, overlaid with the population density grid.

Map A12 Combined rural and urban concentration map of ozone – SOMO35, overlaid with the population density grid.

Map A13 Agriculture areas (all types) at risk / damage map – ozone, AOT40 for crops.

Map A14 Arable land at risk / damage map – ozone, AOT40 for crops.

Map A15 Permanent crops at risk / damage map – ozone, AOT40 for crops

Map A16 Pastures at risk / damage map – ozone, AOT40 for crops.

Map A17 Heterogeneous agricultural areas at risk / damage map – ozone, AOT40 for crops.

Map A18 Forests (all types) at risk / damage map – ozone, AOT40 for forests.

Map A19 Broad-leaved forests at risk / damage map – ozone, AOT40 for forests.

Map A20 Coniferous forests at risk / damage map – ozone, AOT40 for forests.

Map A21 Mixed forests at risk / damage map – ozone, AOT40 for forests.

Table A1 Population exposure and population weights concentration – PM_{10}, annual average.

Table A2 Population exposure and population weights concentration – ozone, SOMO35.

Table A3 Exposure of agriculture areas (all types) – ozone, AOT40 for crops.

Table A4 Exposure of arable land – ozone, AOT40 for crops.

Table A5 Exposure of permanent crops – ozone, AOT40 for crops.

Table A6 Exposure of pastures at risk – ozone, AOT40 for crops.

Table A7 Exposure of heterogeneous agricultural areas – ozone, AOT40 for crops.

Table A8 Exposure of forests (all types) – ozone, AOT40 for forests.

Table A9 Exposure of broad-leaved forests – ozone, AOT40 for forests.

Table A10 Exposure of coniferous forests – ozone, AOT40 for forests.

Table A11 Exposure of mixed forests – ozone, AOT40 for forests.

Map A1. Combined rural and urban concentration map of PM_{10} – annual average, year 2004. Spatial interpolated concentration field and the measured values in the measuring points. Units: µg.m^{-3}.

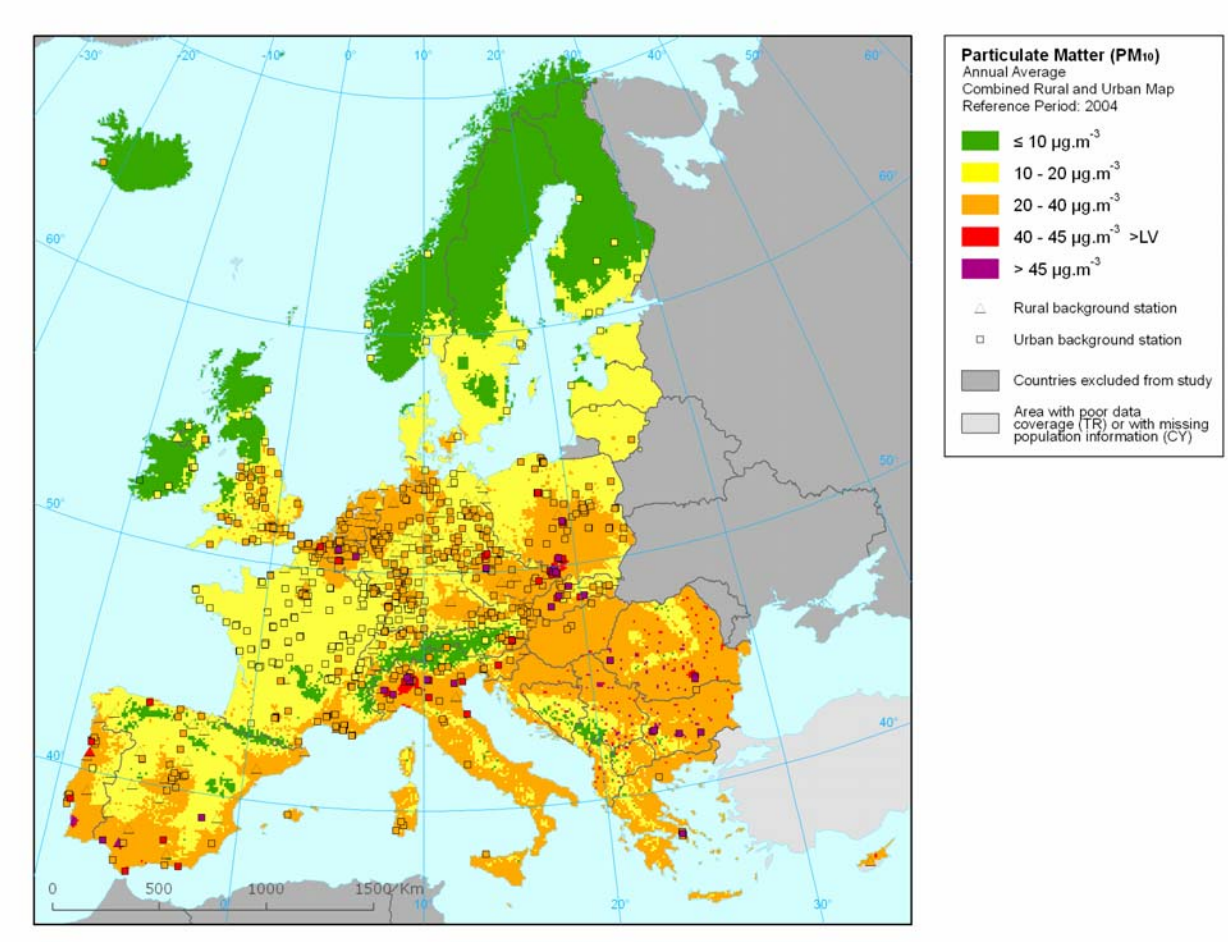

The map was created by combining the rural and urban maps using the population density field and criteria given in Section 3.3 and the introduction to this Annex. The rural map was created by combining the measured PM_{10} concentrations from the rural background stations with supplementary data (EMEP model output, altitude field, surface solar radiation, wind speed), using linear regression followed by interpolation of residuals by ordinary kriging (method 3-P2b-b2). The urban map was created by interpolation of the measured PM_{10} concentrations from the urban and suburban background stations by ordinary kriging (method 2-b2). The areas and stations where the limit value (LV) of 40 µg.m^{-3} is exceeded are coloured red and purple.

The mean interpolation uncertainty of the rural map, expressed by the RMSE from the cross-validation, is 4.6 µg.m^{-3}, i.e. about 23 % of the average of the values measured at all rural background stations. The mean uncertainty of the urban map is 5.5 µg.m^{-3}, i.e. about 21 %

Countries with interpolation based on additional data only: AL, BA, BG, CS, GR, HR, IS, MK, RO. Country with poor data coverage and therefore excluded from the mapping: TR.

Map A2. Combined rural and urban concentration map of PM_{10} – 36th maximum daily average value, year 2004. Units: µg.m^{-3}.

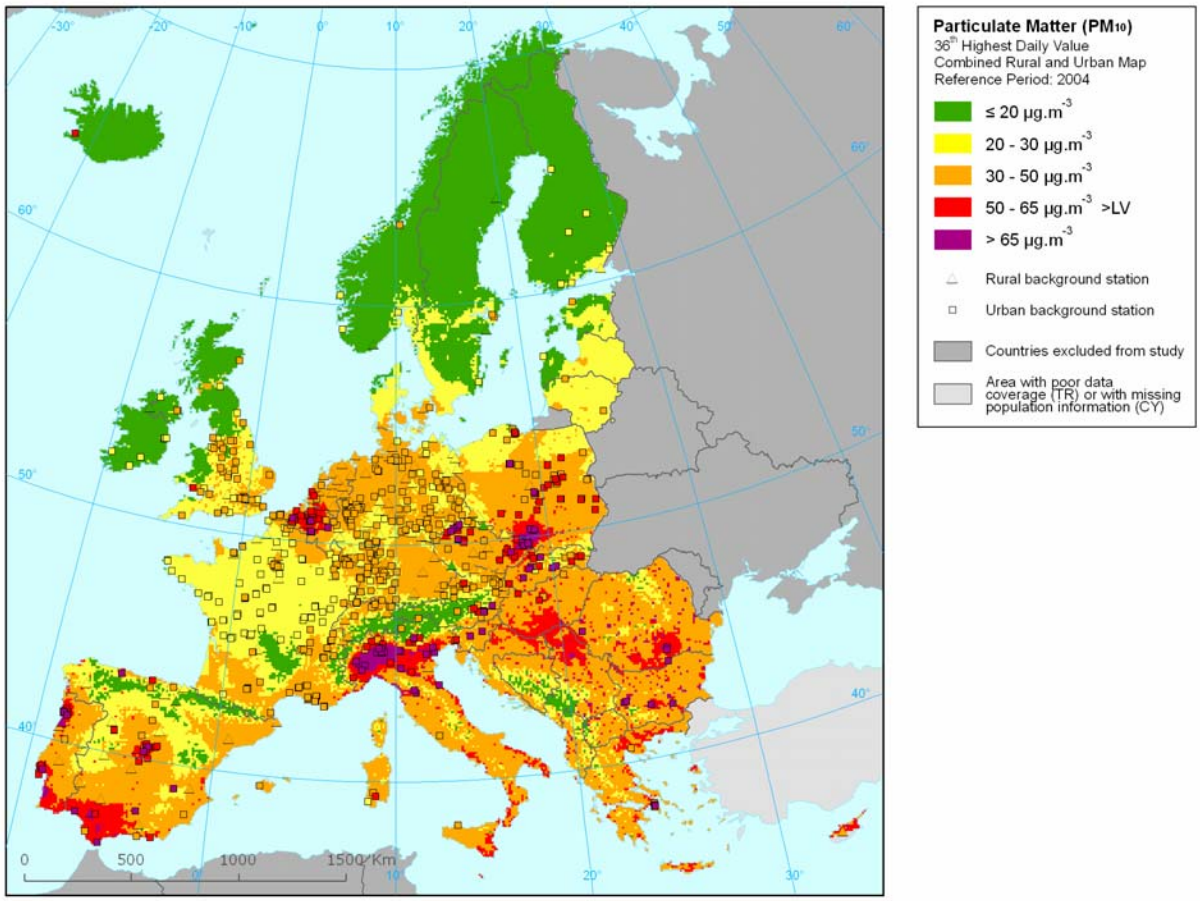

The map was created by combining the rural and urban maps using the population density field and criteria given in Section 3.3 and the introduction to this Annex). The rural map was created by combining the measured PM_{10} concentrations from the rural background stations with supplementary data (EMEP model output, altitude field, surface solar radiation, wind speed), using linear regression followed by interpolation of residuals by ordinary kriging (method 3-P2b-b2). The urban map was created by interpolation of the measured PM_{10} concentrations from the urban and suburban background stations by ordinary kriging (method 2-b2). The areas and stations where the limit value (LV) of 50 µg.m^{-3} is exceeded are coloured red and purple.

The mean interpolation uncertainty of the rural map, expressed by the RMSE from the cross-validation, 8.1 µg.m^{-3}, i.e. about 24 %, for the 36th maximum daily mean value. The mean uncertainty of the urban map is 9.7 µg.m^{-3}, i.e. about 22 %, for the 36th maximum daily mean.

Countries with interpolation based on additional data only: AL, BA, BG, CS, GR, HR, IS, MK, RO. Country with poor data coverage and therefore excluded: TR.

Map A3. Combined rural and urban concentration map of ozone – SOMO35, year 2004. Units: µg.m^{-3}.days.

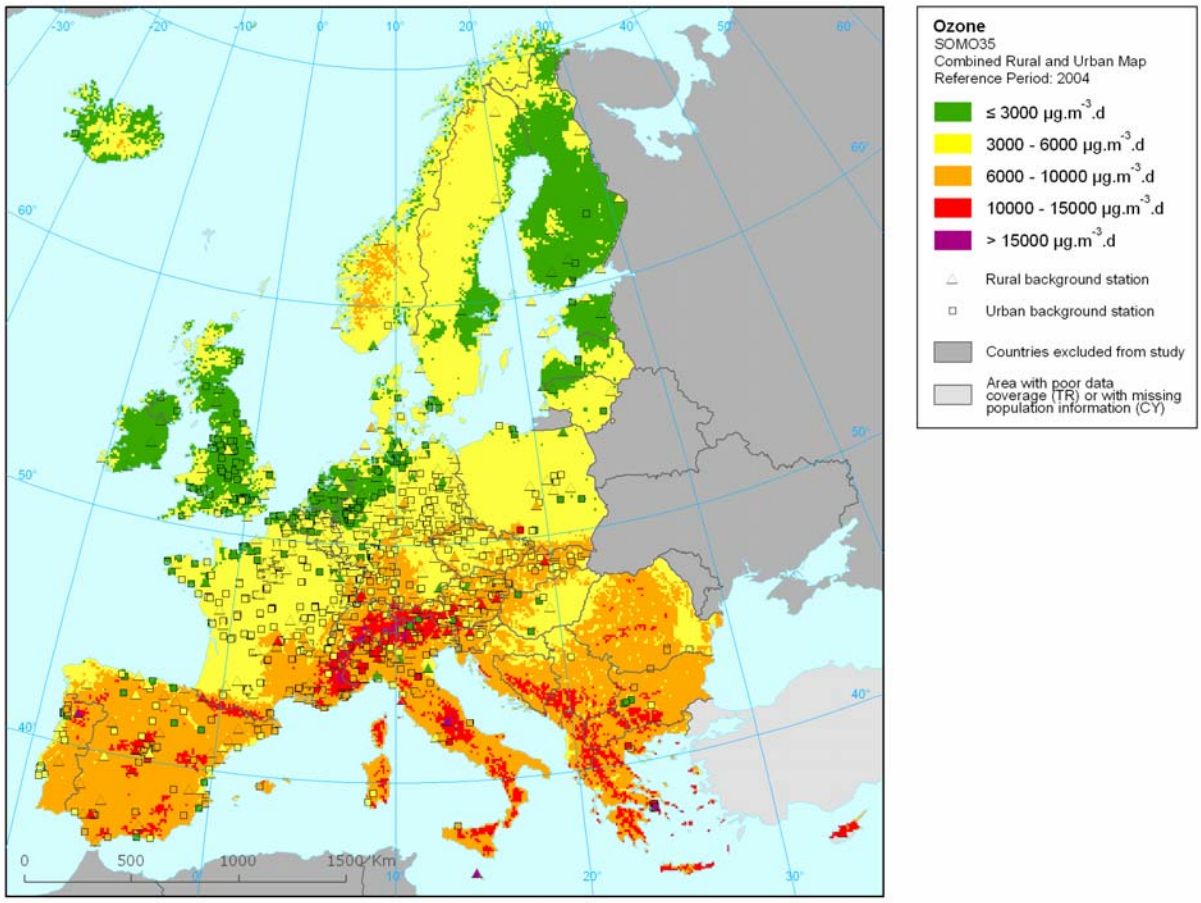

The SOMO35-map was created by the combination of rural and urban maps using the population density field (Section 3.3 and the introduction to this Annex). The rural map of the SOMO35 was created by combining the measured data from the rural background stations with supplementary data (EMEP model output, altitude field, surface solar radiation), using linear regression followed by interpolation of the residuals by ordinary kriging (method 3-O.2c-b2). The urban map of SOMO35 was created by interpolation of measured data from the urban and suburban background stations by ordinary kriging (method 2-b2).

The mean interpolation uncertainty of the rural map, expressed by the RMSE from the cross–validation, is 1865 µg.m^{-3}.days, i.e. about 33 % of the average of SOMO35 values measured at all rural background stations. The mean uncertainty of the urban map is 1411 µg.m^{-3}.days, i.e. about 33 % of the average of measured SOMO35 values at the urban/suburban stations. The differences in the relative values of uncertainties between the SOMO35 and the 26th highest daily maximum 8-hour value (see Map A4) can be explained by larger variability of SOMO35 across the measuring stations.

Countries with interpolation based on additional data only: AL, BA, BG, CS, GR, HR, IS, MK, RO. Country with poor data coverage and therefore excluded from the mapping: TR.

Map A4. Combined rural and urban concentration map of ozone – 26th highest daily maximum 8-hour value, year 2004. Units: µg.m^{-3}.

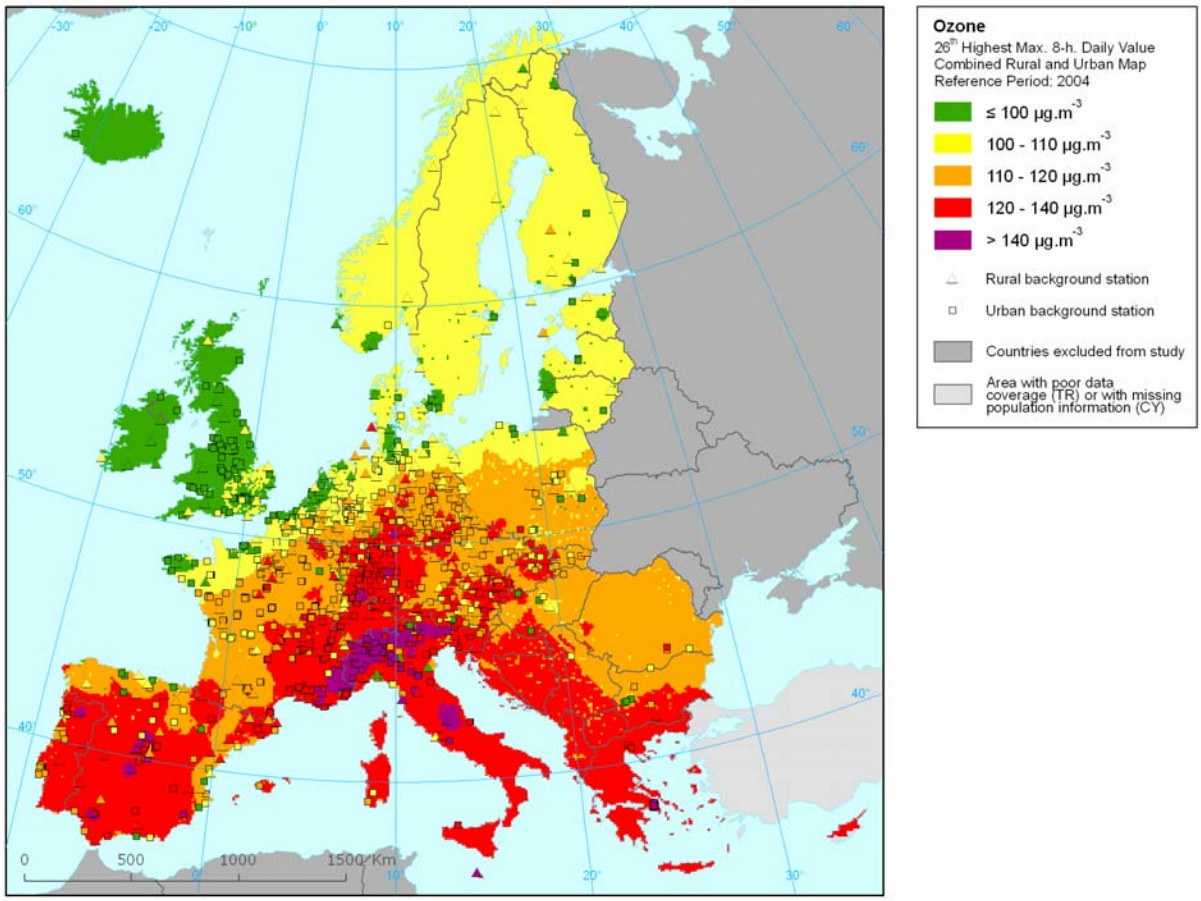

The map is created by the combination of rural and urban maps using the population density field (Section 3.3 and the introduction to this Annex). The rural map of the 26th highest daily maximum 8-hour value was created by the interpolation of the measured values from the rural background stations, using ordinary cokriging with altitude (method 2-c2). The urban map was created by interpolation of measured urban and suburban background data by using the same method, i.e. ordinary cokriging with altitude (method 2-c2).

The mean interpolation uncertainty of the rural map, expressed by the RMSE from the cross-validation, is 10.7 µg.m^{-3}, i.e. about 9 %, for the 26th highest daily maximum 8-hour value. The mean uncertainty of the urban map is 9.1 µg.m^{-3}, i.e. about 8 %, for the 26th highest daily maximum 8-hour value.

Countries with interpolation based on additional data only: AL, BA, BG, CS, GR, HR, IS, MK, RO. Country with poor data coverage and therefore excluded from the mapping: TR.

Map A5. Rural concentration map of ozone – AOT40 for crops, year 2004. Units: µg.m^{-3}.hours.

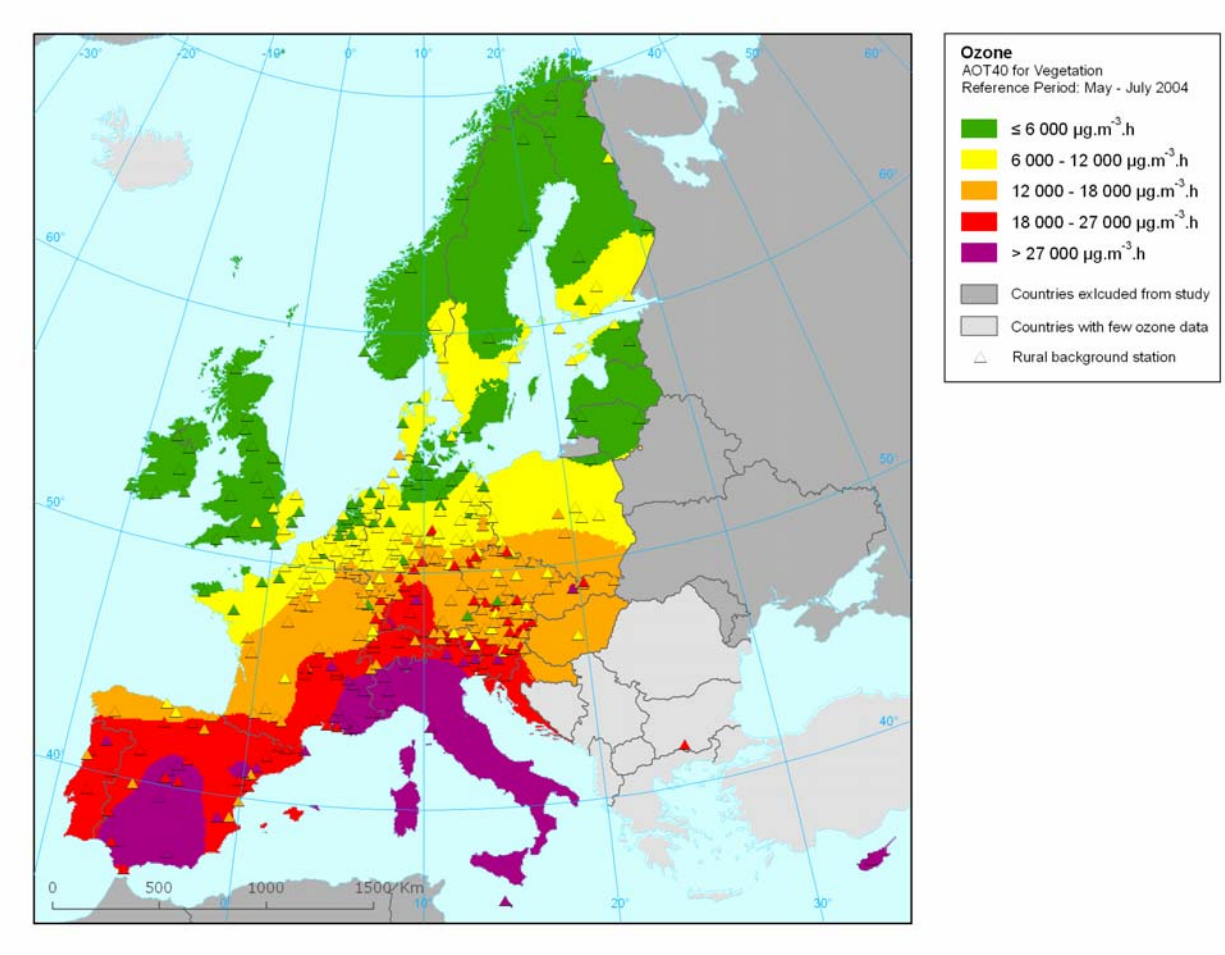

The map of the vegetation-related indicator AOT40 for crops has been created for rural areas only on the basis of rural measuring stations by means of ordinary cokriging, using altitude as supplementary information (method 2-c2). The Balkan region was excluded from the mapping calculations due to its poor measurement station coverage. This map is also used in EEA Core Set Indicator 005 (CSI 005, 2006) on rural areas indicators and the forthcoming EEA air pollution report.

The mean interpolation uncertainty of the map of AOT40 for crops, expressed by the RMSE from the cross-validation, is 5129 µg.m^{-3}.hours, i.e. about 36 % of the average of AOT40 values measured at all stations.

Countries with few ozone data and therefore excluded from the mapping calculations: AL, BA, BG, CS, GR, IS, MK, RO, TR.

Map A6. Rural concentration map of ozone – AOT40 for forests, year 2004. Units: µg.m^{-3}.hours.

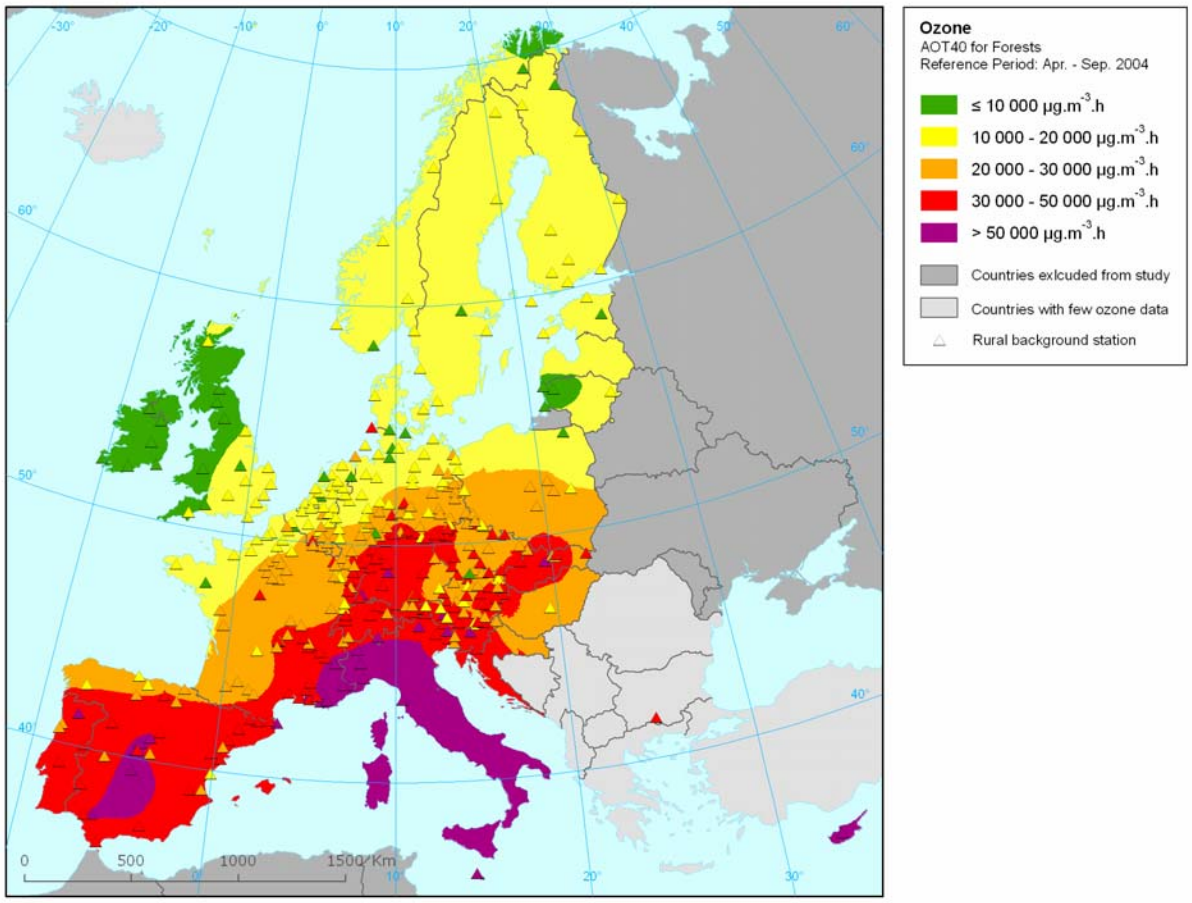

The map of the vegetation-related indicator AOT40 for forests has been created for rural areas only on the basis of rural measuring stations by means of ordinary cokriging, using altitude as supplementary information (method 2-c2). The Balkan region was excluded from the mapping calculations due to its poor measurement station coverage.

The mean interpolation uncertainty of the map of AOT40 for forests, expressed by the RMSE from the cross-validation, is 9004 µg.m^{-3}.hours, i.e. about 33 % of the average of AOT40 values measured at all stations.

Countries with few ozone data and therefore excluded from the mapping calculations: AL, BA, BG, CS, GR, IS, MK, RO, TR.

Map A7. Rural concentration map of NO_x - annual average, year 2004. Units: µg.m^{-3}.

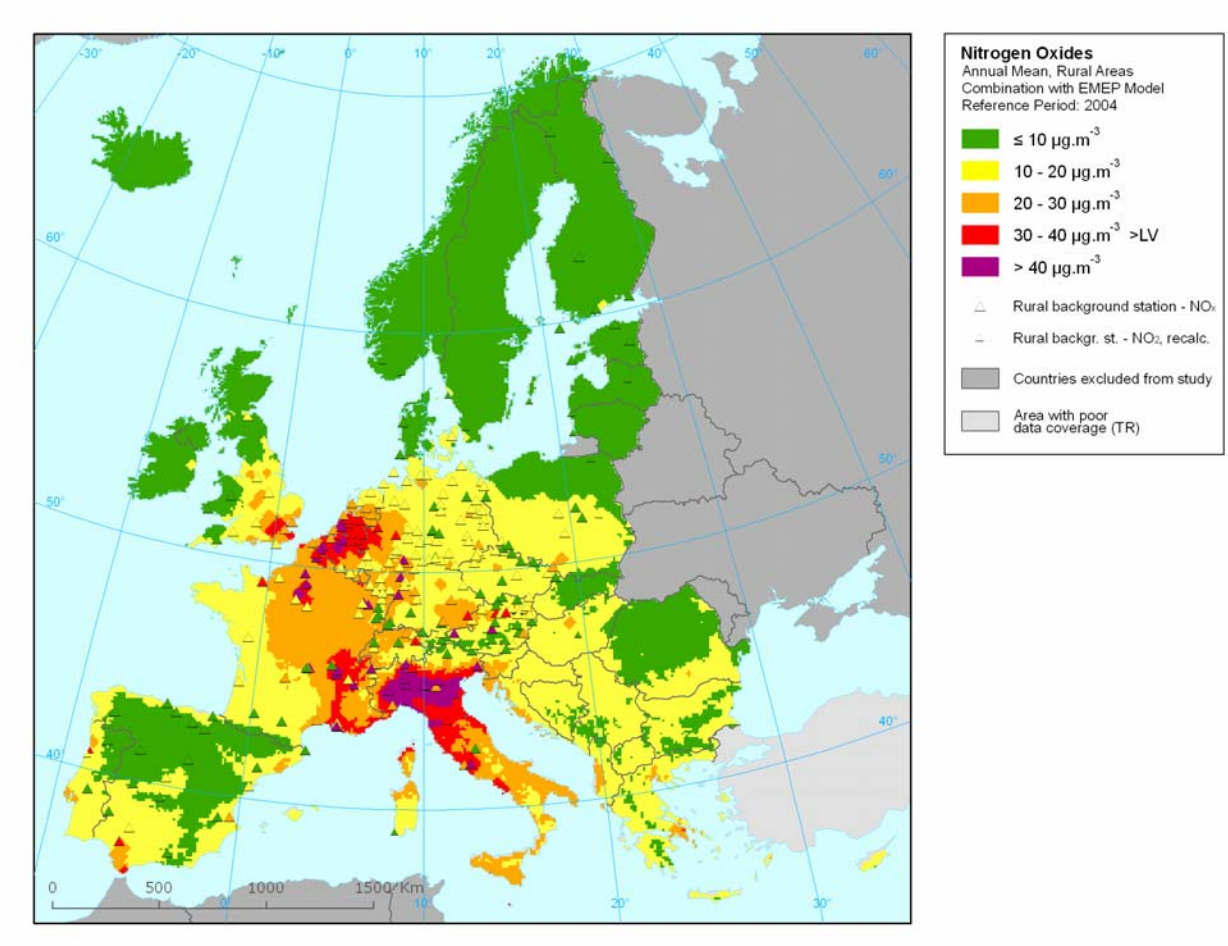

The rural NO_x map was created by combining all the measurement-based data with supplementary data (EMEP model output, altitude field), using interpolation ordinary kriging of the residuals of the linear regression (method 3-N.2-b2). Measurement were used from rural background stations which reported either NO_x or NO + NO_2 monitoring data, with inclusion of an additional 23 rural background stations for which the NO_x concentrations were estimated from the available NO_2 measurements (Section 5.4.3).

The mean interpolation uncertainty of this map expressed in the RMSE from the cross-validation is 10.7 µg.m^{-3}, i.e. about 58 % of the average of the values measured at all rural stations.

Countries with interpolation based on additional data only: AL, BA, BG, CS, CY, GR, HR, IS, MK, RO. Country with poor data coverage and therefore excluded from the mapping: TR.

Map A8. Rural concentration map of SO_2 - annual average, year 2004. Units: µg.m^{-3}.

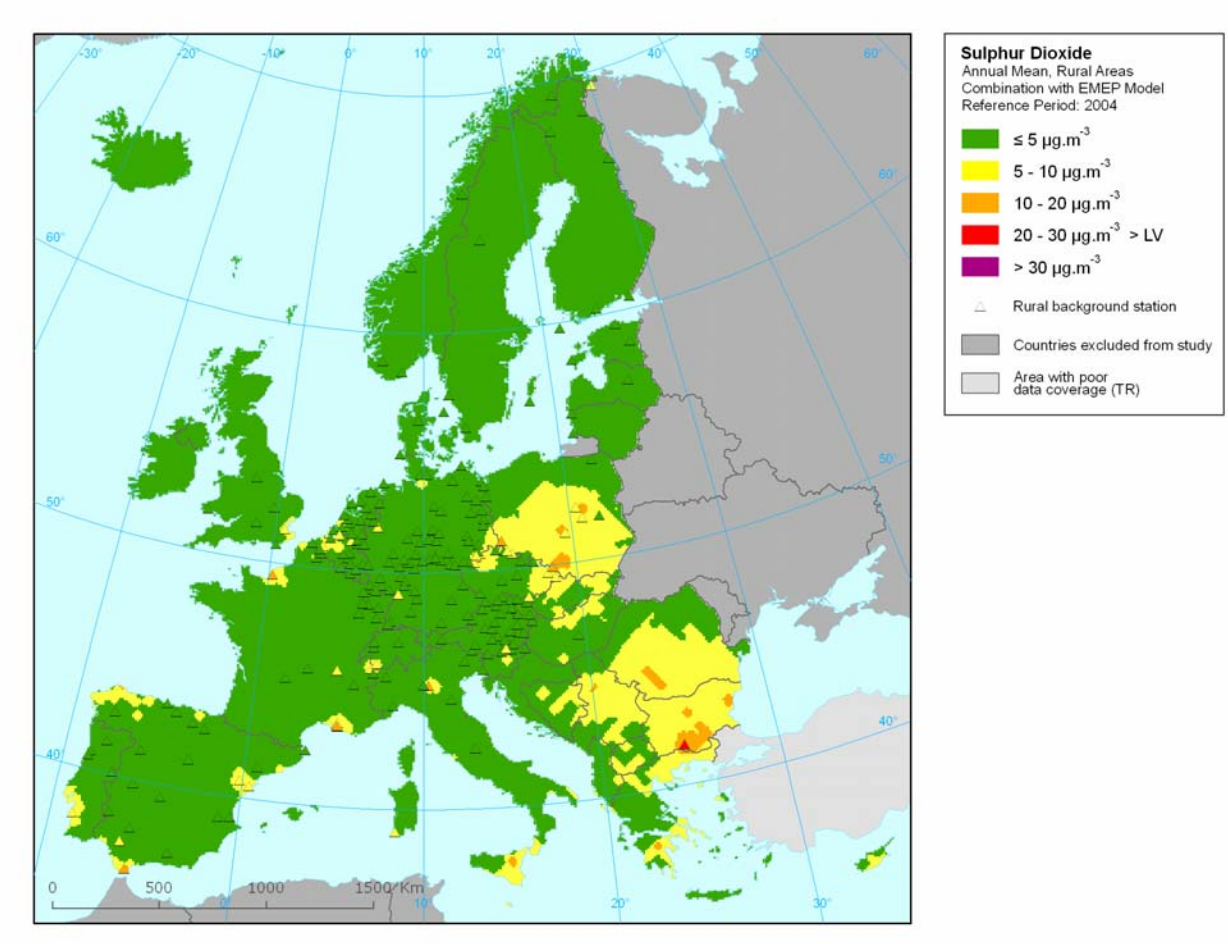

The rural SO_2 map was prepared by combining measurement data with the EMEP model output using linear regression, followed by interpolation of the residuals by ordinary kriging (method 3-S.1-b2).

The mean interpolation uncertainty of this map expressed in cross validation RMSE is 2.0 µg.m^{-3}, i.e. about 60 % of the average of the values measured at all rural stations.

Countries with interpolation based on additional data only: AL, BA, CS, CY, GR, HR, IS, MK, RO.

Country with poor data coverage and therefore excluded from the mapping: TR.

Map A9. Population density map of Europe at 100 m x 100 m grid resolution.

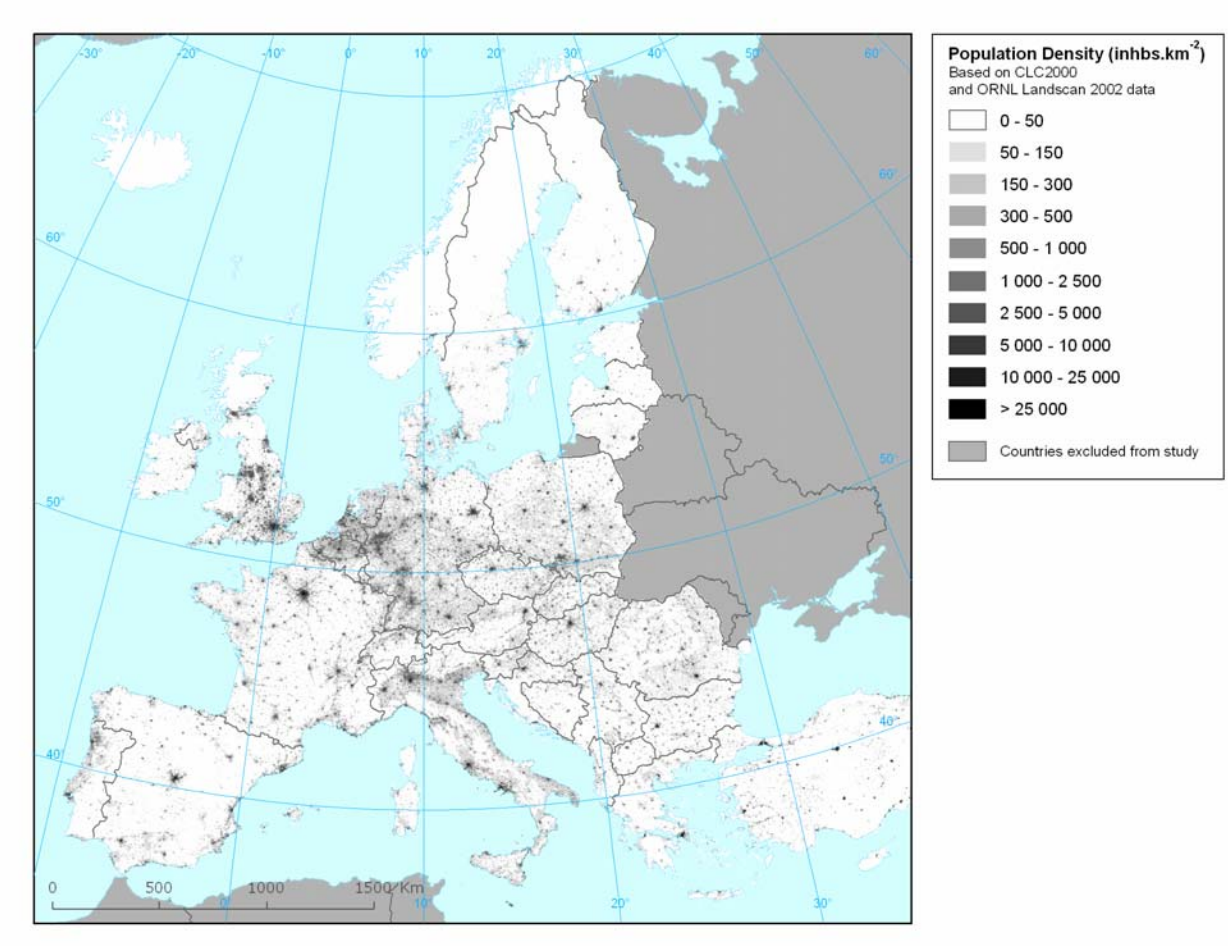

The population density redistribution map done by JRC on basis of the CLC2000 database, with ORNL LandScan 2002 data for the countries lacking in the JRC database: AD, AL, BA, CH, CS, CY, IS, MK, NO and TR.

Map A10. Combined rural and urban concentration map of PM_{10} – annual average, year 2004. Spatial interpolated concentration field overlaid with the population density grid. Units: µg.m^{-3}.

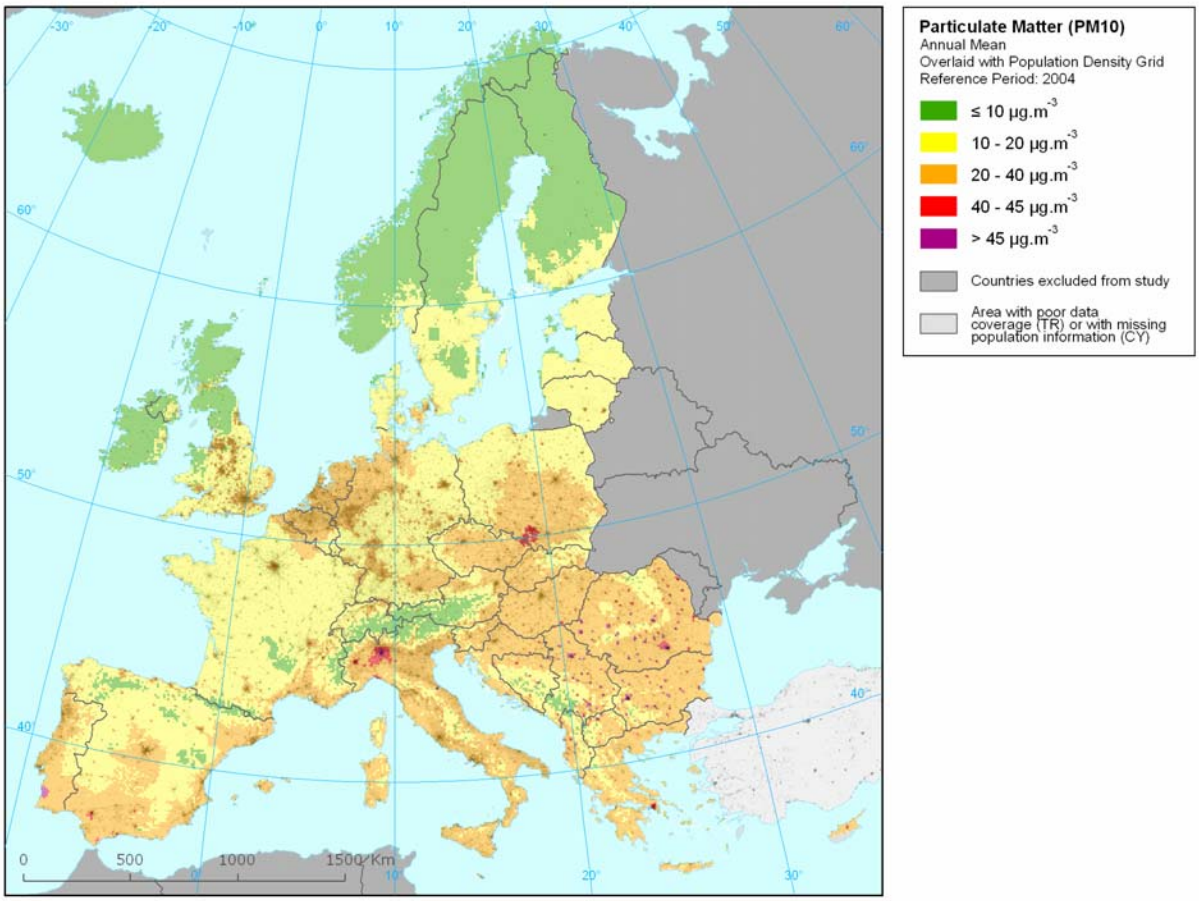

This map is the result of the overlay of Map A1 with a transparency of Map A9 on top. The map shows the spatial match of relative elevated PM_{10} concentrations at the more densely populated and urbanized areas even at those areas without measurements. One can visually conclude that large cities and more populated areas show higher concentration fields than the more rural areas, as expected.

The combined concentration map is created by merging the rural map (method 3-P2a-b2: combination of measured values with EMEP model, altitude, surface solar radiation and wind speed, using linear regression and ordinary kriging of residuals) and the urban map (method 2-b2, i.e. ordinary kriging).

Countries with interpolation based on additional data only: AL, BA, BG, CS, GR, HR, IS, MK, RO.

Country with poor data coverage and therefore excluded from the mapping: TR.

Map A11. Combined rural and urban concentration map of PM_{10} – 36th maximum daily average value, year 2004. Spatial interpolated concentration field overlaid with the population density grid. Units: µg.m^{-3}.

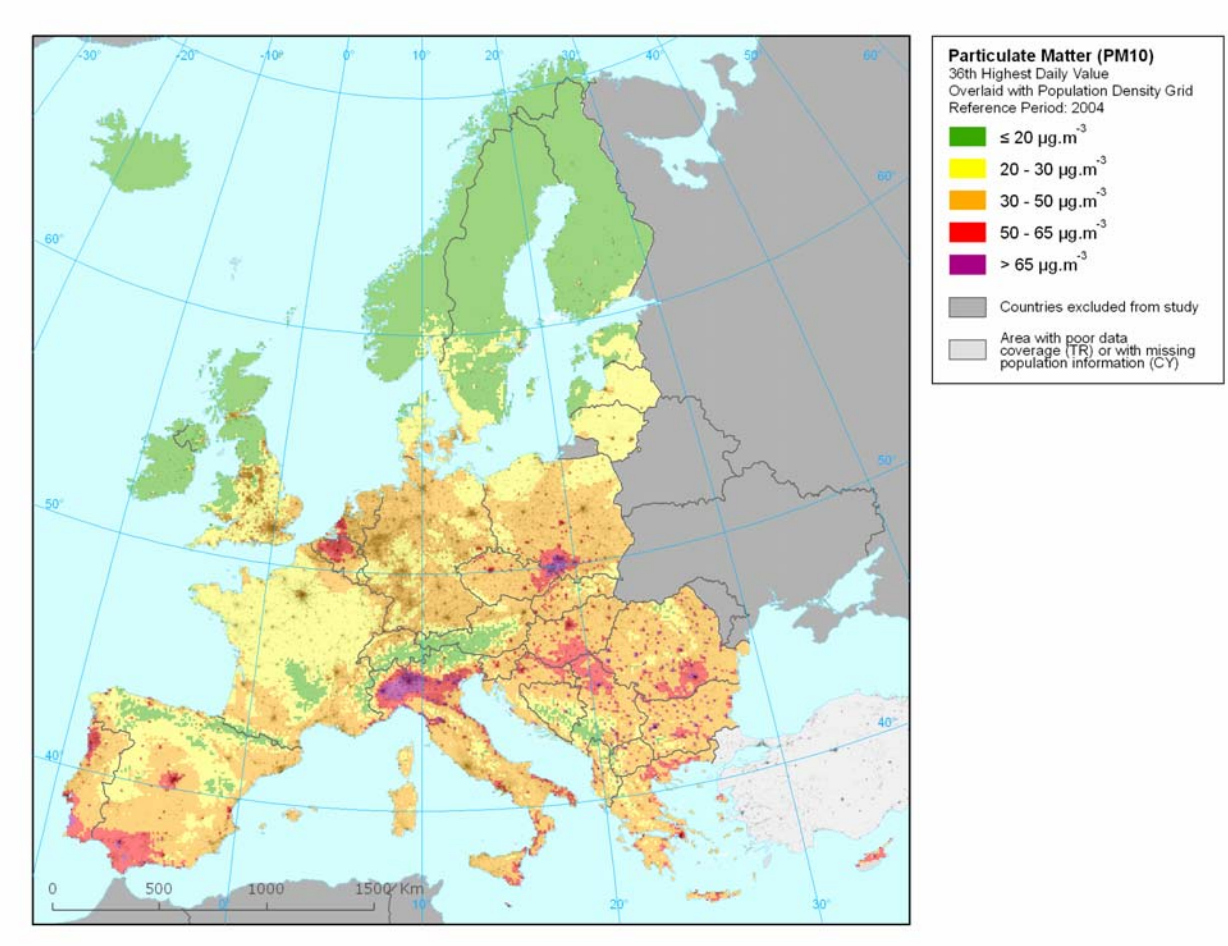

This map is the result of the overlay of Map A2 with a transparency of Map A9 on top. The map shows the spatial match of relative elevated PM_{10} concentrations at the more densely populated and urbanized areas even at those areas without measurements. One can visually conclude that large cities and more populated areas show higher concentration fields than the more rural areas, as expected. This effect is stronger when using the 36th maximum daily mean value compared to the annual average of Map A10.

The combined concentration map is created by merging the rural map (method 3-P2a-b2: combination of measured values with EMEP model, altitude, surface solar radiation and wind speed, using linear regression and ordinary kriging of residuals) and the urban map (method 2-b2, i.e. ordinary kriging). Countries with interpolation based on additional data only: AL, BA, BG, CS, GR, HR, IS, MK, RO.

Country with poor data coverage and therefore excluded from the mapping: TR.

Map A12. Combined rural and urban concentration map of ozone – SOMO35, year 2004. Spatial interpolated concentration field overlaid with the population density grid. Units: µg.m^{-3}.days.

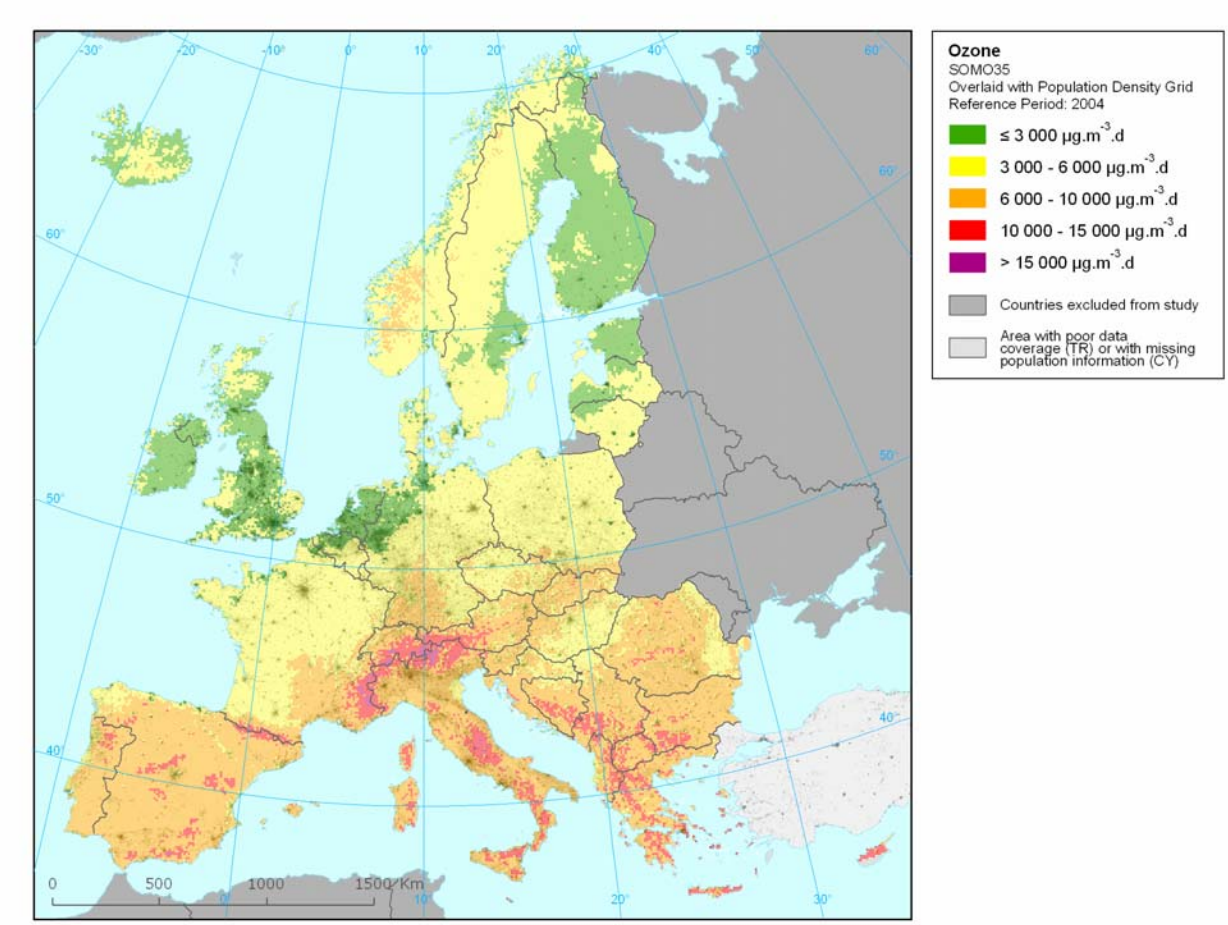

This map is the result of the overlay of Map A3 with a transparency of Map A9 on top. The map shows the spatial match of relative low ozone concentrations at the more densely populated and urbanized areas even at those areas without measurements. One can visually conclude that for ozone the concentrations are generally lower in large cities, as expected.

The combined map is created by merging the rural map (method 3-O2c-b2: combination of measured values with EMEP model, altitude and surface solar radiation, using linear regression and ordinary kriging of residuals) and the urban map (method 2-b2, i.e. ordinary kriging).

Countries with interpolation based on additional data only: AL, BA, BG, CS, GR, HR, IS, MK, RO.

Country with poor data coverage and therefore excluded from the mapping: TR.

Map A13. Agriculture areas (all types) at risk / damage map – ozone, AOT40 for crops, year 2004. Spatial interpolated concentration field map combined with land cover grid of CLC2000. Units: µg.m^{-3}.hours.

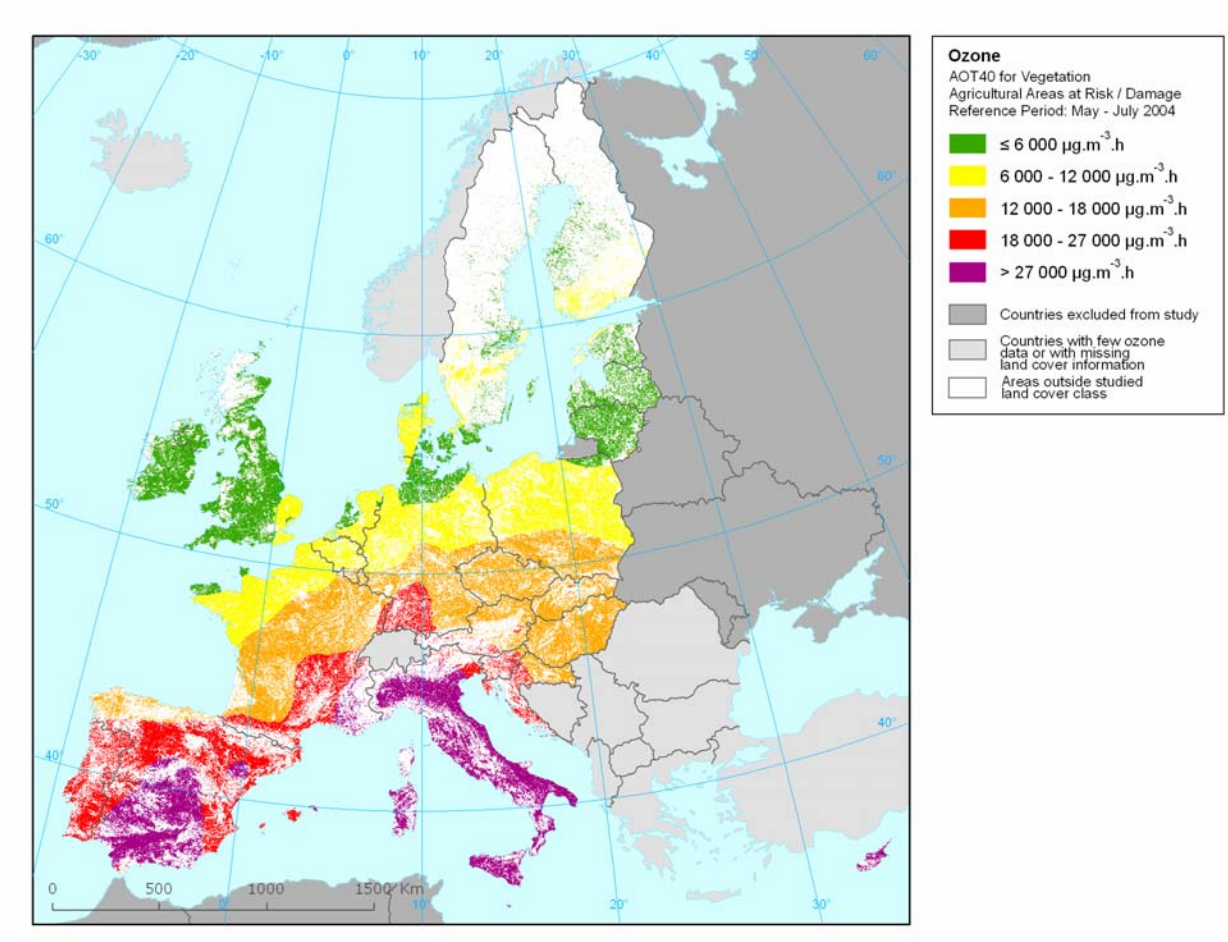

The map shows the accumulated concentrations of AOT40 for crops at areas with CLC2000 level-1 class *2 Agriculture areas*. The spatial concentration field is done by ordinary cokriging, using altitude (method 2-c2).

Countries with missing land cover information are excluded from the mapping: CH, CS, IS, NO, TR.

Countries with few ozone data and therefore excluded from the mapping calculations: AL, BA, BG, GR, MK, RO.

Map A14. Arable land at risk / damage map – ozone, AOT40 for crops, year 2004. Spatial interpolated concentration field map combined with land cover grid of CLC2000. Units: µg.m^{-3}.hours.

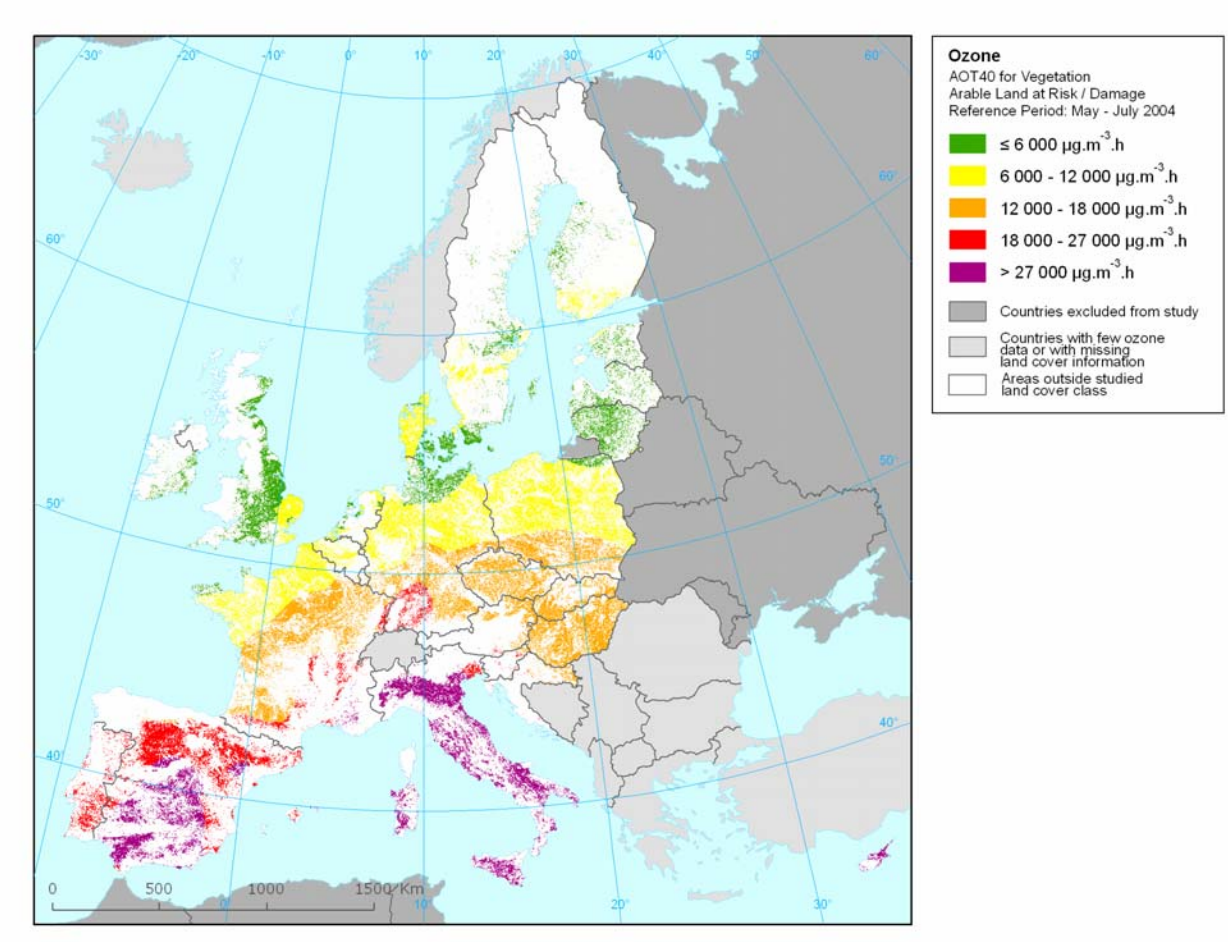

The map shows the accumulated concentrations of AOT40 for crops at areas with CLC2000 level-2 class *2.1 Arable land*, a subclass of Agricultural areas. The spatial concentration field is done by ordinary cokriging, using altitude (method 2-c2).

Countries with missing land cover information are excluded from the mapping: CH, CS, IS, NO, TR.

Countries with few ozone data and therefore excluded from the mapping calculations: AL, BA, BG, GR, MK, RO.

Map A15. Permanent crops at risk / damage map – ozone, AOT40 for crops, year 2004. Spatial interpolated concentration field map combined with land cover grid of CLC2000. Units: µg.m^{-3}.hours.

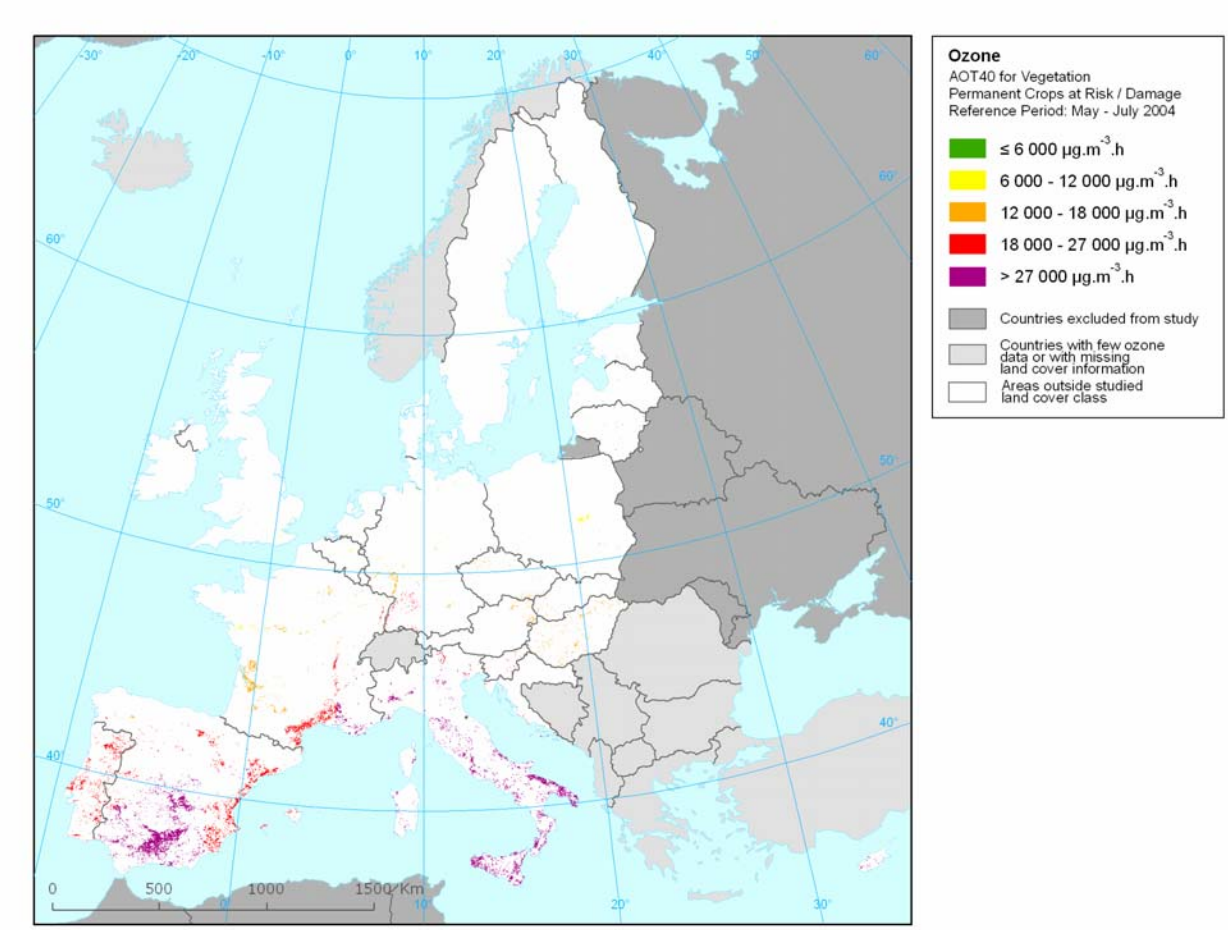

The map shows the accumulated concentration values of AOT40 for crops at areas with CLC2000 level-2 class *2.2 Permanent crops*, a subclass of Agricultural areas. The spatial concentration field is done by ordinary cokriging, using altitude (method 2-c2).

Countries with missing land cover information are excluded from the mapping: CH, CS, IS, NO, TR.

Countries with few ozone data and therefore excluded from the mapping calculations: AL, BA, BG, GR, MK, RO.

Map A16. Pastures at risk / damage map – ozone, AOT40 for crops, year 2004. Spatial interpolated concentration field map combined with land cover grid of CLC2000. Units: µg.m^{-3}.hours.

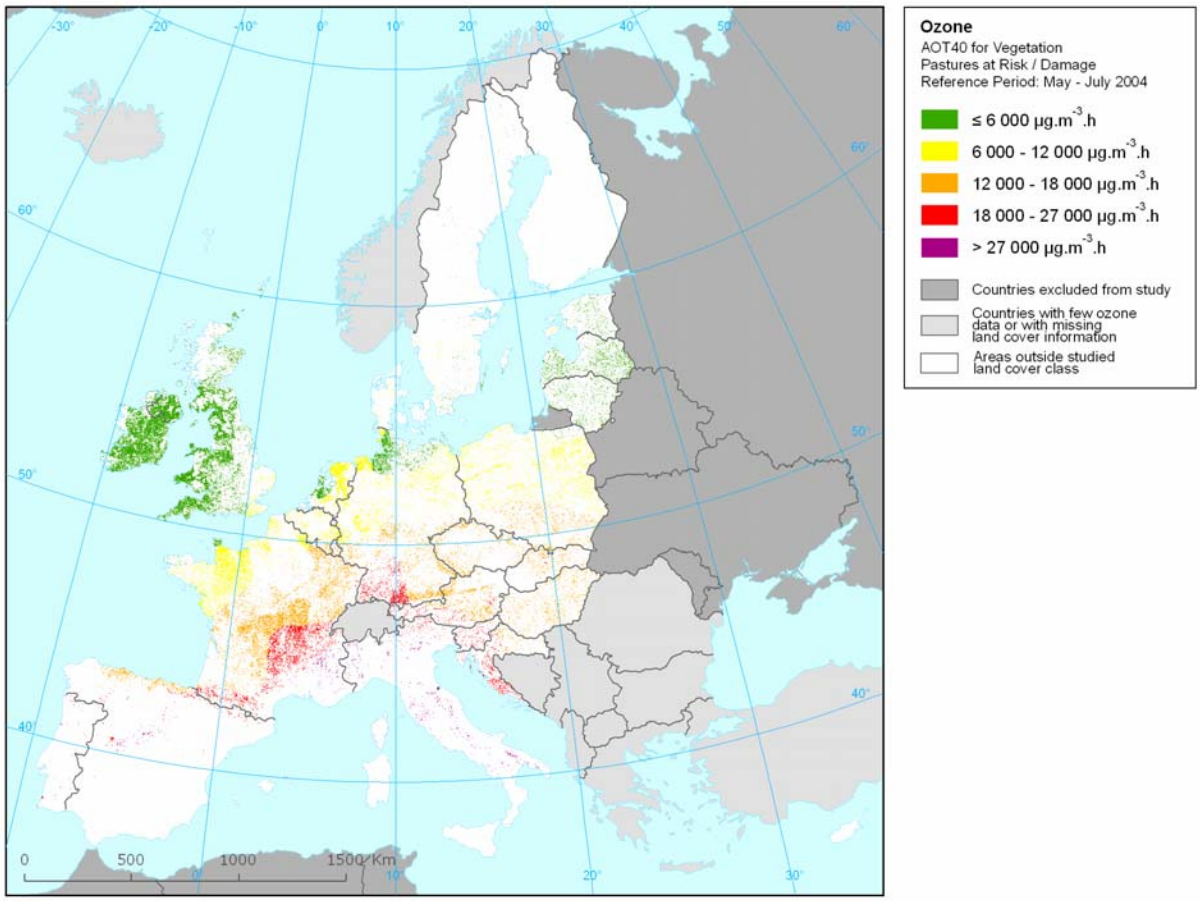

The map shows the concentration values of AOT40 for crops at areas with CLC2000 level-2 class *2.3 Pastures*, a subclass of Agricultural areas. The spatial concentration field is done by ordinary cokriging, using altitude (method 2-c2).

Countries with missing land cover information are excluded from the mapping: CH, CS, IS, NO, TR.

Countries with few ozone data and therefore excluded from the mapping calculations: AL, BA, BG, GR, MK, RO.

Map A17. Heterogeneous agricultural areas at risk / damage map – ozone, AOT40 for crops, year 2004. Spatial interpolated concentration field map combined with land cover grid of CLC2000. Units: µg.m^{-3}.hours.

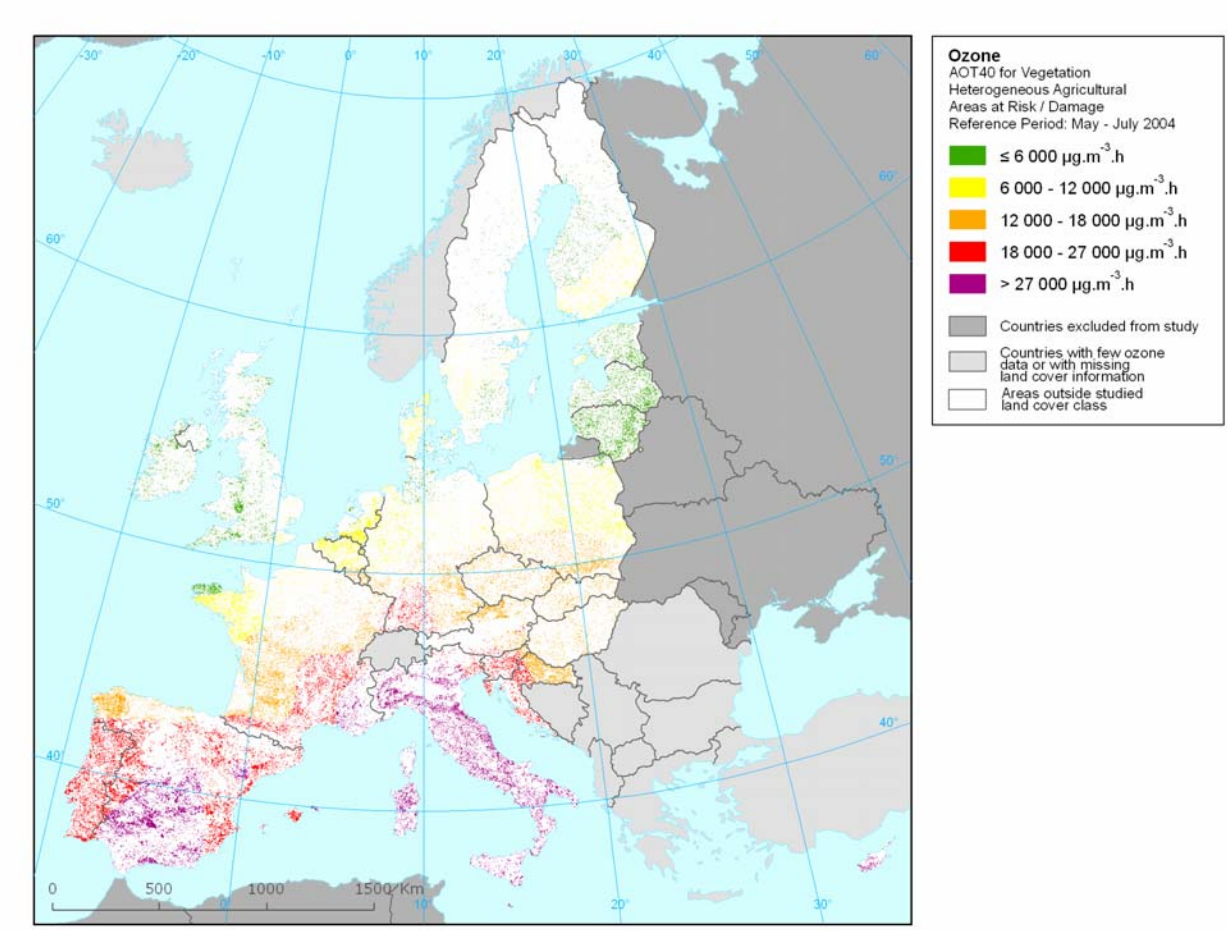

The map shows the accumulated concentrations of AOT40 for crops at areas with CLC2000 level-2 class *2.4 Heterogeneous agricultural areas*, a subclass of Agricultural areas. The spatial concentration field is done by ordinary cokriging, using altitude (method 2-c2).

Countries with missing land cover information are excluded from the mapping: CH, CS, IS, NO, TR.

Countries with few ozone data and therefore excluded from the mapping calculations: AL, BA, BG, GR, MK, RO.

Map A18. Forests (all types) at risk / damage map – ozone, AOT40 for forests, year 2004. Spatial interpolated concentration field map combined with land cover grid of CLC2000. Units: µg.m^{-3}.hours.

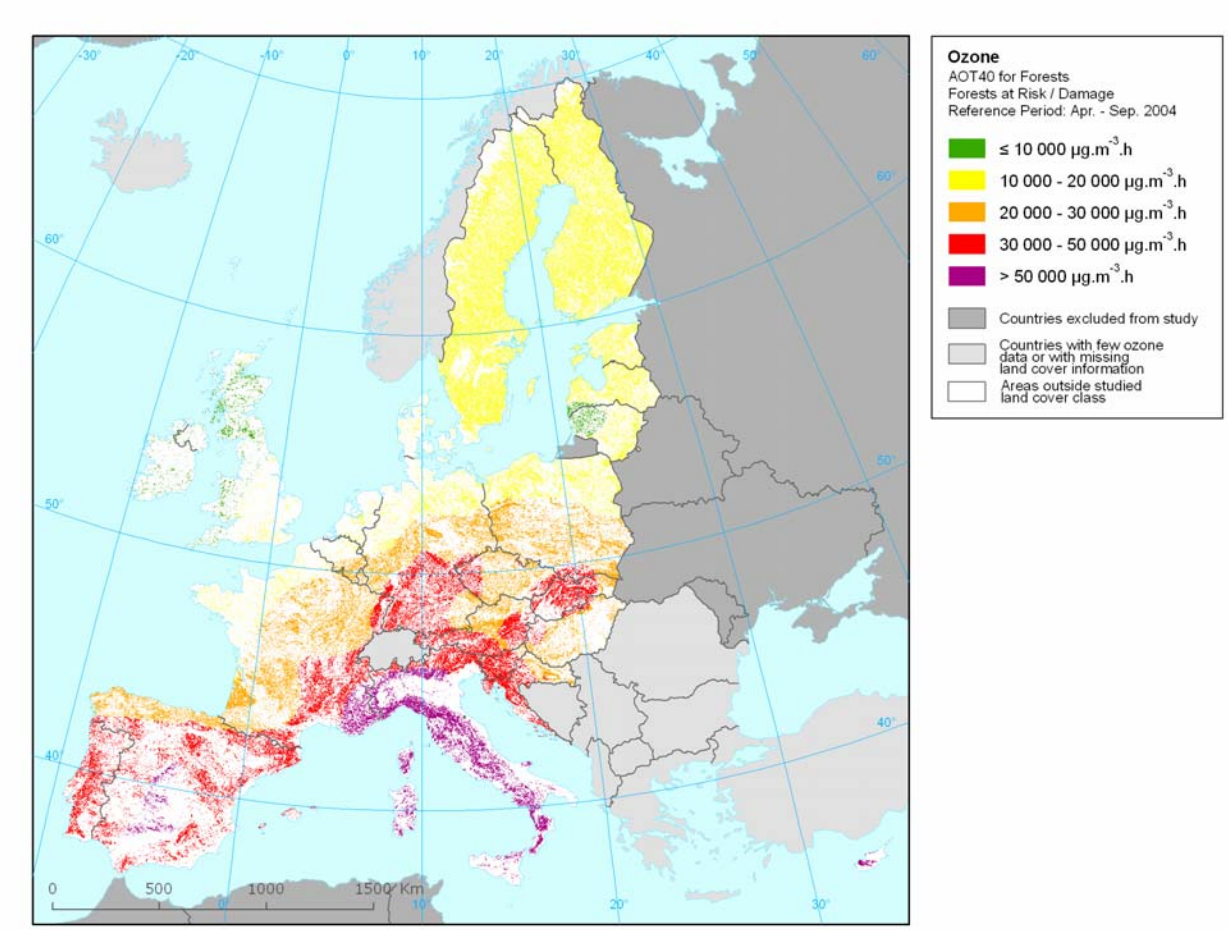

The map shows the accumulated concentrations of AOT40 for forests at areas with CLC2000 level-2 class 3.1 *Forests*. The spatial concentration field is done by ordinary cokriging, using altitude (method 2-c2).

Countries with missing land cover information are excluded from the mapping: CH, CS, IS, NO, TR.

Countries with few ozone data and therefore excluded from the mapping calculations: AL, BA, BG, GR, MK, RO.

Map A19. Broad-leaved forests at risk / damage map – ozone, AOT40 for forests, year 2004. Spatial interpolated concentration field map combined with land cover grid of CLC2000. Units: µg.m^{-3}.hours.

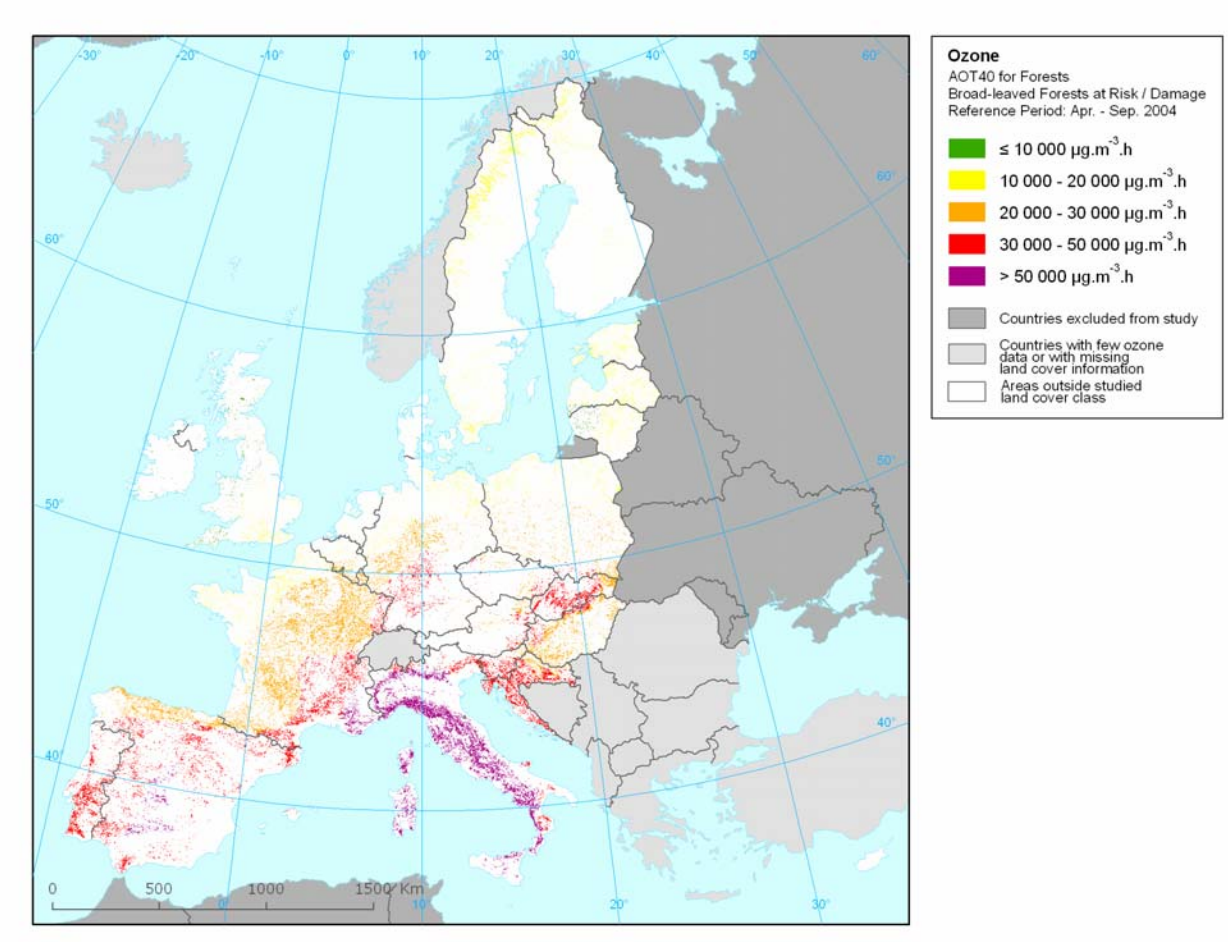

The map shows the concentration values of AOT40 for forests at areas with CLC2000 level-3 class *3.1.1 Broad-leaved forest*s, a sub-class of Forests. The spatial concentration field is done by ordinary cokriging, using altitude (method 2-c2).

Countries with missing land cover information are excluded from the mapping: CH, CS, IS, NO, TR.

Countries with few ozone data and therefore excluded from the mapping calculations: AL, BA, BG, GR, MK, RO.

Map A20. Coniferous forests at risk / damage map – ozone, AOT40 for forests, year 2004. Spatial interpolated concentration field map combined with land cover grid of CLC2000. Units: µg.m^{-3}.hours.

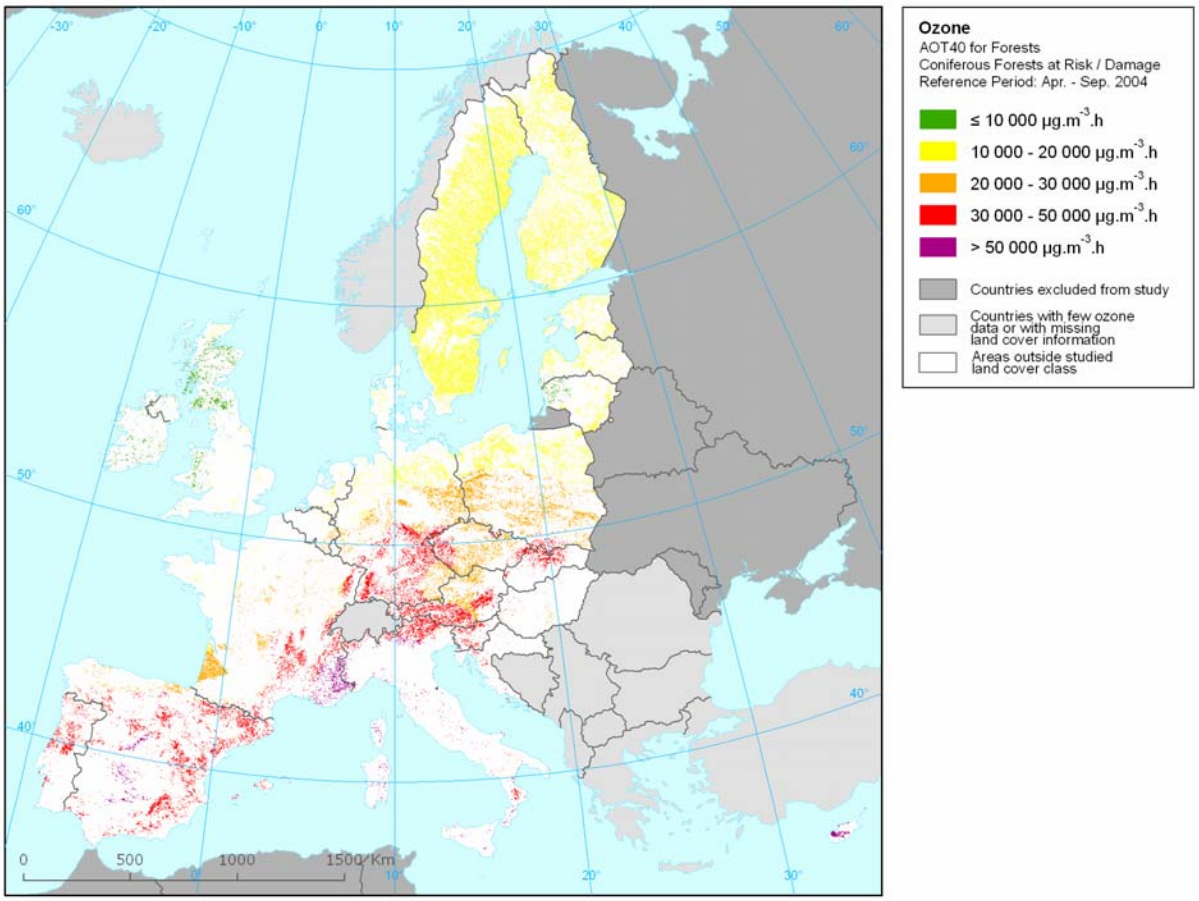

The map shows the concentration values of AOT40 for forests at areas with CLC2000 level-3 class *3.1.2 Coniferous forests*, a sub-class of Forests. The spatial concentration field is done by ordinary cokriging, using altitude (method 2-c2).

Countries with missing land cover information are excluded from the mapping: CH, CS, IS, NO, TR.

Countries with few ozone data and therefore excluded from the mapping calculations: AL, BA, BG, GR, MK, RO.

Map A21. Mixed forests at risk / damage map – ozone, AOT40 for forests, year 2004. Spatial interpolated concentration field map combined with land cover grid of CLC2000. Units: µg.m^{-3}.hours.

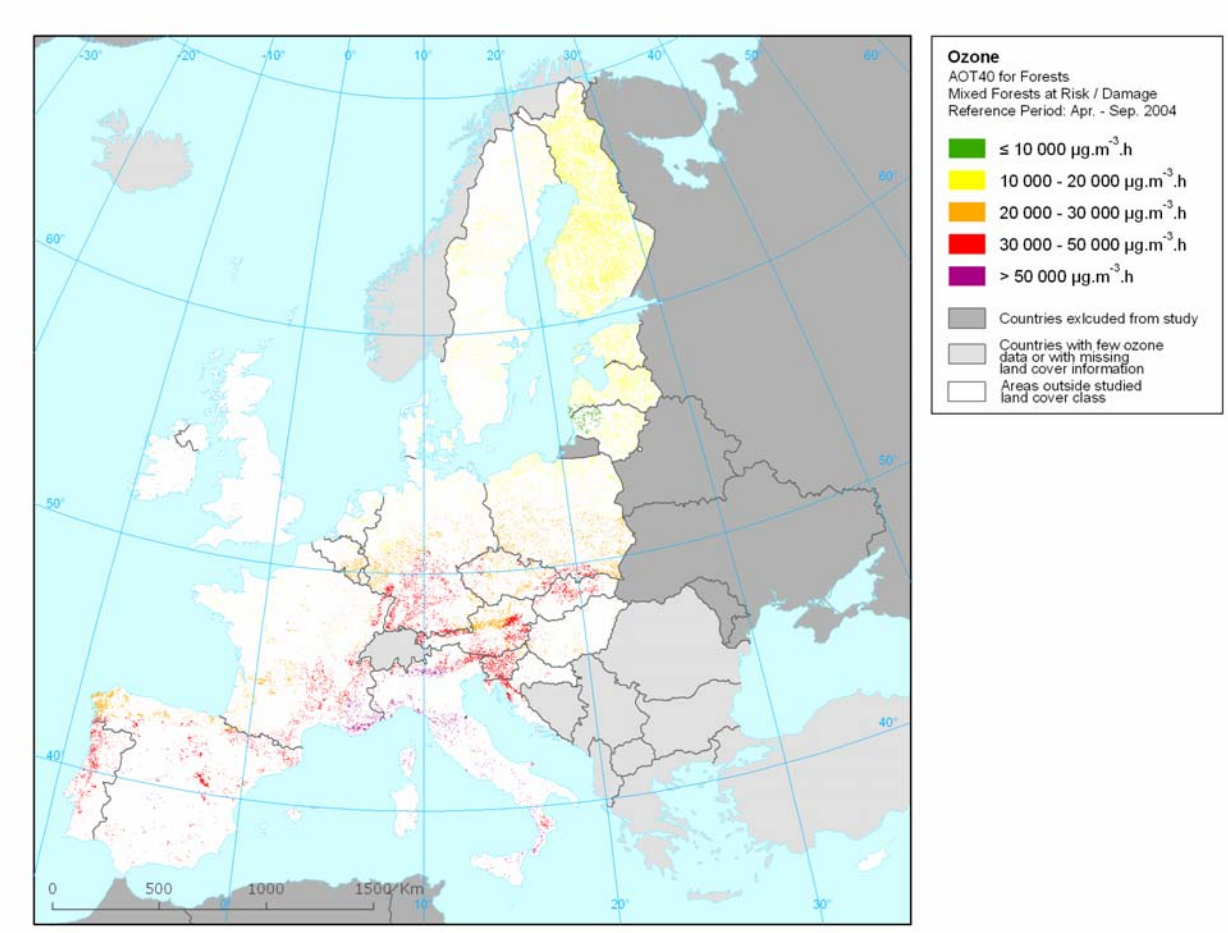

The map shows the concentration values of AOT40 for forests at areas with CLC2000 level-3 class *3.1.3 Mixed forests*, a sub-class of Forests. The spatial concentration field is done by ordinary cokriging, using altitude (method 2-c2).

Countries with missing land cover information are excluded from the mapping: CH, CS, IS, NO, TR.

Countries with few ozone data and therefore excluded from the mapping calculations: AL, BA, BG, GR, MK, RO.

Table A1. Population exposure and population weighted concentration – PM_{10}, annual average, year 2004.

Country	Population (thousands) 2004	2004 *Percent [%]*					Population-weighted concentration [µg.m^{-3}]
		< 10 µg.m^{-3}	10 - 20 µg.m^{-3}	20 - 40 µg.m^{-3}	40 - 45 µg.m^{-3}	> 45 µg.m^{-3}	
Austria	8171	7.9	22.0	70.1	0.0	0.0	21.3
Belgium	10400	0.0	2.3	97.7	0.0	0.0	31.1
Bulgaria	7780	0.0	2.9	55.5	10.9	30.6	38.0
Croatia	4540	0.1	1.6	92.3	6.1	0.0	31.9
Czech Republic	10229	0.0	8.8	84.3	6.9	0.0	28.5
Denmark	5414	1.6	68.2	30.3	0.0	0.0	17.7
Estonia	1335	3.5	96.5	0.0	0.0	0.0	14.2
Finland	5235	34.5	65.5	0.0	0.0	0.0	11.5
France	60257	0.4	59.3	40.2	0.0	0.0	19.5
Germany	82645	0.0	27.4	72.6	0.0	0.0	21.5
Greece	11098	0.0	2.4	63.5	34.1	0.0	34.6
Hungary	10124	0.0	0.1	97.9	2.0	0.0	30.0
Ireland	4080	52.2	47.8	0.0	0.0	0.0	10.4
Italy	58033	0.9	3.1	83.6	8.0	4.4	32.5
Latvia	2318	1.4	94.9	3.7	0.0	0.0	16.3
Liechtenstein	34	0.0	0.0	100.0	0.0	0.0	21.3
Lithuania	3443	0.0	60.0	40.0	0.0	0.0	17.9
Luxembourg	459	0.0	84.9	15.1	0.0	0.0	18.1
Malta	400	0.0	0.0	100.0	0.0	0.0	35.7
Netherlands	16226	0.0	0.0	100.0	0.0	0.0	28.9
Poland	38559	0.0	22.1	68.4	9.5	0.0	26.3
Portugal	10441	0.0	7.5	92.2	0.1	0.2	29.9
Romania	21790	0.1	3.6	57.6	15.3	23.4	35.3
San Marino	28	0.0	0.0	100.0	0.0	0.0	28.0
Slovakia	5401	0.1	12.5	87.4	0.0	0.0	27.0
Slovenia	1967	0.2	9.5	90.3	0.0	0.0	27.9
Spain	42646	0.5	13.3	83.5	2.7	0.0	28.4
Sweden	9008	19.1	77.0	3.9	0.0	0.0	13.2
United Kingdom	59479	4.0	27.7	68.4	0.0	0.0	20.2
Total	**491543**	**1.9**	**24.1**	**68.0**	**3.8**	**2.2**	**25.2**

Countries with missing JRC population density information are excluded from calculations in this paper: AD, AL, BA, CH, CS, CY, IS, MK, NO, TR.

Table A2. Population exposure and population weighted concentration – ozone, SOMO35, year 2004.

Country	Population (thousands) 2004	2004 *Percent [%]*					Population-weighted country concentration [µg.m^{-3}.d]
		< 3000	3000 - 6000	6000 - 10000	10000 - 15000	> 15000	
		µg.m^{-3}.d	µg.m^{-3}.d	µg.m^{-3}.d	µg.m^{-3}.d	µg.m^{-3}.d	
Austria	8171	0.0	60.2	36.8	3.0	0.0	6103
Belgium	10400	63.2	36.8	0.0	0.0	0.0	2934
Bulgaria	7780	0.0	35.8	61.7	2.5	0.0	6433
Croatia	4540	0.0	67.7	32.0	0.4	0.0	5723
Czech Republic	10229	0.0	90.7	9.3	0.0	0.0	5149
Denmark	5414	44.6	55.4	0.0	0.0	0.0	2972
Estonia	1335	94.0	6.0	0.0	0.0	0.0	2226
Finland	5235	95.6	4.4	0.0	0.0	0.0	2456
France	60257	8.1	76.0	15.4	0.5	0.0	4495
Germany	82645	29.9	62.1	8.0	0.0	0.0	4011
Greece	11098	0.0	3.8	85.9	10.3	0.0	8590
Hungary	10124	1.2	83.5	15.2	0.0	0.0	4999
Ireland	4080	98.2	1.8	0.0	0.0	0.0	1558
Italy	58033	0.0	6.5	87.6	5.8	0.1	7850
Latvia	2318	72.5	27.5	0.0	0.0	0.0	2302
Liechtenstein	34	0.0	0.0	100.0	0.0	0.0	6387
Lithuania	3443	51.3	48.7	0.0	0.0	0.0	2869
Luxembourg	459	0.0	100.0	0.0	0.0	0.0	4101
Malta	400	0.0	0.0	100.0	0.0	0.0	7504
Netherlands	16226	96.1	3.9	0.0	0.0	0.0	2354
Poland	38559	5.7	91.5	2.7	0.0	0.0	4245
Portugal	10441	0.0	61.9	36.4	1.8	0.0	5586
Romania	21790	0.0	56.9	42.8	0.3	0.0	5974
San Marino	28	0.0	0.0	100.0	0.0	0.0	7535
Slovakia	5401	0.0	55.3	44.6	0.1	0.0	5903
Slovenia	1967	0.0	45.3	54.3	0.4	0.0	6307
Spain	42646	4.8	48.0	46.5	0.8	0.0	6037
Sweden	9008	53.7	46.3	0.0	0.0	0.0	2840
United Kingdom	59479	94.7	5.3	0.0	0.0	0.0	1712
Total	**491543**	**26.9**	**46.6**	**25.4**	**1.2**	**0.0**	**4659**

Countries with missing JRC population density information are excluded from calculations in this paper: AD, AL, BA, CH, CS, CY, IS, MK, NO, TR.

Table A3. Exposure of agriculture areas (all types) – ozone, AOT40 for crops, year 2004.

Country	Total agricultural area [km^2]	2004 *Percent [%]*				
		0-6 mg.m^{-3}.h	6-12 mg.m^{-3}.h	12-18 mg.m^{-3}.h	18-27 mg.m^{-3}.h	>27 µg.m^{-3}.h
Andorra	14	0.0	0.0	0.0	100.0	0.0
Austria	27451	0.0	0.0	88.3	11.7	0.0
Belgium	17654	0.0	90.7	9.3	0.0	0.0
Croatia	24168	0.0	0.0	52.4	47.6	0.0
Cyprus	4269	0.0	0.0	0.0	0.0	100.0
Czech Republic	45570	0.0	0.0	100.0	0.0	0.0
Denmark	32232	34.4	65.6	0.0	0.0	0.0
Estonia	14680	86.6	13.4	0.0	0.0	0.0
Finland	28893	46.6	53.4	0.0	0.0	0.0
France	328400	2.0	29.3	48.3	17.6	2.8
Germany	213603	13.8	45.9	29.7	10.6	0.0
Hungary	63108	0.0	0.0	100.0	0.0	0.0
Ireland	46396	100.0	0.0	0.0	0.0	0.0
Italy	155704	0.0	0.0	0.0	3.6	96.4
Latvia	28324	100.0	0.0	0.0	0.0	0.0
Liechtenstein	41	0.0	0.0	0.0	100.0	0.0
Lithuania	40002	98.7	1.3	0.0	0.0	0.0
Luxembourg	1410	0.0	4.1	95.9	0.0	0.0
Malta	122	0.0	0.0	0.0	0.0	100.0
Monaco	0	0.0	0.0	0.0	0.0	100.0
Netherlands	24920	20.4	79.6	0.0	0.0	0.0
Poland	200543	3.0	68.6	28.4	0.0	0.0
Portugal	42553	0.0	0.0	0.0	99.9	0.1
San Marino	43	0.0	0.0	0.0	0.0	100.0
Slovakia	24383	0.0	0.0	99.2	0.8	0.0
Slovenia	7133	0.0	0.0	21.9	78.1	0.0
Spain	252381	0.0	0.0	6.5	48.3	45.2
Sweden	38640	57.4	42.6	0.0	0.0	0.0
United Kingdom	141878	88.5	11.5	0.0	0.0	0.0
Total	**1804510**	**19.2**	**24.4**	**26.0**	**15.0**	**15.4**

Countries with few ozone data are excluded from the calculations in this paper: AL, BA, BG, GR, MK, RO. Countries with missing land cover information are also excluded from the calculations: CH, CS, IS, NO, TR.

Table A4. Exposure of arable land – ozone, AOT40 for crops, year 2004.

Country	Total arable land [km^2]	2004 *Percent [%]*				
		0-6 mg.m^{-3}.h	6-12 mg.m^{-3}.h	12-18 mg.m^{-3}.h	18-27 mg.m^{-3}.h	>27 mg.m^{-3}.h
Andorra	0	0.0	0.0	0.0	0.0	0.0
Austria	10973	0.0	0.0	96.4	3.6	0.0
Belgium	6723	0.0	97.5	2.5	0.0	0.0
Croatia	3803	0.0	0.0	92.3	7.7	0.0
Cyprus	2576	0.0	0.0	0.0	0.0	100.0
Czech Republic	32593	0.0	0.0	100.0	0.0	0.0
Denmark	27194	36.5	63.5	0.0	0.0	0.0
Estonia	6605	88.3	11.7	0.0	0.0	0.0
Finland	15950	43.2	56.8	0.0	0.0	0.0
France	153577	1.4	35.5	53.6	8.4	1.0
Germany	136576	13.1	52.3	27.6	7.1	0.0
Hungary	49574	0.0	0.0	100.0	0.0	0.0
Ireland	5385	100.0	0.0	0.0	0.0	0.0
Italy	82877	0.0	0.0	0.0	3.3	96.7
Latvia	9124	100.0	0.0	0.0	0.0	0.0
Liechtenstein	19	0.0	0.0	0.0	100.0	0.0
Lithuania	22265	98.9	1.1	0.0	0.0	0.0
Luxembourg	227	0.0	3.7	96.3	0.0	0.0
Malta	0	0.0	0.0	0.0	0.0	100.0
Monaco	0	0.0	0.0	0.0	0.0	0.0
Netherlands	7618	26.3	73.7	0.0	0.0	0.0
Poland	139563	3.1	69.8	27.1	0.0	0.0
Portugal	13333	0.0	0.0	0.0	100.0	0.0
San Marino	21	0.0	0.0	0.0	0.0	100.0
Slovakia	16682	0.0	0.0	99.5	0.5	0.0
Slovenia	1137	0.0	0.0	50.8	49.2	0.0
Spain	122584	0.0	0.0	0.6	54.2	45.2
Sweden	29594	57.1	42.9	0.0	0.0	0.0
United Kingdom	60549	77.8	22.2	0.0	0.0	0.0
Total	**957119**	**15.6**	**30.2**	**28.5**	**11.1**	**14.6**

Countries with few ozone data are excluded from the calculations in this paper: AL, BA, BG, GR, MK, RO. Countries with missing land cover information are also excluded from the calculations: CH, CS, IS, NO, TR.

Table A5. Exposure of permanent crops – ozone, AOT40 for crops, year 2004.

Country	Total permanent crops [km^2]	2004 *Percent [%]*				
		0-6 mg.m^{-3}.h	6-12 mg.m^{-3}.h	12-18 mg.m^{-3}.h	18-27 mg.m^{-3}.h	>27 mg.m^{-3}.h
Andorra	0	0.0	0.0	0.0	0.0	0.0
Austria	703	0.0	0.0	100.0	0.0	0.0
Belgium	83	0.0	99.7	0.3	0.0	0.0
Croatia	501	0.0	0.0	18.4	81.4	0.2
Cyprus	326	0.0	0.0	0.0	0.0	100.0
Czech Republic	444	0.0	0.0	100.0	0.0	0.0
Denmark	2	66.7	33.3	0.0	0.0	0.0
Estonia	21	93.9	6.1	0.0	0.0	0.0
Finland	0	0.0	0.0	0.0	0.0	0.0
France	14190	0.0	4.2	35.9	46.1	13.8
Germany	2536	6.1	8.5	51.6	33.8	0.0
Hungary	2031	0.0	0.0	100.0	0.0	0.0
Ireland	0	0.0	0.0	0.0	0.0	0.0
Italy	21632	0.0	0.0	0.0	1.8	98.2
Latvia	29	100.0	0.0	0.0	0.0	0.0
Liechtenstein	0	0.0	0.0	0.0	0.0	0.0
Lithuania	98	99.7	0.3	0.0	0.0	0.0
Luxembourg	14	0.0	0.0	100.0	0.0	0.0
Malta	1	0.0	0.0	0.0	0.0	100.0
Monaco	0	0.0	0.0	0.0	0.0	0.0
Netherlands	77	22.4	77.6	0.0	0.0	0.0
Poland	893	0.0	85.4	14.6	0.0	0.0
Portugal	6021	0.0	0.0	0.0	99.9	0.1
San Marino	0	0.0	0.0	0.0	0.0	0.0
Slovakia	361	0.0	0.0	99.9	0.1	0.0
Slovenia	194	0.0	0.0	32.7	67.3	0.0
Spain	34389	0.0	0.0	0.4	34.6	65.0
Sweden	16	76.6	23.4	0.0	0.0	0.0
United Kingdom	177	26.1	73.9	0.0	0.0	0.0
Total	**84737**	**0.4**	**2.2**	**12.2**	**31.0**	**54.2**

Countries with few ozone data are excluded from the calculations in this paper: AL, BA, BG, GR, MK, RO. Countries with missing land cover information are also excluded from the calculations: CH, CS, IS, NO, TR.

Table A6. Exposure of pastures – ozone, AOT40 for crops, year 2004.

Country	Total pastures [km^2]	2004 *Percent [%]*				
		0-6 mg.m^{-3}.h	6-12 mg.m^{-3}.h	12-18 mg.m^{-3}.h	18-27 mg.m^{-3}.h	>27 mg.m^{-3}.h
Andorra	9	0.0	0.0	0.0	100.0	0.0
Austria	8253	0.0	0.0	76.5	23.5	0.0
Belgium	3558	0.0	82.3	17.7	0.0	0.0
Croatia	4716	0.0	0.0	23.1	76.9	0.0
Cyprus	9	0.0	0.0	0.0	0.0	100.0
Czech Republic	5290	0.0	0.0	100.0	0.0	0.0
Denmark	523	12.9	87.1	0.0	0.0	0.0
Estonia	2557	85.7	14.3	0.0	0.0	0.0
Finland	25	80.6	19.4	0.0	0.0	0.0
France	87343	1.3	30.0	45.4	22.1	1.2
Germany	45187	20.5	38.9	26.2	14.3	0.0
Hungary	6605	0.0	0.0	100.0	0.0	0.0
Ireland	35775	100.0	0.0	0.0	0.0	0.0
Italy	4465	0.0	0.0	0.0	19.2	80.8
Latvia	9262	100.0	0.0	0.0	0.0	0.0
Liechtenstein	14	0.0	0.0	0.0	100.0	0.0
Lithuania	4278	96.6	3.4	0.0	0.0	0.0
Luxembourg	303	0.0	0.7	99.3	0.0	0.0
Malta	0	0.0	0.0	0.0	0.0	0.0
Monaco	0	0.0	0.0	0.0	0.0	0.0
Netherlands	10629	25.2	74.8	0.0	0.0	0.0
Poland	27405	1.4	74.2	24.4	0.0	0.0
Portugal	352	0.0	0.0	0.0	100.0	0.0
San Marino	0	0.0	0.0	0.0	0.0	0.0
Slovakia	3026	0.0	0.0	97.1	2.9	0.0
Slovenia	1182	0.0	0.0	9.2	90.8	0.0
Spain	6233	0.0	0.0	66.4	27.1	6.5
Sweden	2434	67.4	32.6	0.0	0.0	0.0
United Kingdom	66521	97.2	2.8	0.0	0.0	0.0
Total	**335949**	**39.1**	**23.4**	**25.5**	**10.5**	**1.5**

Countries with few ozone data are excluded from the calculations in this paper: AL, BA, BG, GR, MK, RO. Countries with missing land cover information are also excluded from the calculations: CH, CS, IS, NO, TR.

Table A7. Exposure of heterogeneous agricultural areas – ozone, AOT40 for crops, year 2004.

Country	Total heterogeneous agricultural area [km^2]	2004 *Percent [%]*				
		0-6 mg.m^{-3}.h	6-12 mg.m^{-3}.h	12-18 mg.m^{-3}.h	18-27 mg.m^{-3}.h	>27 mg.m^{-3}.h
Andorra	5	0.0	0.0	0.0	100.0	0.0
Austria	7523	0.0	0.0	88.2	11.8	0.0
Belgium	7290	0.0	88.5	11.5	0.0	0.0
Croatia	15149	0.0	0.0	52.6	47.4	0.0
Cyprus	1359	0.0	0.0	0.0	0.0	100.0
Czech Republic	7244	0.0	0.0	100.0	0.0	0.0
Denmark	4512	24.0	76.0	0.0	0.0	0.0
Estonia	5497	85.1	14.9	0.0	0.0	0.0
Finland	12919	50.7	49.3	0.0	0.0	0.0
France	73291	4.4	20.2	43.1	26.0	6.3
Germany	29303	7.4	30.2	43.0	19.3	0.0
Hungary	4898	0.0	0.0	100.0	0.0	0.0
Ireland	5237	100.0	0.0	0.0	0.0	0.0
Italy	46730	0.0	0.0	0.0	3.4	96.6
Latvia	9909	100.0	0.0	0.0	0.0	0.0
Liechtenstein	8	0.0	0.0	0.0	100.0	0.0
Lithuania	13361	99.0	1.0	0.0	0.0	0.0
Luxembourg	866	0.0	5.5	94.5	0.0	0.0
Malta	121	0.0	0.0	0.0	0.0	100.0
Monaco	0	0.0	0.0	0.0	0.0	100.0
Netherlands	6596	5.9	94.1	0.0	0.0	0.0
Poland	32682	3.5	58.5	38.0	0.0	0.0
Portugal	22848	0.0	0.0	0.0	99.8	0.2
San Marino	23	0.0	0.0	0.0	0.0	100.0
Slovakia	4314	0.0	0.0	99.2	0.8	0.0
Slovenia	4621	0.0	0.0	17.5	82.5	0.0
Spain	89176	0.0	0.0	12.8	46.9	40.2
Sweden	6596	55.0	45.0	0.0	0.0	0.0
United Kingdom	14631	94.3	5.7	0.0	0.0	0.0
Total	**426706**	**15.2**	**16.4**	**23.8**	**24.1**	**20.4**

Countries with few ozone data are excluded from the calculations in this paper: AL, BA, BG, GR, MK, RO. Countries with missing land cover information are also excluded from the calculations: CH, CS, IS, NO, TR.

Table A8. Exposure of forests (all types) – ozone, AOT40 for forests, year 2004.

Country	Total forests [km^2]	2004 *Percent [%]*				
		0-10 mg.m^{-3}.h	10-20 mg.m^{-3}.h	20-30 mg.m^{-3}.h	30-50 mg.m^{-3}.h	>50 mg.m^{-3}.h
Andorra	61	0.0	0.0	0.0	100.0	0.0
Austria	37598	0.0	0.0	36.9	63.1	0.0
Belgium	6095	0.0	21.8	78.2	0.0	0.0
Croatia	20155	0.0	0.0	27.9	72.1	0.0
Cyprus	1541	0.0	0.0	0.0	0.0	100.0
Czech Republic	25471	0.0	0.0	66.0	34.0	0.0
Denmark	3702	0.0	100.0	0.0	0.0	0.0
Estonia	20781	0.0	100.0	0.0	0.0	0.0
Finland	193300	0.1	99.9	0.0	0.0	0.0
France	144868	0.0	7.5	54.0	29.0	9.5
Germany	103785	0.0	21.5	39.2	39.2	0.0
Hungary	17321	0.0	0.0	74.9	25.1	0.0
Ireland	2908	100.0	0.0	0.0	0.0	0.0
Italy	78801	0.0	0.0	0.0	18.8	81.2
Latvia	26945	6.1	93.9	0.0	0.0	0.0
Liechtenstein	61	0.0	0.0	0.0	100.0	0.0
Lithuania	18671	27.8	72.2	0.0	0.0	0.0
Luxembourg	910	0.0	0.0	100.0	0.0	0.0
Malta	2	0.0	0.0	0.0	0.0	100.0
Monaco	0	0.0	0.0	0.0	0.0	100.0
Netherlands	3105	0.0	100.0	0.0	0.0	0.0
Poland	91776	0.0	43.3	52.2	4.5	0.0
Portugal	24301	0.0	0.0	0.0	100.0	0.0
San Marino	5	0.0	0.0	0.0	0.0	100.0
Slovakia	19270	0.0	0.0	15.4	84.6	0.0
Slovenia	11479	0.0	0.0	4.5	95.5	0.0
Spain	91795	0.0	0.0	22.5	70.3	7.2
Sweden	249898	0.0	100.0	0.0	0.0	0.0
United Kingdom	19693	72.6	27.4	0.0	0.0	0.0
Total	**1214297**	**2.0**	**48.5**	**20.3**	**22.2**	**7.1**

Countries with few ozone data are excluded from the calculations in this paper: AL, BA, BG, GR, MK, RO. Countries with missing land cover information are also excluded from the calculations: CH, CS, IS, NO, TR.

Table A9. Exposure of broad-leaved forests – ozone, AOT40 for forests, year 2004.

Country	Total broad-leaved forests [km^2]	2004 *Percent [%]*				
		0-10 mg.m^{-3}.h	10-20 mg.m^{-3}.h	20-30 mg.m^{-3}.h	30-50 mg.m^{-3}.h	>50 mg.m^{-3}.h
Andorra	0	0.0	0.0	0.0	100.0	0.0
Austria	3415	0.0	0.0	43.9	56.1	0.0
Belgium	2034	0.0	24.8	75.2	0.0	0.0
Croatia	16540	0.0	0.0	33.3	66.7	0.0
Cyprus	6	0.0	0.0	0.0	0.0	100.0
Czech Republic	2558	0.0	0.0	60.4	39.6	0.0
Denmark	680	0.0	100.0	0.0	0.0	0.0
Estonia	4269	0.0	100.0	0.0	0.0	0.0
Finland	7324	2.2	97.8	0.0	0.0	0.0
France	88941	0.0	8.6	63.6	21.8	6.0
Germany	23977	0.0	22.7	48.8	28.6	0.0
Hungary	14776	0.0	0.0	74.7	25.3	0.0
Ireland	294	100.0	0.0	0.0	0.0	0.0
Italy	55194	0.0	0.0	0.0	6.4	93.6
Latvia	5639	9.8	90.2	0.0	0.0	0.0
Liechtenstein	5	0.0	0.0	0.0	100.0	0.0
Lithuania	4142	26.8	73.2	0.0	0.0	0.0
Luxembourg	634	0.0	0.0	100.0	0.0	0.0
Malta	0	0.0	0.0	0.0	0.0	0.0
Monaco	0	0.0	0.0	0.0	0.0	100.0
Netherlands	561	0.0	100.0	0.0	0.0	0.0
Poland	14665	0.0	43.3	52.4	4.4	0.0
Portugal	12169	0.0	0.0	0.0	100.0	0.0
San Marino	5	0.0	0.0	0.0	0.0	100.0
Slovakia	10645	0.0	0.0	25.3	74.7	0.0
Slovenia	4479	0.0	0.0	4.9	95.1	0.0
Spain	37910	0.0	0.0	29.0	61.8	9.2
Sweden	19737	0.0	100.0	0.0	0.0	0.0
United Kingdom	6577	42.8	57.2	0.0	0.0	0.0
Total	**337173**	**1.5**	**19.0**	**33.1**	**28.5**	**17.9**

Countries with few ozone data are excluded from the calculations in this paper: AL, BA, BG, GR, MK, RO. Countries with missing land cover information are also excluded from the calculations: CH, CS, IS, NO, TR.

Table A10. Exposure of coniferous forests – ozone, AOT40 for forests, year 2004.

Country	Total coniferous forests [km^2]	2004 *Percent [%]*				
		0-10 mg.m^{-3}.h	10-20 mg.m^{-3}.h	20-30 mg.m^{-3}.h	30-50 mg.m^{-3}.h	>50 mg.m^{-3}.h
Andorra	59	0.0	0.0	0.0	100.0	0.0
Austria	21504	0.0	0.0	35.2	64.8	0.0
Belgium	1442	0.0	29.0	71.0	0.0	0.0
Croatia	950	0.0	0.0	2.8	97.2	0.0
Cyprus	1532	0.0	0.0	0.0	0.0	100.0
Czech Republic	16867	0.0	0.0	65.8	34.2	0.0
Denmark	1751	0.0	100.0	0.0	0.0	0.0
Estonia	8191	0.0	100.0	0.0	0.0	0.0
Finland	98497	0.0	100.0	0.0	0.0	0.0
France	37050	0.0	6.1	41.1	38.0	14.8
Germany	56156	0.0	24.3	35.9	39.7	0.0
Hungary	981	0.0	0.0	74.0	26.0	0.0
Ireland	2391	100.0	0.0	0.0	0.0	0.0
Italy	13266	0.0	0.0	0.0	60.9	39.1
Latvia	9393	3.2	96.8	0.0	0.0	0.0
Liechtenstein	22	0.0	0.0	0.0	100.0	0.0
Lithuania	7293	22.7	77.3	0.0	0.0	0.0
Luxembourg	118	0.0	0.0	100.0	0.0	0.0
Malta	1	0.0	0.0	0.0	0.0	100.0
Monaco	0	0.0	0.0	0.0	0.0	0.0
Netherlands	1608	0.0	100.0	0.0	0.0	0.0
Poland	54931	0.0	45.7	50.8	3.5	0.0
Portugal	6868	0.0	0.0	0.0	100.0	0.0
San Marino	0	0.0	0.0	0.0	0.0	0.0
Slovakia	5033	0.0	0.0	0.5	99.5	0.0
Slovenia	2497	0.0	0.0	1.3	98.7	0.0
Spain	38944	0.0	0.0	8.3	84.5	7.2
Sweden	214073	0.0	100.0	0.0	0.0	0.0
United Kingdom	12617	88.9	11.1	0.0	0.0	0.0
Total	**614032**	**2.5**	**62.2**	**14.2**	**18.7**	**2.4**

Countries with few ozone data are excluded from the calculations in this paper: AL, BA, BG, GR, MK, RO. Countries with missing land cover information are also excluded from the calculations: CH, CS, IS, NO, TR.

Table A11. Exposure of mixed forests – ozone, AOT40 for forests, year 2004.

Country	Total mixed forests [km^2]	2004 *Percent [%]*				
		0-10 mg.m^{-3}.h	10-20 mg.m^{-3}.h	20-30 mg.m^{-3}.h	30-50 mg.m^{-3}.h	>50 mg.m^{-3}.h
Andorra	2	0.0	0.0	0.0	100.0	0.0
Austria	12679	0.0	0.0	37.9	62.1	0.0
Belgium	2620	0.0	15.5	84.5	0.0	0.0
Croatia	2665	0.0	0.0	3.6	96.4	0.0
Cyprus	3	0.0	0.0	0.0	0.0	100.0
Czech Republic	6046	0.0	0.0	69.0	31.0	0.0
Denmark	1271	0.0	100.0	0.0	0.0	0.0
Estonia	8322	0.0	100.0	0.0	0.0	0.0
Finland	87480	0.0	100.0	0.0	0.0	0.0
France	18877	0.0	5.2	34.4	45.1	15.2
Germany	23652	0.0	13.8	37.5	48.8	0.0
Hungary	1565	0.0	0.0	77.5	22.5	0.0
Ireland	223	100.0	0.0	0.0	0.0	0.0
Italy	10341	0.0	0.0	0.0	30.8	69.2
Latvia	11914	6.5	93.5	0.0	0.0	0.0
Liechtenstein	35	0.0	0.0	0.0	100.0	0.0
Lithuania	7236	33.5	66.5	0.0	0.0	0.0
Luxembourg	158	0.0	0.0	100.0	0.0	0.0
Malta	1	0.0	0.0	0.0	0.0	100.0
Monaco	0	0.0	0.0	0.0	0.0	0.0
Netherlands	936	0.0	100.0	0.0	0.0	0.0
Poland	22180	0.0	37.4	55.8	6.9	0.0
Portugal	5265	0.0	0.0	0.0	100.0	0.0
San Marino	1	0.0	0.0	0.0	0.0	100.0
Slovakia	3591	0.0	0.0	6.8	93.2	0.0
Slovenia	4503	0.0	0.0	6.0	94.0	0.0
Spain	14942	0.0	0.0	43.0	54.9	2.1
Sweden	16089	0.0	100.0	0.0	0.0	0.0
United Kingdom	499	53.6	46.4	0.0	0.0	0.0
Total	**263092**	**1.4**	**54.4**	**18.0**	**22.2**	**3.9**

Countries with few ozone data are excluded from the calculations in this paper: AL, BA, BG, GR, MK, RO. Countries with missing land cover information are also excluded from the calculations: CH, CS, IS, NO, TR.